Technische Universität München

TUM School of Life Sciences

**Impact of gastrically-released dietary bitter peptides on proton secretion and anti-inflammatory processes in immortalized human parietal cells**

Phil Richter

Vollständiger Abdruck der von der TUM School of Life Sciences der Technischen Universität München zur Erlangung eines

Doktors der Naturwissenschaften (Dr. rer. nat.)

genehmigten Dissertation.

Vorsitz: Prof. Dr. Wilfried Schwab

Prüfende der Dissertation:

1. Prof. Dr. Veronika Somoza
2. Prof. Dr. Corinna Dawid
3. Prof. Dr. Barbara Lieder

Die Dissertation wurde am 30.10.2024 bei der Technischen Universität München eingereicht und durch die TUM School of Life Sciences am 23.12.2024 angenommen.

*»There's much to learn. And so much to see.«*

– Elizabeth Woolridge Grant

*Für meine Eltern*

*Katrin und Stefan Richter*

# Preliminary remarks

This thesis was prepared in the period from November 2020 to October 2024 in the Research Group *Metabolic Function & Biosignals* at the Leibniz Institute for Food Systems Biology at the Technical University of Munich under the supervision of Prof. Dr. Veronika Somoza.

The articles *Bitter Peptides YFYPEL, VAPFPEVF, and YQEPVLGPVRGPFPIIV, Released during Gastric Digestion of Casein, Stimulate Mechanisms of Gastric Acid Secretion via Bitter Taste Receptors TAS2R16 and TAS2R38* (Copyright © 2022) and *Sodium-Permeable Ion Channels TRPM4 and TRPM5 are Functional in Human Gastric Parietal Cells in Culture and Modulate the Cellular Response to Bitter-Tasting Food Constituents* (Copyright © 2024) were published in *Journal of Agricultural and Food Chemistry* by the American Chemical Society licensed under CC-BY 4.0 and have been reprinted in this work in accordance with the license terms. The article *Gastric digestion of the sweet-tasting plant protein thaumatin releases bitter peptides that reduce H. pylori induced pro-inflammatory IL-17A release via the TAS2R16 bitter taste receptor* (Copyright © 2024) was published in *Food Chemistry* by Elsevier Society licensed under CC-BY 4.0 and has been reprinted in this work in accordance with the license terms.
All statistics and data presentations were made using GraphPad Prism versions 9 and 10. Illustrations were created with BioRender.com.

# Danksagung

Mein besonderer Dank gilt *Prof. Dr. Veronika Somoza* für die Aufnahme in die Arbeitsgruppe, die Überlassung des interessanten und vielfältigen Forschungsthemas, die hervorragende Betreuung mit wertvollen Gesprächen, Anregungen und Diskussionen und dem stetigen Interesse am Fortschritt der Arbeit. Darüber hinaus danke ich meiner Doktormutter für das mir entgegengebrachte Vertrauen, die Möglichkeit der Teilnahme an nationalen und internationalen Symposien und ihre fortwährende Unterstützung bei der beruflichen Weiterentwicklung.

Des Weiteren möchte ich mich bei meiner Zweitgutachterin *Prof. Dr. Corinna Dawid* für den hilfreichen Austausch bedanken.

Ich danke zudem allen meinen Kollegen am LSB, insbesondere der Arbeitsgruppe *Metabolic Function & Biosignals* für die freundliche Aufnahme am Institut und die produktive Arbeitsatmosphäre.

Meiner Mentorin *Dr. Karin Sebald* danke ich für ihre große Hilfsbereitschaft bei jeglichen Fragen und die zahlreichen heiteren und aufschlussreichen Unterhaltungen.

Bei *Kristin Kahlenberg* möchte ich mich unter anderem für ihre tägliche Unterstützung inner- und außerhalb des Labors, die Gespräche zu sämtlichen fachlichen und persönlichen Themen, die gemeinsame Planung, Durchführung und Auswertung unzähliger Versuche, die Auseinandersetzung mit alltäglichen Problemen, ihr immer offenes Ohr und nicht zuletzt natürlich für die Betreuung und Pflege von Adelheid bedanken.

*Dr. Gaby Andersen* bin ich für ihre schnelle Hilfe bei sämtlichen fachlichen Fragen, die Möglichkeit zur Teilhabe an ihrem einzigartigen Fachwissen und die gelungene Zusammenarbeit, insbesondere am „TRP-Projekt“, dankbar. Die gemeinsame Zeit im Büro hat mich sowohl auf fachlicher Ebene bereichert, als auch maßgeblich zur Erheiterung des Arbeitsalltags beigetragen.

Zudem danke ich *Katrin Gradl* für die schöne gemeinsame Zeit in zwei verschiedenen Büros, den wissenschaftlichen Austausch zu Peptiden und allem voran die überspringende Begeisterung für aquatische Lebewesen.

Bei *Katrin Gradl*, *Sonja Fröhlich* und *Dr. Johanna Kreißl* bedanke ich für die Hilfe bei der Durchführung massenspektrometrischer Analysen und der NMR-Experimente.

Bei *Silke Volkhardt-Rouse*, *Claudia Rehaber* und *Erika Stadler* möchte ich mich für die Unterstützung bei organisatorischen Fragen und insbesondere für die Suche und Überlassung begehrter Terminslots bedanken.

Der Administration danke ich für die Hilfe und Unterstützung bei organisatorischen und verwaltungstechnischen Anliegen.

*Dr. Gaby Andersen*, *Dr. Karin Sebald* und *Kristin Kahlenberg* danke ich nicht nur für das gewissenhafte Korrekturlesen der vorliegenden Arbeit, sondern auch diverser Manuskripte, Abstracts und Poster.

Neben allen Erwähnten, danke ich zudem *Alina Müller*, *Barbara Danzer*, *Eva Bauersachs*, *Dr. Melanie Köhler*, *Miriam Wimmer*, *Dr. Philip Pirkwieser*, *Timm Michel*, *Valeria Palacino Chacon* und *Dr. Verena Mittermeier-Kleßinger* für die schöne gemeinsame Zeit am Institut und auf der ein oder anderen Konferenz.

Ich danke allen Praktikanten, die ich im Rahmen meiner Doktorarbeit betreuen durfte, deren verlässliches Arbeiten einen wichtigen Beitrag zu dieser Arbeit geleistet hat.

Mein größter Dank gilt meinen Eltern, die mir mein Studium ermöglichten, mich glücklicherweise vor ziemlich genau 10 Jahren davon abhielten, mich nach der ersten Woche des Studiums exmatrikulieren zu lassen und auf deren Unterstützung ich immer zählen kann. Auch danke ich meinen Geschwistern, Großeltern und Freunden für ihren Beistand in jeglichen Lebenslagen und die unverzichtbaren Abwechslungen vom Forschungsalltag. Abschließend möchte ich meinem Mann *Konstantin* für seine uneingeschränkte und vielseitige Unterstützung, die Zusprüche und seine Geduld danken.

## Abstract

The digestion of foods in the human gastro-intestinal tract results in structural modification of the ingested food constituents. Since dietary proteins are cleaved into peptides and amino acids during gastric digestion, it was hypothesized that these cleavage products impact *(i)* the bitter taste receptor (TAS2R)-dependent modulation of proton secretion by parietal cells as a fundamental mechanism of gastric acid production, and *(ii)* anti-inflammatory processes.

To investigate this hypothesis, the non-bitter-tasting proteins casein and thaumatin were selected. The cleavage products of both proteins were analyzed in a cell-free experiment mimicking gastric digestion, and subjected to *in silico* bitter prediction tools. The bitterness of the predicted bitter peptides with highest abundancy was confirmed by sensory analysis. Afterwards, the bitter peptides' release was validated and quantified by synthetic reference compounds using LC-MS/MS. Cell-based experiments showed that immortalized human parietal cells (HGT-1) responded to these bitter peptides with an increased proton secretion and a gene regulation of *TAS2R16* and *TAS2R38*. Functional involvement of these TAS2Rs was investigated by selective antagonists, and validated by targeted reduction of *TAS2R16* and *TAS2R38* gene expression using specific siRNA. Subsequently, a new cell model was established based on HGT-1 cells, which reacts with an increased release of interleukin 17A when treated with native proteins from the bacterium *Helicobacter pylori*. Pretreatment of the cells with the bitter thaumatin peptides reduced the *Helicobacter pylori*-induced IL-17A release up to 89.7 ± 21.9%. Functional involvement of TAS2R16 was validated by means of an siRNA approach. Further experiments focusing on the underlying intracellular signaling pathways showed that the activation of a bitter taste receptor leads to an opening of the two transient receptor potential (TRP) channels TRPM4 and TRPM5, whereby extracellular sodium flows into the parietal cells and initiates secretory activity by the $H^+/K^+$ ATPase. Again, the use of antagonists reduced this effect, and the interaction of TAS2Rs with TRPM4 and TRPM5 was validated by CRISPR-Cas9 knock-out and siRNA knock-down approaches, respectively.

Overall, in this work, it was shown that non-bitter-tasting dietary proteins might be cleaved into bitter-tasting peptides during gastric digestion. The resulting gastrically-released bitter peptides modulate proton secretion and the release of pro-inflammatory cytokines from human parietal cells via TAS2Rs. The results can be used to develop palatable food formulations in retrosynthetic approaches that interact with taste receptors in organs and tissues after digestion to achieve the desired physiological effect, while their undigested precursor molecules in the oral cavity do not negatively affect the taste of the food.

# Zusammenfassung

Die Verdauung von Nahrungsmitteln im menschlichen Magen-Darm-Trakt führt zu einer strukturellen Veränderung der aufgenommenen Nahrungsbestandteile. Da Nahrungsproteine während der Verdauung im Magen in Peptide und Aminosäuren gespalten werden, wurde die Hypothese aufgestellt, dass diese Spaltprodukte *(i)* unter Beteiligung von Bittergeschmacksrezeptoren (TAS2Rs) die Protonensekretion und *(ii)* Entzündungsreaktionen von Parietalzellen beeinflussen.

Zur Prüfung der Hypothese wurden die nicht bitter-schmeckenden Proteine Casein und Thaumatin ausgewählt. Die Spaltprodukte beider Proteine wurden in einem zellfreien Experiment, das die Magenverdauung nachahmt, analysiert und mit *in silico* Bittervorhersagetools untersucht. Im Anschluss erfolgte die sensorische Bestätigung der Bitterkeit und die Validierung und Quantifizierung der Peptidfreisetzung durch synthetische Referenzverbindungen mittels LC-MS/MS. Zellbasierte Versuche zeigten, dass immortalisierte menschliche Parietalzellen (HGT-1) mit einer verstärkten Protonensekretion und einer Genregulation von *TAS2R16* und *TAS2R38* auf die bitteren Peptide reagierten. Eine funktionelle Beteiligung der beiden TAS2Rs wurde durch selektive Antagonisten geprüft und durch die gezielte Reduktion der *TAS2R16*- bzw. *TAS2R38*-Genexpression mittels spezifischer siRNA validiert. Anschließend wurde basierend auf HGT-1 Zellen ein neues Zellmodell etabliert, welches durch die Behandlung mit nativen Proteinen aus dem Bakterium *Helicobacter pylori* mit einer verstärkten Freisetzung des Interleukins 17A reagiert. Eine Vorbehandlung der Zellen mit den bitteren Thaumatinpeptiden führte zu einer Reduktion der *Helicobacter pylori*-induzierten IL-17A-Ausschüttung um bis zu 89.7 ± 21.9 %. Eine funktionelle TAS2R16-Beteiligung wurde durch die Anwendung von siRNA validiert. Weiterführende Versuche zu den zugrundeliegenden intrazellulären Signalwegen zeigten, dass die Aktivierung eines TAS2Rs zu einer Öffnung der beiden Transient receptor potential (TRP)-Kanäle TRPM4 und TRPM5 führt, wodurch extrazelluläres Natrium in die Parietalzellen einströmt und schließlich die sekretorische Aktivität durch die $H^+/K^+$-ATPase auslöst. Auch hier verringerte die Anwendung von Antagonisten den Effekt, wobei die Interaktion von TAS2Rs mit TRPM4 und TRPM5 durch CRISPR-Cas9 Knock-Out bzw. siRNA Knock-Down Ansätze validiert wurde.

In dieser Arbeit wurde gezeigt, dass nicht bitter-schmeckende Nahrungsproteine während der Verdauung im Magen in bittere Peptide gespalten werden können, die über TAS2Rs die Protonensekretion und Ausschüttung entzündungsfördernder Zytokine von menschlichen Parietalzellen modulieren. In Zukunft können diese Ergebnisse genutzt werden, um in retrosynthetischen Ansätzen schmackhafte Lebensmittelformulierungen zu entwickeln, die erst nach der Verdauung mit Geschmacksrezeptoren in Organen und Geweben interagieren, um den gewünschten physiologischen Effekt zu erzielen, während deren unverdaute Vorläufermoleküle in der Mundhöhle den Geschmack der Nahrungsmittel nicht negativ beeinflussen.

# Contents

# 1 Introduction

Taste receptors and taste-sensitive ion channels, whose expression was thought to be primarily in the oral cavity, where they are responsible for the perception of taste qualities, have also become increasingly important in relation to various physiological processes over the past 20 years. It is now known that these receptors and ion channels are found in almost all tissues of the human body, although their role and function are far from fully understood. In addition to countless regulatory effects, for example on metabolic processes including the release of hormones and digestive juices in the gastrointestinal tract (Avau et al., 2015; Chou, 2021), bitter taste receptors in particular also play a role in the immune system's defense against pathogens (Dragoș et al., 2022). The complex interplay of a number of receptors and the signaling proteins and pathways associated with them is enhanced by the fact that bioactive food constituents, and therefore also bitter tastants, can be modified not only during the processing of the basic raw materials during food production, but also through digestion and metabolization in the human body. However, the first organ that comes into contact with ingested food is the tongue in the oral cavity.

## 1.1 Taste perception on the tongue

Humans are able to detect and distinguish the five basic taste qualities sweet, umami, bitter, sour and salty. In the oral cavity, taste bud cells of the tongue - being the peripheral organ of gustation - recognize the taste qualities sweet, umami and bitter via highly specialized taste receptor proteins, while salt and acids are sensed through the activation of ion channels (Roper & Chaudhari, 2017). Primary taste transduction originates from cells of taste buds located in circumvallate, foliate or fungiform papillae and involves intra- and intercellular pathways by which the sensory information is passed on to various regions of the brain by glossopharyngeal, chorda tympani and the vagus nerve system. Each taste bud contains about 80–100 neuroepithelial, chemosensory-active taste cells which are classified into the three categories Type I, II and III cells (**Fig. 1**) (Chaudhari & Roper, 2010; Roper & Chaudhari, 2017). The most abundant Type I cells are thought to have a glia-like, structural function and synthesize NTPDase 2 to degrade ATP released by Type II cells for intercellular communication (Chaudhari & Roper, 2010; Roper, 2013). Type II cells are also named “receptor cells” as they express G protein-coupled taste receptor proteins, which are responsible for the transduction of bitter (TAS2R proteins), sweet (TAS1R2/TAS1R3 heterodimer protein) and umami taste (TAS1R1/TAS1R3 heterodimer protein), and express voltage-gated $Na^+$ and $K^+$ channels to mediate depolarization (Chaudhari & Roper, 2010). This is followed by Type II cells releasing ATP to stimulate nerve terminals and Type III cells (Finger et al., 2005; Dando & Roper, 2009). The latter are also named “presynaptic cells” as they

synapse with afferent nerve terminals and release serotonin (Huang et al., 2005; Larson et al., 2015) as well as other neurotransmitters (Huang et al., 2008; Huang et al., 2011; Dando & Roper, 2012), such as acetylcholine and noradrenaline. Type III cells are also involved in sour and salty taste transduction (Gilbertson et al., 2000; Molitor et al., 2020). With the life span of taste cells being limited to only ~10 days, progenitor cells, also classified as Type IV cells and located on the base of the taste bud, constantly replenish the papillae with new mature taste cells (Chaudhari & Roper, 2010; Roper, 2013).

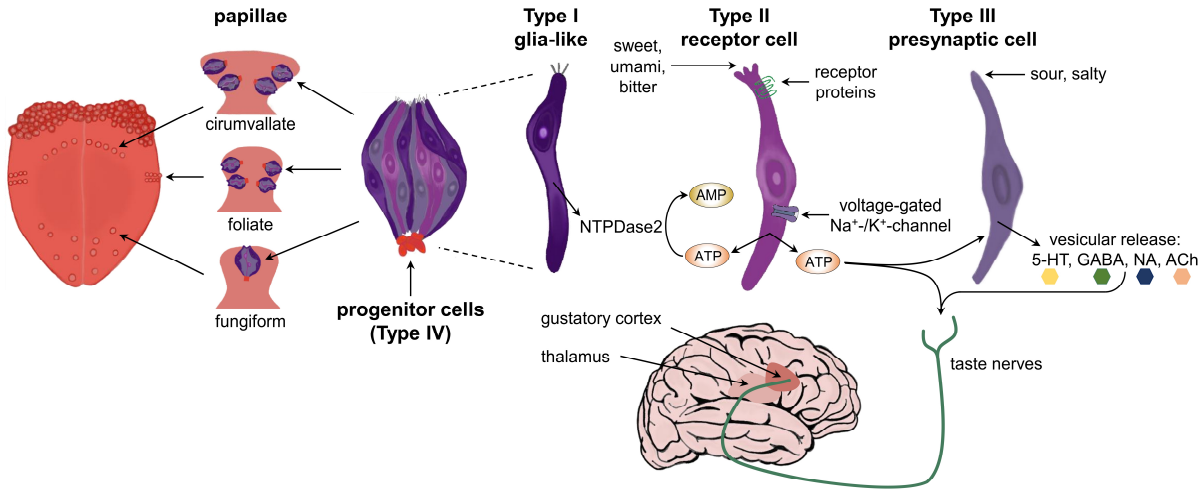


**Figure 1: Schematic overview of organs, tissues and cells facilitating taste perception.** Papillae on the tongue contain progenitor cells, which are composed of glia-like, receptor and presynaptic cells. While Type I cells are mainly responsible for the release of NTPDase 2, which breaks down ATP, Type II cells play a decisive role in the perception of sweet, umami, and bitter and Type III cells in the perception of sour and salty (adapted from Molitor et al., 2020).

While the taste receptors of the TAS1R gene family are responsible for detecting the building blocks of carbohydrates (TAS1R2/TAS1R3), such as glucose, and proteins (TAS1R1/TAS1R3), for instance the sodium salt of L-glutamic acid (Nelson et al., 2001; Max et al., 2001; Montmayeur et al., 2001; Li et al., 2002; Nelson et al., 2002), the proton-channel OTOP1 was recently demonstrated to be involved in the detection of sour stimuli (Tu et al., 2018; Teng et al., 2019; Zhang et al., 2019), consequently protecting from the ingestion of unripe or spoiled food, whereas the sodium channel ENaC serves a role in the maintenance of electrolyte balance eliciting salty perception (Chandrashekar et al., 2010). The most complex family of taste receptors known to date are the TAS2Rs, which consist of around 25 members and are hypothesized to be responsible for preventing the ingestion of potentially toxic compounds, most of which have a bitter taste (**Fig. 2**) (Behrens & Meyerhof, 2018).

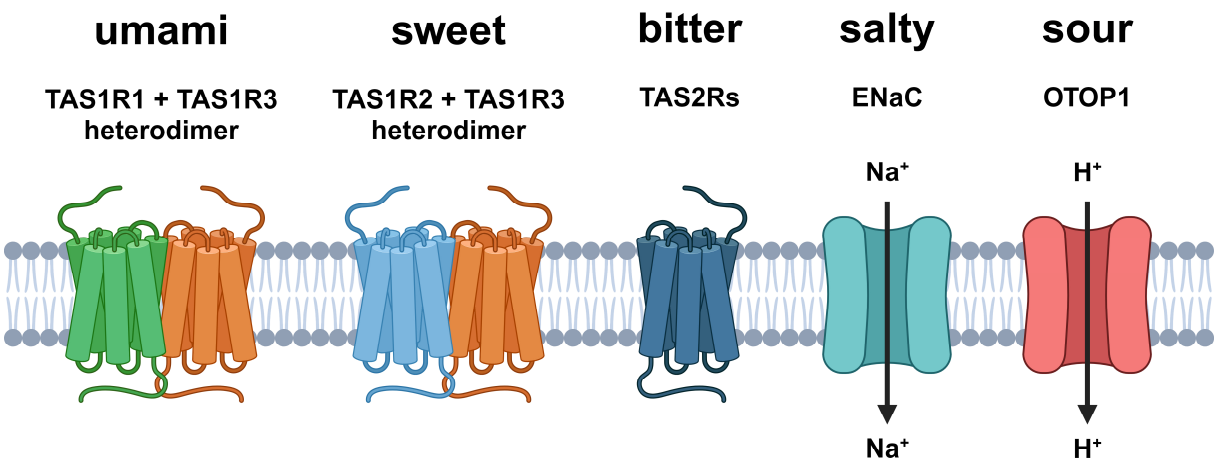


**Figure 2: Illustration of the corresponding receptors or ion channels for the five basic taste qualities.** The heterodimer of TAS1R1 and TAS1R3 for the perception of umami, TAS1R2 and TAS1R3 for sweet, the TAS2R family for bitter taste perception and the two ion channels ENaC and OTOP1 as representatives for salty and sour (Max et al., 2001; Li et al., 2002; Chandrashekar et al., 2010; Behrens & Meyerhof, 2018; Teng et al., 2019). Created with BioRender.com.

The perception of sour and salty through selective ion channels involves the influx of protons (Ramsey & DeSimone, 2018) or sodium ions (Nomura et al., 2020) into the intracellular space. This is contrasted by the signaling of the G protein-coupled taste receptors.

## 1.2 Cellular pathways in response to sweet or bitter-tasting compounds

### 1.2.1 Downstream cellular signaling pathways of taste receptors

Taste-receptor cells on the tongue and various types of enteroendocrine cells, e.g. L cells of the ileum and colon, express components essential for sensing of tastants and nutrients. These include apical G protein-coupled receptors of the TAS1R and the TAS2R family for sweet, umami and bitter-tasting compounds and the G protein isoforms Gα-gustducin, Gβ3, and Gγ13. After activation of a TAS2R by binding a ligand, a conformational change is induced. This causes the dissociation of the G protein into its α and βγ subunit. In the subsequent pathway (**Fig. 3**), the βγ subunit leads to an activation of the phospholipase C β2 (PLC β2) which catalyzes the cleavage of phosphatidylinositol 4,5-bisphosphate ($PIP_2$) into inositol 1,4,5-trisphosphate ($IP_3$) and diacylglycerol (DAG). In term, the $IP_3$ receptors expressed on the endoplasmic reticulum (ER) are activated by the released $IP_3$, resulting in a release of $Ca^{2+}$ ions from the ER into the cytosol (calcium mobilization) (Rozengurt et al., 2006; Sanematsu et al., 2014; Jalševac et al., 2022). Increasing $Ca^{2+}$ levels in the cytosol activate transient receptor potential channels TRPM4 and TRPM5, resulting in sodium influx into the cell and membrane depolarization, leading to ATP release (Dutta Banik & Medler, 2023; Kaske et al., 2007; Clapp et al., 2008).

While the signaling pathway originating from the βγ subunit of gustducin is well described and elucidated, little is known about the involvement of the dissociated α subunit. In the past, it has been hypothesized that this is associated with changes in intracellular cyclic adenosine monophosphate (cAMP) levels. For example, there is evidence that dissociation of the α subunit leads to activation of phosphodiesterase (PDE), which catalyzes the degradation of cAMP, resulting in decreased cAMP levels and maintained $IP_3$ type 3 receptor hypophosphorylation and sensitization (Clapp et al., 2008; Jalševac et al., 2022). Therefore, the tonic activity of α-gustducin regulates taste cell responsivity. Transducin, a similar G protein also present in taste cells, can replace the function of α-gustducin (Ruiz-Avila et al., 1995; He et al., 2002). In contrast, there are also several studies that have shown that the treatment of immortalized human parietal cells with bitter compounds can also lead to an increase in intracellular cAMP concentration (Rubach et al., 2010; Liszt et al., 2017). In both, taste buds and parietal cells, the signaling cascades include a cAMP-dependent and a PLC β2/$IP_3$/$Ca^{2+}$-dependent pathway (Roper, 2007).

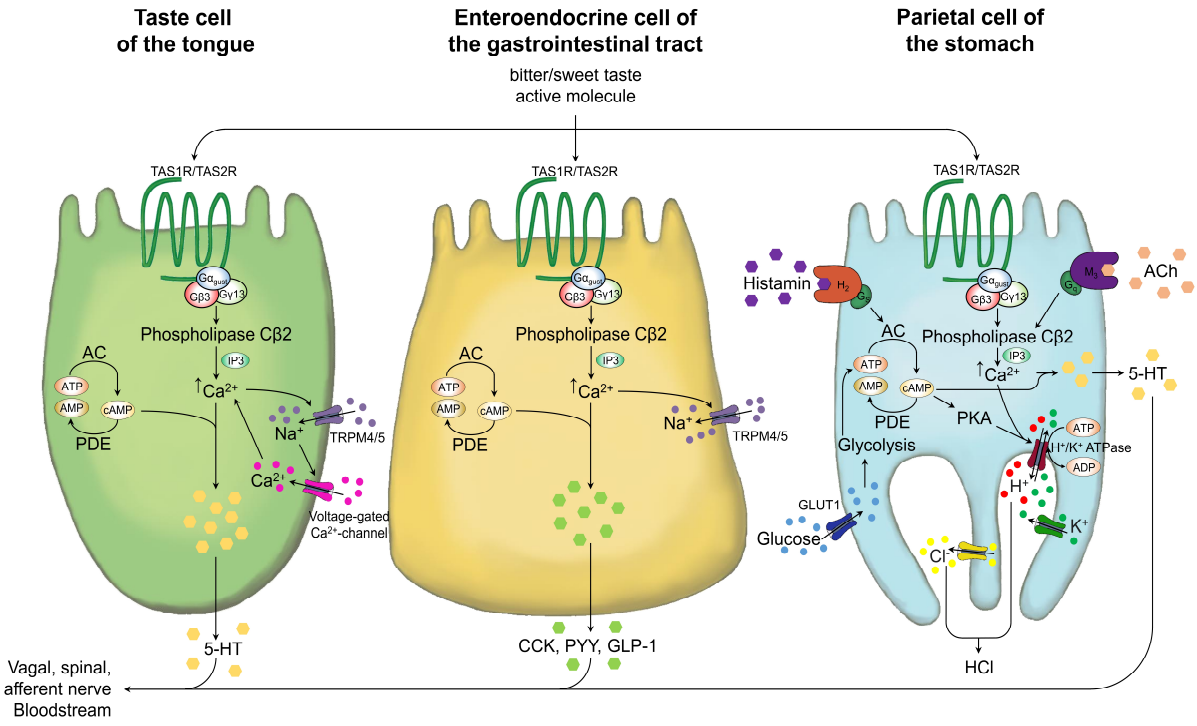


**Figure 3: Similarities in nutrient-sensing mechanisms used by taste-receptor cells of the tongue (summarized representation of the cell types), enteroendocrine cells of the intestine and parietal cells of stomach.** All three cell types express bitter taste receptors that lead to different outcomes via similar intracellular signaling pathways (adapted from Cummings & Overduin, 2007; Zopun et al., 2018a; Zopun et al., 2018b; excerpts previously published by Richter et al., 2022).

So far, $K^+$ channels and voltage-gated $Ca^{2+}$ channels that are important for taste sensation in the tongue have not yet been confirmed in enteroendocrine cells. However, both cell types

share the final pathway for activation, which includes an increase in intracellular calcium mobilization. This triggers basolateral exocytosis of neurotransmitters, e.g. serotonin, into synapses with nerve fibers that transfer information to the hindbrain. In enteroendocrine cells, intracellular calcium mobilization results in the release of satiating peptides that also delay gastric emptying, e.g. via GLP-1 (Jang et al., 2007) or PYY (additionally reduces intestinal motility) (Yuzuriha et al., 2007; Abrol et al., 2015). These peptides diffuse across extracellular fluids to enter the circulation or to interact with nearby afferent nerve terminals from vagal, spinal, and myenteric neurons (Baggio & Drucker, 2014; Wachsmuth et al., 2022). In addition to stimulating peptide release directly, sweet-taste-receptor activation by extracellular tastants also upregulates glucose transporters in enteroendocrine cells (Cummings & Overduin, 2007; Lee & Owyang, 2017), possibly amplifying release of satiation peptides by enhancing intracellular glucose uptake and metabolism (Dyer et al., 2005). Moreover, L cells secrete cholecystokinin (CCK), which results in delayed gastric emptying and increased release of digestive enzymes (Lieverse et al., 1994; Liou et al., 2011; Daly et al., 2013).

In the stomach, the activation of calcium-dependent ion channels regulates the hunger hormone ghrelin through P/D1 cells (Engelstoft et al., 2013; Vancleef et al., 2015; Steensels et al., 2016). Furthermore, G (in the stomach and duodenum) and S cells (in the jejunum and duodenum) are involved in the release of gastrin and somatostatin, which stimulate or inhibit the secretion of pepsinogen and gastric acid, respectively (Feng et al., 2010; Haid et al., 2012). The secretion of gastric acid by parietal cells can be activated by histamine or acetylcholine binding to their cognate histamine $H_2$ or acetylcholine $M_3$ receptors (J. G. Forte, 2010). Activation of these receptors results, either by $G_s$- and adenylyl cyclase/cAMP- or by $G_q$- and PLC β2/$IP_3$/$Ca^{2+}$-dependent pathways, which are also present in taste cells of the tongue and in enteroendocrine cells, in the stimulation of the $H^+/K^+$ ATPase, which pumps protons into the stomach lumen (J. G. Forte, 2010). Previous studies demonstrated TAS1Rs and TAS2Rs being expressed in gastric cells (**Tab. 1** and **Fig. 4**), and are involved in mechanisms regulating proton secretion in a well-established cell model of immortalized human parietal cells (HGT-1) that resembles all functional characteristics of human parietal cells (Liszt et al., 2017; Zopun et al., 2018b; Stoeger et al., 2020).

The TAS2R-mediated stimulation of cellular proton secretion was verified in a human intervention trial in which a bolus dose of 120 mg of the bitter-tasting compound caffeine (targeting TAS2R7/10/14/43/46; Meyerhof et al., 2010) increased gastric acid secretion. This effect was ameliorated by the TAS2R antagonist homoeriodictyol (HED), which has an antagonistic effect on TAS2R20/31/43/50 but activates TAS2R14 and 39 (Roland et al., 2013; Liszt et al., 2017). Notably, activation of gastric TAS2Rs by caffeine was more effective in stimulating gastric acid secretion by reducing the reacidification time in healthy subjects than activation of oral TAS2Rs.

**Table 1: Comparative representation of mRNA expression in HGT-1 cells normalized to the expression of the acetylcholine receptor (*CHRM3*).** The specific transcripts of 22 of the 25 known human bitter taste receptors were identified by RT-qPCR (Liszt et al., 2017).

| receptor gene | mean | ± | SEM |
|---|---|---|---|
| *TAS2R1* | 0.20 | ± | 0.05 |
| *TAS2R3* | 9.87 | ± | 0.85 |
| *TAS2R4* | 5.66 | ± | 0.77 |
| *TAS2R5* | 12.08 | ± | 0.82 |
| *TAS2R7* | 0.32 | ± | 0.07 |
| *TAS2R8* | no specific product | | |
| *TAS2R9* | 0.12 | ± | 0.02 |
| *TAS2R10* | 0.97 | ± | 0.10 |
| *TAS2R13* | 1.69 | ± | 0.14 |
| *TAS2R14* | 12.39 | ± | 1.35 |
| *TAS2R16* | 0.71 | ± | 0.24 |
| *TAS2R19* | 4.40 | ± | 0.68 |
| *TAS2R20* | 9.09 | ± | 1.14 |
| *TAS2R30* | 8.02 | ± | 0.72 |
| *TAS2R31* | 4.00 | ± | 1.77 |
| *TAS2R38* | 0.14 | ± | 0.05 |
| *TAS2R39* | 3.64 | ± | 0.81 |
| *TAS2R40* | 0.51 | ± | 0.05 |
| *TAS2R41* | 0.66 | ± | 0.14 |
| *TAS2R42* | 2.24 | ± | 0.44 |
| *TAS2R43* | 6.47 | ± | 0.32 |
| *TAS2R45* | not detected | | |
| *TAS2R46* | 2.59 | ± | 0.42 |
| *TAS2R50* | 2.91 | ± | 0.29 |
| *TAS2R60* | no specific product | | |

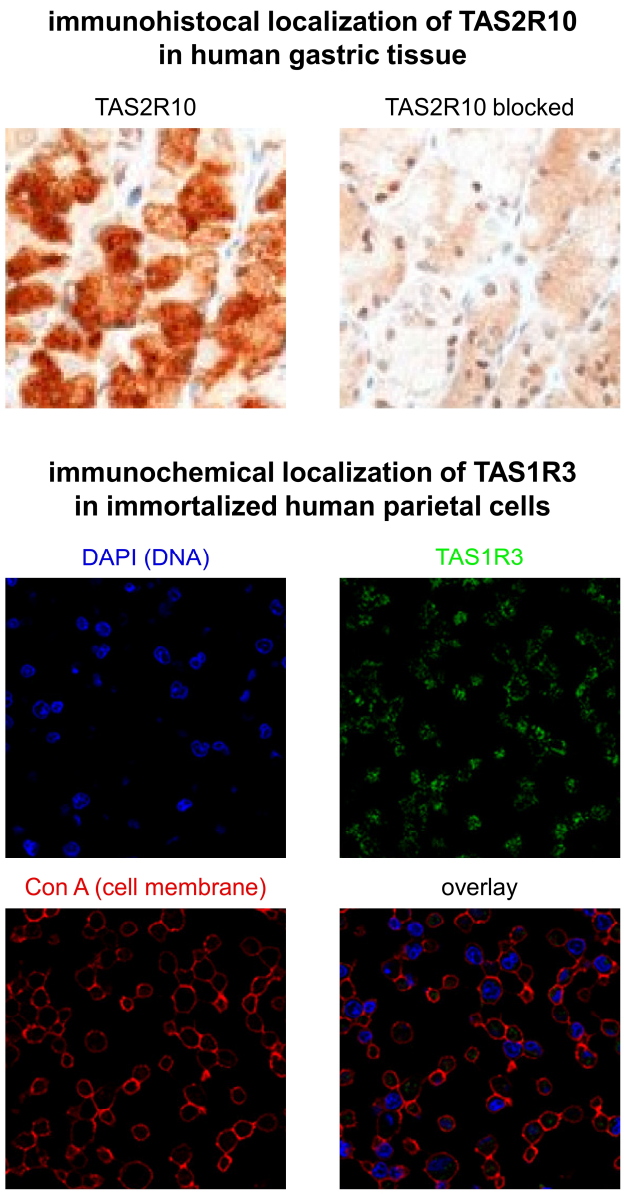


**Figure 4: Exemplary visualization of the expression of taste receptors in human gastric tissue and human parietal cells using immunohistology and immunocytochemistry.** The expression of TAS2R10 could be detected in biopsy samples of the human stomach, while the expression of TAS1R3 could be localized immunochemically in HGT-1 cells (adapted from Liszt et al., 2017; Zopun et al., 2018b).

Comparatively little is known about the intracellular signaling pathways in cells other than taste cells, which also express taste receptors, especially TAS2Rs. For instance, in contrast to other cell types, a possible involvement of TRPM4 and TRPM5 in parietal cells has not yet been confirmed, although this would be a potentially key target in the regulation of gastric acid secretion and associated symptoms.

## 1.3 Role of taste receptors in the oral cavity and in extra-oral tissues

Although taste receptor proteins were first discovered in the oral gustatory system (Ekoff et al., 2014; Gilca & Dragos, 2017), research over the past 20 years revealed their expression in multiple extra-oral tissues and organs that play critical roles in the maintenance of metabolic homeostasis and in disease response (Edgar et al., 2002; Barrett et al., 2013). Even gene expression levels of taste receptor proteins, like for many other G protein-coupled receptors (GPCRs), are typically low, they can utilize a powerful intracellular amplification cascade for signaling, which is a common feature of GPCRs (Ross, 2014), making high expression levels not be required for significant physiological effects. This knowledge has opened a new field investigating the distribution, functionality and physiological roles of extra-oral taste receptors (Lee et al., 2019).

### 1.3.1 Functional role of the sweet taste receptor (TAS1R2/TAS1R3)

Taste receptor cells sensing sweet (TAS1R2/TAS1R3) (Kim et al., 2017) and umami (TAS1R1/TAS1R3) (Han et al., 2018) have also been hypothesized to impact food intake (Depoortere, 2014). One of the central questions associated with this hypothesis is whether the sweet taste of a compound has an impact on total energy intake. Answering this question is of global importance since the excessive consumption of sugar, particularly in sugar-sweetened beverages, has been linked to the rising rates of obesity worldwide (Malik et al., 2006; Bermudez & Gao, 2010). For more than the past two decades, one of the strategies to combat the current obesity crisis has been to reduce energy intake by replacing sugar with high intensity sweeteners in commercial products (Benton, 2005; Swithers et al., 2010). Unfortunately, the prevalence of obesity has continued to increase. A meta-analysis of controlled human intervention studies and prospective cohort trials in 2014 even revealed that consumption of high intensity sweeteners was not associated with a reduced energy intake (Miller & Perez, 2014), instead suggesting that habitual consumption of sweetness without the associated energy may actually increase appetite and encourage the intake of alternative foods (Mattes & Popkin, 2009). However, the molecular mechanisms by which and to which extend sweet-tasting compounds stimulate food intake via activation of sweet taste receptors have not been studied comprehensively so far. Although the identification of sweet taste receptors in the oral cavity (Hoon et al., 1999; Nelson et al., 2001) and the gastro-intestinal tract (Dyer et al., 2005; Jang et al., 2007) provided important insights, it is still unclear whether the habitual use of large amounts of sugar or high intensity sweeteners impairs mechanisms regulating food intake by modulation of oral, gastro-intestinal or brain sensing mechanisms of sweetness (Bartoshuk et al., 2006; Westerterp, 2006; Duffy, 2007). A recent human intervention study published in 2020 demonstrated that an addition of 60 ppm of the TAS1R3 antagonist lactisol to a 10% sucrose-in-water drink increased total energy intake from a

subsequent standardized ad libitum breakfast and reduced plasma concentrations of the satiating neurotransmitter serotonin compared to administration of the sucrose solution solely (Schweiger et al., 2020). Since the addition of the same dose of lactisol to a 10% glucose-in-water drink, targeting TAS1R2, did not affect total energy intake, a pivotal role of TAS1R3 in mechanisms regulating energy intake might be hypothesized (Inoue et al., 2004; DuBois, 2016; Zhao et al., 2018).

However, this study neither investigated the underlying molecular mechanisms nor discriminated between TAS1R3 sweet sensing in the oral cavity, the gastro-intestinal tract, the brain and the periphery. All these sites are involved in the complex interplay of a plethora of hormonal, neural, and metabolic signals transmitted to the brain to regulate satiation, which refers to processes that promote meal termination, thereby limiting meal size (Blundell & Halford, 1994; Smith, 1998), and satiety, which refers to postprandial events that affect the interval to the next meal, i.e. regulating meal frequency, which is also influenced by learned habits (Strubbe & Woods, 2004).

In a cell model, immortalized human parietal cells (HGT-1) were exposed to various sweeteners, e.g. cyclamate, targeting the TAS1R2/3 sweet receptor which not only stimulated proton secretion but also the release of the neurotransmitter serotonin by cAMP- and $Ca^{2+}$-dependent signaling pathways (Zopun et al., 2018a; Zopun et al., 2018b). Since these effects were reduced by the TAS1R3 antagonist lactisole, involvement of the TAS1R2/3 heterodimer is strongly hypothesized. However, knowledge regarding the role of the stomach in gastro-intestinal serotonin secretion and its impact on satiation is scarce. Although very early studies from the 1980ies showed that peripherally administered serotonin decreases food intake in rats, only central serotonin has been considered as satiating (Pollock & Rowland, 1981). This assumption might be re-evaluated as also in 2004, gastric distension-induced released serotonin was demonstrated to stimulate c-Fos expression in specific brain nuclei via 5-$HT_3$ receptors in conscious rats, indicating a satiating potential of peripheral serotonin (Mazda et al., 2004).

In mice, a diet-induced obesity led to a reduced number of taste buds on the tongue and increased food intake which is associated with reduced taste perception (Kaufman et al., 2018). In addition, another study has shown that by pharmacologically blocking of sweet taste receptors in humans using *Gymnema sylvestre*, the desire for sweet taste qualities decreases (Turner et al., 2020). This could mean that people with a reduced sense of sweet taste, like the obese mice (Kaufman et al., 2018), need more intense stimuli and therefore a higher energy intake to achieve a feeling of satiation and reward (Noel et al., 2017).

### 1.3.2 Functional role of bitter taste receptors (TAS2Rs)

One of the early studies showing an extra-oral functionality of TAS2Rs was published by Deshpande et al., 2010, who demonstrated that TAS2Rs on airway smooth muscle cells trigger bronchodilation through localized calcium signaling, resulting in the reversal of airway obstruction. TAS2Rs and their downstream signaling molecules have also been identified in the intestinal tract, where a functional role for a small number of these receptors in the detection of nutrients and resulting hormonal and neural cascades regulating food intake has been shown (Chen et al., 2006; Le Nevé et al., 2010). Specifically, for some of the 25 receptors of the human TAS2R family, which help to avoid ingestion of bitter-tasting, potentially toxic food ingredients (Behrens & Meyerhof, 2018), a pivotal role has been demonstrated in the delay of gastric emptying (e.g. mice TAS2R108; Avau et al., 2015) stimulated by denatonium benzoate, one of the most bitter-tasting compounds known (Zeece, 2020a), as well as gastric acid secretion and gastric motility (e.g. human TAS2R43) induced by the bitter-tasting compound caffeine and ameliorated by the bitter-masking compound homoeriodictyol (Liszt et al., 2017).

The feeling of satiation is triggered, among other factors, by an increased serotonin level in the brain due to its appetite-suppressing effect (Wurtman & Wurtman, 1995; Blundell & Halford, 1998). But not only the serotonin level in the brain has an effect on the digestion of foods and associated metabolic processes. Serotonin secreted into the intestinal mucosa leads to the activation of serotonin receptors. Subsequent stimulus transmission by excitatory motor neurons via acetylcholine and inhibitory motor neurons via nitric oxide results in peristalsis of the intestinal muscles (Costedio et al., 2007). The following results, in which their effects were suppressed, show that bitter tastants also play a role here (Hochkogler et al., 2017). When the bitter-masking compound homoeriodictyol was consumed by moderately overweight male subjects, their energy intake from an ad libitum breakfast increased, especially the intake of protein. In addition, a reduced release of serotonin into plasma was observed. However, there are not only compounds that reduce the effects of bitter compounds, but also those that enhance their impact. The synthetic capsaicinoid nonivamide, for example, has a satiating effect, reduces the energy intake and increases the serotonin level in the plasma (Hochkogler et al., 2014). Recent results show that the addition of nonivamide and the amino acid L-arginine to wheat protein hydrolysate further enhances these effects. Furthermore, increased serotonin levels in plasma and delayed gastric emptying were observed (Stoeger et al., 2019). In terms of satiety, it has long been known that proteins are the most effective macronutrients (Morell & Fiszman, 2017). One point to bear in mind here is that proteins ingested through foods are broken down by pepsin into peptides and amino acids, such as L-arginine, during gastric digestion, especially under the acidic conditions in the stomach (Heda et al., 2024). The gastrointestinal digestion of compounds in the human body plays another important role.

Starting with digestion in the mouth, the structure of consumed compounds is changed, which can lead to the activation of different receptors during the digestion. The fact that peptides released during digestion have effects on functions and physiology of the human body is also shown by a patent, in which casein-derived hexapeptides have anxiolytic activity (Balandras et al., 2007). In another patent it was shown that peptides released from casein affect the production of fibrillin in fibroblasts (Smith, 2003).

However, an overall satiating effect of TAS2R agonists, resulting in reduced food and/or energy intake, is currently under debate since human intervention studies reveal conflicting results. Whereas oral administration of about 500 µg/kg denatonium benzoate (Avau et al., 2015) as well as 18 mg quinine as TAS2R agonists increased satiation and reduced total food intake in healthy subjects by about 10% (Andreozzi et al., 2015), and an oral bolus dose of 30 mg homoeriodictyol as TAS2R antagonist, in contrast, increased appetite and total energy intake from a standardized breakfast by about 7% (Hochkogler et al., 2017), intra-duodenal infusion of high amounts of up to 225 mg quinine failed to affect energy intake (Bitarafan et al., 2019). These contradictory results show that the site of action of the bitter compounds used is of central importance. In addition to the different functions of the targeted cell types, it should be considered that besides proteins, digestion and metabolization can also lead to structural changes of other food constituents and consequently to changes in their effect, for instance on satiation. While these factors have been very well investigated and described for drugs, there is not yet sufficient evidence available for bioactive food ingredients. In the case of quinine, it would be conceivable, that the orally ingested compound is already modified in the stomach in such a way that hardly any equivalents of the intact quinine reach the intestine. It has been shown, for instance, that quinine can undergo inversions and additions when exposed to low pH levels given in the stomach by gastric acid, which can lead to a loss of the hydrophobic vinyl group (Dawidowicz et al., 2018) and thus to a change in the impact of the compound, for example on the described energy intake.

In addition to the results from human and animal studies, fundamental involvement of bitter taste receptors in physiological outcomes has also been demonstrated in cell culture. Since treatment of immortalized human parietal cells with the bitter-tasting amino acid L-arginine (targeting at least TAS2R1 and TAS2R38) also stimulated proton secretion and the release of serotonin from HGT-1 cells (Stoeger et al., 2020), it can be assumed that amino acids and bitter peptides, which are released during digestion, can also have a bitter taste receptor-mediated influence on gastric functions. While activation of TAS2R1 and TAS2R4 could be shown for other amino acids than L-arginine, such as L-phenylalanine and L-tryptophan, bitter peptides such as LLL, YPFPGPIHNS, and LVYPFPGPIHNXX also activate TAS2R1/4/39 (Kohl et al., 2013). Experiments with casein hydrolysates showed not only activation of the classic receptors associated with bitter peptides like TAS2R1/4/14/39/46, but additionally

intercellular calcium mobilization by HEK293 cells overexpressing TAS2R16 (Maehashi et al., 2008; Dai et al., 2024). In the context of TAS2R16, it was shown that the dipeptide L-tryptophan-L-tryptophan, which activates TAS2R1/4/39 (Kohl et al., 2013), also has inhibitory effects on TAS2R14/16/43/46 (Ojiro et al., 2021), resulting in an interesting interplay involving several different receptors, as present in native cells, which has not yet been investigated further. This demonstrates that the potential digestion products of dietary proteins, namely amino acids and peptides, have an influence on digestive processes and satiation both in animal and human experiments and at the cellular level.

While obesity as a state of low-grade chronic inflammation can lead to numerous metabolic diseases (Hildebrandt et al., 2023), inflammatory processes are another aspect alongside satiety and overweight in which bitter taste receptors can play a role. To understand how bitter compounds can counteract the release of pro-inflammatory cytokines and where the underlying signaling pathways may intersect, the processes of inflammatory responses in the human body need to be introduced.

### 1.4 Inflammatory responses in the human organism

There are a variety of factors that can induce inflammatory processes in response to a pro-inflammatory stimulus or event in the human body. In addition to chemical factors, such as alcohol and heavy metals like nickel, or physical influences, like burns, frostbite or foreign bodies, infectious factors are considered to be the most complex ones (Chen et al., 2017). These include viruses, bacteria and other microorganisms that exhibit so-called pathogen-associated molecular patterns (PAMPs), such as the lipopolysaccharides (LPS) of gram-negative bacteria. However, non-infectious influences also trigger the release of damage-associated molecular patterns in the organism, which initiate the inflammatory response (Kawai & Akira, 2010). Basically, all inflammations are defense mechanisms (Nathan & Ding, 2010), primarily intended to eliminate the initiator and subsequently induce healing (Ferrero-Miliani et al., 2007). Mechanistically, inflammatory responses are characterized by pain, swelling, redness, heat, and even loss of function of the respective tissue (Takeuchi & Akira, 2010). These are caused, for instance, by the recruitment and accumulation of leukocytes, the secretion of chemokines and cytokines, but also by changes in vascular permeability (Chertov et al., 2000; Ferrero-Miliani et al., 2007). The leukocytes involved, which are recruited to the site of inflammation, include macrophages, monocytes and lymphocytes (**Fig. 5**).

Macrophages recognize foreign structures (antigens) of bacteria and viruses, which are taken up by phagocytosis and undergo intracellular digestion, making them harmless. Macrophages are also able to release cytokines and present antigens to activate other leukocytes (Fujiwara & Kobayashi, 2005). Monocytes are considered to be the main source of pro- and anti-inflammatory cytokines and therefore play an important role in transmitting signals to the

surrounding tissue and in attracting other immunocompetent cells (Wrigley et al., 2011). Lymphocytes can in turn be divided into different classes, with T and B lymphocytes making up the two main classes, both of which are also involved in the above-mentioned release of cytokines (Srikakulapu & McNamara, 2020). While T lymphocytes are activated by antigen-presenting cells, such as macrophages, leading also to the release of cytotoxic proteins that induce apoptosis of the targeted cell, B lymphocytes are involved in the production of antibodies (Burger & Dayer, 2002; Srikakulapu & McNamara, 2020). In addition to the aspects in which the functions of the various cell types differ, they share a common feature, namely the release of pro- and anti-inflammatory cytokines that stimulate or inhibit inflammatory responses. In addition to interleukins (IL), a differentiation is also made between tumor necrosis factors (TNF), interferons (IFN), colony-stimulating factors (CSF) and chemokines, whereby these are primarily intended to recruit leukocytes to the site of inflammation (Turner et al., 2014). While the cause of inflammation is usually neutralized by normal cytokine production through regulation of the immune response, excessive cytokine release can lead to serious consequences such as metabolic disorders, tissue damage, allergies, organ failure and even death (Czaja, 2014; Liu et al., 2016).

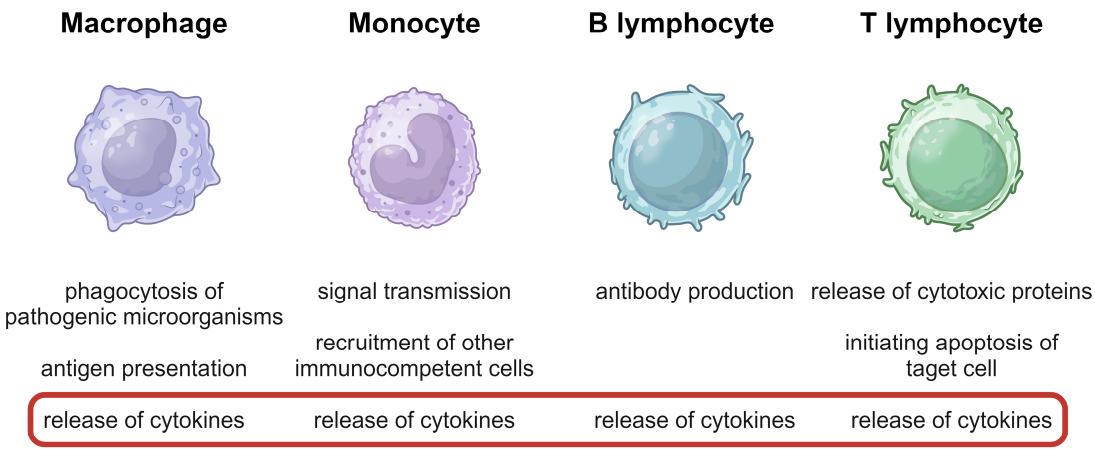


**Figure 5: Illustration of the cell types mainly involved in inflammatory responses.** While macrophages, monocytes and B and T lymphocytes differ in some of their functions, they are all involved in the release of cytokines (Burger & Dayer, 2002; Fujiwara & Kobayashi, 2005; Wrigley et al., 2011; Srikakulapu & McNamara, 2020). Created with BioRender.com.

With regard to infections affecting the stomach, for instance caused by the specialized bacterium *Helicobacter pylori* (*H. pylori*), which has already infected around half of the world's population (Pormohammad et al., 2019), an overproduction of pro-inflammatory cytokines can also be found in the gastric mucosa. In the case of long-term inflammation, immunocompetent cells can cause damage to the mucosa through the formation of reactive oxygen species,

among other factors, which can promote the development of gastritis and consequently also the risk of gastric ulcers and cancer (Crabtree, 1996; McColl et al., 2000; Wei et al., 2024).

### 1.4.1 Underlying cellular signaling pathways

Looking at the intracellular processes that are induced by inflammation, two main signaling pathways can be distinguished that make it possible to map most of the underlying cellular mechanisms, namely the NF-κB and the MAPK signaling pathway (**Fig. 6**) (Chen et al., 2017). PAMPs are recognized via receptors with extracellular domains, such as Toll-like receptors (TLRs), whereby activation of the IκB kinase can be initiated via the adapter molecules TIRAP and MyD88, which are associated with TRAF6, as part of the NF-κB signaling pathway. When bound, IκB prevents nuclear translocation of the two transcription factors RelA and p50 (Kadhim et al., 2001). The phosphorylation of the protein catalyzed by the IκB kinase, followed by intracellular degradation, releases RelA and p50 and causes increased transcription of cytokine-encoding genes in the nucleus (Lawrence, 2009; Hayden & Ghosh, 2012). Binding of pro-inflammatory cytokines to their corresponding receptors, such as IL-17 binding to IL-17R, also leads to activation of IκB kinase via TRAF6, thereby triggering the NF-κB pathway (Dainichi et al., 2019). However, TRAF6 is not only the link to the NF-κB signaling pathway, but can also initiate the activation of MAP kinase kinase kinases (MAPKKKs) as part of the MAPK pathway. The active form of MAPKKKs catalyzes the phosphorylation of MAPKKs, which in turn catalyze the phosphorylation of MAPKs (Dhillon et al., 2007). The MAP kinase group includes numerous transcription factors, such as Erk1/2, JNK, and p38, which, after activation by phosphorylation followed by nuclear translocation, also stimulate the transcription of genes that are finally responsible for the increased cytokine expression (Kim & Choi, 2010). They also induce the expression of the cyclooxygenases (COX-) 1 and 2 (Patel et al., 2012), which form the basis for prostaglandin synthesis. All these enzymes mentioned here are therefore involved in inflammatory processes in the human body and provide potential targets for anti-inflammatory compounds.

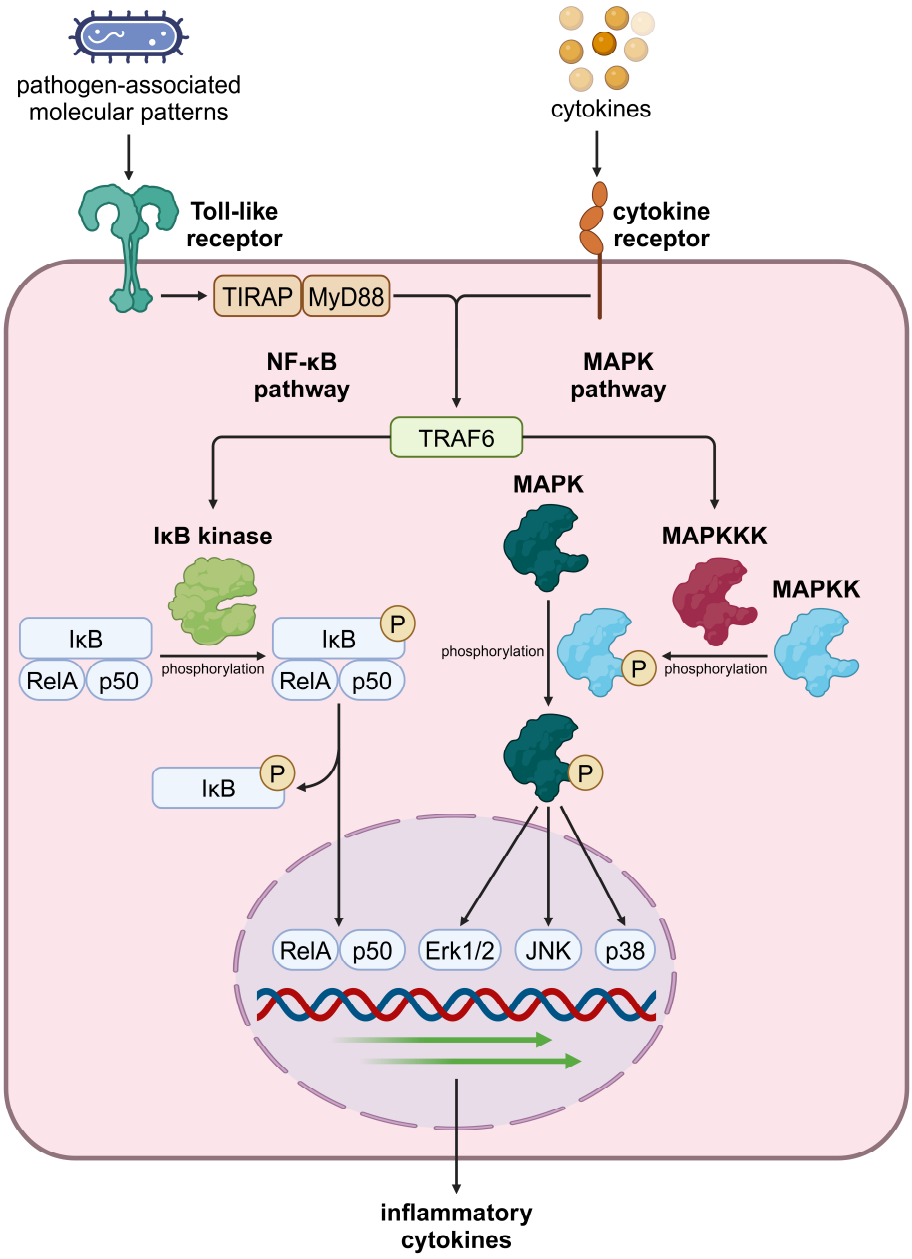


**Figure 6: Schematic overview of the intracellular processes involved in inflammation via the two main signaling pathways NF-κB and MAPK.** The two adapter proteins TIRAP (TIR domain containing adaptor protein) and MyD88 (myeloid differentiation primary response 88) are used to initiate TRAF6 (tumor necrosis factor receptor associated factor 6)-dependent activation of IκB kinase or MAPKKK (mitogen-activated protein kinase kinase kinase). As part of the NF-κB signaling pathway, phosphorylation of IκB by IκB kinase leads to the release of the two transcription factors RelA and p50, which results in nuclear translocation, leading to the expression of relevant cytokine genes. The MAPKKK of the MAPK signaling pathway catalyzes the phosphorylation of MAPKK, which in turn activates MAPK by phosphorylation. MAPKs include Erk (extracellular-signal regulated kinases) 1/2, JNK (c-Jun N-terminal kinases) and p38, which also act as transcription factors. Both signaling pathways increase the expression and ultimately the release of pro-inflammatory cytokines (adapted from Kadhim et al., 2001; Dhillon et al., 2007; Lawrence, 2009; Kim & Choi, 2010; Hayden & Ghosh, 2012; Chen et al., 2017; Dainichi et al., 2019). Created with BioRender.com.

## 1.5 Cellular mode of action of anti-inflammatory compounds

### 1.5.1 Mechanisms of anti-inflammatory medications

The two most well-known anti-inflammatory drugs, ibuprofen and acetylsalicylic acid, are COX inhibitors, which prevent the synthesis of prostaglandin $H_2$ from arachidonic acid by inhibiting the activity of COX-1 and pro-inflammatory cytokine-induced COX-2 (Vane, 1971; Davies, 1998). The hormone cortisol, which is also used as an anti-inflammatory drug, intervenes much earlier in the signaling cascade. On the one hand, cortisol leads to a reduction in the mRNA expression of toll-like receptors and various pro-inflammatory cytokines. On the other hand, the decisive phosphorylation steps in both the NF-κB and MAPK pathways are inhibited. As a result, the transcription factors RelA and p50 are neither released nor can the gene sequences that code for inflammatory cytokines be read if the phosphorylation of MAPK fails to occur (Barnes, 2010; Dong et al., 2018). Acetylsalicylic acid and ibuprofen are synthetically produced drugs that are used to treat inflammation in the human body and are classified as non-steroidal anti-inflammatory drugs (NSAIDs), while cortisol is a hormone that is produced in the adrenal cortex and, like the synthetic prednisone, belongs to the group of steroids. In general, NSAIDs can be divided into four groups (Bacchi et al., 2012; Bindu et al., 2020): while drugs such as ibuprofen and aspirin, but also diclofenac, belong to category I and non-selectively inhibit both COX-1 and COX-2, celecoxib from category II has a preference for inhibiting COX-2, although it still blocks COX-1 at the same time. This selectivity is even more pronounced in group III drugs, for example rofecoxib shows almost no inhibition of COX-1. Sodium salicyclate, which belongs to the last group, is considered to be a weak inhibitor of both cyclooxygenases. At this point it should be mentioned that the bitter-tasting β-glucopyranoside salicin from willow bark (Hänsel, 2010), which is able to trigger selective TAS2R16 activation (Meyerhof et al., 2010), is metabolized in the human liver to salicylic acid (Mahdi, 2014), and is therefore representative of active compounds that are formed during digestion in the human organism. This shows that not only synthetic drugs or the body's own messengers, but also a variety of bioactive compounds that are ingested with foods can act as anti-inflammatory agents.

### 1.5.2 Functional role of food constituents in inflammatory processes

Besides the intake of medication that specifically reduces inflammation in the human body, food constituents can also influence inflammatory responses. In addition to polyphenols, such as epigallocatechin-3-gallate (Ahmad et al., 2000), curcumin (Kumar et al., 1998), and resveratrol (Tiroch et al., 2021), which are found in numerous plants, a variety of terpenoids, such as celastrol (Jin et al., 2002) and kamebakaurin (Lee et al., 2004), are also considered inhibitors within the NF-κB signaling pathway. This means that various types of fruit and vegetables such as apples, cherries, grapes, broccoli, peppers and onions, as well as coffee

and tea, provide some compounds that can potentially minimize inflammatory responses in the body (Nam, 2006).

For primary human gingival fibroblasts (HGF) it could be shown that both the LPS-induced enhancement of *IL-6* and *IL-8* gene expression and an increased secretion of IL-8 could be reduced by treatment with the TAS2R16 agonist salicin. A knock-down by siRNA targeting *TAS2R16* abolished this effect, demonstrating the involvement of TAS2R16 in the reduced secretion of pro-inflammatory cytokines (Zhou et al., 2021). Anti-inflammatory effects of bitter compounds have also been shown with immortalized human gingival fibroblasts (HGF-1). While a reduction in the LPS-induced release of IL-6 and IL-8 in HGF-1 cells by flavanones and erionic acids was demonstrated in 2016 (Walker et al., 2016) without considering the possible involvement of bitter taste receptors in these processes, their role was clarified and validated five years later. Here it was shown that *trans*-resveratrol, which has a bitter taste that can be reduced by the bitter masking-compound HED, can reduce the LPS-induced secretion of IL-6 by HGF-1 cells with the involvement of TAS2R50 (Tiroch et al., 2021). Furthermore, a correlation between the bitter taste perception threshold of various polyphenols, as well as other bitter-tasting food constituents such as L-arginine and caffeine, and their ability to reduce LPS-induced IL-6 release was demonstrated (Tiroch et al., 2023). Those compounds with lower threshold values, such as quinine and sinensetin, led to a stronger inhibition of IL-6 secretion. Although there are other bitter-tasting amino acids and peptides besides L-arginine that can induce physiological reactions via TAS2Rs, a connection between the anti-inflammatory effects of these compound classes and bitter taste receptors has not yet been found (Tagliamonte et al., 2024).

Nevertheless, peptides have become increasingly important in recent years, as their structure is extremely diverse due to their composition of different amino acids, which is why they have a wide range of applications (Bhandari et al., 2020). Of particular interest here is the fact that the digestion of proteins leads to amino acids and peptides that could potentially influence physiological processes such as gastric acid secretion or gastric inflammation. Since bovine milk and dairy products are important components of the diet of a large part of the world's population (Haug et al., 2007), caseins are among the most important animal proteins in the human nutrition. Casein peptides, in particular casokinins, are known to have ACE inhibitory effects (Ibrahim et al., 2016), which lead to a reduction in blood pressure by inhibiting the conversion of angiotensin I to angiotensin II, while casein-derived glycomacropeptides and casoplateins have anti-bacterial (Hayes et al., 2006) and anti-thrombotic effects (Liu et al., 2019), respectively, and casoxins act as opioid receptor agonists (**Fig. 7**) (Teschemacher et al., 1997; Kazimierska & Kalinowska-Lis, 2021). However, the beneficial effects found relate to the direct examination of the peptides and not to possible concentrations that may be generated during the digestion of the corresponding precursor proteins.

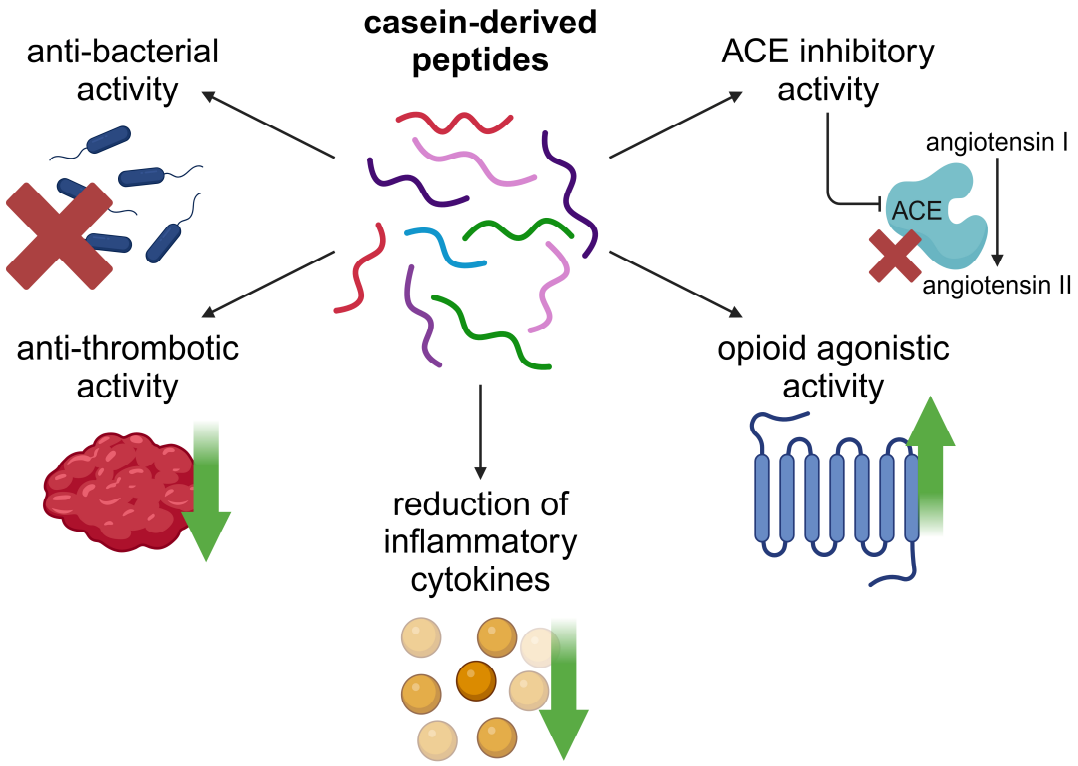


**Figure 7: Overview of the various pathways via which casein-derived peptides can induce anti-inflammatory effects.** In addition to inhibitory effects on ACE (angiotensin-converting enzyme) activity, the release of cytokines and thrombotic activity, agonistic effects on opioid receptors and anti-bacterial effects caused by casein peptides were also demonstrated (Kazimierska & Kalinowska-Lis, 2021). Created with BioRender.com.

With regard to the content of the present work, the anti-inflammatory effects of peptides mediated by TAS2Rs should also be focused, especially in view of the frequently occurring bitter taste of peptides. For instance, the peptide YFYPEL from $\alpha_{S2}$-casein has been shown to reduce LPS-induced *IL-6* mRNA expression in human intestinal epithelial cells (Chen et al., 2023). Casein hydrolysates are known to have anti-inflammatory effects through the downregulation of COX-2, the inhibition of the NF-κB signaling pathway (Nielsen et al., 2012) or a reduction in leukocyte recruitment (Aihara et al., 2009). Peptides of other origins have also shown beneficial effects in terms of inflammation in the past. In addition to whey and fish protein hydrolysates, which also reduced expression of *IL-8* and apoptosis (Marchbank et al., 2009; Piccolomini et al., 2012; Iskandar et al., 2013), hydrolysates of plant proteins such as soy and wheat also revealed such a reduction (Sato et al., 2013) and an inhibition of NF-κB (Mejia & Dia, 2009) and the reduction of oxidative stress (Kovacs-Nolan et al., 2012). However, peptides in general may not only have anti-inflammatory effects, but also pro-inflammatory properties in their function as antigens (Depraetere, 2000). On a mechanistic level, incubation of macrophages with the thaumatin-like protein from *Litchi chinensis* could show enhanced

gene expression of *nitric oxide synthase* and *COX-2* and increased production of TNF-α and interleukin 1β (Chen et al., 2020).

In general, food-derived peptides have been shown to interfere with various cellular signaling pathways. In addition to the aforementioned influences on the expression of inflammatory cytokines or enzymes associated with inflammation and the NF-κB pathway, peptides can also reduce TLR4 expression or inhibit the MAPK pathway (Galland et al., 2022). With all these modes of action, it cannot be ruled out that the taste quality and the associated ability of bitter peptides to activate extra-oral TAS2Rs also play a part in this. In particular, since the two bitter compounds resveratrol (Tiroch et al., 2021) and salicin (Zhou et al., 2021) were able to reduce the LPS-induced expression of pro-inflammatory cytokines via TAS2R50 and TAS2R16, as described above.

## 1.6 Aim of this work and hypotheses

The here presented dissertation hypothesized that bitter-tasting food constituents may have beneficial effects on physiological functions of the stomach with regard to gastric acid secretion, as key mechanism of digestion, and the release of pro-inflammatory cytokines. For their mode of action, it must be ensured that the dietary-derived bitter compounds are released upon gastric digestion to reach their site of action. While bitter taste receptors in the oral cavity are activated directly by bitter-tasting food constituents, activation of gastric bitter taste receptors requires the presence of bitter-tasting compounds during and/or after gastric digestion. So far, very little is known regarding the effects of bitter-tasting peptides that are released from dietary, especially non-bitter-tasting, proteins during gastric digestion.

The aim of this work was to *(i)* identify and characterize bitter-tasting peptides released during gastric digestion of the non-bitter-tasting proteins casein und thaumatin, and *(ii)* to demonstrate their TAS2R-dependent effects on proton secretion, as the fundamental mechanism of gastric acid production, and on anti-inflammatory processes in immortalized human parietal cells. While the majority of previously published work is focused on the interaction of extra-oral TAS2Rs with bitter-tasting compounds that are found in foods, the results of this work were aimed at demonstrating that bitter-tasting peptides, released from non-bitter-tasting dietary proteins, have beneficial effects on mechanisms regulating gastric acid secretion and the *Helicobacter pylori*-evoked release of pro-inflammatory cytokines.

# 2 Materials and Methods

**Cell culture**

Cultivation of immortalized human parietal cells (HGT-1) in DMEM with 10% FBS and 1% penicillin and streptomycin was performed under standard conditions at 37 °C and 5% $CO_2$. More detailed information on this can be found in the integrated publications Richter et al., 2022; Richter et al., 2024a; Richter et al., 2024b and in the work of Liszt et al., 2015.

**Determination of cell viability using the MTT assay**

Cell toxic effects of the compounds used were excluded by incubating the cells for the time periods and in the concentrations relevant for the subsequent experiments. The cells were then treated with MTT (3-(4,5-dimethylthiazol-2-yl)-2,5-diphenyltetrazolium bromide). This yellow tetrazolium salt is reduced to the water-insoluble formazan by NADH and NADPH, which is formed by living cells with normal metabolic activity. Its absorption in DMSO ultimately allows conclusions about the cell viability and therefore the toxicity of the investigated compounds. More detailed information on this can be found in the integrated publications Richter et al., 2022; Richter et al., 2024a; Richter et al., 2024b and in the work of Liszt et al., 2015.

**Measuring the influence of food constituents on proton secretion by means of the pH-sensitive fluorescent dye SNARF™-1**

The determination of the proton secretion by HGT-1 cells was performed by measuring the intracellular pH value. For this purpose, the cells were stained with the pH-sensitive fluorescent dye 5-(and-6)-carboxy SNARF™-1 and then stimulated with the compounds to be examined. Based on the measured changes in the fluorescence intensities, the IPX values were calculated, which allow conclusions to be drawn about secretory activity. More detailed information on this can be found in the integrated publications Richter et al., 2022; Richter et al., 2024a; Richter et al., 2024b and in the work of Liszt et al., 2012; Liszt et al., 2015.

**Measurements of intracellular calcium and sodium concentrations with specific fluorescent dyes**

Analogous to the determination of the proton concentrations, the intracellular calcium and sodium concentrations were measured using the specific fluorescent dyes SBFI and Cal-520, which emit different strong fluorescence intensities depending on the complexation status. More detailed information on this can be found in the integrated publication Richter et al., 2024a.

**Measurement of intracellular sodium concentrations using laser-ablation inductively coupled plasma mass spectrometry (LA-ICP-MS)**

To validate the intracellular sodium concentrations determined by means of the sodium-sensitive fluorescent dye, the sodium content in the cytosol of the HGT-1 cells after treatment with food constituents was also examined by LA-ICP-MS. More detailed information on the parameters used can be found in the integrated publication Richter et al., 2024a.

**Reduction of the expression of specific genes via transient siRNA knock-down approaches**

To detect the involvement of certain receptors or ion channels, the expression of this specific protein was reduced by using small interfering RNA (siRNA). The siRNA was transferred into the cells as a complex with Lipofectamine™ RNAiMAX, whereby the strongest reduction in expression was achieved after 72 hours of transfection. As a negative control, cells were treated analogously with unspecific siRNA (mock-transfection). The cells were then analyzed with the corresponding cell-based assays. More detailed information on this can be found in the integrated publications Richter et al., 2022; Richter et al., 2024a; Richter et al., 2024b and in the work of Zopun et al., 2018b.

**Experiments with TAS2R43 knock-out HGT-1 cells**

To investigate the involvement of the bitter taste receptor TAS2R43, the identical TAS2R43 Homozygous KO clone as in the work of Liszt et al., 2017 was used.

**Real-time quantitative PCR (RT-qPCR)**

To determine the quantitative expression of selected genes, the cells were incubated with the relevant compounds and then lysed. After RNA isolation using silica gel centrifugation columns, any DNA present was digested before the RNA was subsequently transcribed into cDNA using the reverse transcriptase enzyme. Quantitation was done after each PCR doubling step by SYBR, which allowed the calculations for a relative comparison (double delta Ct analysis). More detailed information on this can be found in the integrated publications Richter et al., 2022; Richter et al., 2024a; Richter et al., 2024b and also in the work of Liszt et al., 2017.

**Immunocytochemistry**

To detect the expression of the investigated ion channels at the protein level, they were localized using fluorescence labeling. The exact procedure and the antibodies used can be found in the integrated publication Richter et al., 2024a.

**Quantitation of chemokines and cytokines by means of Enzyme-linked immunosorbent assay (ELISA) and proteome profiler**

The first step in quantifying the chemokines and cytokines investigated was to screen the cell supernatants using the Proteome Profiler Human Cytokine Array Kit according to the manufacturer's protocol to establish a suitable cell model. More specific analyses of the influence of food constituents and the involvement of bitter taste receptors were then carried out by ELISA according to the standard protocol. More detailed information on this can be found in the integrated publication Richter et al., 2024b.

**Quantitative protein determination by Bradford assay**

To determine the physiologically achievable concentrations of thaumatin-derived peptides in the stomach, the protein content of commercially available sweetener tablets was determined using Bradford solution. More detailed information on this can be found in the integrated publication Richter et al., 2024b.

***In vitro* digestion**

For simulated digestion, the intact proteins were first dissolved or suspended in a buffer that mimicked the composition of saliva (SSF). After a five-minute incubation at 37 °C, simulated gastric fluid (SGF), which adjusted the pH to 3 and contained pepsin, was added to the solution. During the continuous incubation at 37 °C, samples were taken at periodic intervals. The resulting peptides were then either purified for the cell-based assays or analyzed by mass spectrometry. The protocol used is mainly based on the work of Brodkorb et al., 2019, whereby more detailed information on this can be found in the integrated publications Richter et al., 2022; Richter et al., 2024b.

***In vivo* digestion**

To validate the functionality of the *in vitro* digestion, the proteins were additionally administered to pigs whose peptide-containing stomach contents were collected after two hours and identified and quantified by mass spectrometry. More detailed information on this can be found in the integrated publications Richter et al., 2022; Richter et al., 2024b.

**Identification, quantitation and validation of the formed peptides using Liquid Chromatography-Mass Spectrometry (LC-MS) approaches**

The samples generated *in vitro* and *in vivo* were analyzed using Liquid Chromatography Time-of-Flight Mass Spectrometry (LC-ToF-MS) and the recorded spectra were compared with spectra generated *in silico* using the MaxQuant software (Cox & Mann, 2008), based on the amino acid sequences of the intact proteins. The peptides identified from the transitions were

then checked for their taste quality using bitter prediction tools and their formation during gastric digestion was validated by targeted Liquid Chromatography Tandem Mass Spectrometry (LC-MS/MS) measurements of the samples and externally synthesized reference peptides. The selected peptides were also quantified by LC-MS/MS. More detailed information on the parameters used can be found in the integrated publications Richter et al., 2022; Richter et al., 2024b and in the work of Sebald et al., 2018; Sebald et al., 2020.

**Sensory trials**

To validate the bitter taste quality of the selected peptides, solutions of these were sensory evaluated. For this purpose, three-alternative forced choice (3-AFC) tests as well as studies on the most dominant taste sensation were carried out. More detailed information on this can be found in the integrated publications Richter et al., 2022; Richter et al., 2024b and in the work of Frank et al., 2014; Meilgaard et al., 2016.

# 3 Results

## 3.1 Integrated publication I: Bitter Peptides YFYPEL, VAPFPEVF, and YQEPVLGPVRGPFPIIV, Released during Gastric Digestion of Casein, Stimulate Mechanisms of Gastric Acid Secretion via Bitter Taste Receptors TAS2R16 and TAS2R38

All references to tables and figures in this section refer to the following publication, which can be found in the appendix to this thesis from page 68, including published supplementary data.

Richter, P., Sebald, K., Fischer, K., Behrens, M., Schnieke, A., & Somoza, V. (2022).
**Bitter Peptides YFYPEL, VAPFPEVF, and YQEPVLGPVRGPFPIIV, Released during Gastric Digestion of Casein, Stimulate Mechanisms of Gastric Acid Secretion via Bitter Taste Receptors TAS2R16 and TAS2R38.**
In: *Journal of Agricultural and Food Chemistry* (Vol. 70, Issue 37, pp. 11591–11602).
American Chemical Society (ACS). https://doi.org/10.1021/acs.jafc.2c05228

In the past, bitter-tasting amino acids such as L-arginine and L-tryptophan have been shown to stimulate the proton secretion by immortalized human parietal cells (HGT-1). In this work, it was hypothesized that bitter peptides generated from non-bitter casein during gastric digestion influence the proton secretion by HGT-1 cells via the involvement of bitter taste receptors (TAS2Rs) (**Fig. S1**). Using an *in vitro* gastric digestion approach, 238 different peptides derived from casein (mixture of $\alpha_{S1}$-, $\alpha_{S2}$-, $\beta_{A1/2}$-, and κ-casein) were identified using LC-ToF-MS and MaxQuant software. An *in vivo* validation in pigs resulted in 270 unique peptides, whereby all of the peptides identified in the *in vitro* approach were also found here. By applying various *in silico* bitter prediction tools, five potential bitter peptides (PVVVPPFLQPEVM from $\beta_{A1/A2}$-$CN_{81–93}$, VAPFPEVF from $\alpha_{S1}$-$CN_{25–32}$, YFYPEL from $\alpha_{S1}$-$CN_{144–149}$, YQEPVLGPVRGPFPIIV from $\beta_{A1/A2}$-$CN_{193–209}$, and YYVPLGTQ from $\alpha_{S1}$-$CN_{165–172}$) were selected and their formation was confirmed both *in vitro* and *in vivo* by targeted proteomics (**Tab. S2**) by comparison with commercially synthesized reference peptides (**Fig. S2**). The resulting peptide concentrations were determined *in vitro* (**Fig. 1A**) with the corresponding release rates (**Fig. 1B**) and *in vivo* (**Fig. 1C**) by LC-MS/MS, whereby the peptide fragments shown in **Fig. S7** were identified for the degradation of peptide YQEPVLGPVRGPFPIIV. Investigations on the bitterness of the peptides showed a stimulation of proton secretion associated with TAS2R-involvement with hormetic concentration dependence in the cellular bitter response assay with HGT-1 cells (**Fig. 2**) and the assignment of the bitter taste quality to all five peptides by sensory tests (**Fig. S5**). For the three peptides with the strongest impact

on the secretory activity of HGT-1 cells (**Fig. S3**), the most effective concentrations were determined (**Fig. S4**) and their time-dependent influence on the gene expression of all 25 human TAS2Rs known to date was investigated (**Fig. 3**, **Tab. S1**, and **Tab. S3**). Since a particular modulatory effect on the abundance of *TAS2R16* and *TAS2R38* mRNA transcripts was observed (**Fig. 4**), their involvement was further investigated by simultaneous treatment of HGT-1 cells with the antagonist probenecid, whereby the bitter peptide-induced stimulation of proton secretion was reduced (**Fig. 5A**). To confirm the TAS2R16 and TAS2R38 dependency, knock-down experiments were performed in which the expression of both receptors was reduced by siRNA (**Fig. S8**) and a reduction of the stimulatory effects on proton secretion by the three bitter peptides was shown in *TAS2R16*kd (**Fig. 5B-D**) and *TAS2R38*kd (**Fig. 5E-G**) cells, respectively, while stimulation with histamine led to the same effect size in all cases (**Fig. S9**).

**Phil Richter:** Writing – review & editing, Writing – original draft, Validation, Methodology, Investigation, Formal analysis, Conceptualization. **Karin Sebald:** Writing – review & editing, Methodology, Conceptualization. **Konrad Fischer:** Writing – review & editing, Methodology, Investigation. **Maik Behrens:** Writing – review & editing, Methodology. **Angelika Schnieke:** Writing – review & editing, Methodology. **Veronika Somoza:** Writing – review & editing, Validation, Supervision, Resources, Project administration, Methodology, Funding acquisition, Conceptualization.

## 3.2 Integrated publication II: Gastric digestion of the sweet-tasting plant protein thaumatin releases bitter peptides that reduce *H. pylori* induced pro-inflammatory IL-17A release via the TAS2R16 bitter taste receptor

All references to tables and figures in this section refer to the following publication, which can be found in the appendix to this thesis from page 96, including published supplementary data.

Richter, P., Sebald, K., Fischer, K., Schnieke, A., Jlilati, M., Mittermeier-Klessinger, V., & Somoza, V. (2024).
**Gastric digestion of the sweet-tasting plant protein thaumatin releases bitter peptides that reduce *H. pylori* induced pro-inflammatory IL-17A release via the TAS2R16 bitter taste receptor.**
In: *Food Chemistry* (Vol. 448, p. 139157).
Elsevier BV. https://doi.org/10.1016/j.foodchem.2024.139157

Recent studies show that bitter taste receptors can also play a decisive role in inflammatory processes. Since anti-inflammatory effects of peptides are also known, it was hypothesized in this project that gastric digestion of thaumatin, a sweet-tasting plant-derived protein, also releases bitter peptides that could have a TAS2R-mediated effect on inflammatory processes by reducing the release of pro-inflammatory cytokines. The *in vitro* gastric digestion of thaumatin with subsequent identification by LC-ToF-MS and MaxQuant resulted in 66 different peptides, which could be assigned to the two thaumatin forms I and II. The number of relevant peptides could be reduced to the three bitter peptides DAGGRQLNSGES (TH-I/II$_{25–36}$), FNVPMDF (TH-I/II$_{108–114}$), and WTINVEPGTKGGKIW (TH-II$_{37–51}$) and the non-bitter reference peptide AAASKGDAAL (TH-I/II$_{15–24}$) by using *in silico* bitter prediction tools (**Tab. S2**). In addition to the formation of the four selected peptides from the *in vitro* approach, validation experiments in pigs resulted in 64 further peptides after two hours of gastric digestion of thaumatin. Targeted LC-MS/MS measurements (**Tab. S1**) allowed a clear comparison of the peptides formed and selected *in vitro* and *in vivo* with purchased synthesized reference peptides (**Fig. S2**). The time-dependent quantitation of *in vitro* gastric digests showed a rapid release of the peptides within the first 15 minutes, whereby the concentrations of DAGGRQLNSGES and WTINVEPGTKGGKIW stabilized and FNVPMDF and AAASKGDAAL were further degraded (**Fig. 2**). Peptide concentrations in the nanomolar range were found in the stomach contents of the pigs (**Fig. 3**). To verify the taste qualities determined *in silico*, the peptides were examined by sensory analysis, confirming the bitterness of DAGGRQLNSGES, WTINVEPGTKGGKIW, and FNVPMDF and the non-bitterness of AAASKGDAAL (**Tab. S3** and **Fig. 1**). In addition, a model system of immortalized human parietal cells (HGT-1) was

established to investigate inflammatory responses caused by incubation with native proteins from *Helicobacter pylori* (*H. pylori*), whereby their cell toxicity was excluded beforehand (**Fig. S3**). This resulted in gene regulation at the mRNA level and the release of various chemokines and cytokines (**Tab. 1**, **Tab. S4**, and **Fig. S4**). While there was a *H. pylori*-induced release of IL-17A, this could be reduced by pre-treatment with the bitter peptides, but not with the non-bitter peptide (**Fig. 5B**). To investigate TAS2R involvement in these processes, HGT-1 cells were treated with the peptides, showing no cytotoxic effects (**Fig. S1**) while the bitter peptides and intact thaumatin led to hormetic stimulation of proton secretion (**Fig. 4A**, **Fig. S5**, and **Fig. S6**), which was not induced by co-treatment with the TAS2R16/38/43 antagonist probenecid (**Fig. S8**). Investigations of mRNA regulation showed a higher expression of *TAS2R16* in HGT-1 cells compared to TAS2R transcripts whose expression was also modulated by the bitter peptides (**Fig. S7**). A concentration dependency was found for *TAS2R16* gene expression induced by thaumatin and the bitter peptides (**Fig. 4B**). Knock-down of *TAS2R16* expression in HGT-1 cells (**Fig. 5A**) resulted in the same *H. pylori*-induced release of IL-17A as in cells treated with the native *H. pylori* proteins alone, regardless of pre-treatment with the bitter peptides (**Fig. 5B**).

**Authorship contribution:**

**Phil Richter:** Writing – review & editing, Writing – original draft, Validation, Methodology, Investigation, Formal analysis, Conceptualization. **Karin Sebald:** Writing – review & editing, Methodology, Conceptualization. **Konrad Fischer:** Writing – review & editing, Methodology, Investigation. **Angelika Schnieke:** Writing – review & editing, Methodology. **Malek Jlilati:** Investigation. **Verena Mittermeier-Klessinger:** Writing – review & editing, Methodology. **Veronika Somoza:** Writing – review & editing, Validation, Supervision, Resources, Project administration, Methodology, Funding acquisition, Conceptualization.

## 3.3 Integrated publication III: Sodium-Permeable Ion Channels TRPM4 and TRPM5 are Functional in Human Gastric Parietal Cells in Culture and Modulate the Cellular Response to Bitter-Tasting Food Constituents

All references to tables and figures in this section refer to the following publication, which can be found in the appendix to this thesis from page 122, including published supplementary data.

Richter, P., Andersen, G., Kahlenberg, K., Mueller, A. U., Pirkwieser, P., Boger, V., & Somoza, V. (2024).
**Sodium-Permeable Ion Channels TRPM4 and TRPM5 are Functional in Human Gastric Parietal Cells in Culture and Modulate the Cellular Response to Bitter-Tasting Food Constituents.**
In: *Journal of Agricultural and Food Chemistry* (Vol. 72, Issue 9, pp. 4906–4917).
American Chemical Society (ACS). https://doi.org/10.1021/acs.jafc.3c09085

To gain a better understanding of the cellular processes underlying the TAS2R-mediated modulation of proton secretion by parietal cells, the role of the transient receptor potential cation channels (TRP)M4 and M5 known from taste cells was investigated in immortalized human parietal (HGT-1) cells. The expression of both sodium-selective ion channels was validated by RT-qPCR at the mRNA level (**Fig. 1**) and by immunofluorescence microscopy at the protein level (**Fig. 2** and **Fig. S2**). The bitter coffee constituent caffeine and the bitter-tasting amino acid L-arginine served as non-cytotoxic (**Fig. S1**) model compounds, with the former leading to a decrease in the cytosolic calcium concentration measured using a calcium-sensitive fluorescent dye (Cal-520), while L-arginine caused an increase in the level of calcium in the cytosol (**Fig. S3A** and **C**). The positive control ionomycin (**Fig. S3B**) and the $M_3$ receptor agonist carbachol (**Fig. S3D**) both led to an increase in the measured fluorescence caused by the calcium-sensitive dye used. The two model compounds induced a concentration-dependent increase in the fluorescence of the sodium-binding dye SBFI in HGT-1 cells (**Fig. 3A** and **Fig. S4**), while histamine had no effect on the fluorescence signal at the concentrations tested (**Fig. 3B**). Simultaneous treatment of the cells with caffeine or L-arginine and the bitter-masking compound HED led in both cases to lower measured intensities than were evoked by the two bitter compounds alone (**Fig. 4A** and **B**). Incubation of TAS2R43ko HGT-1 cells with caffeine also showed a lower increase in sodium-dependent signals compared to wild-type cells (**Fig. 4C**). The application of ICP-MS laser ablation (**Tab. S1**) showed an increase in intracellular sodium concentrations after incubation of the cells with caffeine or L-arginine (**Fig. 5A** and **B**). Replacing the surrounding medium of HGT-1 cells with sodium-free buffer during incubation with the two bitter compounds showed lower

cytosolic sodium concentrations compared to untreated control cells (**Fig. 5C**). While co-treatment of cells with caffeine and the TRPM5 antagonist nicotine resulted in a reduction of the caffeine-induced increase in sodium levels (**Fig. 6A**), co-treatment with triphenylphosphine oxide (TPPO) resulted in higher intracellular sodium concentrations (**Fig. 6B**) than caffeine alone. Treatment of cells with nicotine alone resulted in no change in the intracellular sodium concentration associated with the measured fluorescence intensity, whereas TPPO increased it. Since caffeine triggered a downregulation of both genes after 30 minutes (**Fig. S6**), the involvement of TRPM4 and TRPM5 in the bitter compound-induced stimulation of proton secretion was to be investigated by reducing the mRNA expression of the two ion channels using siRNA (**Fig. S5**). It was found that both the cells with reduced TRPM4 and TRPM5 expression showed a lower increase in intracellular sodium than HGT-1 cells with normal TRP expression (**Fig. 6C**). Carbachol also no longer led to the previously observed sodium influx in the transfected cells (**Fig. 7**). From the perspective of proton secretion, which was induced by both caffeine and L-arginine, simultaneous treatment of the cells with the TRPM4-specific inhibitor 9-phenanthrol or the TRPM5-specific inhibitors nicotine and TPPO led to a reduction in the effect size (**Fig. S7**). Similarly, the stimulation of proton secretion by caffeine was lower in sodium-free buffer, whereas histamine led to the same secretory activity in both this and sodium-containing buffer (**Fig. 5D**). Finally, the effects of the bitter compounds caffeine and L-arginine and the $H_2$ receptor agonist histamine on proton secretion were compared in mock-transfected and *TRPM4*kd and *TRPM5*kd cells. No differentiation was possible when the cells were incubated with histamine, but the lower expression of the two TRP channels led to less proton secretion when the cells were stimulated with caffeine or L-arginine (**Fig. 8**), resulting in the hypothesized signaling pathway (**Fig. 9**).

**Authorship contribution:**

**Phil Richter:** Writing – review & editing, Validation, Methodology, Investigation, Formal analysis, Conceptualization. **Gaby Andersen:** Writing – original draft, Methodology, Conceptualization. **Kristin Kahlenberg:** Validation, Investigation, Formal analysis. **Alina Ulrike Mueller:** Validation, Investigation, Formal analysis. **Philip Pirkwieser:** Validation, Methodology, Investigation, Formal analysis. **Valerie Boger:** Validation, Investigation, Formal analysis. **Veronika Somoza:** Writing – review & editing, Validation, Supervision, Resources, Project administration, Methodology, Funding acquisition, Conceptualization.

**Phil Richter** and **Gaby Andersen** contributed equally to this work.

# 4 Discussion

Previous studies have shown that bitter-tasting food constituents, such as polyphenols and amino acids, stimulate proton secretion by immortalized human parietal (HGT-1) cells with the functional involvement of TAS2Rs. Similarly, the reduced release of pro-inflammatory cytokines by the interaction of bitter-tasting compounds and TAS2Rs is known. However, potential structural changes associated with digestion and metabolization were neglected. But especially proteins that do not yet have a bitter taste in the oral cavity during food ingestion might be cleaved into bitter peptides during gastric digestion, which could then interact with extra-oral TAS2Rs and thereby stimulate proton secretion and reduce the release of cytokines from HGT-1 cells. In addition to the tasteless milk protein casein, the plant-derived protein thaumatin was selected for this work, as society's demand for substitutes for animal products and protein sources from plant sources is increasing in view of climate change and for health reasons (Henchion et al., 2017).

## 4.1 Breakdown of the milk protein casein during gastric digestion led to the formation of bitter peptides that stimulated the proton secretion by HGT-1 cells with the involvement of TAS2R16 and TAS2R38

Although the milk protein casein does not cause a bitter taste, its hydrolysates often have a bitter off-taste (Sparrer & Belitz, 1975), which is why it was hypothesized that the cleavage of proteins during gastric digestion releases bitter peptides. This would mean that structural changes catalyzed in the stomach by amide-cleaving enzymes such as pepsin release bitter peptides from food proteins, which are then able to influence gastric proton secretion via bitter taste receptors.

To investigate this hypothesis, bovine casein, a mixture of the proteins $\alpha_{S1}$-, $\alpha_{S2}$-, β-, and κ-casein (Gigli, 2016), was subjected to an *in vitro* digestion approach. The selected digestion method has been adapted from the Nature protocol published by Brodkorb et al. in 2019, in which no validation by the precise identification and quantitation of the resulting peptides had been carried out, but rather a comparison of the peptide patterns for κ-casein found *in vitro* or *in vivo* in pigs. As described in the first integrated publication (Richter et al., 2022), samples were taken at different time points during the simulation of gastric digestion at acidic pH with the enzyme pepsin at 37 °C to ensure the identification of the resulting peptides over the entire digestion process of up to six hours. Mass spectra were recorded for the peptides using LC-ToF-MS, which were then compared with spectra generated *in silico* using the MaxQuant software (Cox & Mann, 2008). The software utilizes the classic known fragmentation pattern of peptides and calculates all mass spectra for potential peptides based on the known amino acid sequence of the intact proteins ($\alpha_{S1}$- (P02662), $\alpha_{S2}$- (P02663), β- (P02666) and κ-casein

(P02668); The UniProt Consortium, 2021). After comparison with the spectra actually recorded, by applying this software, the Andromeda score was calculated, which reflects the probability of the presence of a particular peptide sequence. In this work, the following sequences with an Andromeda score above 150 indicating a highly probable formation during *in vitro* digestion, were identified: FVAPFPEVF ($\alpha_{S1}$-$CN_{24–32}$), INNQFLPYPYYAKPAA (κ-$CN_{51–66}$), LTDVENLHLPLPLL ($\beta_{A2}$-$CN_{127–140}$), PVVVPPFLQPEVM ($\beta_{A1/A2}$-$CN_{81–93}$), TDVENLHLPLPLL ($\beta_{A2}$-$CN_{128–140}$), TDVENLHLPLPLLQS ($\beta_{A2}$-$CN_{128–142}$), VAPFPEVF ($\alpha_{S1}$-$CN_{25–32}$), YFYPEL ($\alpha_{S1}$-$CN_{144–149}$), YQEPVLGPVRGPFPIIV ($\beta_{A1/A2}$-$CN_{193–209}$), YTDAPSF ($\alpha_{S1}$-$CN_{173–179}$), and YYVPLGTQ ($\alpha_{S1}$-$CN_{165–172}$). A comparison of these with the literature revealed distinct physiological activities in organs and tissues beyond the stomach. In addition to stimulating the secretion of the satiety hormones CCK and GLP-1 (Santos-Hernández et al., 2018), some of the identified peptides also exhibit ACE-inhibitory and antihypertensive activities (Del Contreras et al., 2009; Dallas et al., 2016; Corrons et al., 2017). Anti-inflammatory and anti-bacterial effects have also been attributed to some of these peptides (Rizzello et al., 2005; Chen et al., 2023).

However, the existing literature did not describe any connection between these described effects and the involvement of TAS2Rs. To close this gap, and since the focus of this work was on the bitter taste receptor-mediated effects of peptides, three prediction tools were used in the following to limit the subsequent experiments to potentially bitter peptides. Ney's calculation, established in 1971 (Ney, 1971), is based on the hydrophobicity of the individual amino acids, assuming that hydrophobic side chains tend to cause bitter taste sensations, while hydrophilic residues do not cause a bitterness. Furthermore, the tools BERT4Bitter (Bidirectional Encoder Representations from Transformers) and iBitter-SCM (scoring card method) enable more complex forecasting using automated computer models (Charoenkwan et al., 2020; Charoenkwan et al., 2021).

The bitterness of the peptides PVVVPPFLQPEVM ($\beta_{A1/A2}$-$CN_{81–93}$), VAPFPEVF ($\alpha_{S1}$-$CN_{25–32}$), YFYPEL ($\alpha_{S1}$-$CN_{144–149}$), YQEPVLGPVRGPFPIIV ($\beta_{A1/A2}$-$CN_{193–209}$), and YYVPLGTQ ($\alpha_{S1}$-$CN_{165–172}$) classified as potentially bitter by means of these tools was confirmed by a 3-alternative forced choice (AFC) sensory trail with untrained panelists. This showed that the bitter taste of peptides can be reliably predicted by combining different bitterness prediction tools and, even more important, that the gastric digestion of non-bitter-tasting proteins, in this case casein, can lead to the release of bitter-tasting peptides in the stomach.

To monitor the time course of this release and the possible further peptide degradation, the samples obtained by *in vitro* digestion were subjected to quantitation by LC-MS/MS. This showed a rapid formation of the peptides PVVVPPFLQPEVM, YFYPEL, YYVPLGTQ, and YQEPVLGPVRGPFPIIV within the first hour, while the latter was degraded into smaller peptides and amino acids in the further course of digestion. Notably, the concentration of

VAPFPEVF increased continuously throughout the entire process. However, the concentration of all peptides examined exceeded 200 µM only for a short time, which is why only concentrations of a maximum of 200 µM were considered for follow-up *in vitro* experiments. These findings are also consistent with theoretical calculations of the maximum concentrations achievable in the stomach on the basis that one liter of cow's milk contains about 27.5 g of casein (Bijl et al., 2013), the amounts of which are in turn distributed among the various subforms $\alpha_{S1}$-, $\alpha_{S2}$-, β-, and κ-casein (Davies & Law, 1977).

In addition to validating the sequences output by MaxQuant using synthesized reference peptides, the peptides produced by *in vitro* digestion were validated by means of an *in vivo* approach with pigs. Here, the strong similarity of the gastrointestinal tract of pigs and humans was utilized to reproduce digestion in the human body in as much detail as possible (Patterson et al., 2008). Two hours after administration of the intact casein, the stomach contents of the animals were collected and analyzed analogously to the *in vitro* samples via LC-ToF-MS and quantified via LC-MS/MS. Identification using MaxQuant showed high concordance with the peptides formed *in vitro*, as all previously identified peptides were found. Targeted proteomics was used to validate the formation of the five selected bitter peptides of the *in vitro* approach with commercially synthesized reference compounds as well as with the peptides formed *in vivo*. The quantitation of the peptides in the *in vivo* digests revealed lower concentrations compared to the *in vitro* samples. The reasons for this might be the varying stomach volumes of the biological systems and incomplete uptake of the casein administered, as it is difficult to ensure complete suspension in this approach. The solution to this issue might be a gavage, but this involves a major intervention and makes the biological system more artificial.

The effects of casein and the validated bitter-tasting peptides on secretory activity were then investigated in cell experiments. In the past, a TAS2R-dependent stimulation of proton secretion by HGT-1 cells has been shown for various bitter compounds, such as caffeine and different polyphenols (Liszt et al., 2018; Sterneder et al., 2021; Tiroch et al., 2021). The influence of caffeine on proton secretion by HGT-1 cells as a surrogate model of human parietal cells could be validated in a human intervention study (Liszt et al., 2017), which makes the HGT-1 cell model a suitable bitter response assay without exposing panelists of sensory trials to potentially toxic compounds (Liszt et al., 2015).

An impact on secretory activity of HGT-1 cells was also shown for other bitter tastants, such as L-amino acids. For instance, incubation of HGT-1 cells with the bitter-tasting amino acid L-arginine led to a stimulation of proton secretion via TAS2R1, which could be reduced by the bitter-masking compound HED (Stoeger et al., 2018; Stoeger et al., 2020). This suggests that bitter peptides may also influence proton secretion with the involvement of TAS2Rs. Incubation of the cells with the mixture of intact caseins, as present in bovine milk, reduced proton secretion compared to untreated control cells (Richter et al., 2022). This means that the intact

protein reduced the secretory activation of the immortalized parietal cells, while the hydrolysate generated by the *in vitro* digestion as a mixture of different peptides caused a stimulation of precisely this secretion. This was further evidence, that the hypothesized change in the taste quality of a food protein during digestion may also alter the effect on proton secretion caused by that compound.

The observed stimulatory effect could also be attributed to the identified bitter peptides. Each of the five bitter peptides led to a significant stimulation of proton secretion within the concentration range of 0.01 - 200 µM. The concentration dependency found here resulted in a hormetic pattern in which a medium concentration triggered the maximum effect in terms of stimulation, while higher or lower concentrations caused less strong effects or no effects at all. Such a concentration curve has also been shown in the past for the serotonin-induced modulation of proton secretion by HGT-1 cells. Here, a concentration of 0.1 µM led to the strongest effect, while higher concentrations (≥ 0.5 µM) did not allow any differentiation from untreated control cells (Holik et al., 2021). There are several possible reasons for this. For instance, the bitter peptides could not only modulate proton secretion, but also influence other proteins involved in cell signaling, such as peptide transporters, at higher concentrations. As the peptide concentrations in the stomach rarely exceed 200 µM under physiological conditions, these effects were neglected in the further course.

In the previously described bitter compound-induced modulations of proton secretion, a functional involvement of bitter taste receptors was present in all cases. To be able to attribute a functional involvement of TAS2Rs in the bitter peptide-mediated stimulation of secretory activity, the influence on gene expression of the three casein-derived bitter peptides that elicited the strongest effect was examined. Incubation of HGT-1 cells with the peptides YFYPEL, VAPFPEVF and YQEPVLGPVRGPFPIIV at the most effective concentrations, as determined by curve fit calculations, resulted in the regulation of various TAS2Rs at the mRNA level at the investigated time points between 15 minutes and two hours. Although these data cannot be used to determine whether stronger or weaker mRNA expression correlates with the protein level, the involvement of a specific TAS2Rs in cellular signaling pathways can possibly be deduced from the altered frequency of transcripts. This does not necessarily have to be a ligand-receptor-interaction leading to activation, as a role of these receptors as signaling proteins within complex cellular responses cannot be excluded.

Nevertheless, it was evident from the gene regulation data that the expression of *TAS2R16*, *TAS2R38* and *TAS2R41* in particular was affected across the different time points and peptides. Considering the fact that *TAS2R41* was expressed significantly lower by HGT-1 cells than *TAS2R16* and *TAS2R38*, a closer look at the transcript levels for *TAS2R16* showed a upregulation after treatment with each of the identified peptides at all time points. A similar picture resulted when looking at TAS2R38. Here, there was no significant regulation for peptide

VAPFPEVF at two time points, while all other data points also showed an upregulation of the TAS2R38-encoding transcripts. It was concluded that the treatment of the cells with the bitter peptides caused a change in the gene expression of *TAS2R16* and *TAS2R38*, which ultimately indicated the involvement of these two receptors in the cellular response to the bitter peptides. So far, no specific peptides were known to interact with TAS216 and TAS2R38, as experience has shown that the agonists of these two highly selective bitter taste receptors are mainly limited to β-glucopyranosides, phenylthiocarbamide (PTC) and 6-propyl-2-thiouracil (PROP), respectively (Meyerhof et al., 2010). Nevertheless, calcium mobilization has been found in the past in TAS2R16 overexpressing HEK293 cells treated with casein hydrolysates (Maehashi et al., 2008). For TAS2R38, there are also first indications showing a connection with amino acids, as there are evidences that the bitter taste of L-arginine could be TAS2R38-mediated (Stoeger et al., 2020).

Evidence of the functional involvement of receptors in certain cellular responses could be obtained, for instance, by using known inhibitors or antagonists. A suitable antagonist for both, TAS2R16 and TAS2R38, is the compound probenecid (Greene et al., 2011). In the past, it has been shown that in TAS2R16 overexpressing HEK-293T cells, calcium mobilization triggered by the specific agonist salicin could be reduced by pre-incubation with probenecid. The same could also be shown for the activation of TAS2R38 overexpressing cells with PROP or PTC. Apart from cellular assays, a reduced perception of bitterness triggered by salicin, could also be determined by the prior administration of probenecid to panelists in sensory trails.

To investigate this inhibition approach in the HGT-1 cell model to measure the stimulatory properties of bitter-tasting peptides on proton secretion in this work, the cells were again treated with the three most active bitter peptides at the determined most effective concentrations. Incubation without the presence of probenecid showed the previously observed stimulation of proton secretion, whereas co-treatment with probenecid prevented the bitter peptide-induced stimulation of secretory. Therefore, it was shown that simultaneous incubation of the cells with the identified peptides and a known antagonist of TAS2R16 and TAS2R38 no longer induces stimulation, suggesting that the two receptors indeed played a role in the cellular response to the bitter peptides.

One issue with pharmacological inhibition, however, is the occurrence of off-target effects, which can never be excluded. Probenecid, for example, also prevents TAS2R43-dependent activation by aloin (Greene et al., 2011), or is known as an inhibitor of the organic anion transporters 1 and 3 (Hagos et al., 2017) and as an activator of the transient receptor potential channel V2 (Bang et al., 2007). In contrast to the use of inhibitors, much clearer results can be impacted by knock-down experiments. For this purpose, specific RNA fragments, so-called small interfering RNA (siRNA), are introduced into the cell, which selectively bind to mRNAs coding for a specific gene and ultimately induce their intracellular degradation (Dana et al.,

2017). In this way, the gene expression of selected genes can be specifically reduced to analyze the consequences of the absence of the corresponding protein. To establish the knock-down approach in this work, the expression of the very well expressed *MAPK1* gene was first reduced in the HGT-1 cells. The strongest downregulation was observed three days after transfection with lipofectamine. The investigation of two different siRNA sequences that target different positions of the TAS2R16- or TAS2R38-encoding mRNA showed different efficiencies, whereby the siRNA that caused the strongest downregulation after three days was chosen for the subsequent experiments. Incubation of HGT-1 cells with reduced *TAS2R16* or *TAS2R38* expression showed a reduction in secretory activity of HGT-1 cells induced by the three bitter peptides. Since the cells are in a harsh environment during transfection, it has to be excluded that the transfection process itself has any influence on the cellular proton secretion. For this purpose, a mock-transfection was carried out in which the cells are treated under identical conditions but with an untargeted, random siRNA that does not match any corresponding mRNA sequence inside the cell. Treatment of these mock-transfected cells with YFYPEL, VAPFPEVF, and YQEPVLGPVRGPFPIIV showed an identical response compared to non-transfected cells in terms of stimulation of proton secretion. This experiment ruled out the possibility that the cells' proton secretion properties were influenced by the transfection process. The fact that the proton secretion by HGT-1 cells is also stimulated by the neurotransmitter histamine (Yao & Forte, 2003; Liszt et al., 2017) makes it possible to control the TAS2R-independent functionality of proton secretion after successful reduction of TAS2R16- or TAS2R38-expression by transfection. In this control experiment, it was shown that the same histamine-induced stimulation of proton secretion occurs in non- and mock-transfected cells as well as in cells with reduced TAS2R16- or TAS2R38-expression, demonstrating that the underlying signaling pathway was not affected by any of the applied transfections, except for the expression of the respective bitter taste receptor.

The final knock-down experiments clearly demonstrated that both TAS2R16 and TAS2R38 are involved in the bitter peptide-induced stimulation of secretory activity of immortalized human parietal cells. Consequently, it cannot be ruled out that all the effects found in earlier studies, such as the secretion of satiety hormones (Santos-Hernández et al., 2018) and anti-hypertensive activities (Del Contreras et al., 2009), do not also result from the involvement of bitter taste receptors. Furthermore, it cannot be denied that the anti-inflammatory effects of peptides in particular may also be TAS2R-dependent, as current studies increasingly suggest that bitter taste receptors in extra-oral tissues may have a significant influence on the reduced release of pro-inflammatory cytokines (Tiroch et al., 2021; Zhou et al., 2021; Tiroch et al., 2023). Especially for YFYPEL, which was identified as bitter casein-derived peptide in this thesis, anti-inflammatory effects could be shown last year by reducing the LPS-induced stimulation of *IL-6* gene expression (Chen et al., 2023).

## 4.2 Bitter-tasting thaumatin-derived peptides stimulated proton secretion and reduced *H. pylori*-induced IL-17A release of HGT-1 cells via TAS2R16

After the tasteless milk protein casein was shown to be broken down by digestion into bitter-tasting peptides that stimulate the secretory activity of HGT-1 cells, the following study focused on the sweet-tasting thaumatin. To meet the increased demand for plant-derived foods, this protein was selected to investigate the TAS2R-dependent effects of its cleavage products on proton secretion and the release of pro-inflammatory cytokines in the stomach.

Thaumatin is a mixture of two proteins (thaumatin I (P02883) and II (P02884); The UniProt Consortium, 2021), which occurs naturally in the plant *Thaumatococcus daniellii*, tastes about 2000 times sweeter than sucrose (Zeece, 2020b) and has therefore been approved as a sweetener (E 957) in the EU since 1994 (Das Europäische Parlament und der Rat der Europäischen Union, 1994). Due to the substantially lower amount of thaumatin that has to be used to achieve the same sweetening power as sucrose, the energy content is minimized to 0.05% in the context of the sugar used in the sweetened foods or beverages.

To investigate which peptides are formed during gastric digestion of the two thaumatin forms I and II, the two digestion approaches were used in the first step of the second integrated publication (Richter et al., 2024b), analogous to the models established with casein. *In vitro* digestion under acidic conditions with pepsin resulted in the release of 66 different peptides over a screened time period of six hours. The spectra were also recorded using LC-ToF-MS and the peptides were identified using MaxQuant (Cox & Mann, 2008). In contrast to the various casein forms, which differ fundamentally in their amino acid composition, the two thaumatin forms studied only vary at four positions (46N>K; 63S>R; 67K>R; 76R>Q) (The UniProt Consortium, 2021). This resulted in eight peptides that could be attributed specifically to the sequence of thaumatin I and five to that of thaumatin II, while the release of the remaining 53 peptides was possible from both forms. By applying the proven bitter prediction tools of Ney (Ney, 1971), BERT4Bitter (Charoenkwan et al., 2021) and iBitter-SCM (Charoenkwan et al., 2020), the set of potentially bitter peptides was narrowed down to DAGGRQLNSGES (TH-I/II$_{25-36}$), FNVPMDF (TH-I/II$_{108-114}$), WTINVEPGTKGGKIW (TH-II$_{37-51}$). To carry out control experiments, peptide AAASKGDAAL (TH-I/II$_{15-24}$), which was classified as non-bitter by the *in silico* tools, was also included in the follow-up experiments.

The formation of the peptides under *in vivo* conditions was validated by experiments with pigs to reproduce human gastric digestion as authentically as possible. Among the 68 peptides that were identified in the stomach contents of the pigs after two hours of thaumatin digestion using LC-ToF-MS and MaxQuant (Cox & Mann, 2008) were the three selected bitter peptides DAGGRQLNSGES, FNVPMDF, and WTINVEPGTKGGKIW as well as the non-bitter peptide AAASKGDAAL. Overall, a comparison of the peptides found here with the 66 sequences identified in the *in vitro* samples resulted in a match of 83.7 ± 1.8%, whereby the *in vitro* model

of digestion developed by Brodkorb et al. once again showed a very good and comparable performance. In addition to the factor of the Andromeda score calculated by MaxQuant as a validation parameter, which indicates the probability with which the mass transitions found match the spectra generated *in silico* on the basis of the amino acid sequences, commercially synthesized reference peptides of the corresponding sequences were acquired. The actual presence of the selected peptides in the digestion samples generated *in vitro* and *in vivo* was ensured by using a targeted LC-MS/MS approach. By comparing the MRM transitions and the retention times, it was finally possible to validate that the selected peptides DAGGRQLNSGES, FNVPMDF, WTINVEPGTKGGKIW, and AAASKGDAAL are formed during the gastric digestion of thaumatin.

While the majority of the peptides formed during the digestion of casein had already been shown to have bioactive effects, such as stimulating the secretion of the satiety hormones (Santos-Hernández et al., 2018) and ACE inhibition (Corrons et al., 2017), no match was found in literature for the four thaumatin peptides identified in this thesis, meaning that the structures and potential effects were still completely unknown. Only for some thaumatin-like proteins, physiological functions could be identified in the past. For instance, thaumatin-like protein 1a found in *Annurca* apple was shown to have an inhibitory effect on acetyl cholinesterase, monoamine oxidase A, and A$\beta_{1\text{-}40}$ aggregation, which are key components in Alzheimer's and Parkinson's disease (D'Errico et al., 2024). In addition, antifungal activities and affinities for carbohydrate binding, but also pro-inflammatory properties were observed for thaumatin-like peptides in the past (Liu et al., 2010; Chen et al., 2020).

Furthermore, prior to the thesis presented here, no information on specific taste qualities of the thaumatin-derived peptides was known. For this reason, the bitterness predicted by the used *in silico* tools was to be confirmed in a further sensory trail, in which the panelists were asked to determine the most dominant taste quality (bitter, sweet or other). This showed that the three peptides DAGGRQLNSGES, FNVPMDF, and WTINVEPGTKGGKIW previously classified as bitter actually had a bitter taste, while no clear assignment to a bitter taste was possible for AAASKGDAAL. In addition, the already known sweet taste of thaumatin was also confirmed in this sensory test, whereby a bitter aftertaste, which was also previously described in the literature, was also detected (Healey et al., 2017). This once again confirmed the hypothesis stated at the beginning of this thesis about the change in taste quality of food constituents during digestion using another example.

To investigate the bioactivity of the validated peptides in the following, the physiologically achievable concentrations of these were determined. However, the strong sweetness of thaumatin described at the beginning and the associated sparing use of the protein in food limits the concentration of the resulting peptides that can be achieved in the organism after habitual food intake, although the bioactivity of the peptides in the present work was not

dependent on absorption or other parameters, as the direct effects on the stomach cells were investigated. The time-dependent quantitation of the peptides generated *in vitro* again showed a rapid cleavage of thaumatin and the corresponding release of the selected peptides within the first 15 minutes. The concentrations found for the peptides DAGGRQLNSGES and WTINVEPGTKGGKIW were stable around 300 and 200 µM, respectively, for the entire course of gastric digestion up to six hours, while for FNVPMDF and the non-bitter AAASKGDAAL a degradation of both peptides was detectable within the first hour. The targeted LC-MS/MS measurements of the samples obtained by *in vivo* digestion in pigs showed significantly lower concentrations in the nanomolar range after two hours, as was already observed for the release of the casein peptides. Considering the release rates of thaumatin peptides accessible in this way, it was possible to determine that peptide concentrations in the single-digit nanomolar range can be achieved in the stomach after ingestion of a typical amount of thaumatin, for example through sweetener tablets. To investigate the effect of the peptides on inflammatory processes, a suitable cell model was established.

As part of this work, a suitable cell model was established, to investigate the effect of the bitter-tasting peptides in the context of inflammatory processes, that have already been modulated by bitter food constituents in the past (Tiroch et al., 2023). Here, immortalized human parietal cells (HGT 1), for which no information on the release of pro-inflammatory signaling proteins was known, were also used to analyze inflammatory processes in the stomach. To obtain information on the mRNA transcripts of known chemo- and cytokines, the influence of a mixture of native *Helicobacter pylori* proteins on the gene regulation of HGT-1 cells was investigated. This led to the regulation of a variety of chemokines and cytokines that are already associated with *H. pylori* infections in the literature (Moss et al., 1994; Yang et al., 2024). To be able to derive an actual physiological effect, the focus of this work was primarily on the release of signaling proteins at the protein level. In addition to the increased release of interleukins (IL)-1β, -6, -11, -15, -16, -17A, -19, -31, and -34 by the treated cells, increased concentrations of C-C and C-X-C motif chemokine ligands CCL19, CCL20, CXCL5, CXCL10, and CXCL11 were also determined in the cell supernatants. Since the amount of bound IL-17A was highest in the experiments and this interleukin has been linked to *H. pylori*-mediated gastric carcinogenesis in previous studies (Kang et al., 2023), the effects of the peptides on *H. pylori*-induced IL-17A release were investigated in the following.

A one-hour pre-incubation of HGT-1 cells with the non-bitter-tasting peptide AAASKGDAAL and subsequent incubation with the *H. pylori* native proteins resulted in the same IL-17A release as in cells treated with *H. pylori* alone. In contrast, pre-treatment of the cells with the previously determined bitter peptides DAGGRQLNSGES, FNVPMDF, and WTINVEPGTKGGKIW led to a strong reduction of the *H. pylori*-induced IL-17A release. The fact that the three bitter peptides led to a reduction in the *H. pylori*-induced release of the

pro-inflammatory cytokine IL-17A and consequently show anti-inflammatory effects, while the non-bitter-tasting peptide showed no influence, suggests that TAS2Rs are also involved here. This is not the first known case of anti-inflammatory effects of bitter compounds mediated by TAS2Rs. In a cell model with human gingival fibroblasts, a correlation between the bitter taste of food constituents such as quinine, epigallocatechin gallate, sinensetin, L-arginine and their ability to reduce the LPS-induced release of the pro-inflammatory cytokine IL-6 has been shown in the past (Tiroch et al., 2023). Previously, it was demonstrated that bitter-tasting *trans*-resveratrol, a polyphenol, also has a reducing effect on the release of IL-6 from human gingival fibroblasts, whereby a crucial involvement of TAS2R50 could be verified (Tiroch et al., 2021). TAS2R16 is a candidate bitter taste receptor that already played a major role in the work with the bitter casein peptides. This receptor was also shown to be involved in anti-inflammatory reactions, in that salicin, a known specific TAS2R16 agonist, led to a reduction in the LPS-induced release of IL-8 (Zhou et al., 2021). Whether the thaumatin peptide-mediated effects are also based on the involvement of specific TAS2Rs was investigated by further studies of the four peptides.

In the experiments with the casein peptides, the cellular bitter response assay has proven its worth in identifying compounds that influence the proton secretion by HGT-1 cells and potentially evoke a bitter taste. Taking into account the previously determined concentrations that are achievable under physiological conditions in the human stomach, the bitter peptides DAGGRQLNSGES, FNVPMDF, and WTINVEPGTKGGKIW showed a stimulation of the secretory activity of the cells. As already observed with the casein peptides, a hormetic concentration dependence could be deduced. Interestingly, the concentration range determined (5 - 30 pM), in which the thaumatin peptides caused the strongest effect with regard to the stimulation of proton secretion, was lower than the most effective concentrations determined for the casein peptides (0.03 - 17.5 µM). In comparison with the minimum concentrations of established bitter compounds that led to calcium mobilization in TAS2R-overexpressing HEK-293T cells, the concentrations determined for casein peptides are comparably low, such as for denatonium benzoate, which induces an activation of TAS2R47 from a concentration of 0.03 µM, or quinine, which shows an interaction with TAS2R4/7/10/14/39/40/43/44/46 at 10 µM (Meyerhof et al., 2010). The even lower most effective concentrations of the thaumatin peptides in the picomolar range are below the lowest concentration of a compound for which calcium mobilization by TAS2R activation has been demonstrated to date, namely 1.3 nM aristolochic acid leads to activation of TAS2R43 (Meyerhof et al., 2010). However, it should be emphasized at this point that the physiological effects of bitter compounds involving TAS2Rs, such as modulation of inflammation, might not be solely based on traditional ligand-receptor interactions. The participation of TAS2Rs in other

cellular processes is also conceivable, which is why a comparison with known minimum activation concentrations and $EC_{50}$ values should be treated with caution.

Independently of this, the non-bitter peptide AAASKGDAAL did not affect the stimulation of proton secretion by HGT-1 cells observed for the bitter peptides in the concentration range tested. A connection can therefore already be found here between the anti-inflammatory abilities of bitter peptides and their influence on proton secretion. Unlike intact casein, which had no effect, undigested thaumatin also led to a stimulation of secretory activity. One explanation for this could be the possible spatial accessibility of an amino acid sequence in the complex-folded protein for bitter taste receptors, which could also explain the bitter aftertaste of sweet-tasting thaumatin. Thaumatin would not be the first sweetener to interact with TAS2Rs in addition to sweet receptors (TAS1R2/TAS1R3), which is known for acesulfame K and saccharin, for instance, which activate TAS2R43 and TAS2R44 (Meyerhof et al., 2010). Furthermore, an involvement of the receptors TAS1R1 and TAS1R3, which are both expressed by HGT-1 cells and could have an influence on the proton secretion by the cells, cannot be ruled out. It has been shown in the past that the two sweeteners cyclamate and acesulfame K can also modulate the cellular secretion of protons with the contribution of TAS1R3 (Zopun et al., 2018b).

With regard to the involvement of bitter taste receptors in the observed physiological outcomes, the effects of bitter-tasting thaumatin-derived peptides on the gene regulation of TAS2Rs were investigated analogously to the approach with casein (Richter et al., 2022). Again, there was a significant modulation of the mRNA expression of the receptors *TAS2R16*, *TAS2R38* and *TAS2R41*. In the following, the focus was placed on the role of *TAS2R16*, as it is expressed more strongly than *TAS2R41*, as already mentioned and also than *TAS2R38* in the selected cell model. The analysis of the concentration-dependent changes in the abundance of the *TAS2R16* transcripts after treatment with the respective peptides showed a correlation with the effects of these on the proton secretion by HGT-1 cells. The correlations found were not equally pronounced for all compounds investigated, as both the bitter-tasting peptide WTINVEPGTKGGKIW and the sweet-tasting protein thaumatin also increased the expression of *TAS2R16* to a particularly high level at concentrations that exhibited strong secretion-promoting properties, while the opposite effect was observed for DAGGRQLNSGES. In this case, lower concentrations led to a reduced influence on the proton secretion by HGT-1 cells, but at the same time to a stronger downregulation of *TAS2R16* at the mRNA level. A hybrid of both influences was observed for the third bitter peptide FNVPMDF. Here, lower concentrations also led to stronger stimulation of proton secretion with a simultaneous reduction in the *TAS2R16* mRNA transcripts present, but higher concentrations, which no longer caused a significant increase in secretory activities due to the hormetic course of the concentration dependence, were able to cause a strong upregulation of *TAS2R16*. This

demonstrates that different compounds, which all have a bitter taste and comparable effects on proton secretion but differ structurally, can elicit different responses in gene regulation. Both upregulation and downregulation may therefore indicate the involvement of a specific receptor protein in cellular processes, while the participation of a receptor cannot be ruled out if the transcript level in question is not affected (Vohradský, 2001; Gry et al., 2009).

The next step in identifying receptor involvement was taken by using pharmacological inhibitors as described above. Since TAS2R16 was again of central importance here, the influence of the TAS2R16 inhibitor probenecid with regard to the stimulation of proton secretion by HGT-1 cells induced by the bitter peptides and the sweet-tasting thaumatin was investigated again. Since the effect on the secretory activity of two of the bitter peptides was strongest at 30 pM, both, the peptides and the intact thaumatin were used at this concentration to ensure better comparability. While treatment of the cells with the compounds alone led to the expected increase in proton secretion, this could no longer be observed with co-treatment with probenecid. The fact that probenecid alone showed no influence on the intracellular proton concentration and that histamine-induced secretion was also not influenced by probenecid, indicates that the inhibitor indeed leads to blocking via antagonistic effects on specific TAS2Rs, as described earlier (Greene et al., 2011).

With the use of the cellular bitter response assay, it was therefore possible to provide mechanistic insights into the sensorially determined taste quality of the bitter-tasting peptides and to show a potential bitter taste receptor dependency. To investigate the possible involvement of TAS2R16 in the anti-inflammatory effects of the peptides DAGGRQLNSGES, FNVPMDF, and WTINVEPGTKGGKIW, the expression of this receptor was again reduced by using specific siRNA. This reduction in *TAS2R16* expression resulted in HGT-1 cells treated with the bitter peptides prior to treatment with the native *H. pylori* proteins secreting more IL-17A than native cells with normal *TAS2R16* expression. While the thaumatin-derived peptides led to reduced *H. pylori*-induced IL-17A release in native HGT-1 cells with normal TAS2R16 expression, a reduction in *TAS2R16* expression caused the cells to show increased IL-17A secretion, despite treatment with the bitter peptides. For other isoforms of IL-17, namely IL-17E and IL-17F, it was recently shown that food constituents such as folic acid, vitamins $B_6$ (pyridoxine hydrochloride) and C, but also ions such as potassium or iron can lead to a reduction in IL-17 release (Polak-Szczybyło & Tabarkiewicz, 2022). While the underlying molecular mechanisms are not fully understood, it should be noted that vitamin $B_6$ as well as metal ions are able to activate bitter taste receptors. While divalent metal ions such as $Fe^{2+}$ and $Mn^{2+}$ are known agonists for TAS2R7 (Behrens et al., 2019), pyridoxine hydrochloride also activates TAS2R7 and TAS2R14 (Delompré et al., 2022). This leads to the assumption that the bitter taste quality of the investigated micronutrients could also play a role in their significance in the context of IL-17 release.

Consequently, it was shown that the release of IL-17A induced by *H. pylori* can be reduced by pre-treatment with bitter peptides, which were released from thaumatin during gastric digestion. In addition, the experiments showed that these bitter peptide-mediated anti-inflammatory effects are functionally dependent on TAS2R16.

These two parts of the thesis have shown that physiological effects induced by food constituents may not be predictable if only their original structure is considered. Digestion begins immediately after the ingestion of food and with it the breakdown, metabolization and structural transformation of its constituents. This fact can be utilized in the future by conjugating bioactive ingredients with compounds, primarily peptides, which change the taste quality and therefore address other families of receptors after cleavage in the human organism than in the oral cavity. Furthermore, by continuing this approach, it may also be possible to mask bioactive, less palatable compounds so that they are only released at their destination by enzymes present in these organs. Nevertheless, this requires further research as part of a human intervention study.

## 4.3 Sodium permeable ion channels TRPM4 and TRPM5 are functionally required for TAS2R-induced proton secretion by HGT-1 cells

If only digestion-related changes in a molecule can cause such decisive differences in the context of their impact on stomach physiology, it should also be noted that cellular signaling pathways are also not so simple that they could only be dependent on one receptor-agonist-interaction. For example, the perception of bitter taste sensations by TAS2Rs on the tongue is known to involve sodium permeable ion channels, which are opened by the increase in cytosolic calcium levels associated with the activation of G protein-coupled receptors, causing an increase in intracellular sodium concentrations (Dutta Banik et al., 2018; Wu et al., 2020; Dutta Banik & Medler, 2023). The involvement of these channels, namely transient receptor potential cation channels (TRP) M4 and M5, has also been validated in other cell types. TRPM4, for instance, is involved in inflammatory processes in neurons (Schattling et al., 2012) and in the reaction of macrophages to infections (Serafini et al., 2012). TRPM5, on the other hand, was shown to play a decisive role in the glucose-induced release of insulin from the pancreatic islets (Colsoul et al., 2010). The expression and function of the two ion channels in parietal cells has not yet been investigated, which is why this question was examined in more detail in this thesis.

A first step in investigating whether a particular protein is expressed in a cell type was to screen for the presence of the corresponding mRNA using RT-qPCR. Here, not only the transcripts of the channels in question, TRPM4 and TRPM5, but also those of 24 of the 25 other members of the transient receptor potential channels family of cellular ion channels, with the exception of TRPC5, were found in HGT-1 cells. However, as already mentioned, the strength of

expression at the mRNA level does not necessarily reflect protein expression in all cases (Gry et al., 2009). To investigate the expression of TRPM4 and TRPM5 at the protein level, the ion channels were therefore also localized using immunocytochemistry and both were detected in the cell membrane of HGT-1 cells.

After demonstrating the expression, the functional role of the two sodium-permeable ion channels in HGT-1 cells was investigated. For this purpose, a sodium-selective fluorescent dye was used, with the help of which sodium ions can be detected in the presence of other monovalent cations. The dye used, SBFI (sodium-binding benzofuran isophthalate), complexes free sodium ions through an aza-crown ether, changing its emission ratio through a spectral response to ion binding (Minta & Tsien, 1989).

To establish a link between TAS2Rs and TRPM4 and TRPM5, the two bitter-tasting compounds caffeine and L-arginine were used to investigate the cellular signaling pathways of HGT-1 cells. Caffeine has been shown to stimulate proton secretion by HGT-1 cells involving TAS2R43 (Liszt et al., 2017), while the bitter amino acid L-arginine has an impact on secretory activity via TAS2R1 (Stoeger et al., 2020). Both compounds also led to a concentration-dependent increase in sodium-dependent fluorescence signals in the experiments to investigate intracellular sodium levels.

As already discussed in the third integrated publication (Richter et al., 2024a), the $EC_{50}$ values determined for caffeine and L-arginine of 0.65 and 10.38 mM, respectively, were in very good agreement with the bitter recognition thresholds known from the literature, which vary between 0.7 and 3.7 mM for caffeine (Guinard et al., 1994; Izawa et al., 2010) and 75 mM for L-arginine (Sonntag et al., 2010). To investigate the intracellular processes up to this point in more detail, a further aspect that is particularly associated with G protein-coupled receptors was investigated, namely intracellular calcium mobilization (Nash et al., 2001). The conformational change of a TAS2R through binding of a bitter compound leads to dissociation of the coupled G protein with subsequent activation of phospholipase C β2. The $IP_3$ formed by this from $PIP_2$ binds to corresponding $IP_3$ receptors on the ER, triggering release of the calcium stores into the cytosol (Tuzim & Korolczuk, 2021). This fact has been utilized for years to identify agonists for bitter taste receptors (Meyerhof et al., 2010; Behrens & Meyerhof, 2018). To analyze the role of calcium in immortalized human parietal cells, the HGT-1 cells were incubated with another fluorescent dye, Cal-520. This complexes calcium ions in the same way as EDTA, which changes the fluorescence properties of the covalently bound fluorophore (Liao et al., 2021). Here, as expected, L-arginine led to an increase in cytosolic calcium levels in the HGT-1 cells, while reduced fluorescence intensities were determined for caffeine directly after addition. However, it has already been shown in the past that caffeine can quench the fluorescence of dyes due to its heteroaromatic properties (Muschol et al., 1999). Since treatment of the cells with ionomycin as a positive control, which transports extracellular

calcium ions through the cell membrane, also showed an increase in cytosolic calcium levels, the functionality of the assay was validated. Modulation of intracellular calcium levels by bitter compounds for this cell line was demonstrated for the first time in this project.

In terms of controls, two other compounds were investigated that activate two different groups of GPCRs, triggering different intracellular signaling pathways. While the muscarinic acetylcholine receptor ($M_3$) is activated by carbachol and consequently leads to calcium mobilization, histamine is an agonist of the histamine $H_2$ receptor, which influences cellular processes via the cAMP-dependent pathway (Chew et al., 1992; Engevik et al., 2020). While carbachol led to calcium mobilization and sodium influx into HGT-1 cells, histamine had no effect on the cytosolic concentrations of either cation. Nevertheless, histamine has always shown a stimulating effect on the proton secretion by the cells in the past, which is why treatment with histamine has long proven to be a positive control in the investigation of secretory activity (Liszt et al., 2017; Liszt et al., 2018). Consequently, the observed effects of the controls are consistent with those described in the literature (Chew et al., 1992; Engevik et al., 2020).

To establish a link between the bitter compound-modulated changes in intracellular sodium concentrations and TAS2Rs, the cells were incubated with caffeine or L-arginine and the bitter-masking compound HED (Roland et al., 2013). In both cases, a reduction in caffeine- or L-arginine-induced sodium influx was observed, indicating that HED also reduces the bitter compound-triggered increase in cytosolic sodium levels through its antagonistic effects on TAS2Rs. The fact that not only antagonistic effects on TAS2R20/31/43/50 but also agonistic effects on TAS2R14 and TAS2R39 have been observed for HED in the past (Roland et al., 2013) explains that treatment of HGT-1 cells with HED alone also showed increased sodium levels compared to untreated control cells in the here presented thesis.

This illustrated once again that although the use of antagonists or inhibitors can provide indications of the involvement of receptors, further validation is necessary. Therefore, TAS2R43ko HGT-1 cells were examined to finally conclude the involvement of a specific TAS2R in bitter compound-induced increases in intracellular sodium levels. The use of the same clone already allowed Liszt et al. in 2017 to demonstrate a reduced response to the stimulation of proton secretion by caffeine in the absence of TAS2R43. In the present work, a comparison of wild-type cells with native TAS2R expression pattern and TAS2R43ko cells showed a reduction in the caffeine-induced increase in intracellular sodium levels. As expected, despite the lack of expression of TAS2R43, sodium influx still occurred because caffeine is not only an agonist of TAS2R43 but also for TAS2R7/10/14/46 (Meyerhof et al., 2010). It was concluded that the increase in sodium concentrations by caffeine involved TAS2R43, but that other caffeine-targeted bitter taste receptors also led to increased cytosolic sodium levels.

After validating the involvement of TAS2Rs in the observed changes in sodium concentration, the next step was to investigate whether it was actually sodium, as the dye used primarily binds these ions, but can also complex other monovalent cations such as potassium (Minta & Tsien, 1989). Measurements using ICP-MS laser ablation showed increased sodium concentrations in cells previously treated with caffeine or L-arginine compared to untreated control cells at the single cell level. A further verification was possible by repeating the influx experiments in nominally sodium-free buffer. Since the increase in cytosolic sodium levels after incubation of the cells with caffeine or L-arginine did not occur if no sodium was present in the extracellular space, it was clearly shown that this is a TAS2R-controlled influx of sodium ions. Since the intracellular sodium concentrations were lower when the cells were treated with the bitter compounds in the sodium-free buffer compared to untreated cells, it was hypothesized that an opening of sodium-permeable ion channels still occurs, but would result in sodium efflux along the concentration gradient out of the cell. For instance, sodium efflux from human erythrocytes cultured in sodium-free buffer has been observed before (Maizels, 1968).

Although TRPM4 and TRPM5 are already associated with TAS2R-induced sodium influx in taste cells (Dutta Banik et al., 2018), there are many more sodium-permeable ion channels. ENaC, for example, is also an ion channel involved in the perception of taste (salty) and is permeable to sodium ions (Chandrashekar et al., 2010). To investigate the hypothesis that sodium influx was mainly controlled by TRPM4 and TRPM5, a further set of experiments was performed. Pharmacological blocking of TRPM5 by nicotine (Gees et al., 2014) resulted in a reduction of the measured caffeine-induced sodium influxes, while another inhibitor, triphenylphosphine oxide (TPPO) (Palmer et al., 2010), already caused a sodium influx alone, the effect of which added up to the caffeine-induced influxes upon co-incubation. Notably, it was not possible to investigate TRPM4 involvement by using inhibitors, as the inhibitor 9-phenanthrol (Guinamard et al., 2014) exhibits fluorescence at the same wavelength that is required to excite the sodium-sensitive fluorescent dye. Overall, the experiments with the different inhibitors generated inconsistent results, which was why a siRNA knock-down approach was developed to obtain conclusive results. By reducing the gene expression of *TRPM4* or *TRPM5*, a reduced increase in cytosolic sodium levels was observed after incubation with caffeine targeting at least TAS2R43 and L-arginine targeting TAS2R1, among others. Mock-transfected cells showed the increase in intracellular sodium concentrations previously observed in native cells upon treatment with the two bitter compounds. This demonstrated that both TRPM4 and TRPM5 play crucial roles in the TAS2R-mediated sodium influx into HGT-1 cells. An unchanged sodium concentration in the treated cells compared to the untreated cells was not observed for any of the knock-down approaches, which is likely to be based on the fact that only one of the two TRP channels was targeted in each case and the expression of the proteins concerned is merely reduced, but not completely prevented as in

knock-out experiments. Stimulation of the cells with carbachol also showed a reduction in sodium influx for *TRPM4*kd and *TRPM5*kd cells, whereas the expected influx was observed in mock-transfected cells.

As studied in this thesis, a key physiological outcome of the immortalized human parietal cells is the secretion of protons associated with the production of gastric acid. Conclusively, to elaborate on the understanding of the signaling pathway responsible for this, experiments were carried out on the role of TRPM4 and TRPM5 in the secretory activity of HGT-1 cells. The previously reported ability of caffeine (Liszt et al., 2017; Liszt et al., 2018) and L-arginine (Stoeger et al., 2020) to stimulate proton secretion could be reproduced in this model. However, when the cell-surrounding medium was again replaced with nominal sodium-free buffer and the cells were stimulated with caffeine, the increase in secretory activity was not observed. The situation was different when proton secretion was induced by histamine. The activation of the sodium-independent signaling pathway led to the same stimulation in both sodium-containing and sodium-free buffer. The dependence of the increased proton secretion triggered by bitter compounds on a sodium influx through TRPM4 and TRPM5 was demonstrated both by using the inhibitors already mentioned and by the knock-down approach. Since the intracellular pH values were measured at wavelengths that do not interfere with the fluorescence of the TRPM4 antagonist 9-phenanthrol (Guinamard et al., 2014), a lower proton stimulation triggered by simultaneous treatment with caffeine was observed both in this case and for the two TRPM5-specfic inhibitors nicotine (Gees et al., 2014) and TPPO (Palmer et al., 2010). A reduction in *TRPM4* or *TRPM5* expression also led to a significant reduction in the caffeine- or L-arginine-induced stimulation of the secretory activity of HGT-1 cells. In contrast, the expression of the two sodium-permeable ion channels played no role in the initiation of proton secretion by histamine.

Summarizing the results of the previous understanding of the cellular signaling pathways relevant for the stimulation of proton secretion by human parietal cells by bitter food constituents (Chew et al., 1992; Yao & Forte, 2003; J. G. Forte, 2010; Zopun et al., 2018a; Zopun et al., 2018b; Engevik et al., 2020), extended by the findings obtained in this study, the sodium-dependent signaling pathway emerges on the one hand. Here, the bitter compound is targeting the bitter taste receptor, which triggers activation of the phospholipase C β2 by the dissociated G protein. A cleavage of $PIP_2$ to $IP_3$ leads to calcium mobilization within the cell, which is followed by an opening of the calcium-sensitive ion channels TRPM4 and TRPM5. A sodium influx occurs through the sodium-permeable channels, which triggers a depolarization of the cell and finally initiates the active export of protons by the $H^+/K^+$ ATPase. On the other hand, there is the TAS2R- and sodium-independent pathway. Triggered by histamine, the modulation of intracellular cAMP concentrations leads to activation of protein kinase A, which also influences the proton pump. The results of this section show that the activation of TAS2Rs

triggers a complex intracellular signaling pathway, leading to the typical outcome of proton secretion by parietal cells. However, other pathways, such as the involvement of cAMP signaling, cannot be ruled out, as it is not yet conclusively known to which G proteins TAS2Rs are coupled in other tissues and organs. While βγ-controlled calcium mobilization may always play a more or less important role to a certain extent, $G\alpha_q$ coupling would trigger stronger calcium signals. The involvement of $G\alpha_s$, on the other hand, would cause an increase in intracellular cAMP levels by stimulating the adenylyl cyclase. In contrast, $G\alpha_i$ coupling would have the opposite effect by increasing the rate of phosphodiesterase and hydrolysis of cAMP. The here presented work demonstrated that the induction of physiological effects by food constituents, which primarily target bitter taste receptors, requires additional cellular components, such as the two TRP channels TRPM4 and TRPM5, which in turn could be suitable targets for ingredients and drugs to minimize or abolish undesirable reactions.

## 4.4 Conclusion and Perspectives

In the past, the effects of flavoring compounds or food constituents primarily present in plant- or animal-based products or formed during production and processing (e.g. through fermentation) were studied for their impact on TAS2R-mediated cellular processes, such as, e.g. inflammation (Tiroch et al., 2021) or proton secretion (Liszt et al., 2017; Liszt et al., 2018). This thesis focused on bitter compounds that are formed during digestion of non-bitter-tasting dietary peptides and whose flavor quality cannot be perceived in this form in the oral cavity. Since it is known for over 20 years that receptor proteins for the perception of taste qualities are not only found in the oral cavity, but also in many extra-oral tissues and organs, it is essential to consider the enzymatic degradation and metabolization during digestion to better assess and predict effects on physiological processes mediated by these receptors. The beneficial effects associated with extra-oral TAS2Rs can only occur if the compounds ingested with food retain their bitterness during digestion and metabolization or are transformed during this process into compounds capable of interacting with TAS2Rs.

As summarized in **Fig. 8**, the here presented work shows that both non-bitter-tasting dietary proteins, caseins, a protein mixture of animal origin, as well as thaumatins, being plant proteins, are cleaved into bitter-tasting peptides during gastric digestion. In addition to gastrically-released casein peptides already known in the literature, previously unknown peptides resulting from the cleavage of thaumatin were identified in this thesis. The sensory bitterness of the peptides identified was, for the first time, linked to a TAS2R-dependent proton secretion controlled by parietal cells, which is an essential component of gastric acid production, linked to protein digestion and satiety. Furthermore, anti-inflammatory TAS2R-mediated effects were deduced for the bitter peptides derived from thaumatin, whereby the release of pro-inflammatory cytokines induced by *H. pylori* was reduced. To further elucidate the underlying signaling pathways, sodium-permeable ion channels TRPM4 and TRPM5 were also shown to be involved in TAS2R-mediated stimulation of proton secretion for the first time in this work. A limiting factor is that the involvement of receptors or ion channels in the native context can only be clearly validated by knock-out or knock-down approaches. With regard to the cellular signaling pathways downstream of binding bitter-tasting ligands to TAS2Rs, not everything is known yet. In particular, further impact of bitter compounds and the underlying signaling pathways on extra-oral TAS2R-expressing organs and tissues should be investigated in the future.

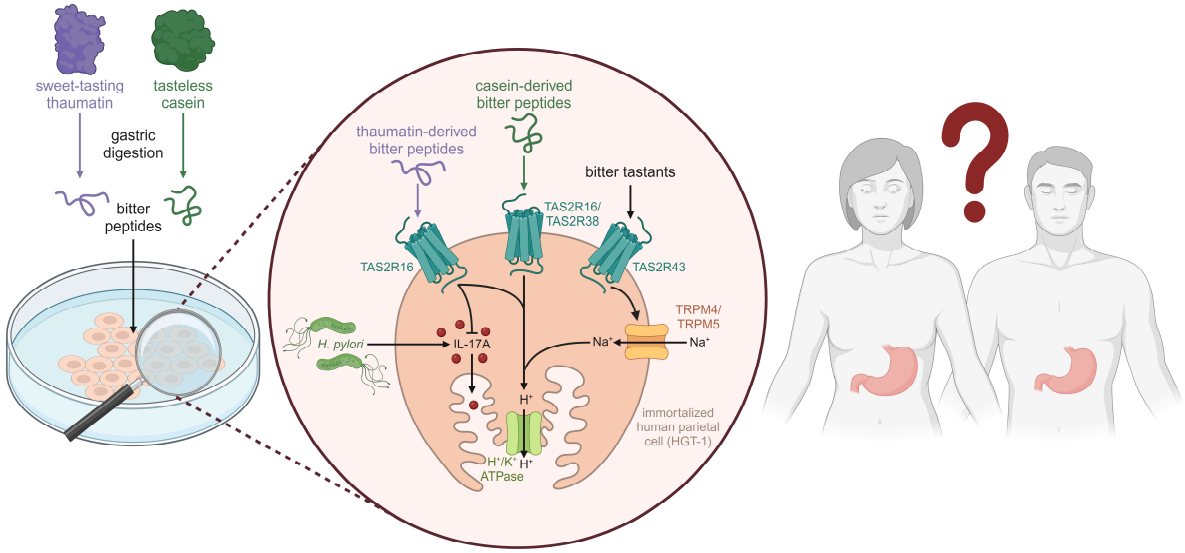


**Figure 8: Summary of the results obtained in this work on the mechanistic processes in immortalized human parietal cells. Based on the conclusions of this thesis, clinical studies are now essential to evaluate the transferability.** Created with BioRender.com.

In the long term, this work represents a way of masking undesirable taste sensations by using a retrosynthetic approach to conjugate bioactive peptides or even other active ingredients with peptides that are cleaved during digestion in the stomach, releasing the active constituent. The additional peptides produced in this process do not represent an additional burden for the organism and only serve to change the taste quality. However, in contrast to these intentionally induced changes in taste quality, the results of this work should also raise awareness that even tasteless or sweet-tasting food components, in this case proteins, can be cleaved during digestion into peptides that have a bitter taste quality and thereby influence gastric physiology via TAS2Rs by stimulating secretory activity or reducing the release of pro-inflammatory cytokines. Other potential targets for masking undesirable taste sensations or modulating cellular functions such as proton secretion are the TRPM4 and TRPM5 ion channels, which also play an important role from a mechanistic perspective.

The results obtained in the *in vitro* experiments of this work are promising and indicate potential health impacts of the released bitter-tasting peptides. However, human intervention studies are needed to confirm the relevance and safety of these findings for the human organism, particularly with regard to the release amounts of the respective peptides after habitual dietary intake.

# 5 References

Abrol, R., Tan, J., Hui, H., Goddard III, W. A., & Pandol, S. J. (2015). Structural basis for bitter taste receptor activation and its potential role in targeting diabetes. *Functional Foods in Health and Disease*, *5*, 117.

Ahmad, N., Gupta, S., & Mukhtar, H. (2000). Green tea polyphenol epigallocatechin-3-gallate differentially modulates nuclear factor kappaB in cancer cells versus normal cells. *Archives of Biochemistry and Biophysics*, *376*, 338–346.

Aihara, K., Ishii, H., & Yoshida, M. (2009). Casein-derived tripeptide, Val-Pro-Pro (VPP), modulates monocyte adhesion to vascular endothelium. *Journal of Atherosclerosis and Thrombosis*, *16*, 594–603.

Andreozzi, P., Sarnelli, G., Pesce, M., Zito, F. P., Alessandro, A. D., Verlezza, V., Palumbo, I., Turco, F., Esposito, K., & Cuomo, R. (2015). The Bitter Taste Receptor Agonist Quinine Reduces Calorie Intake and Increases the Postprandial Release of Cholecystokinin in Healthy Subjects. *Journal of Neurogastroenterology and Motility*, *21*, 511–519.

Avau, B., Rotondo, A., Thijs, T., Andrews, C. N., Janssen, P., Tack, J., & Depoortere, I. (2015). Targeting extra-oral bitter taste receptors modulates gastrointestinal motility with effects on satiation. *Scientific Reports*, *5*, 15985.

Bacchi, S., Palumbo, P., Sponta, A., & Coppolino, M. F. (2012). Clinical pharmacology of non-steroidal anti-inflammatory drugs: a review. *Anti-Inflammatory & Anti-Allergy Agents in Medicinal Chemistry*, *11*, 52–64.

Baggio, L. L., & Drucker, D. J. (2014). Glucagon-like peptide-1 receptors in the brain: controlling food intake and body weight. *The Journal of Clinical Investigation*, *124*, 4223–4226.

Balandras, F., Miclo, L., Gaillard, J. L., Le, R. Y., & Laurent, F. (2007). *Casein-Derived Peptides having Anxiolytic Activity*. FR20060010855;WO2007EP63863, *A01K67/027;A23L33/00;A61K38/08;A61P25/22;C07H21/00;C07K7/06;C12N1/19;C12N1/21;C12P21/00*.

Bang, S., Kim, K. Y., Yoo, S., Lee, S.-H., & Hwang, S. W. (2007). Transient receptor potential V2 expressed in sensory neurons is activated by probenecid. *Neuroscience Letters*, *425*, 120–125.

Barnes, P. J. (2010). Mechanisms and resistance in glucocorticoid control of inflammation. *The Journal of Steroid Biochemistry and Molecular Biology*, *120*, 76–85.

Barrett, T., Wilhite, S. E., Ledoux, P., Evangelista, C., Kim, I. F., Tomashevsky, M., Marshall, K. A., Phillippy, K. H., Sherman, P. M., Holko, M., Yefanov, A., Lee, H., Zhang, N., Robertson, C. L., Serova, N., Davis, S., & Soboleva, A. (2013). NCBI GEO: archive for functional genomics data sets--update. *Nucleic Acids Research*, *41*, D991-5.

Bartoshuk, L. M., Duffy, V. B., Hayes, J. E., Moskowitz, H. R., & Snyder, D. J. (2006). Psychophysics of sweet and fat perception in obesity: problems, solutions and new perspectives. *Philosophical Transactions of the Royal Society of London. Series B, Biological Sciences*, *361*, 1137–1148.

Behrens, M., & Meyerhof, W. (2018). Vertebrate Bitter Taste Receptors: Keys for Survival in Changing Environments. *Journal of Agricultural and Food Chemistry*, *66*, 2204–2213.

Behrens, M., Redel, U., Blank, K., & Meyerhof, W. (2019). The human bitter taste receptor TAS2R7 facilitates the detection of bitter salts. *Biochemical and Biophysical Research Communications*, *512*, 877–881.

Benton, D. (2005). Can artificial sweeteners help control body weight and prevent obesity? *Nutrition Research Reviews*, *18*, 63–76.

Bermudez, O. I., & Gao, X. (2010). Greater consumption of sweetened beverages and added sugars is associated with obesity among US young adults. *Annals of Nutrition and Metabolism*, *57*, 211–218.

Bhandari, D., Rafiq, S., Gat, Y., Gat, P., Waghmare, R., & Kumar, V. (2020). A Review on Bioactive Peptides: Physiological Functions, Bioavailability and Safety. *International Journal of Peptide Research and Therapeutics*, *26*, 139–150.

Bijl, E., van Valenberg, H. J. F., Huppertz, T., & van Hooijdonk, A. C. M. (2013). Protein, casein, and micellar salts in milk: current content and historical perspectives. *Journal of Dairy Science*, *96*, 5455–5464.

Bindu, S., Mazumder, S., & Bandyopadhyay, U. (2020). Non-steroidal anti-inflammatory drugs (NSAIDs) and organ damage: A current perspective. *Biochemical Pharmacology*, *180*, 114147.

Bitarafan, V., Fitzgerald, P. C. E., Little, T. J., Meyerhof, W., Wu, T., Horowitz, M., & Feinle-Bisset, C. (2019). Effects of Intraduodenal Infusion of the Bitter Tastant, Quinine, on Antropyloroduodenal Motility, Plasma Cholecystokinin, and Energy Intake in Healthy Men. *Journal of Neurogastroenterology and Motility*, *25*, 413–422.

Blundell, J. E., & Halford, J. C. (1994). Regulation of nutrient supply: the brain and appetite control. *The Proceedings of the Nutrition Society*, *53*, 407–418.

Blundell, J. E., & Halford, J. C. (1998). Serotonin and Appetite Regulation. *CNS Drugs*, *9*, 473–495.

Brodkorb, A., Egger, L., Alminger, M., Alvito, P., Assunção, R., Ballance, S., Bohn, T., Bourlieu-Lacanal, C., Boutrou, R., Carrière, F., Clemente, A., Corredig, M., Dupont, D., Dufour, C., Edwards, C., Golding, M., Karakaya, S., Kirkhus, B., Le Feunteun, S., Lesmes, U., Macierzanka, A., Mackie, A. R., Martins, C., Marze, S., McClements, D. J., Ménard, O., Minekus, M., Portmann, R., Santos, C. N., Souchon, I., Singh, R. P., Vegarud, G. E.,

Wickham, M. S. J., Weitschies, W., & Recio, I. (2019). INFOGEST static in vitro simulation of gastrointestinal food digestion. *Nature Protocols*, *14*, 991–1014.

Burger, D., & Dayer, J.-M. (2002). The role of human T-lymphocyte-monocyte contact in inflammation and tissue destruction. *Arthritis Research*, *4 Suppl 3*, S169-76.

Chandrashekar, J., Kuhn, C., Oka, Y., Yarmolinsky, D. A., Hummler, E., Ryba, N. J. P., & Zuker, C. S. (2010). The cells and peripheral representation of sodium taste in mice. *Nature*, *464*, 297–301.

Charoenkwan, P., Nantasenamat, C., Hasan, M. M., Manavalan, B., & Shoombuatong, W. (2021). BERT4Bitter: a bidirectional encoder representations from transformers (BERT)-based model for improving the prediction of bitter peptides. *Bioinformatics*, *37*, 2556–2562.

Charoenkwan, P., Yana, J., Schaduangrat, N., Nantasenamat, C., Hasan, M. M., & Shoombuatong, W. (2020). iBitter-SCM: Identification and characterization of bitter peptides using a scoring card method with propensity scores of dipeptides. *Genomics*, *112*, 2813–2822.

Chaudhari, N., & Roper, S. D. (2010). The cell biology of taste. *The Journal of Cell Biology*, *190*, 285–296.

Chen, H., Wang, K., Xiao, H., Hu, Z., & Zhao, L. (2020). Structural Characterization and Pro-inflammatory Activity of a Thaumatin-Like Protein from Pulp Tissues of Litchi chinensis. *Journal of Agricultural and Food Chemistry*, *68*, 6439–6447.

Chen, L., Deng, H., Cui, H., Fang, J., Zuo, Z., Deng, J., Li, Y., Wang, X., & Zhao, L. (2017). Inflammatory responses and inflammation-associated diseases in organs. *Oncotarget*, *9*, 7204–7218.

Chen, M. C., Wu, S. V., Reeve, J. R., & Rozengurt, E. (2006). Bitter stimuli induce Ca2+ signaling and CCK release in enteroendocrine STC-1 cells: role of L-type voltage-sensitive Ca2+ channels. *American Journal of Physiology-Cell Physiology*, *291*, C726-39.

Chen, W., Chen, Y., Qian, Y., Zhang, J., Hu, X., Yan, X., Jiang, C., Yao, S., Yu, Q., Chen, X., & Han, S. (2023). The casein-derived peptide YFYPEL alleviates intestinal epithelial cell dysfunction associated with NEC by regulating the PI3K/AKT signaling pathway. *Food & Function*, *14*, 3769–3778.

Chertov, O., Yang, D., Howard, O. M., & Oppenheim, J. J. (2000). Leukocyte granule proteins mobilize innate host defenses and adaptive immune responses. *Immunological Reviews*, *177*, 68–78.

Chew, C. S., Nakamura, K., & Ljungström, M. (1992). Calcium signaling mechanisms in the gastric parietal cell. *The Yale Journal of Biology and Medicine*, *65*, 561–623.

Chou, W.-L. (2021). Therapeutic potential of targeting intestinal bitter taste receptors in diabetes associated with dyslipidemia. *Pharmacological Research*, *170*, 105693.

Clapp, T. R., Trubey, K. R., Vandenbeuch, A., Stone, L. M., Margolskee, R. F., Chaudhari, N., & Kinnamon, S. C. (2008). Tonic activity of Galpha-gustducin regulates taste cell responsivity. *FEBS letters*, *582*, 3783–3787.

Colsoul, B., Schraenen, A., Lemaire, K., Quintens, R., van Lommel, L., Segal, A., Owsianik, G., Talavera, K., Voets, T., Margolskee, R. F., Kokrashvili, Z., Gilon, P., Nilius, B., Schuit, F. C., & Vennekens, R. (2010). Loss of high-frequency glucose-induced Ca2+ oscillations in pancreatic islets correlates with impaired glucose tolerance in Trpm5-/- mice. *Proceedings of the National Academy of Sciences of the United States of America*, *107*, 5208–5213.

Corrons, M. A., Liggieri, C. S., Trejo, S. A., & Bruno, M. A. (2017). ACE-inhibitory peptides from bovine caseins released with peptidases from Maclura pomifera latex. *Food Research International*, *93*, 8–15.

Costedio, M. M., Hyman, N., & Mawe, G. M. (2007). Serotonin and its role in colonic function and in gastrointestinal disorders. *Diseases of the Colon and Rectum*, *50*, 376–388.

Cox, J., & Mann, M. (2008). MaxQuant enables high peptide identification rates, individualized p.p.b.-range mass accuracies and proteome-wide protein quantification. *Nature Biotechnology*, *26*, 1367–1372.

Crabtree, J. E. (1996). Gastric mucosal inflammatory responses to Helicobacter pylori. *Alimentary Pharmacology & Therapeutics*, *10 Suppl 1*, 29–37.

Cummings, D. E., & Overduin, J. (2007). Gastrointestinal regulation of food intake. *The Journal of Clinical Investigation*, *117*, 13–23.

Czaja, A. J. (2014). Hepatic inflammation and progressive liver fibrosis in chronic liver disease. *World Journal of Gastroenterology*, *20*, 2515–2532.

Dai, W., Xiang, A., Pan, D., Xia, Q., Sun, Y., Wang, Y., Wang, W., Cao, J., & Zhou, C. (2024). Insights into the identification of bitter peptides from Jinhua ham and its taste mechanism by molecular docking and transcriptomics analysis. *Food Research International*, *189*, 114534.

Dainichi, T., Matsumoto, R., Mostafa, A., & Kabashima, K. (2019). Immune Control by TRAF6-Mediated Pathways of Epithelial Cells in the EIME (Epithelial Immune Microenvironment). *Frontiers in Immunology*, *10*, 1107.

Dallas, D. C., Citerne, F., Tian, T., Silva, V. L. M., Kalanetra, K. M., Frese, S. A., Robinson, R. C., Mills, D. A., & Barile, D. (2016). Peptidomic analysis reveals proteolytic activity of kefir microorganisms on bovine milk proteins. *Food Chemistry*, *197*, 273–284.

Daly, K., Al-Rammahi, M., Moran, A., Marcello, M., Ninomiya, Y., & Shirazi-Beechey, S. P. (2013). Sensing of amino acids by the gut-expressed taste receptor T1R1-T1R3 stimulates CCK secretion. *American Journal of Physiology-Gastrointestinal and Liver Physiology*, *304*, G271-82.

Dana, H., Chalbatani, G. M., Mahmoodzadeh, H., Karimloo, R., Rezaiean, O., Moradzadeh, A., Mehmandoost, N., Moazzen, F., Mazraeh, A., Marmari, V., Ebrahimi, M., Rashno, M. M., Abadi, S. J., & Gharagouzlo, E. (2017). Molecular Mechanisms and Biological Functions of siRNA. *International Journal of Biomedical Science IJBS*, *13*, 48–57.

Dando, R., & Roper, S. D. (2009). Cell-to-cell communication in intact taste buds through ATP signalling from pannexin 1 gap junction hemichannels. *The Journal of Physiology*, *587*, 5899–5906.

Dando, R., & Roper, S. D. (2012). Acetylcholine is released from taste cells, enhancing taste signalling. *The Journal of Physiology*, *590*, 3009–3017.

Das Europäische Parlament und der Rat der Europäischen Union (1994). *Richtlinie 94/35/EG der Europäischen Parlaments und des Rates*.

Davies, D. T., & Law, A. J. R. (1977). The composition of whole casein from the milk of Ayrshire cows. *Journal of Dairy Research*, *44*, 447–454.

Davies, N. M. (1998). Clinical pharmacokinetics of ibuprofen. The first 30 years. *Clinical Pharmacokinetics*, *34*, 101–154.

Dawidowicz, A. L., Bernacik, K., Typek, R., & Stankevič, M. (2018). Possibility of quinine transformation in food products: LC–MS and NMR techniques in analysis of quinine derivatives. *Zeitschrift für Lebensmittel-Untersuchung und -Forschung*, *244*, 105–116.

Del Contreras, M. M., Carrón, R., Montero, M. J., Ramos, M., & Recio, I. (2009). Novel casein-derived peptides with antihypertensive activity. *International Dairy Journal*, *19*, 566–573.

Delompré, T., Belloir, C., Martin, C., Salles, C., & Briand, L. (2022). Detection of Bitterness in Vitamins Is Mediated by the Activation of Bitter Taste Receptors. *Nutrients*, *14*.

Depoortere, I. (2014). Taste receptors of the gut: emerging roles in health and disease. *Gut*, *63*, 179–190.

Depraetere, V. (2000). Origins of antigenic peptides. *Nature Cell Biology*, *2*, E75.

D'Errico, A., Nasso, R., Di Maro, A., Landi, N., Chambery, A., Russo, R., D'Angelo, S., Masullo, M., & Arcone, R. (2024). Identification and Characterization of Neuroprotective Properties of Thaumatin-like Protein 1a from Annurca Apple Flesh Polyphenol Extract. *Nutrients*, *16*.

Deshpande, D. A., Wang, W. C. H., McIlmoyle, E. L., Robinett, K. S., Schillinger, R. M., An, S. S., Sham, J. S. K., & Liggett, S. B. (2010). Bitter taste receptors on airway smooth muscle bronchodilate by localized calcium signaling and reverse obstruction. *Nature Medicine*, *16*, 1299–1304.

Dhillon, A. S., Hagan, S., Rath, O., & Kolch, W. (2007). MAP kinase signalling pathways in cancer. *Oncogene*, *26*, 3279–3290.

Dong, J., Qu, Y., Li, J., Cui, L., Wang, Y., Lin, J., & Wang, H. (2018). Cortisol inhibits NF-κB and MAPK pathways in LPS activated bovine endometrial epithelial cells. *International Immunopharmacology*, *56*, 71–77.

Dragoș, D., Petran, M., Gradinaru, T.-C., & Gilca, M. (2022). Phytochemicals and Inflammation: Is Bitter Better? *Plants*, *11*, 2991.

DuBois, G. E. (2016). Molecular mechanism of sweetness sensation. *Physiology & Behavior*, *164*, 453–463.

Duffy, V. B. (2007). Variation in oral sensation: implications for diet and health. *Current Opinion in Gastroenterology*, *23*, 171–177.

Dutta Banik, D., Martin, L. E., Freichel, M., Torregrossa, A.-M., & Medler, K. F. (2018). TRPM4 and TRPM5 are both required for normal signaling in taste receptor cells. *Proceedings of the National Academy of Sciences of the United States of America*, *115*, E772-E781.

Dutta Banik, D., & Medler, K. F. (2023). Defining the role of TRPM4 in broadly responsive taste receptor cells. *Frontiers in Cellular Neuroscience*, *17*, 1148995.

Dyer, J., Salmon, K. S. H., Zibrik, L., & Shirazi-Beechey, S. P. (2005). Expression of sweet taste receptors of the T1R family in the intestinal tract and enteroendocrine cells. *Biochemical Society Transactions*, *33*, 302–305.

Edgar, R., Domrachev, M., & Lash, A. E. (2002). Gene Expression Omnibus: NCBI gene expression and hybridization array data repository. *Nucleic Acids Research*, *30*, 207–210.

Ekoff, M., Choi, J.-H., James, A., Dahlén, B., Nilsson, G., & Dahlén, S.-E. (2014). Bitter taste receptor (TAS2R) agonists inhibit IgE-dependent mast cell activation. *The Journal of Allergy and Clinical Immunology*, *134*, 475–478.

Engelstoft, M. S., Park, W.-M., Sakata, I., Kristensen, L. V., Husted, A. S., Osborne-Lawrence, S., Piper, P. K., Walker, A. K., Pedersen, M. H., Nøhr, M. K., Pan, J., Sinz, C. J., Carrington, P. E., Akiyama, T. E., Jones, R. M., Tang, C., Ahmed, K., Offermanns, S., Egerod, K. L., Zigman, J. M., & Schwartz, T. W. (2013). Seven transmembrane G protein-coupled receptor repertoire of gastric ghrelin cells. *Molecular Metabolism*, *2*, 376–392.

Engevik, A. C., Kaji, I., & Goldenring, J. R. (2020). The Physiology of the Gastric Parietal Cell. *Physiological Reviews*, *100*, 573–602.

Feng, J., Petersen, C. D., Coy, D. H., Jiang, J.-K., Thomas, C. J., Pollak, M. R., & Wank, S. A. (2010). Calcium-sensing receptor is a physiologic multimodal chemosensor regulating gastric G-cell growth and gastrin secretion. *Proceedings of the National Academy of Sciences of the United States of America*, *107*, 17791–17796.

Ferrero-Miliani, L., Nielsen, O. H., Andersen, P. S., & Girardin, S. E. (2007). Chronic inflammation: importance of NOD2 and NALP3 in interleukin-1beta generation. *Clinical and Experimental Immunology*, *147*, 227–235.

Finger, T. E., Danilova, V., Barrows, J., Bartel, D. L., Vigers, A. J., Stone, L., Hellekant, G., & Kinnamon, S. C. (2005). ATP signaling is crucial for communication from taste buds to gustatory nerves. *Science (New York, N.Y.)*, *310*, 1495–1499.

Frank, O., Kreissl, J. K., Daschner, A., & Hofmann, T. (2014). Accurate determination of reference materials and natural isolates by means of quantitative (1)h NMR spectroscopy. *Journal of Agricultural and Food Chemistry*, *62*, 2506–2515.

Fujiwara, N., & Kobayashi, K. (2005). Macrophages in inflammation. *Current Drug Targets-Inflammation and Allergy*, *4*, 281–286.

Galland, F., Espindola, J. S. de, Lopes, D. S., Taccola, M. F., & Pacheco, M. T. B. (2022). Food-derived bioactive peptides: Mechanisms of action underlying inflammation and oxidative stress in the central nervous system. *Food Chemistry Advances*, *1*, 100087.

Gees, M., Alpizar, Y. A., Luyten, T., Parys, J. B., Nilius, B., Bultynck, G., Voets, T., & Talavera, K. (2014). Differential effects of bitter compounds on the taste transduction channels TRPM5 and IP3 receptor type 3. *Chemical Senses*, *39*, 295–311.

Gigli, I. (2016). *Milk Proteins: From Structure to Biological Properties and Health Aspects*. Erscheinungsort nicht ermittelbar: IntechOpen.

Gilbertson, T. A., Damak, S., & Margolskee, R. F. (2000). The molecular physiology of taste transduction. *Current Opinion in Neurobiology*, *10*, 519–527.

Gilca, M., & Dragos, D. (2017). Extraoral Taste Receptor Discovery: New Light on Ayurvedic Pharmacology. *Evidence-based Complementary and Alternative Medicine*, *2017*, 5435831.

Greene, T. A., Alarcon, S., Thomas, A., Berdougo, E., Doranz, B. J., Breslin, P. A. S., & Rucker, J. B. (2011). Probenecid inhibits the human bitter taste receptor TAS2R16 and suppresses bitter perception of salicin. *PloS One*, *6*, e20123.

Gry, M., Rimini, R., Strömberg, S., Asplund, A., Pontén, F., Uhlén, M., & Nilsson, P. (2009). Correlations between RNA and protein expression profiles in 23 human cell lines. *BMC Genomics*, *10*, 365.

Guinamard, R., Hof, T., & Del Negro, C. A. (2014). The TRPM4 channel inhibitor 9-phenanthrol. *British Journal of Pharmacology*, *171*, 1600–1613.

Guinard, J. X., Hong, D. Y., Zoumas-Morse, C., Budwig, C., & Russell, G. F. (1994). Chemoreception and perception of the bitterness of isohumulones. *Physiology & Behavior*, *56*, 1257–1263.

Hagos, F. T., Daood, M. J., Ocque, J. A., Nolin, T. D., Bayir, H., Poloyac, S. M., Kochanek, P. M., Clark, R. S. B., & Empey, P. E. (2017). Probenecid, an organic anion transporter 1 and 3 inhibitor, increases plasma and brain exposure of N-acetylcysteine. *Xenobiotica*, *47*, 346–353.

Haid, D. C., Jordan-Biegger, C., Widmayer, P., & Breer, H. (2012). Receptors responsive to protein breakdown products in g-cells and d-cells of mouse, swine and human. *Frontiers in Physiology*, *3*, 65.

Han, P., Keast, R., & Roura, E. (2018). TAS1R1 and TAS1R3 Polymorphisms Relate to Energy and Protein-Rich Food Choices from a Buffet Meal Respectively. *Nutrients*, *10*.

Hänsel, R. (2010). *Pharmakognosie - Phytopharmazie (Springer-Lehrbuch) (German Edition).* (9th ed.). Springer-Lehrbuch. Dordrecht: Springer.

Haug, A., Høstmark, A. T., & Harstad, O. M. (2007). Bovine milk in human nutrition – a review. *Lipids in Health and Disease*, *6*, 25.

Hayden, M. S., & Ghosh, S. (2012). NF-κB, the first quarter-century: remarkable progress and outstanding questions. *Genes & Development*, *26*, 203–234.

Hayes, M., Ross, R. P., Fitzgerald, G. F., Hill, C., & Stanton, C. (2006). Casein-Derived Antimicrobial Peptides Generated by Lactobacillus acidophilus DPC6026. *Applied and Environmental Microbiology*, *72*, 2260–2264.

He, W., Danilova, V., Zou, S., Hellekant, G., Max, M., Margolskee, R. F., & Damak, S. (2002). Partial rescue of taste responses of alpha-gustducin null mice by transgenic expression of alpha-transducin. *Chemical Senses*, *27*, 719–727.

Healey, R. D., Lebhar, H., Hornung, S., Thordarson, P., & Marquis, C. P. (2017). An improved process for the production of highly purified recombinant thaumatin tagged-variants. *Food Chemistry*, *237*, 825–832.

Heda, R., Toro, F., & Tombazzi, C. R. (2024). *StatPearls: Physiology, Pepsin*. Treasure Island (FL).

Henchion, M., Hayes, M., Mullen, A. M., Fenelon, M., & Tiwari, B. (2017). Future Protein Supply and Demand: Strategies and Factors Influencing a Sustainable Equilibrium. *Foods*, *6*.

Hildebrandt, X., Ibrahim, M., & Peltzer, N. (2023). Cell death and inflammation during obesity: "Know my methods, WAT(son)". *Cell Death and Differentiation*, *30*, 279–292.

Hochkogler, C. M., Liszt, K., Lieder, B., Stöger, V., Stübler, A., Pignitter, M., Hans, J., Widder, S., Ley, J. P., Krammer, G. E., & Somoza, V. (2017). Appetite-Inducing Effects of Homoeriodictyol: Two Randomized, Cross-Over Interventions. *Molecular Nutrition & Food Research*, *61*.

Hochkogler, C. M., Rohm, B., Hojdar, K., Pignitter, M., Widder, S., Ley, J. P., Krammer, G. E., & Somoza, V. (2014). The capsaicin analog nonivamide decreases total energy intake from a standardized breakfast and enhances plasma serotonin levels in moderately overweight men after administered in an oral glucose tolerance test: a randomized, crossover trial. *Molecular Nutrition & Food Research*, *58*, 1282–1290.

Holik, A.-K., Schweiger, K., Stoeger, V., Lieder, B., Reiner, A., Zopun, M., Hoi, J. K., Kretschy, N., Somoza, M. M., Kriwanek, S., Pignitter, M., & Somoza, V. (2021). Gastric Serotonin Biosynthesis and Its Functional Role in L-Arginine-Induced Gastric Proton Secretion. *International Journal of Molecular Sciences*, *22*.

Hoon, M. A., Adler, E., Lindemeier, J., Battey, J. F., Ryba, N. J., & Zuker, C. S. (1999). Putative Mammalian Taste Receptors. *Cell*, *96*, 541–551.

Huang, Y. A., Maruyama, Y., & Roper, S. D. (2008). Norepinephrine is coreleased with serotonin in mouse taste buds. *The Journal of Neuroscience*, *28*, 13088–13093.

Huang, Y. A., Pereira, E., & Roper, S. D. (2011). Acid stimulation (sour taste) elicits GABA and serotonin release from mouse taste cells. *PloS One*, *6*, e25471.

Huang, Y.-J., Maruyama, Y., Lu, K.-S., Pereira, E., Plonsky, I., Baur, J. E., Wu, D., & Roper, S. D. (2005). Mouse taste buds use serotonin as a neurotransmitter. *The Journal of Neuroscience*, *25*, 843–847.

Ibrahim, H. R., Ahmed, A. S., & Miyata, T. (2016). Novel angiotensin-converting enzyme inhibitory peptides from caseins and whey proteins of goat milk. *Journal of Advanced Research*, *8*, 63–71.

Inoue, M., Reed, D. R., Li, X., Tordoff, M. G., Beauchamp, G. K., & Bachmanov, A. A. (2004). Allelic variation of the Tas1r3 taste receptor gene selectively affects behavioral and neural taste responses to sweeteners in the F2 hybrids between C57BL/6ByJ and 129P3/J mice. *The Journal of Neuroscience*, *24*, 2296–2303.

Iskandar, M. M., Dauletbaev, N., Kubow, S., Mawji, N., & Lands, L. C. (2013). Whey protein hydrolysates decrease IL-8 secretion in lipopolysaccharide (LPS)-stimulated respiratory epithelial cells by affecting LPS binding to Toll-like receptor 4. *The British Journal of Nutrition*, *110*, 58–68.

Izawa, K., Amino, Y., Kohmura, M., Ueda, Y., & Kuroda, M. (2010). Human–Environment Interactions – Taste. In *Comprehensive Natural Products II* (pp. 631–671): Elsevier.

J. G. Forte (2010). The gastric parietal cell: at home and abroad. *European Surgery*.

Jalševac, F., Terra, X., Rodríguez-Gallego, E., Beltran-Debón, R., Blay, M. T., Pinent, M., & Ardévol, A. (2022). The Hidden One: What We Know About Bitter Taste Receptor 39. *Frontiers in Endocrinology*, *13*, 854718.

Jang, H.-J., Kokrashvili, Z., Theodorakis, M. J., Carlson, O. D., Kim, B.-J., Zhou, J., Kim, H. H., Xu, X., Chan, S. L., Juhaszova, M., Bernier, M., Mosinger, B., Margolskee, R. F., & Egan, J. M. (2007). Gut-expressed gustducin and taste receptors regulate secretion of glucagon-like peptide-1. *Proceedings of the National Academy of Sciences of the United States of America*, *104*, 15069–15074.

Jin, H. Z., Hwang, B. Y., Kim, H. S., Lee, J. H., Kim, Y. H., & Lee, J. J. (2002). Antiinflammatory constituents of Celastrus orbiculatus inhibit the NF-kappaB activation and NO production. *Journal of Natural Products*, *65*, 89–91.

Kadhim, H., Tabarki, B., Verellen, G., Prez, C. de, Rona, A. M., & Sébire, G. (2001). Inflammatory cytokines in the pathogenesis of periventricular leukomalacia. *Neurology*, *56*, 1278–1284.

Kang, J. H., Park, S., Rho, J., Hong, E.-J., Cho, Y.-E., Won, Y.-S., & Kwon, H.-J. (2023). IL-17A promotes Helicobacter pylori-induced gastric carcinogenesis via interactions with IL-17RC. *Gastric Cancer: Official Journal of the International Gastric Cancer Association and the Japanese Gastric Cancer Association*, *26*, 82–94.

Kaske, S., Krasteva, G., König, P., Kummer, W., Hofmann, T., Gudermann, T., & Chubanov, V. (2007). TRPM5, a taste-signaling transient receptor potential ion-channel, is a ubiquitous signaling component in chemosensory cells. *BMC Neuroscience*, *8*, 49.

Kaufman, A., Choo, E., Koh, A., & Dando, R. (2018). Inflammation arising from obesity reduces taste bud abundance and inhibits renewal. *PLoS Biology*, *16*, e2001959.

Kawai, T., & Akira, S. (2010). The role of pattern-recognition receptors in innate immunity: update on Toll-like receptors. *Nature Immunology*, *11*, 373–384.

Kazimierska, K., & Kalinowska-Lis, U. (2021). Milk Proteins-Their Biological Activities and Use in Cosmetics and Dermatology. *Molecules*, *26*.

Kim, E. K., & Choi, E.-J. (2010). Pathological roles of MAPK signaling pathways in human diseases. *Biochimica et Biophysica Acta*, *1802*, 396–405.

Kim, S.-K., Chen, Y., Abrol, R., Goddard, W. A., & Guthrie, B. (2017). Activation mechanism of the G protein-coupled sweet receptor heterodimer with sweeteners and allosteric agonists. *Proceedings of the National Academy of Sciences of the United States of America*, *114*, 2568–2573.

Kohl, S., Behrens, M., Dunkel, A., Hofmann, T., & Meyerhof, W. (2013). Amino acids and peptides activate at least five members of the human bitter taste receptor family. *Journal of Agricultural and Food Chemistry*, *61*, 53–60.

Kovacs-Nolan, J., Zhang, H., Ibuki, M., Nakamori, T., Yoshiura, K., Turner, P. V., Matsui, T., & Mine, Y. (2012). The PepT1-transportable soy tripeptide VPY reduces intestinal inflammation. *Biochimica et Biophysica Acta*, *1820*, 1753–1763.

Kumar, A., Dhawan, S., Hardegen, N. J., & Aggarwal, B. B. (1998). Curcumin (Diferuloylmethane) inhibition of tumor necrosis factor (TNF)-mediated adhesion of monocytes to endothelial cells by suppression of cell surface expression of adhesion molecules and of nuclear factor-kappaB activation. *Biochemical Pharmacology*, *55*, 775–783.

Larson, E. D., Vandenbeuch, A., Voigt, A., Meyerhof, W., Kinnamon, S. C., & Finger, T. E. (2015). The Role of 5-HT3 Receptors in Signaling from Taste Buds to Nerves. *The Journal of Neuroscience*, *35*, 15984–15995.

Lawrence, T. (2009). The nuclear factor NF-kappaB pathway in inflammation. *Cold Spring Harbor Perspectives in Biology*, *1*, a001651.

Le Nevé, B., Foltz, M., Daniel, H., & Gouka, R. (2010). The steroid glycoside H.g.-12 from Hoodia gordonii activates the human bitter receptor TAS2R14 and induces CCK release

from HuTu-80 cells. *American Journal of Physiology-Gastrointestinal and Liver Physiology*, *299*, G1368-75.

Lee, A. A., & Owyang, C. (2017). Sugars, Sweet Taste Receptors, and Brain Responses. *Nutrients*, *9*.

Lee, J.-H., Choi, J. K., Noh, M. S., Hwang, B. Y., Hong, Y. S., & Lee, J. J. (2004). Anti-inflammatory effect of kamebakaurin in in vivo animal models. *Planta Medica*, *70*, 526–530.

Lee, S.-J., Depoortere, I., & Hatt, H. (2019). Therapeutic potential of ectopic olfactory and taste receptors. *Nature Reviews. Drug discovery*, *18*, 116–138.

Li, X., Staszewski, L., Xu, H., Durick, K., Zoller, M., & Adler, E. (2002). Human receptors for sweet and umami taste. *Proceedings of the National Academy of Sciences of the United States of America*, *99*, 4692–4696.

Liao, J., Patel, D., Zhao, Q., Peng, R., Guo, H., & Diwu, Z. (2021). A novel Ca2+ indicator for long-term tracking of intracellular calcium flux. *BioTechniques*, *70*, 271–277.

Lieverse, R. J., Jansen, J. B., Masclee, A. A., & Lamers, C. B. (1994). Satiety effects of cholecystokinin in humans. *Gastroenterology*, *106*, 1451–1454.

Liou, A. P., Sei, Y., Zhao, X., Feng, J., Lu, X., Thomas, C., Pechhold, S., Raybould, H. E., & Wank, S. A. (2011). The extracellular calcium-sensing receptor is required for cholecystokinin secretion in response to L-phenylalanine in acutely isolated intestinal I cells. *American Journal of Physiology-Gastrointestinal and Liver Physiology*, *300*, G538-46.

Liszt, K. I., Eder, R., Wendelin, S., & Somoza, V. (2015). Identification of Catechin, Syringic Acid, and Procyanidin B2 in Wine as Stimulants of Gastric Acid Secretion. *Journal of Agricultural and Food Chemistry*, *63*, 7775–7783.

Liszt, K. I., Hans, J., Ley, J. P., Köck, E., & Somoza, V. (2018). Characterization of Bitter Compounds via Modulation of Proton Secretion in Human Gastric Parietal Cells in Culture. *Journal of Agricultural and Food Chemistry*, *66*, 2295–2300.

Liszt, K. I., Ley, J. P., Lieder, B., Behrens, M., Stöger, V., Reiner, A., Hochkogler, C. M., Köck, E., Marchiori, A., Hans, J., Widder, S., Krammer, G., Sanger, G. J., Somoza, M. M., Meyerhof, W., & Somoza, V. (2017). Caffeine induces gastric acid secretion via bitter taste signaling in gastric parietal cells. *Proceedings of the National Academy of Sciences of the United States of America*, *114*, E6260-E6269.

Liszt, K. I., Walker, J., & Somoza, V. (2012). Identification of organic acids in wine that stimulate mechanisms of gastric acid secretion. *Journal of Agricultural and Food Chemistry*, *60*, 7022–7030.

Liu, H., Tu, M., Cheng, S., Chen, H., Wang, Z., & Du, M. (2019). An anticoagulant peptide from beta-casein: identification, structure and molecular mechanism. *Food & Function*, *10*, 886–892.

Liu, J.-J., Sturrock, R., & Ekramoddoullah, A. K. M. (2010). The superfamily of thaumatin-like proteins: its origin, evolution, and expression towards biological function. *Plant Cell Reports*, *29*, 419–436.

Liu, Z., Wang, Y., Wang, Y., Ning, Q., Zhang, Y., Gong, C., Zhao, W., Jing, G., & Wang, Q. (2016). Dexmedetomidine attenuates inflammatory reaction in the lung tissues of septic mice by activating cholinergic anti-inflammatory pathway. *International Immunopharmacology*, *35*, 210–216.

Maehashi, K., Matano, M., Wang, H., Vo, L. A., Yamamoto, Y., & Huang, L. (2008). Bitter peptides activate hTAS2Rs, the human bitter receptors. *Biochemical and Biophysical Research Communications*, *365*, 851–855.

Mahdi, J. G. (2014). Biosynthesis and metabolism of β-d-salicin: A novel molecule that exerts biological function in humans and plants. *Biotechnology Reports*, *4*, 73–79.

Maizels, M. (1968). Effect of sodium content on sodium efflux from human red cells suspended in sodium-free media containing potassium, rubidium, caesium or lithium chloride. *The Journal of Physiology*, *195*, 657–679.

Malik, V. S., Schulze, M. B., & Hu, F. B. (2006). Intake of sugar-sweetened beverages and weight gain: a systematic review. *The American Journal of Clinical Nutrition*, *84*, 274–288.

Marchbank, T., Elia, G., & Playford, R. J. (2009). Intestinal protective effect of a commercial fish protein hydrolysate preparation. *Regulatory Peptides*, *155*, 105–109.

Mattes, R. D., & Popkin, B. M. (2009). Nonnutritive sweetener consumption in humans: effects on appetite and food intake and their putative mechanisms. *The American Journal of Clinical Nutrition*, *89*, 1–14.

Max, M., Shanker, Y. G., Huang, L., Rong, M., Liu, Z., Campagne, F., Weinstein, H., Damak, S., & Margolskee, R. F. (2001). Tas1r3, encoding a new candidate taste receptor, is allelic to the sweet responsiveness locus Sac. *Nature Genetics*, *28*, 58–63.

Mazda, T., Yamamoto, H., Fujimura, M., & Fujimiya, M. (2004). Gastric distension-induced release of 5-HT stimulates c-fos expression in specific brain nuclei via 5-HT3 receptors in conscious rats. *American Journal of Physiology-Gastrointestinal and Liver Physiology*, *287*, G228-35.

McColl, K. E., el-Omar, E., & Gillen, D. (2000). Helicobacter pylori gastritis and gastric physiology. *Gastroenterology Clinics of North America*, *29*, 687-703, viii.

Meilgaard, M., Meilgaard, M. C., Civille, G. V., & Carr, B. T. (2016). *Sensory evaluation techniques.* (Fifth edition). Boca Raton, London, New York: CRC Press Taylor & Francis Group CRC Press is an imprint of the Taylor & Francis Group an Informa business.

Mejia, E. G. de, & Dia, V. P. (2009). Lunasin and lunasin-like peptides inhibit inflammation through suppression of NF-kappaB pathway in the macrophage. *Peptides*, *30*, 2388–2398.

Meyerhof, W., Batram, C., Kuhn, C., Brockhoff, A., Chudoba, E., Bufe, B., Appendino, G., & Behrens, M. (2010). The molecular receptive ranges of human TAS2R bitter taste receptors. *Chemical Senses*, *35*, 157–170.

Miller, P. E., & Perez, V. (2014). Low-calorie sweeteners and body weight and composition: a meta-analysis of randomized controlled trials and prospective cohort studies. *The American Journal of Clinical Nutrition*, *100*, 765–777.

Minta, A., & Tsien, R. Y. (1989). Fluorescent indicators for cytosolic sodium. *Journal of Biological Chemistry*, *264*, 19449–19457.

Molitor, E. von, Riedel, K., Hafner, M., Rudolf, R., & Cesetti, T. (2020). Sensing Senses: Optical Biosensors to Study Gustation. *Sensors*, *20*.

Montmayeur, J. P., Liberles, S. D., Matsunami, H., & Buck, L. B. (2001). A candidate taste receptor gene near a sweet taste locus. *Nature Neuroscience*, *4*, 492–498.

Morell, P., & Fiszman, S. (2017). Revisiting the role of protein-induced satiation and satiety. *Food Hydrocolloids*, *68*, 199–210.

Moss, S. F., Legon, S., Davies, J., & Calam, J. (1994). Cytokine gene expression in Helicobacter pylori associated antral gastritis. *Gut*, *35*, 1567–1570.

Muschol, M., Dasgupta, B. R., & Salzberg, B. M. (1999). Caffeine interaction with fluorescent calcium indicator dyes. *Biophysical Journal*, *77*, 577–586.

Nam, N.-H. (2006). Naturally occurring NF-kappaB inhibitors. *Mini Reviews in Medicinal Chemistry*, *6*, 945–951.

Nash, M. S., Young, K. W., Challiss, R. A., & Nahorski, S. R. (2001). Intracellular signalling. Receptor-specific messenger oscillations. *Nature*, *413*, 381–382.

Nathan, C., & Ding, A. (2010). Nonresolving inflammation. *Cell*, *140*, 871–882.

Nelson, G., Chandrashekar, J., Hoon, M. A., Feng, L., Zhao, G., Ryba, N. J. P., & Zuker, C. S. (2002). An amino-acid taste receptor. *Nature*, *416*, 199–202.

Nelson, G., Hoon, M. A., Chandrashekar, J., Zhang, Y., Ryba, N. J., & Zuker, C. S. (2001). Mammalian Sweet Taste Receptors. *Cell*, *106*, 381–390.

Ney, K. H. (1971). Voraussage der Bitterkeit von Peptiden aus deren Aminosäurezusammensetzung. *Zeitschrift für Lebensmittel-Untersuchung und -Forschung*, *147*, 64–68.

Nielsen, D. S. G., Theil, P. K., Larsen, L. B., & Purup, S. (2012). Effect of milk hydrolysates on inflammation markers and drug-induced transcriptional alterations in cell-based models. *Journal of Animal Science*, *90 Suppl 4*, 403–405.

Noel, C. A., Sugrue, M., & Dando, R. (2017). Participants with pharmacologically impaired taste function seek out more intense, higher calorie stimuli. *Appetite*, *117*, 74–81.

Nomura, K., Nakanishi, M., Ishidate, F., Iwata, K., & Taruno, A. (2020). All-Electrical Ca2+-Independent Signal Transduction Mediates Attractive Sodium Taste in Taste Buds. *Neuron*, *106*, 816-829.e6.

Ojiro, I., Nishio, H., Yamazaki-Ito, T., Nakano, S., Ito, S., Toyohara, Y., Hiramoto, T., Terada, Y., & Ito, K. (2021). Trp-Trp acts as a multifunctional blocker for human bitter taste receptors, hTAS2R14, hTAS2R16, hTAS2R43, and hTAS2R46. *Bioscience, Biotechnology, and Biochemistry*, *85*, 1526–1529.

Palmer, R. K., Atwal, K., Bakaj, I., Carlucci-Derbyshire, S., Buber, M. T., Cerne, R., Cortés, R. Y., Devantier, H. R., Jorgensen, V., Pawlyk, A., Lee, S. P., Sprous, D. G., Zhang, Z., & Bryant, R. (2010). Triphenylphosphine oxide is a potent and selective inhibitor of the transient receptor potential melastatin-5 ion channel. *Assay and Drug Development Technologies*, *8*, 703–713.

Patel, S., Vetale, S., Teli, P., Mistry, R., & Chiplunkar, S. (2012). IL-10 production in non-small cell lung carcinoma patients is regulated by ERK, P38 and COX-2. *Journal of Cellular and Molecular Medicine*, *16*, 531–544.

Patterson, J. K., Lei, X. G., & Miller, D. D. (2008). The pig as an experimental model for elucidating the mechanisms governing dietary influence on mineral absorption. *Experimental Biology and Medicine*, *233*, 651–664.

Piccolomini, A. F., Iskandar, M. M., Lands, L. C., & Kubow, S. (2012). High hydrostatic pressure pre-treatment of whey proteins enhances whey protein hydrolysate inhibition of oxidative stress and IL-8 secretion in intestinal epithelial cells. *Food & Nutrition Research*, *56*.

Polak-Szczybyło, E., & Tabarkiewicz, J. (2022). IL-17A, IL-17E and IL-17F as Potential Biomarkers for the Intensity of Low-Grade Inflammation and the Risk of Cardiovascular Diseases in Obese People. *Nutrients*, *14*.

Pollock, J. D., & Rowland, N. (1981). Peripherally administered serotonin decreases food intake in rats. *Pharmacology, Biochemistry, and Behavior*, *15*, 179–183.

Pormohammad, A., Mohtavinejad, N., Gholizadeh, P., Dabiri, H., Salimi Chirani, A., Hashemi, A., & Nasiri, M. J. (2019). Global estimate of gastric cancer in Helicobacter pylori-infected population: A systematic review and meta-analysis. *Journal of Cellular Physiology*, *234*, 1208–1218.

Ramsey, I. S., & DeSimone, J. A. (2018). Otopetrin-1: A sour-tasting proton channel. *The Journal of General Physiology*, *150*, 379–382.

Richter, P., Andersen, G., Kahlenberg, K., Mueller, A. U., Pirkwieser, P., Boger, V., & Somoza, V. (2024a). Sodium-Permeable Ion Channels TRPM4 and TRPM5 are Functional in Human Gastric Parietal Cells in Culture and Modulate the Cellular Response to Bitter-Tasting Food Constituents. *Journal of Agricultural and Food Chemistry*, *72*, 4906–4917.

Richter, P., Sebald, K., Fischer, K., Behrens, M., Schnieke, A., & Somoza, V. (2022). Bitter Peptides YFYPEL, VAPFPEVF, and YQEPVLGPVRGPFPIIV, Released during Gastric Digestion of Casein, Stimulate Mechanisms of Gastric Acid Secretion via Bitter Taste

Receptors TAS2R16 and TAS2R38. *Journal of Agricultural and Food Chemistry*, *70*, 11591–11602.

Richter, P., Sebald, K., Fischer, K., Schnieke, A., Jlilati, M., Mittermeier-Klessinger, V., & Somoza, V. (2024b). Gastric digestion of the sweet-tasting plant protein thaumatin releases bitter peptides that reduce H. pylori induced pro-inflammatory IL-17A release via the TAS2R16 bitter taste receptor. *Food Chemistry*, *448*, 139157.

Rizzello, C. G., Losito, I., Gobbetti, M., Carbonara, T., Bari, M. D. de, & Zambonin, P. G. (2005). Antibacterial activities of peptides from the water-soluble extracts of Italian cheese varieties. *Journal of Dairy Science*, *88*, 2348–2360.

Roland, W. S. U., van Buren, L., Gruppen, H., Driesse, M., Gouka, R. J., Smit, G., & Vincken, J.-P. (2013). Bitter taste receptor activation by flavonoids and isoflavonoids: modeled structural requirements for activation of hTAS2R14 and hTAS2R39. *Journal of Agricultural and Food Chemistry*, *61*, 10454–10466.

Roper, S. D. (2007). Signal transduction and information processing in mammalian taste buds. *Pflugers Archiv: European Journal of Physiology*, *454*, 759–776.

Roper, S. D. (2013). Taste buds as peripheral chemosensory processors. *Seminars in Cell & Developmental Biology*, *24*, 71–79.

Roper, S. D., & Chaudhari, N. (2017). Taste buds: cells, signals and synapses. *Nature Reviews. Neuroscience*, *18*, 485–497.

Ross, E. M. (2014). G Protein-coupled receptors: Multi-turnover GDP/GTP exchange catalysis on heterotrimeric G proteins. *Cellular Logistics*, *4*, e29391.

Rozengurt, N., Wu, S. V., Chen, M. C., Huang, C., Sternini, C., & Rozengurt, E. (2006). Colocalization of the alpha-subunit of gustducin with PYY and GLP-1 in L cells of human colon. *American Journal of Physiology-Gastrointestinal and Liver Physiology*, *291*, G792-802.

Rubach, M., Lang, R., Skupin, C., Hofmann, T., & Somoza, V. (2010). Activity-guided fractionation to characterize a coffee beverage that effectively down-regulates mechanisms of gastric acid secretion as compared to regular coffee. *Journal of Agricultural and Food Chemistry*, *58*, 4153–4161.

Ruiz-Avila, L., McLaughlin, S. K., Wildman, D., McKinnon, P. J., Robichon, A., Spickofsky, N., & Margolskee, R. F. (1995). Coupling of bitter receptor to phosphodiesterase through transducin in taste receptor cells. *Nature*, *376*, 80–85.

Sanematsu, K., Yoshida, R., Shigemura, N., & Ninomiya, Y. (2014). Structure, function, and signaling of taste G-protein-coupled receptors. *Current Pharmaceutical Biotechnology*, *15*, 951–961.

Santos-Hernández, M., Tomé, D., Gaudichon, C., & Recio, I. (2018). Stimulation of CCK and GLP-1 secretion and expression in STC-1 cells by human jejunal contents and in vitro gastrointestinal digests from casein and whey proteins. *Food & Function*, *9*, 4702–4713.

Sato, K., Egashira, Y., Ono, S., Mochizuki, S., Shimmura, Y., Suzuki, Y., Nagata, M., Hashimoto, K., Kiyono, T., Park, E. Y., Nakamura, Y., Itabashi, M., Sakata, Y., Furuta, S., & Sanada, H. (2013). Identification of a hepatoprotective peptide in wheat gluten hydrolysate against D-galactosamine-induced acute hepatitis in rats. *Journal of Agricultural and Food Chemistry*, *61*, 6304–6310.

Schattling, B., Steinbach, K., Thies, E., Kruse, M., Menigoz, A., Ufer, F., Flockerzi, V., Brück, W., Pongs, O., Vennekens, R., Kneussel, M., Freichel, M., Merkler, D., & Friese, M. A. (2012). TRPM4 cation channel mediates axonal and neuronal degeneration in experimental autoimmune encephalomyelitis and multiple sclerosis. *Nature Medicine*, *18*, 1805–1811.

Schweiger, K., Grüneis, V., Treml, J., Galassi, C., Karl, C. M., Ley, J. P., Krammer, G. E., Lieder, B., & Somoza, V. (2020). Sweet Taste Antagonist Lactisole Administered in Combination with Sucrose, But Not Glucose, Increases Energy Intake and Decreases Peripheral Serotonin in Male Subjects. *Nutrients*, *12*.

Sebald, K., Dunkel, A., & Hofmann, T. (2020). Mapping Taste-Relevant Food Peptidomes by Means of Sequential Window Acquisition of All Theoretical Fragment Ion-Mass Spectrometry. *Journal of Agricultural and Food Chemistry*, *68*, 10287–10298.

Sebald, K., Dunkel, A., Schäfer, J., Hinrichs, J., & Hofmann, T. (2018). Sensoproteomics: A New Approach for the Identification of Taste-Active Peptides in Fermented Foods. *Journal of Agricultural and Food Chemistry*, *66*, 11092–11104.

Serafini, N., Dahdah, A., Barbet, G., Demion, M., Attout, T., Gautier, G., Arcos-Fajardo, M., Souchet, H., Jouvin, M.-H., Vrtovsnik, F., Kinet, J.-P., Benhamou, M., Monteiro, R. C., & Launay, P. (2012). The TRPM4 channel controls monocyte and macrophage, but not neutrophil, function for survival in sepsis. *Journal of Immunology*, *189*, 3689–3699.

Smith, G. P. (1998). *Satiation: From Gut to Brain*: Oxford University Press.

Smith, J. A. (2003). *USE OF ALPHA-S2 CASEIN PRECURSOR-DERIVED PEPTIDES*. GB20020009384;WO2003GB01439, *A61K8/64;A61K38/17;A61P1/02;A61P17/00;A61P17/16;A61P43/00;A61Q11/00;A61Q19/08;C07K14/47;C07K16/04;A61K38/17;A61K7/48;A61P1/02;A61P17/00;C07K14/47*.

Sonntag, T., Kunert, C., Dunkel, A., & Hofmann, T. (2010). Sensory-guided identification of N-(1-methyl-4-oxoimidazolidin-2-ylidene)-alpha-amino acids as contributors to the thick-sour and mouth-drying orosensation of stewed beef juice. *Journal of Agricultural and Food Chemistry*, *58*, 6341–6350.

Sparrer, D., & Belitz, H. D. (1975). Bittere Peptide aus Casein nach Hydrolyse mit alpha-Chymotrypsin und Trypsin. *Zeitschrift für Lebensmittel-Untersuchung und -Forschung*, *157*, 197–204.

Srikakulapu, P., & McNamara, C. A. (2020). B Lymphocytes and Adipose Tissue Inflammation. *Arteriosclerosis, Thrombosis, and Vascular Biology*, *40*, 1110–1122.

Steensels, S., Vancleef, L., & Depoortere, I. (2016). The Sweetener-Sensing Mechanisms of the Ghrelin Cell. *Nutrients*, *8*.

Sterneder, S., Stoeger, V., Dugulin, C. A., Liszt, K. I., Di Pizio, A., Korntheuer, K., Dunkel, A., Eder, R., Ley, J. P., & Somoza, V. (2021). Astringent Gallic Acid in Red Wine Regulates Mechanisms of Gastric Acid Secretion via Activation of Bitter Taste Sensing Receptor TAS2R4. *Journal of Agricultural and Food Chemistry*, *69*, 10550–10561.

Stoeger, V., Holik, A.-K., Hölz, K., Dingjan, T., Hans, J., Ley, J. P., Krammer, G. E., Niv, M. Y., Somoza, M. M., & Somoza, V. (2020). Bitter-Tasting Amino Acids l-Arginine and l-Isoleucine Differentially Regulate Proton Secretion via T2R1 Signaling in Human Parietal Cells in Culture. *Journal of Agricultural and Food Chemistry*, *68*, 3434–3444.

Stoeger, V., Lieder, B., Riedel, J., Schweiger, K., Hoi, J., Ruzsanyi, V., Klieber, M., Rust, P., Hans, J., Ley, J. P., Krammer, G. E., & Somoza, V. (2019). Wheat Protein Hydrolysate Fortified With l-Arginine Enhances Satiation Induced by the Capsaicinoid Nonivamide in Moderately Overweight Male Subjects. *Molecular Nutrition & Food Research*, *63*, e1900133.

Stoeger, V., Liszt, K. I., Lieder, B., Wendelin, M., Zopun, M., Hans, J., Ley, J. P., Krammer, G. E., & Somoza, V. (2018). Identification of Bitter-Taste Intensity and Molecular Weight as Amino Acid Determinants for the Stimulating Mechanisms of Gastric Acid Secretion in Human Parietal Cells in Culture. *Journal of Agricultural and Food Chemistry*, *66*, 6762–6771.

Strubbe, J. H., & Woods, S. C. (2004). The timing of meals. *Psychological Review*, *111*, 128–141.

Swithers, S. E., Martin, A. A., & Davidson, T. L. (2010). High-intensity sweeteners and energy balance. *Physiology & Behavior*, *100*, 55–62.

Tagliamonte, S., Oliviero, V., & Vitaglione, P. (2024). *Food bioactive peptides: functionality beyond bitterness*.

Takeuchi, O., & Akira, S. (2010). Pattern recognition receptors and inflammation. *Cell*, *140*, 805–820.

Teng, B., Wilson, C. E., Tu, Y.-H., Joshi, N. R., Kinnamon, S. C., & Liman, E. R. (2019). Cellular and Neural Responses to Sour Stimuli Require the Proton Channel Otop1. *Current Biology*, *29*, 3647-3656.e5.

Teschemacher, H., Koch, G., & Brantl, V. (1997). Milk protein-derived opioid receptor ligands. *Biopolymers*, *43*, 99–117.

The UniProt Consortium (2021). UniProt: the universal protein knowledgebase in 2021. *Nucleic Acids Research*, *49*, D480-D489.

Tiroch, J., Dunkel, A., Sterneder, S., Zehentner, S., Behrens, M., Di Pizio, A., Ley, J. P., Lieder, B., & Somoza, V. (2023). Human Gingival Fibroblasts as a Novel Cell Model Describing the Association between Bitter Taste Thresholds and Interleukin-6 Release. *Journal of Agricultural and Food Chemistry*, *71*, 5314–5325.

Tiroch, J., Sterneder, S., Di Pizio, A., Lieder, B., Hoelz, K., Holik, A.-K., Pignitter, M., Behrens, M., Somoza, M., Ley, J. P., & Somoza, V. (2021). Bitter Sensing TAS2R50 Mediates the trans-Resveratrol-Induced Anti-inflammatory Effect on Interleukin 6 Release in HGF-1 Cells in Culture. *Journal of Agricultural and Food Chemistry*, *69*, 13339–13349.

Tu, Y.-H., Cooper, A. J., Teng, B., Chang, R. B., Artiga, D. J., Turner, H. N., Mulhall, E. M., Ye, W., Smith, A. D., & Liman, E. R. (2018). An evolutionarily conserved gene family encodes proton-selective ion channels. *Science (New York, N.Y.)*, *359*, 1047–1050.

Turner, M. D., Nedjai, B., Hurst, T., & Pennington, D. J. (2014). Cytokines and chemokines: At the crossroads of cell signalling and inflammatory disease. *Biochimica et Biophysica Acta*, *1843*, 2563–2582.

Turner, S., Diako, C., Kruger, R., Wong, M., Wood, W., Rutherfurd-Markwick, K., & Ali, A. (2020). Consuming Gymnema sylvestre Reduces the Desire for High-Sugar Sweet Foods. *Nutrients*, *12*.

Tuzim, K., & Korolczuk, A. (2021). An update on extra-oral bitter taste receptors. *Journal of Translational Medicine*, *19*, 440.

Vancleef, L., van den Broeck, T., Thijs, T., Steensels, S., Briand, L., Tack, J., & Depoortere, I. (2015). Chemosensory signalling pathways involved in sensing of amino acids by the ghrelin cell. *Scientific Reports*, *5*, 15725.

Vane, J. R. (1971). Inhibition of prostaglandin synthesis as a mechanism of action for aspirin-like drugs. *Nature: New Biology*, *231*, 232–235.

Vohradský, J. (2001). Neural network model of gene expression. *Federation of American Societies for Experimental Biology*, *15*, 846–854.

Wachsmuth, H. R., Weninger, S. N., & Duca, F. A. (2022). Role of the gut–brain axis in energy and glucose metabolism. *Experimental & Molecular Medicine*, *54*, 377–392.

Walker, J., Reichelt, K. V., Obst, K., Widder, S., Hans, J., Krammer, G. E., Ley, J. P., & Somoza, V. (2016). Identification of an anti-inflammatory potential of Eriodictyon angustifolium compounds in human gingival fibroblasts. *Food & Function*, *7*, 3046–3055.

Wei, Y.-F., Xie, S.-A., & Zhang, S.-T. (2024). Current research on the interaction between Helicobacter pylori and macrophages. *Molecular Biology Reports*, *51*, 497.

Westerterp, K. R. (2006). Perception, passive overfeeding and energy metabolism. *Physiology & Behavior*, *89*, 62–65.

Wrigley, B. J., Lip, G. Y. H., & Shantsila, E. (2011). The role of monocytes and inflammation in the pathophysiology of heart failure. *European Journal of Heart Failure*, *13*, 1161–1171.

Wu, H., Cui, Y., He, C., Gao, P., Li, Q., Zhang, H., Jiang, Y., Hu, Y., Wei, X., Lu, Z., Ma, T., Liu, D., & Zhu, Z. (2020). Activation of the bitter taste sensor TRPM5 prevents high salt-induced cardiovascular dysfunction. *Science China. Life Sciences*, *63*, 1665–1677.

Wurtman, R. J., & Wurtman, J. J. (1995). Brain serotonin, carbohydrate-craving, obesity and depression. *Obesity Research*, *3 Suppl 4*, 477S-480S.

Yang, X.-T., Niu, P.-Q., Li, X.-F., Sun, M.-M., Wei, W., Chen, Y.-Q., & Zheng, J.-Y. (2024). Differential cytokine expression in gastric tissues highlights helicobacter pylori's role in gastritis. *Scientific Reports*, *14*, 7683.

Yao, X., & Forte, J. G. (2003). Cell biology of acid secretion by the parietal cell. *Annual Review of Physiology*, *65*, 103–131.

Yuzuriha, H., Inui, A., Asakawa, A., Ueno, N., Kasuga, M., Meguid, M. M., Miyazaki, J., Ninomiya, M., Herzog, H., & Fujimiya, M. (2007). Gastrointestinal hormones (anorexigenic peptide YY and orexigenic ghrelin) influence neural tube development. *Federation of American Societies for Experimental Biology*, *21*, 2108–2112.

Zeece, M. (2020a). Flavors. In *Introduction to the Chemistry of Food* (pp. 213–250): Elsevier.

Zeece, M. (2020b). *Introduction to the Chemistry of Food*. San Diego: Elsevier Science & Technology.

Zhang, J., Jin, H., Zhang, W., Ding, C., O'Keeffe, S., Ye, M., & Zuker, C. S. (2019). Sour Sensing from the Tongue to the Brain. *Cell*, *179*, 392-402.e15.

Zhao, M., Xu, X.-Q., Meng, X.-Y., & Liu, B. (2018). The Heptahelical Domain of the Sweet Taste Receptor T1R2 Is a New Allosteric Binding Site for the Sweet Taste Modulator Amiloride That Modulates Sweet Taste in a Species-Dependent Manner. *Journal of Molecular Neuroscience*, *66*, 207–213.

Zhou, Z., Xi, R., Liu, J., Peng, X., Zhao, L., Zhou, X., Li, J., Zheng, X., & Xu, X. (2021). TAS2R16 Activation Suppresses LPS-Induced Cytokine Expression in Human Gingival Fibroblasts. *Frontiers in Immunology*, *12*, 726546.

Zopun, M., Lieder, B., Holik, A.-K., Ley, J. P., Hans, J., & Somoza, V. (2018a). Noncaloric Sweeteners Induce Peripheral Serotonin Secretion via the T1R3-Dependent Pathway in Human Gastric Parietal Tumor Cells (HGT-1). *Journal of Agricultural and Food Chemistry*, *66*, 7044–7053.

Zopun, M., Liszt, K. I., Stoeger, V., Behrens, M., Redel, U., Ley, J. P., Hans, J., & Somoza, V. (2018b). Human Sweet Receptor T1R3 is Functional in Human Gastric Parietal Tumor Cells (HGT-1) and Modulates Cyclamate and Acesulfame K-Induced Mechanisms of Gastric Acid Secretion. *Journal of Agricultural and Food Chemistry*, *66*, 4842–4852.

# 6 Appendix

## 6.1 Publication I and published supplementary data

Richter, P., Sebald, K., Fischer, K., Behrens, M., Schnieke, A., & Somoza, V. (2022).
**Bitter Peptides YFYPEL, VAPFPEVF, and YQEPVLGPVRGPFPIIV, Released during Gastric Digestion of Casein, Stimulate Mechanisms of Gastric Acid Secretion via Bitter Taste Receptors TAS2R16 and TAS2R38.**
In: *Journal of Agricultural and Food Chemistry* (Vol. 70, Issue 37, pp. 11591–11602).
American Chemical Society (ACS). https://doi.org/10.1021/acs.jafc.2c05228

JOURNAL OF AGRICULTURAL AND FOOD CHEMISTRY

pubs.acs.org/JAFC

Article

# Bitter Peptides YFYPEL, VAPFPEVF, and YQEPVLGPVRGPFPIIV, Released during Gastric Digestion of Casein, Stimulate Mechanisms of Gastric Acid Secretion *via* Bitter Taste Receptors TAS2R16 and TAS2R38

Phil Richter, Karin Sebald, Konrad Fischer, Maik Behrens, Angelika Schnieke, and Veronika Somoza*

Cite This: *J. Agric. Food Chem.* 2022, 70, 11591−11602

Read Online

ACCESS | Metrics & More | Article Recommendations | Supporting Information

**ABSTRACT:** Eating satiating, protein-rich foods is one of the key aspects of modern diet, although a bitter off-taste often limits the application of some proteins and protein hydrolysates, especially in processed foods. Previous studies of our group demonstrated that bitter-tasting food constituents, such as caffeine, stimulate mechanisms of gastric acid secretion as a signal of gastric satiation and a key process of gastric protein digestion *via* activation of bitter taste receptors (TAS2Rs). Here, we tried to elucidate whether dietary non-bitter-tasting casein is intra-gastrically degraded into bitter peptides that stimulate mechanisms of gastric acid secretion in physiologically achievable concentrations. An *in vitro* model of gastric digestion was verified by casein-fed pigs, and the peptides resulting from gastric digestion were identified by liquid chromatography−time-of-flight-mass spectrometry. The bitterness of five selected casein-derived peptides was validated by sensory analyses and by an *in vitro* screening approach based on human gastric parietal cells (HGT-1). For three of these peptides (YFYPEL, VAPFPEVF, and YQEPVLGPVRGPFPIIV), an upregulation of gene expression of *TAS2R16* and *TAS2R38* was observed. The functional involvement of these TAS2Rs was verified by siRNA knockdown (kd) experiments in HGT-1 cells. This resulted in a reduction of the mean proton secretion promoted by the peptides by up to 86.3 ± 9.9% for TAS2R16kd ($p < 0.0001$) cells and by up to 62.8 ± 7.0% for TAS2R38kd ($p < 0.0001$) cells compared with mock-transfected cells.

**KEYWORDS:** *casein, bitter peptides, gastric acid secretion, bitter taste receptors, HGT-1, gastric digestion*



## 1. INTRODUCTION

The consumption of protein-rich foods and the reduction of fats and carbohydrates are high on the priority list in modern diets. Numerous studies have shown that increased protein intake can reduce food intake and, consequently, the body fat mass and body weight.[1] One of the key studies from the group of Westerterp-Plantenga[2] shows that a higher casein content in the diet of healthy subjects (10% *vs* 25% of energy) leads to an increased feeling of fullness and satiety. Mechanistically, dietary protein has been shown to stimulate the release of hormones in the intestine, such as glucagon-like peptide 1 (GLP-1), cholecystokinin, and peptide YY, which promote the feeling of satiation.[3] For example, the plasma concentration of GLP-1, which is released in the ileum and colon, increased after administration of a high-protein breakfast (60% protein) compared to a high-fat or high-carbohydrate breakfast.[4]

However, mechanisms of satiation are not only initiated during digestion in the intestines but also already in the stomach. Here, food ingredients regulate gastric motility and emptying as well as gastric acid secretion.[5] Dietary satiating effects have been demonstrated not only for complex proteins but also for a number of their constituents, namely, peptides and amino acids.[6]

Besides the effects on hormones promoting satiation, a reduction of food intake by dietary proteins can also be achieved by regulation of the so-called "hunger hormone" ghrelin, which promotes the feeling of hunger.[7] In a previous study by Blom *et al.*,[8] mean gastric ghrelin release was reduced by 46% after intake of a high-protein diet (58.1% of energy from protein and 14.1% of energy from carbohydrate) as compared to a high-carbohydrate diet (19.3% of energy from protein and 47.3% of energy from carbohydrate). A similar involvement of the stomach in the regulation of food intake was shown by Uchida *et al.*,[9] where administration of a dose of 1 g per kg body weight of the bitter-tasting amino acid L-arginine to male Sprague−Dawley rats resulted in slowing of gastric emptying. In one of our own previous studies, L-arginine also promoted slowing of gastric emptying and a decrease in energy intake in healthy subjects.[10] In addition, ingestion of L-arginine-enriched wheat protein hydrolysate increased plasma concentrations of the satiating neurotransmitter serotonin.[10]

For L-arginine, one of the most bitter-tasting amino acids in our diet, our group also demonstrated a stimulation of cellular mechanisms regulating gastric acid secretion in cultured

Received: July 24, 2022
Revised: August 13, 2022
Accepted: August 15, 2022
Published: September 2, 2022

human parietal cells (HGT-1) *via* TAS2R1 signaling.[11,12] The underlying hypothesis of bitter-taste-sensing chemoreceptors being involved in gastric acid secretion was verified by preceding experiments, showing that the bitter-tasting caffeine stimulates (i) proton secretion *via* TAS2R signaling in TAS2R43 CRISPR-Cas9-edited human parietal HGT-1 cells in culture and (ii) promotes gastric acid secretion in healthy subjects, which was reduced by co-administration of the TAS2R antagonist homoeriodictyol.[13] Notably, administration of bitter-masking homoeriodictyol not only reduced the caffeine-evoked effect on gastric acid secretion but also increased gastric motility and emptying, decreased peripheral serotonin levels, and stimulated appetite.[14]

From a physiological perspective, the stomach is able to sense peptides and amino acids, which then regulates the release of hormones gastrin and motilin, stimulating gastric acid secretion as well as gastric motility and emptying.[15] Motilin receptors are activated not only by the hormone itself but also by agonists such as the bitter-tasting drug erythromycin, which activates TAS2R10[16] or denatonium benzoate, targeting various TAS2Rs. In addition to amino acids,[11] peptides present in casein hydrolysates are well-known for their bitter taste.[17] Already seven decades ago, the bitter taste of dairy products was ascribed to casein peptides generated upon casein hydrolysis.[18] The molecular mechanisms underlying the bitter taste of casein peptides have been elucidated more recently, that is, by Maehashi *et al.*[19] who demonstrated that casein hydrolysates activate TAS2R16 in transfected HEK293 cells. Since then, several peptides have been demonstrated to activate a number of bitter receptors, namely TAS2R1, TAS2R4, TAS2R14, TAS2R39, and TAS2R46,[20] although no specific peptide sequences are known to chiefly result in TAS2R16 activation, and peptides do not conform with the so far identified selectivity of TAS2R16 for $\beta$-D-glucopyranosides.

Activation of the G-protein-coupled TAS2Rs in gastric parietal cells is based on binding of taste-active compounds, resulting in increased enzymatic activity of phospholipase C $\beta$2.[13] In some cases, the presence of agonists in the nanomolar range is sufficient to activate TAS2Rs.[21,22] The product resulting from the phospholipase C $\beta$2 activity, phosphatidylinositol-4,5-bisphosphate ($PIP_2$), is cleaved into diacylglycerol and inositol trisphosphate ($IP_3$), which leads to calcium release from the endoplasmic reticulum.[23] The increased calcium concentration in the cell promotes the activity of $H^+$,$K^+$-ATPase, which transports protons out of the parietal cell by cleaving ATP.[24] Similarly, activation of the G-protein-coupled receptors $H_2$ by histamine and $M_3$ by acetylcholine increases proton secretion in gastric parietal cells. Binding of acetylcholine also causes activation of phospholipase C $\beta$2, and receptor $H_2$ activates adenylyl cyclase, which catalyzes the formation of cAMP.[25] For the proposed mechanism of proton secretion induced by bitter compounds in parietal cells, see Supporting Information Figure-SI 1.

Dietary intake of bitter compounds is recognized by TAS2Rs located on taste cells of the tongue's taste buds. However, structural changes of food constituents during gastric digestion may also lead to the formation of compounds with bitter taste quality, which are not sensed as bitter tasting due to the lack of appropriate nerve connections between the stomach and the brain. For example, tryptic digestion of bovine casein releases peptides that have a bitter taste, whereas the intact protein does not taste bitter.[26] The formation of peptides in the stomach is catalyzed by the gastric enzyme pepsin.[27] Its inactive precursor pepsinogen is autocatalytically cleaved into the active form pepsin at pH values below 6.[28] Pepsin preferably cleaves next to the amino acids phenylalanine, tyrosine, and leucine, but it is able to hydrolyze almost all peptide bonds.[29] At pH 7 and higher, the enzyme denatures irreversibly.

In this work, we hypothesize (i) that bitter peptides are formed during gastric digestion of non-bitter-tasting bovine casein, and (ii) that these bitter peptides have an effect on mechanisms regulating gastric acid secretion *via* TAS2Rs. Verification of this hypothesis could foster research on taste qualities of dietary proteins and their potential as food constituents that help to modulate food intake and, ultimately, maintain a healthy body weight.

## 2. MATERIALS AND METHODS

**2.1. Chemicals.** 1,5-Carboxy-seminaphtorhodafluor acetoxymethylester (SNARF-1-AM) and Dulbecco's modified Eagle's medium GlutaMAX (DMEM) were purchased from Thermo Fisher Scientific. Fetal bovine serum (FBS Supreme), trypsin/ethylenediaminetetraacetic acid, and penicillin−streptomycin were obtained from PAN-Biotech GmbH (Aidenbach, Germany). Phosphate buffered saline was bought from Biozym Scientific GmbH (Hessisch Oldendorf, Germany). Dimethyl sulfoxide (DMSO) was purchased from Carl Roth (Karlsruhe, Germany). $CaCl_2$, casein from bovine milk, 3-(4,5-dimethylthiazol-2-yl)-2,5-diphenyltetrazolium bromide (MTT), D-glucose, formic acid, HCl, 4-(2-hydroxyethyl)-1-piperazineethanesulfonic acid (HEPES), KCl, $KH_2PO_4$, KOH, MeCN, $MgCl_2(H_2O)_6$, $MgSO_4$, NaCl, $NaHCO_3$, $(NH_4)_2CO_3$, and pepsin from porcine gastric mucosa were ordered from Merck KGaA (Darmstadt, Germany). Custom peptides (PVVVPPFLQPEVM, VAPFPEVF, YFYPEL, YQEPVLGPVRGPFPIIV, and YYVPLGTQ) were synthesized by Genscript Biotech with a purity of >95% (New Jersey, USA). Double-distilled water ($ddH_2O$) from Elga Purelab Classic (Veolia Water Solutions & Technologies, France) was used for all experiments. Krebs-Ringer−HEPES buffer (KRHB) contains 130 mM NaCl, 4.7 mM KCl, 1.3 mM $CaCl_2$, 1.2 mM $MgSO_4$, 1.2 mM $KH_2PO_4$, 11.7 mM D-glucose, and 10 mM HEPES; the pH was adjusted to 7.4 with KOH.

**2.2. *In Vitro* Digestion.** The *in vitro* digestion was based on the Nature protocol established by Brodkorb *et al.*[30] For this, simulated salivary fluid (SSF, containing 15.1 mM KCl, 3.7 mM $KH_2PO_4$, 13.6 mM $NaHCO_3$, 0.15 mM $MgCl_2(H_2O)_6$, 0.06 mM $(NH_4)_2CO_3$, 1.1 mM HCl, and 1.5 mM $CaCl_2(H_2O)_2$) and simulated gastric fluid (SGF, containing 6.9 mM KCl, 0.9 mM $KH_2PO_4$, 25.0 mM $NaHCO_3$, 47.2 mM NaCl, 0.12 mM $MgCl_2(H_2O)_6$, 0.5 mM $(NH_4)_2CO_3$, 15.6 mM HCl, and 0.15 mM $CaCl_2(H_2O)_2$) were prepared. A total amount of 100 mg casein was suspended in 3 mL of SSF and incubated for 5 min at 37 °C in the tube rotator. After taking a sample (500 $\mu$L, $t$ = 0 h), 2 mL of SGF was added and the pH was adjusted to 3 with 100 $\mu$L of HCl (1 M). After addition of 125 $\mu$L of pepsin solution (80,000 U/mL in 10 mM HCl), 275 $\mu$L of $H_2O$ was added to fill up to 5 mL. This was followed by further incubation at 37 °C in a tube rotator for 6 h. 500 $\mu$L of samples was taken at 0.25, 0.5, 0.75, 1, 2, 3, 4, 5, and 6 h, respectively. The samples were frozen in liquid nitrogen and stored at −80 °C until further analysis. For MS experiments, all samples were diluted 1:1 with 10% MeCN. To prepare the casein hydrolysate after 1 h of digestion for use in cell assays, the samples were desalted (20 mL $H_2O$ + 0.1% formic acid) by solid phase extraction (HyperSep C18, 5 g, Thermo Scientific) and peptide fraction was then eluted with 20 mL each of 20% MeCN + 0.1% formic acid and 60% MeCN + 0.1% formic acid.[31]

**2.3. *In Vivo* Digestion.** For *in vivo* experiments, 1 g of casein was suspended in 5 mL of $H_2O$ and fed to pigs (German Landrace, German Landrace × minipig, age: 16−27 weeks). After 2 h, the pigs were anesthetized and killed and the stomach was removed. The stomach contents were aliquoted, frozen in liquid nitrogen, and stored


https://doi.org/10.1021/acs.jafc.2c05228
J. Agric. Food Chem. 2022, 70, 11591−11602

at −80 °C until further analysis. To remove any impurities, the samples were desalted (1 mL $H_2O$ + 0.1% formic acid) by solid phase extraction (Discovery DSC-18, 100 mg, Sigma-Aldrich) and the peptide fraction was then eluted with 750 μL each of 20% MeCN + 0.1% formic acid and 60% MeCN + 0.1% formic acid. After solvent removal, the peptides were dissolved in 5% MeCN.

**2.4. Ultra-performance Liquid Chromatography−Time-of-Flight Mass Spectrometry and Peptide Identification.** Measurements were performed using a Sciex ExionLC AC (Sciex, Darmstadt, Germany) coupled to a Sciex TripleTOF 6600 mass spectrometer (Sciex, Darmstadt, Germany). Data acquisition and instrumentation control were performed with AnalystTF software (v 1.7.1; Sciex, Darmstadt, Germany). Separation was performed using a 100 × 2.1 mm, 1.7 μm, Kinetex C18 column (Phenomenex, Aschaffenburg, Germany) with a guard column of the same type with 0.1% aqueous formic acid and acetonitrile containing 0.1% formic acid at a flow rate of 0.3 mL/min. The gradient was based on the following scheme: 0 min, 5% B; 0.5 min, 5% B; 14 min, 40% B; 15 min, 98% B; 16 min, 98% B; 17 min, 5% B; and 20 min, 5% B. The column oven temperature was set at 40 °C, and the injection volume was 1 μL per sample. For ToF-MS measurements, the same parameters[32,33] were used for all samples (ion spray voltage 5500 eV, source temperature 550 °C, nebulizing gas 55 psi, and heating gas 65 psi). Nitrogen was set to 35 psi and served as a curtain gas to effectively dissolve the ions. In IDA mode, a ToF-MS survey scan was acquired from $m/z$ 100 to 1500 using an accumulation time of 250 ms (declustering potential DP 80 V and collision energy CE 10 V). Product ion spectra for the 15 most abundant compounds in the $m/z$ range of 100−1500 were recorded in high sensitivity mode for 50 ms (DP 80 V, CE 45 V, CE spread *CES* 15 V). MaxQuant software (v 1.6.3.4; Max Planck Institute of Biochemistry, Planegg, Germany) compares the data found in the recorded MS/MS spectra with in silico-generated spectra.[34] With the selected settings (peptide length between 4 and 25 amino acids, unspecific digestion, variable modifications: oxidation M, acetyl protein N-term, carbamidomethyl C, phospho STY, andromeda score > 10) and imported sequences of $\alpha_{S1}$-casein (UniProt P02662), $\alpha_{S2}$-casein (UniProt P02663), $\beta_{A1}$-casein (UniProt P02666, natural variant A1), $\beta_{A2}$-casein (UniProt P02666, natural variant A2), and κ-casein (UniProt P02668), which have lengths between 190 and 224 amino acids, ≈12,000 different peptides are possible. The specific cleavage pattern of pepsin limits the number of peptides that can be generated. However, in order not to exclude the pepsin-independent formation of peptides caused by gastric acid, an enzyme-independent in silico digest with all possible ≈12,000 peptide spectra was chosen.

**2.5. Quantitative $^1$H Nuclear Magnetic Resonance Spectroscopy.** The synthesized reference peptides were dissolved in $D_2O$. 600 μL of each of the peptide solutions was loaded into NMR tubes (178 × 5 mm inner diameter, USC tubes, Bruker, Rheinstetten, Germany) and analyzed using a 400 MHz Avance III NMR spectrometer (Bruker, Rheinstetten, Germany). Instrument calibration and data processing were performed as detailed earlier.[35] The specific proton resonance signal at 3.55 ppm (s, 3H) of the external standard caffeine (3.58 mmol/L) was used for calibration. The calibration was verified immediately before the measurement with L-tyrosine (4.34 mmol/L, 7.10 ppm, d, 2H).

**2.6. Targeted Proteomics.** All targeted proteomics LC−MS/MS measurements were performed using a Sciex ExionLC AC (Sciex, Darmstadt, Germany) coupled to a 6500+ QTrap LC−MS/MS system (Sciex, Darmstadt, Germany) operating in the positive electrospray ionization mode. Data acquisition and instrumentation control were performed with AnalystTF software (v 1.7.1; Sciex, Darmstadt, Germany). Separation was performed using a 100 × 2.1 mm, 1.7 μm, Kinetex C18 column (Phenomenex, Aschaffenburg, Germany) with a guard column of the same type with 0.1% aqueous formic acid and acetonitrile containing 0.1% formic acid at a flow rate of 0.25 mL/min. The gradient was based on the following scheme: 0 min, 15% B; 7 min, 40% B; 7.5 min, 98% B; 10.5 min, 98% B; 10.8 min, 15% B; and 15 min, 15% B. The column oven temperature was set at 40 °C, and the injection volume was 1 μL per sample. For MS/MS measurements, the same parameters were used for all samples (ion spray voltage 5500 eV, source temperature 450 °C, nebulizing gas 60 psi, and heating gas 30 psi). Nitrogen was set to 35 psi and served as a curtain gas to effectively dissolve the ions. To optimize the parameters DP, CE, and collision cell exit potential for each peptide and transition (Supporting Information Table-SI 2), standard solutions of the five synthesized peptides were injected directly into the MS ion source. Ionization parameters were optimized in positive ESI mode using AnalystTF software (v 1.7.1; Sciex, Darmstadt, Germany). For the preparation of the calibration curves, five peptides were dissolved individually in $D_2O$ (600 μL) and the concentration of the stock solutions was determined by qNMR.[35] For each peptide, seven calibration solutions (0.5, 1, 5, 10, 50, 100, and 200 μM) were diluted in 5% MeCN from these stock solutions. The data were analyzed using MultiQuant software (v 3.0.3; Sciex, Darmstadt, Germany).

**2.7. Sensory Study.** To verify the bitterness of the selected peptides, each peptide was dissolved in bottled, non-carbonated water (1.5 mM) and tested by 17 panelists in a three-alternative forced choice (3-AFC) test against the bottled, non-carbonated water.[36] To prevent ingestion of toxic substances, the purity of the peptides was checked (>95%, LC−MS) and the solutions were spit out and not swallowed.

**2.8. Cell Culture.** Human gastric tumor cells (HGT-1), provided by Dr. C. Laboisse, Nantes (France), were cultivated at 37 °C in a humidified atmosphere at 5% $CO_2$ in DMEM containing 10% FBS and 1% penicillin and streptomycin. Cells between passages 15 and 29 were used for all experiments. 50,000 cells per well were seeded 1 day before the experiment into a transparent 96-well plate, for cell viability assays, or into a black 96-well plate, for proton secretion assays. For the detection of gene expression, 800,000 cells per well were seeded into a T25 cell culture flask.

**2.9. Cell Viability.** To exclude cytotoxic effects of all used substances on HGT-1 cells, their metabolic activity was tested using MTT dye. For this purpose, cells were treated with solutions of casein (10 μM), hydrolysates (10 μM), peptides (250 μM), and probenecid (1 mM) in KRHB or the transfection reagents for either 30 min or 72 h under standard conditions. The solutions were removed, and 100 μL of MTT solution (0.83 mg/mL in DMEM) was added to each well. After another incubation for 15 min under standard conditions, the MTT solution was removed, and the formed formazan was dissolved in DMSO. Absorbance was measured at 570 nm (reference 650 nm) using an Infinite M200 plate reader (Tecan, Switzerland). Cell viability was calculated relative to cells treated with KRHB only (=100%).

**2.10. Proton Secretion Assay.** The measurement of proton secretion from HGT-1 cells represents a well-established model for the identification of bitter compounds. By affecting extraoral bitter taste receptors with bitter compounds, a modulatory effect on proton secretion can be measured. For this purpose, cells were washed with KRHB and incubated with 3 μM of the intracellular pH indicator 1,5 carboxy-seminaphto-rhodafluor acetoxymethyl ester (SNARF-1-AM) under standard conditions. After 30 min, the cells were washed again with KRHB and then incubated with casein (0.01−10 μM equimolar related to the relevant forms $\alpha_{S1}$- and β-casein), hydrolysate (0.01−10 μM), or the peptides (0.01−200 μM). For co-incubation experiments, peptides were incubated together with probenecid (1 mM). All substances were dissolved and diluted in KRHB. 1 mM histamine was used as a positive control. Measurements were performed using FlexStation 3 (Molecular Devices, USA). The excitation wavelength was 488 nm, and the emission wavelengths were 580 and 640 nm. For calibration (pH range 7.0−8.0), the intracellular and extracellular pH was adjusted with 2 μM nigericin in potassium buffer (20 mM NaCl, 110 mM KCl, 1 mM $CaCl_2$, 1 mM $MgSO_4$, 18 mM D-glucose, and 20 mM HEPES). The intracellular proton index (IPX) was calculated as the log2 value of the 580/640 ratio and compared with cells without treatment. Negative values represent increased secretion of protons and therefore stimulation of mechanisms regulating gastric acid secretion in HGT-1 cells. In contrast, positive values represent an inhibition of secretion compared to the untreated control.


https://doi.org/10.1021/acs.jafc.2c05228
J. Agric. Food Chem. 2022, 70, 11591−11602

**2.11. Quantitation of mRNA Expression.** For mRNA expression analysis, 800,000 cells were seeded in a T25 cell culture flask (25 $cm^2$) 1 day before the experiment. After incubation with 17.5 $\mu$M VAPFPEVF, 0.03 $\mu$M YFYPEL, or 0.4 $\mu$M YQEPVLGPVRGPFPIIV for 15, 30, 60, and 120 min, RNA was isolated using the peqGOLD RNA Kit (VWR Peqlab, USA) following the manufacturer's protocol. Determination of RNA concentration (A260/A280 between 2.03 and 2.09) was performed on a NanoDrop One$^c$ (Thermo Fisher Scientific Inc., USA). RNA integrity number (RIN 9.9−10.0, version 2.6, assay class Eukaryote Total RNA Nano) was analyzed using a 2100 Bioanalyzer (Agilent Technologies, USA). Removal of gDNA and synthesis of cDNA were performed using the iScript gDNA Clear cDNA Synthesis Kit (BioRad, Feldkirchen, Germany) following the manufacturer's protocol. Real-time-qPCR (RT-qPCR) was performed with 50 ng cDNA amplified with SsoAdvanced Universal SYBR Green Supermix (Bio-Rad Laboratories, Inc., USA). The sequences of the forward and reverse primers of the 25 TAS2Rs were taken from Liszt *et al.*[13] (Supporting Information Table-SI 3). Verified primers for the TAS1Rs (TAS1R1: qHsaCID0013443; TAS1R2: qHsaCID0016106; TAS1R3: qHsaCED0002321) and for MAPK1 (qHsaCEP0050000) were obtained from Bio-Rad Laboratories. PPIA[37] and GAPDH[38] were used as reference genes. The effects of the peptides on gene expression were analyzed in comparison to untreated control cells.

**2.12. Transient Knock-Down of TAS2R16 or TAS2R38 Expression in HGT-1 Cells.** Expression of TAS2R16 and TAS2R38 was reduced by treatment of HGT-1 cells with siRNA. 100,000 cells per well were seeded 1 day before the experiment into a 24-well plate. All reagents and siRNA were purchased from Thermo Fisher Scientific, USA (cytotoxicity was excluded by MTT). Transfection was performed with Lipofectamine RNAiMAX in Opti-Medium according to the manufacturer's protocol. 1−50 nM of different siRNA sequences (HSS121396 and HSS181763 for TAS2R16 and HSS108754 and HSS108756 for TAS2R38) and three different incubation times (24, 48, and 72 h) were tested. Mock control experiments were performed analogously with 1 or 10 nM Stealth RNAi siRNA negative control. To verify the functionality of the transfection process, verified 10 nM siRNA targeting MAPK1 (VHS40312) was used (positive control). The transfection rate was checked by qPCR as described in section 2.11. For the proton secretion assays, 20,000 cells per well were seeded 1 day before transfection into a black 96-well plate. After 72 h of transfection, proton secretion activities of TAS2R16 knock-down or TAS2R38 knock-down HGT-1 were compared with the mock transfected cells by means of ΔIPX.

**2.13. Statistical Analysis.** All data are presented as mean ± standard error of the mean (SEM) unless otherwise indicated. At least three biological replicates were prepared from each experiment. Statistical analyses of different treatments with the untreated control were performed using the one-way ANOVA Holm-Šidák *post hoc* test or *t*-test Holm-Šidák method, after the Nalimov outlier test. Different $p$ values are indicated with asterisks according to the following scheme: * = $p \leq 0.05$, ** = $p \leq 0.01$, *** = $p \leq 0.001$, **** = $p \leq 0.0001$.

## 3. RESULTS AND DISCUSSION

**3.1. *In Vitro* Digestion under Gastric Conditions Produces Bitter Peptides.** Protein digestion in the human stomach is essentially characterized by two important aspects: one is the low pH caused by gastric acid. The other is the presence of the enzyme pepsin, which cleaves peptide bonds.[28] In order to elucidate the formation of peptides during digestion of casein over a wide time spectrum, samples were taken for identification at seven different time points during a simulated *in vitro* digestion (0−6 h of digestion). All samples were analyzed in four biological replicates in untargeted ToF-MS-IDA mode.

After the first hour, 77.8 ± 9.8 different peptides were identified increasing to 91.3 ± 2.2 after 2 h. At all later time points, no major changes in the number of peptides were detected (3 h: 87.5 ± 9.6, 4 h: 94.0 ± 11.9, 5 h: 93.3 ± 13.5, and 6 h: 97.0 ± 12.9), but a large number of different peptides were found. Comparison of the resulting peptides at all 6 time points resulted in a peptide library of 238 different casein peptides (67 for $\alpha_{S1}$-casein, 21 for $\alpha_{S2}$-casein, 21 for $\beta_{A1}$-casein, 30 for $\beta_{A2}$-casein, 62 for $\beta_{A1/A2}$-casein, and 37 for $\kappa$-casein). To exclude possible peptide contamination of the casein used, a sample was also taken before reduction of pH to 3 and addition of the enzyme pepsin (0 h). Here, 2.5 ± 1.1 peptides were identified. To assess if pH change alone caused peptide formation, incubation of casein at pH 3 and 7 without pepsin was carried out over the same time period. This resulted in the formation of 3.6 ± 1.4 (at pH 3) and 4.0 ± 0.8 (at pH 7) peptides within 6 h, respectively. It shows that the low pH alone is not sufficient to release peptides from casein. Nevertheless, the low pH is necessary to ensure the activity of pepsin since it denatures at higher pH values.[28]

To focus on the most important peptide candidates in the next experiments, the following criteria were used for selection. The Andromeda score indicates how closely a spectrum generated in silico matches the measured MS/MS spectra. Above an Andromeda score of 100, the identified peptides match in almost all cases.[39] Therefore, only peptides with a score above 150 were considered. As a result, peptide selection was limited to the following 11: FVAPFPEVF ($\alpha_{S1}$-$CN_{24-32}$), INNQFLPYPYYAKPAA ($\kappa$-$CN_{51-66}$), LTDVENLHLPLPLL ($\beta_{A2}$-$CN_{127-140}$), PVVVPPFLQPEVM ($\beta_{A1/A2}$-$CN_{81-93}$), TDVENLHLPLPLL ($\beta_{A2}$-$CN_{128-140}$), TDVENLHLPLPLLQS ($\beta_{A2}$-$CN_{128-142}$), VAPFPEVF ($\alpha_{S1}$-$CN_{25-32}$), YFYPEL ($\alpha_{S1}$-$CN_{144-149}$), YQEPVLGPVRGPFPIIV ($\beta_{A1/A2}$-$CN_{193-209}$), YTDAPSF ($\alpha_{S1}$-$CN_{173-179}$), and YYVPLGTQ ($\alpha_{S1}$-$CN_{165-172}$).

To predict bitterness in the second step, three different prediction tools were applied. First, the $Q$ values of the peptides were calculated, indicating the average hydrophobicity.[33,40] Only one peptide (YTDAPSF; $Q$ value = 1323) had a value below 1400 cal/mol and was excluded. The two tools iBitter-SCM[41] and BERT4Bitter[42] predict the bitterness of peptides based on their amino acids and their sequence. This allowed the number of peptides to be reduced to six. Although both FVAPFPEVF (iBitter-SCM score 451.3) and VAPFPEVF (iBitter-SCM score 469.3) are predicted to be bitter peptides according to all three tools, FVAPFPEVF was excluded to avoid the study of peptides with overlapping sequences.

The sequences of the five selected peptides are PVVVPPFLQPEVM ($\beta_{A1/A2}$-$CN_{81-93}$), VAPFPEVF ($\alpha_{S1}$-$CN_{25-32}$), YFYPEL ($\alpha_{S1}$-$CN_{144-149}$), YQEPVLGPVRGPFPIIV ($\beta_{A1/A2}$-$CN_{193-209}$), and YYVPLGTQ ($\alpha_{S1}$-$CN_{165-172}$). All of these peptides selected were released from $\alpha_{S1}$- or $\beta$-casein, with the peptides derived from $\beta$-casein found in both natural variants (A1 and A2). The fact that $\alpha_{S1}$- and $\beta$-casein represent the majority of casein present in cow's milk (38.4% and 36.5%) is another aspect in favor of the five selected peptides.[43]

To verify the five selected peptides, synthesized reference peptides were purchased and ultra-high performance liquid-chromatography (UHPLC)−MS/MS-MRM spectra were recorded (Supporting Information Figure-SI 2A). The retention times [ultra-performance liquid chromatography (UPLC)] and SRM mass transitions (MS/MS) of peptides in *in vitro* samples were compared with the previously recorded


https://doi.org/10.1021/acs.jafc.2c05228
J. Agric. Food Chem. 2022, 70, 11591−11602

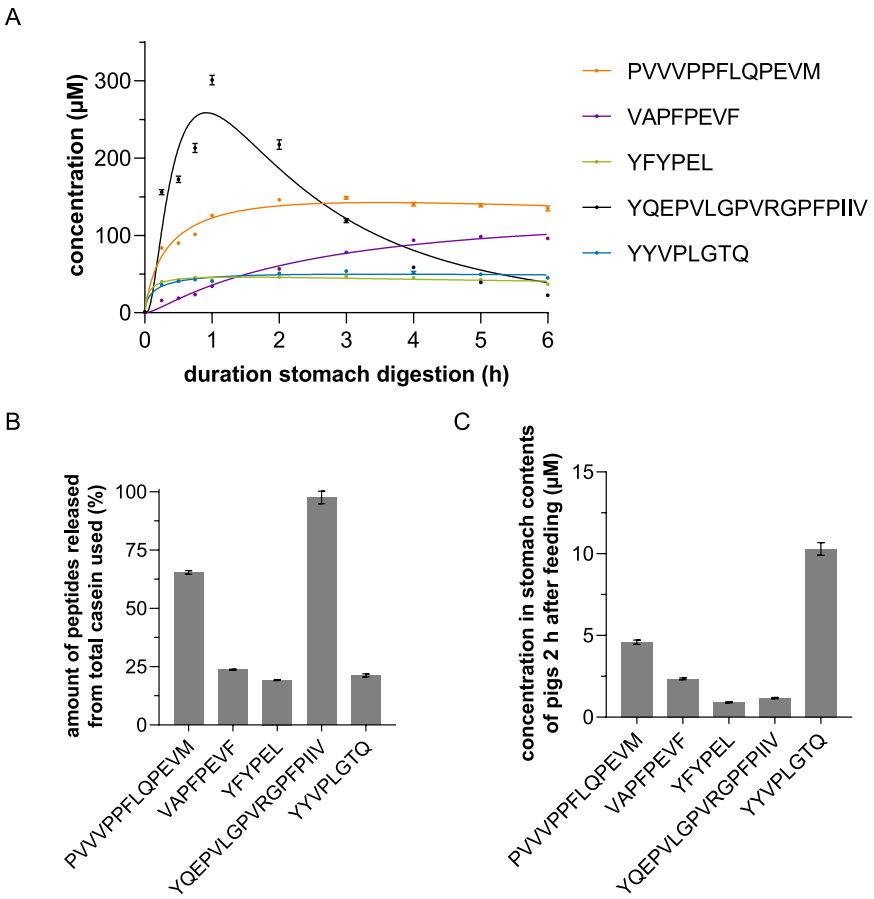


**Figure 1.** (A) Peptide concentrations in the course of in vitro digestion. Samples were taken after 0, 0.25, 0.5, 0.75, 1, 2, 3, 4, 5, and 6 h of digestion and quantitated by means of targeted UHPLC−MS/MS-MRM measurements. Data shown as mean ± SEM, $n$ = 4, transitions per peptide = 5. (B) Release rates of the five investigated peptides related to $\alpha_{S1}$- or $\beta$-casein after 2 h of in vitro digestion. Data are shown as mean ± SEM, $n$ = 4, transitions per peptide = 5. (C) Concentrations of the five investigated peptides related to $\alpha_{S1}$- or $\beta$-casein after 2 h of in vivo digestion. Data are shown as mean ± SEM, $n$ = 6, transitions per peptide = 5.

spectra of externally synthesized peptides. The identification of all five selected peptides was clearly confirmed (Supporting Information Figure-SI 2B). For quality control, reference solutions were analyzed between LC−MS measurements of the samples. The following recovery rates were obtained: PVVVPPFLQPEVM: 102.6 ± 2.2%, VAPFPEVF: 100.0 ± 3.6%, YFYPEL: 97.5 ± 3.7%, YQEPVLGPVRGPFPIIV: 103.5 ± 2.1%, and YYVPLGTQ: 97.2 ± 4.9%.

All five selected peptides have already been described in the literature as cleavage products of casein digestion.[44] Various bioactivities have already been found for three of the peptides. YQEPVLGPVRGPFPIIV is the best known representative and exhibits antimicrobial[45] and immunomodulatory abilities[46] as well as angiotensin-converting-enzyme inhibitory activity.[47] YFYPEL was found to increase the expression of MUC5AC in human intestinal cells. The resulting increase in the mucus barrier may prevent gastrointestinal diseases.[48] In addition, transport through Caco-2 cell monolayers was observed for YQEPVLGPVRGPFPIIV and PVVVPPFLQPEVM.[49]

After verifying the formation of the selected peptides in *in vitro* digestion, sensory analyses were performed to confirm their bitter taste. After purity tests by reversed-phase-(HPLC) and quantitative $^1$H NMR, Three AFC tests ($n$ = 17−18) of all peptides (1.5 mM in water) were performed against two samples containing water. This showed that all five peptides exhibit a distinct bitter taste (Supporting Information Figure-SI 5, $p \leq 0.001$). The results of the bitter prediction tools used at the beginning could be confirmed. This demonstrates that bitter peptides were released during the gastric digestion of non-bitter casein.

**3.2. Monitoring of the Formation of Bitter Peptides PVVVPPFLQPEVM, VAPFPEVF, YFYPEL, YQEPVLGPVRGPFPIIV, and YYVPLGTQ during *In Vitro* Digestion.** To investigate the formation and degradation of peptides during digestion, their concentrations were determined at different time points. For this purpose, a suitable LC−MS/MS-MRM method was developed. Since the untargeted measurements of the samples showed a high release of different peptides already in the first hour of *in vitro* digestion, a sample was taken every 15 min for quantitation within the first hour (Figure 1A). The *in vitro* digestion was highly reproducible, showing only small deviations between experiments (SEM).

The highest release was observed for the peptides YQEPVLGPVRGPFPIIV (up to 300.8 µM) and PVVVPPFLQPEVM (up to 148.7 µM). While PVVVPPFLQPEVM was not further degraded during the digestion, YQEPVLGPVRGPFPIIV underwent a continuous cleavage over the 6 h, so that its final concentration was lower (22.5 µM) than that of all other peptides analyzed. For example, the peptides YQEPVLG ($\beta_{A1/A2}$-CN$_{193-199}$) and PVRGPFPIIV ($\beta_{A1/A2}$-CN$_{200-209}$) were identified as cleavage


https://doi.org/10.1021/acs.jafc.2c05228
J. Agric. Food Chem. 2022, 70, 11591−11602

products (for all peptide fragments found, see Supporting Information Figure-SI 7). The peptides VAPFPEVF, YFYPEL, and YYVPLGTQ were released in lower concentrations at the beginning (between 34.3 and 42.3 $\mu$M after 1 h), and there is no noticeable degradation during further digestion, similar to PVVVPPFLQPEVM.

No formation of the five peptides in the control digests at pH 3 and 7 without pepsin could be detected by the targeted measurements.

**3.3. Selected Peptides Are Also Formed during *In Vivo* Digestion Experiments.** To confirm that the peptides formed *in vitro* are also generated *in vivo*, feeding experiments were performed in pigs, as the function of their digestive tract is very similar to humans.[50] The pH of the stomach contents was 2.9 ± 0.7, close to the *in vitro* conditions. Two hours after administration of casein, the stomach content of the animals was analyzed in six biological replicates by means of LC−MS/MS and LC−ToF-MS in IDA mode as detailed in sections 3.1 and 3.2. This resulted in a peptide library consisting of 270 peptides. All previously identified peptides from the *in vitro* approaches after 2 h ($n$ = 4) were found in this library. The high correlation of peptides formed *in vitro* and *in vivo* is consistent with the results described by Egger *et al.*[51]

In particular, the five selected peptides were unambiguously identified in both ToF-MS-IDA and targeted UHPLC−MS/MS-MRM measurements (Supporting Information Figure-SI 2C). The quantitation was also performed analogously to the *in vitro* samples. As the volume of gastric contents varied between 100 and 1000 mL, the concentrations of released peptides were normalized to 100 mL gastric volume. The concentrations of the five peptides ranged from 0.91 ± 0.03 $\mu$M for YFYPEL to 10.30 ± 0.38 $\mu$M for YYVPLGTQ (Figure 1C). The release rates of the peptides were lower than those during *in vitro* digestion. This could be due to incomplete suspension of the ingested casein.

**3.4. Determination of Physiological Concentrations of Peptides in the Stomach.** In order to study meaningful effects of peptides on human digestion, it is essential to determine concentrations that are actually achievable in the stomach after habitual dietary intake of dairy products. The concentrations of peptides released from $\alpha_{S1}$- and $\beta$-casein in *in vitro* and *in vivo* digestion were in a micromolar range. A similar range of casein concentrations can be expected in the human stomach after ingestion of dairy products. This is based on the assumption that 1 L of cow's milk contains about 27.5 g of casein,[17] with $\alpha_{S1}$-casein ($m_w$ = 24.5 kDa; UniProt: P02662) and $\beta$-casein ($m_w$ = 25.1 kDa; UniProt: P02666) accounting for 38.4% and 36.5%, respectively,[43] resulting in maximum concentrations of 460 $\mu$M for $\alpha_{S1}$-casein or 425 $\mu$M for $\beta_{A1/A2}$-casein. However, the actual concentrations are likely to be much lower due to dilution by gastric acid. In addition, pepsin cleaves at different sites within the amino acid sequences, leading to the formation of competing peptides with similar sequences and consequently to a lower release of the peptides under investigation. Depending on the sequence, the peptides were released in variable amounts (related to the respective casein variant). The peptide YQEPVLGPVRGPFPIIV showed the highest release after 2 h with almost 100% (Figure 1B). One reason for this could be the position of the sequence at the C-terminus of $\beta$-casein. In addition, pepsin preferably cleaves between tyrosine and leucine.[29] The release rates of the other peptides ranged from 19.3% (YFYPEL) to 65.5% (PVVVPPFLQPEVM). In the case of YQEPVLGPVRGPFPIIV, further degradation took place during the course of digestion, resulting in low concentrations of parental peptides. For these reasons, peptide concentrations between 0.01 and 200 $\mu$M were chosen for further experiments.

**3.5. Effect of Casein-Derived Bitter Peptides on Mechanisms Regulating Gastric Acid Secretion by HGT-1 Cells.** To cover the range of physiological concentrations of the selected peptides possible in the human stomach, peptide concentrations between 0.01 and 200 $\mu$M were chosen as described above. Cell viability after incubation with the peptides, hydrolysate, and intact casein was tested before (≥97.5% compared to control).

In order to check if intact casein (before digestion) already has an effect on the proton secretion of HGT-1 cells, the impact of 0.01−10 $\mu$M casein (equimolar related to the relevant forms $\alpha_{S1}$- and $\beta$-casein) was analyzed by proton secretion assay. The intercellular proton index IPX indicates the secretory activity. Negative values represent increased secretion of protons and therefore stimulation of mechanisms regulating gastric acid secretion in HGT-1 cells. In contrast, positive values represent an inhibition of secretions compared to the untreated control. No significant change in mean IPX was found for casein concentrations below 5 $\mu$M (Figure 2).

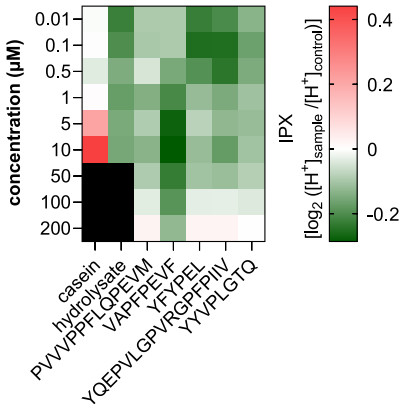


**Figure 2.** Heatmap showing the change in mean secretory activity (IPX) in HGT-1 cells on incubation with casein (equimolar related to the relevant forms $\alpha_{S1}$- and $\beta$-casein), casein-hydrolysate (equimolar related to the relevant forms $\alpha_{S1}$- and $\beta$-casein; after 1 h of gastric digestion), and the five selected peptides PVVVPPFLQPEVM, VAPFPEVF, YFYPEL, YQEPVLGPVRGPFPIIV, and YYVPLGTQ at concentrations between 0.01 and 10 or 200 $\mu$M. Red shades represent inhibition of activity (positive IPX values) and green shades represent stimulation of proton secretion (negative IPX values). Data are shown as mean after incubation for 10 min, $n$ = 4−8, t.r. = 4−6.

Treatment of the HGT-1 cells with casein concentrations of 5 $\mu$M (ΔIPX = +0.212 ± 0.029; $p \leq 0.001$) and 10 $\mu$M (ΔIPX = +0.441 ± 0.037; $p \leq 0.0001$) inhibited proton secretion. This shows that intact casein at low concentrations has no effect on mechanisms regulating gastric acid secretion by HGT-1 cells, whereas higher concentrations have a regulatory effect and inhibit secretion. Investigation of the effects of higher concentrations was not possible due to the poor solubility of casein.

To test the effects of peptides produced during digestion on proton secretion, cells were incubated with 0.01−10 $\mu$M casein hydrolysate (after 1 h of gastric digestion). It was found that concentrations between 5 and 10 $\mu$M did not inhibit mechanisms regulating gastric acid secretion (Figure 2). At


https://doi.org/10.1021/acs.jafc.2c05228
J. Agric. Food Chem. 2022, 70, 11591−11602

concentrations of 0.01 and 0.1 $\mu$M hydrolysate, significant ($p \leq 0.05$) stimulation of secretion was detected, with ΔIPX changes of −0.222 ± 0.046 and −0.199 ± 0.055, respectively. Consequently, the peptides produced during gastric digestion of non-bitter casein as a mixture have a stimulating effect on mechanisms regulating gastric acid secretion, suggesting that bitter-tasting peptides, among others, were released. For all five selected peptides, a significant hormetic concentration-dependent influence on the secretory activity was found. Holik *et al.*[52] showed a hormetic dose−response when HGT-1 cells were incubated with L-arginine. HGT-1 cells released more serotonin when treated with lower L-arginine concentrations (10 mM) than with higher L-arginine concentrations (50 mM). This effect was additionally found upon serotonin-induced stimulation of proton secretion from HGT-1 cells.

While significant ΔIPX was analyzed for the peptide PVVVPPFLQPEVM at 1 and 10 $\mu$M only, the other four peptides showed a significant increase in secretory activities of HGT-1 cells over a wider concentration range. Incubation with VAPFPEVF at a concentration of 10 $\mu$M showed the highest change in ΔIPX with −0.286 ± 0.037 ($p \leq 0.0001$; Supporting Information Figure-SI 3). In addition, also the peptides YFYPEL (0.1 $\mu$M; ΔIPX −0.253 ± 0.027; $p \leq 0.0001$), YQEPVLGPVRGPFPIIV (0.1 $\mu$M; ΔIPX −0.203 ± 0.048; $p \leq 0.0001$), and YYVPLGTQ (0.1 $\mu$M; ΔIPX −0.166 ± 0.017; $p \leq 0.0001$) stimulated the secretion of protons (Figure 2).

Interestingly, the IPX profiles of YFYPEL and YQEPVLGPVRGPFPIIV were very similar. Despite different lengths, different side chains, and different origins (YFYPEL ($\alpha_{S1}$-$CN_{144-149}$) and YQEPVLGPVRGPFPIIV ($\beta_{A1/A2}$-$CN_{193-209}$)), both peptides show great similarity in concentration-dependent stimulating mechanisms, regulating gastric acid secretion in HGT-1 cells (Supporting Information Figure-SI 3).

Overall, mechanisms regulating proton secretion by HGT-1 cells were not affected by low concentrations of casein (<5 $\mu$M), whereas they were inhibited at concentrations of 5 $\mu$M and higher compared to untreated cells. In contrast, the peptide mixture consisting of casein hydrolyzed by pepsin already demonstrated stimulatory effects on the mechanisms regulating proton secretion by HGT-1 cells. This was consistent with the result that bitter peptides were also produced during the digestion process, which cause even greater stimulation of proton secretion when administered in their isolated forms. The three peptides with the greatest effects on proton secretory activity (VAPFPEVF, YFYPEL, and YQEPVLGPVRGPFPIIV) were selected to investigate their effects on taste (TAS1R) and bitter (TAS2R) receptor gene expression.

**3.6. Bitter Peptides Affect the Expression of Various Bitter Receptors, Especially TAS2R16 and TAS2R38.** To determine which peptide concentrations between the tested 0.01−200 $\mu$M have the highest impact on secretory activity, a curve fit calculation was performed for each peptide (Supporting Information Figure-SI 4). The minima obtained represent the respective concentrations with the lowest IPX values, thereby showing highest impact on secretory activity. Incubation of HGT-1 cells with VAPFPEVF (17.5 $\mu$M), YFYPEL (0.03 $\mu$M), and YQEPVLGPVRGPFPIIV (0.4 $\mu$M) resulted in both up- and down-regulation of bitter receptor gene expressions at all four time points investigated (Figure 3 and Supporting Information Table-SI 1). Expression of *TAS2R60* could not be detected in HGT-1 cells, either with

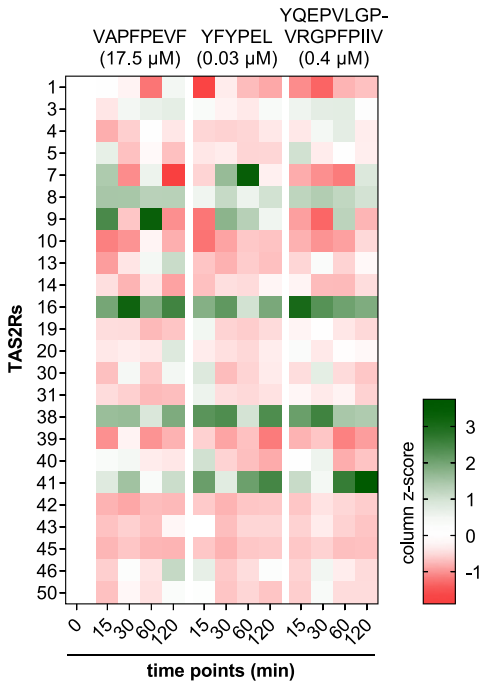


**Figure 3.** Auto-scaled changes (column z-score) in gene expressions of 24 bitter receptors at each time point found in HGT-1 cells after incubation for 15/30/60/120 min with VAPFPEVF (17.5 $\mu$M), YFYPEL (0.03 $\mu$M), or YQEPVLGPVRGPFPIIV (0.4 $\mu$M). Normalized to the expression of PPIA and GAPDH (reference genes). Data are shown as mean, $n$ = 3−5, t.r. = 3.

or without treatment. The change in gene expression for *TAS2R16* and *TAS2R38* was differently affected (Figure 4). *TAS2R41* showed variable upregulation after treatment with the peptides but did not reach statistical significance (Figure 3).

For *TAS2R16*, an upregulation was found at all time points and for all three peptides ($p \leq 0.05$). The highest fold changes in the regulation of *TAS2R16* were found for VAPFPEVF (3.70 ± 0.97, $p < 0.0001$, df = 16, $t$ = 5.4), YFYPEL (3.19 ± 0.50, $p < 0.0001$, df = 16, $t$ = 6.3), and YQEPVLGPVRGPFPIIV (3.46 ± 0.58, $p < 0.0001$, df = 16, $t$ = 7.4), respectively, after an incubation with the respective peptide of 30 min (Figure 4, top). Since all three peptides caused an upregulation ($p \leq 0.05$) of gene expression of the *TAS2R16* at all time points between 15 min and 2 h, it was hypothesized that this receptor plays a crucial role in the increased secretion of gastric acid in HGT-1 cells incubated with bitter peptides. It has already been observed that *TAS2R16*, among other bitter receptors, is targeted by peptides from casein hydrolysates.[19]

In addition, upregulation of *TAS2R38* was also observed. For peptides with similar IPX profiles YFYPEL and YQEPVLGPVRGPFPIIV, this regulation was also significant ($p \leq 0.05$) at all time points (Figure 4, bottom). When HGT-1 cells were incubated with the peptide VAPFPEVF, no significant changes in gene regulation of *TAS2R38* could be detected after 15 and 60 min, while this was the case after 30 (2.42 ± 0.55, $p < 0.01$, df = 15, $t$ = 3.1) and 120 min (2.45 ± 0.26, $p < 0.01$, df = 15, $t$ = 3.8).

The most effective upregulation of gene expression for each peptide was observed for VAPFPEVF on *TAS2R16*, as described above, for YFYPEL (after 60 min, fold change 6.71 ± 1.56, $p < 0.05$, df = 14, $t$ = 2.6) in TAS2R7 and for

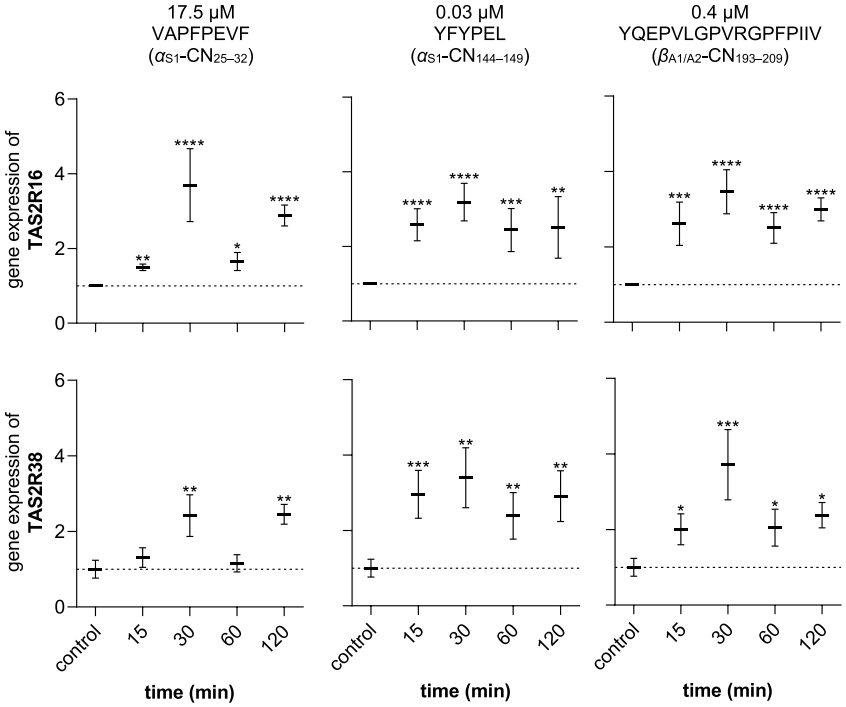


**Figure 4.** Changes in gene expressions (fold change) of bitter receptors TAS2R16 (top) and TAS2R38 (bottom) after incubation with peptides VAPFPEVF (17.5 $\mu$M; left), YFYPEL (0.03 $\mu$M; center), and YQEPVLGPVRGPFPIIV (0.4 $\mu$M; right) for 15/30/60/120 min. Normalized to the expression of PPIA and GAPDH (reference genes). Data are shown as mean ± SEM, $n$ = 3−5, t.r. = 3, statistics: $t$-test Holm-Šidák method; significant differences are expressed with * = $p \leq 0.05$, ** = $p \leq 0.01$, *** = $p \leq 0.001$, **** = $p \leq 0.0001$.

YQEPVLGPVRGPFPIIV (after 120 min, fold change 4.61 ± 2.03, $p \leq 0.01$, df = 14, $t$ = 3.1) in *TAS2R41*. The most pronounced down-regulation was found for *TAS2R10* for all three peptides after incubation with VAPFPEVF after 15 min (0.34 ± 0.05, $p < 0.0001$, df = 16, $t$ = 6.1), with YFYPEL after 30 min (0.41 ± 0.05, $p < 0.001$, df = 16, $t$ = 4.2), and with YQEPVLGPVRGPFPIIV after 15 min (0.52 ± 0.06, $p < 0.01$, df = 16, $t$ = 4.0) (Supporting Information Table-SI 1).

Taken together, it was found that the gene expression of *TAS2R16* and *TAS2R38* was significantly upregulated after only 15 min of incubation in the case of almost all three bitter peptides. This upregulation became even stronger after 30 min. This indicates that these two receptors play a decisive role in the mechanism of gastric acid secretion from HGT-1 cells, when they are treated with bitter peptides. For TAS2R16, a high specificity for glycosides has been found in the past,[53] whereas TAS2R38 is known for the perception of phenylthiocarbamides.[54,55] However, no prior knowledge existed regarding the effect of the peptides identified here on TAS2R16 and TAS2R38. To validate the involvement of these two receptors, knock-down experiments were performed in HGT-1 cells.

**3.7. Peptides Slightly Affect the Expression of Taste Receptors TAS1R.** Proton secretion has been shown in the past to be affected not only by bitter substances involving TAS2Rs but also by sweeteners.[56] For this reason, the gene expression of TAS1R1, TAS1R2, and TAS1R3 was investigated. While the receptors responsible for umami taste, TAS1R1 and TAS1R3, could be detected in HGT-1 cells, no gene expression of TAS1R2 was found. Consequently, no heterodimer of TAS1R2 and TAS1R3 can be formed and, therefore, no sweet taste sensing can be hypothesized by HGT-1 cells, as previously reported.[56] After incubation of HGT-1 cells with the selected peptides, a significant increase ($p < 0.0001$, df = 16, $t$ = 5.6) in the expression of TAS1R3 was found only for 0.03 $\mu$M YFYPEL after 15 min and a decrease ($p < 0.001$, df = 16, $t$ = 4.3) in the expression of TAS1R1 after 30 min (Supporting Information Figure-SI 6, center). No significant changes in TAS1R1 and TAS1R3 expression were detected after 60 and 120 min. Also, peptides VAPFPEVF (17.5 $\mu$M) and YQEPVLGPVRGPFPIIV (0.4 $\mu$M) had no significant effect on the expression (Supporting Information Figure-SI 6). Overall, the changes in the expression of *TAS1R1* and *TAS1R3* were minor compared to those of the bitter receptor genes and, presumably, of only minor biological significance.

**3.8. Impact of TAS2R16 and TAS2R38 on Peptide-Induced Stimulation of Proton Secretion in HGT-1 Cells.** To verify the involvement of TAS2R16 and TAS2R38 in the increased proton secretion after incubation of HGT-1 cells with the bitter peptides, the cells were co-treated with 1 mM of the TAS2R16 and TAS2R38 antagonist probenecid (cell viability ≥ 97.5% compared to control). Probenecid is known to selectively inhibit TAS2R16, TAS2R38, and TAS2R43.[57] HGT-1 cells treated with the bitter peptides alone (VAPFPEVF (17.5 $\mu$M), YFYPEL (0.03 $\mu$M), and YQEPVLGPVRGPFPIIV (0.4 $\mu$M)) showed increased proton secretion compared to untreated control cells ($p < 0.01$). Co-incubation with probenecid (1 mM) reduced this stimulation back to baseline levels (for VAPFPEVF ΔIPX = +0.043 ± 0.031; $p > 0.92$; for YFYPEL ΔIPX = −0.001 ± 0.019; $p > 0.99$; for YQEPVLGPVRGPFPIIV ΔIPX = −0.020 ± 0.036; $p > 0.99$), so that no changes in proton secretion could be detected anymore compared to untreated cells (Figure 5A).

To confirm the respective involvement of TAS2R16 and TAS2R38 in the increased proton secretion by HGT-1 cells,

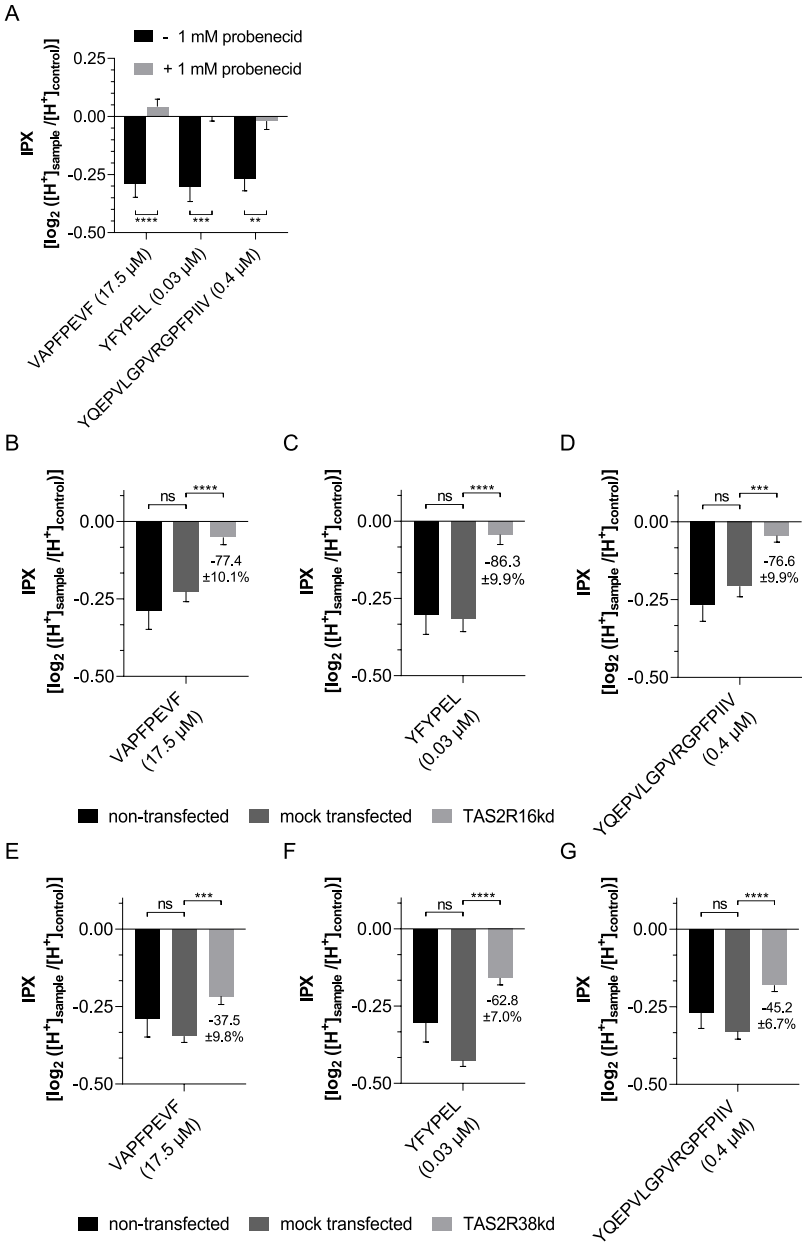


**Figure 5.** Effect on proton secretion after incubation with VAPFPEVF (17.5 $\mu$M), YFYPEL (0.03 $\mu$M), and YQEPVLGPVRGPFPIIV (0.4 $\mu$M), respectively, of (A) HGT-1 cells with (light gray bars) and without (black bars) 1 mM probenecid; (B−D) non-transfected (black bars), mock-transfected (dark gray bars), and TAS2R16kd (light gray bars) HGT-1 cells; and (E−G) non-transfected (black bars), mock-transfected (dark gray bars), and TAS2R38kd (light gray bars) HGT-1 cells. Data are shown as mean ± SEM after incubation for 10 min, $n$ = 4−8, t.r. = 4−12, control: KRHB, statistics: one-way ANOVA Holm-Šidák post hoc test; significant differences are expressed with ** = $p \leq 0.01$, *** = $p \leq 0.001$, **** = $p \leq 0.0001$.

knock-down experiments were performed. The highest knock-down efficiency was observed by RT-qPCR after 72 h of transfection with 10 nM siRNA targeting *TAS2R16* (HSS121396) and 1 nM siRNA targeting *TAS2R38* (HSS108754), respectively. The expression of *TAS2R16* was reduced to 42.2 ± 1.7% ($p < 0.001$) and to 62.8 ± 10.7% ($p < 0.01$) for *TAS2R38* (Supporting Information Figure-SI 6). Cytotoxic effects of siRNA were excluded before performing the experiments (≥97.5% compared to control). Cell viability after transfection was 93.2 ± 1.2% (compared to DMEM control), which is consistent with the manufacturer's data. To monitor the transfection process, the expression of MAPK1 was reduced to 60.2 ± 3.9% ($p < 0.01$).

To investigate the involvement of TAS2R16 in the increased proton secretion activity induced by incubation with the peptides, the proton secretion assays were repeated with TAS2R16kd and mock transfected HGT-1 cells. This showed that the increase in proton secretion activity in TAS2R16kd cells was decreased by 77.4 ± 10.1% for VAPFPEVF (17.5 $\mu$M, $p < 0.0001$), by 86.3 ± 9.9% for YFYPEL (0.03 $\mu$M, $p < 0.0001$), and by 76.6 ± 9.9% for YQEPVLGPVRGPFPIIV (0.4 $\mu$M, $p < 0.001$) (Figure 5B). Analogously, the stimulatory effect of bitter peptides in TAS2R38kd HGT-1 cells also


https://doi.org/10.1021/acs.jafc.2c05228
J. Agric. Food Chem. 2022, 70, 11591−11602

decreased. Stimulation by incubation with VAPFPEVF was reduced by 37.5 ± 9.8% (17.5 μM, $p < 0.001$), with YFYPEL by 62.8 ± 7.0% (0.03 μM, $p < 0.0001$), and with YQEPVLGPVRGPFPIIV by 45.2 ± 6.7% (0.4 μM, $p < 0.0001$) (Figure 5C).

Mock-transfected cells showed no significant differences from non-transfected cells in both cases. TAS2R-independent histamine-induced stimulation of proton secretion does not differ from non-transfected cells in either mock-transfected or TAS2R16 or TAS2R38 knockdown HGT-1 cells (Supporting Information Figure-SI 9). This shows that the secretory activity of the cells was not affected by transfection, except for the receptor in question.

The above results indicate that both TAS2R16 and TAS2R38 play a functional role in the increased proton secretion by HGT-1 cells exposed to the bitter peptides tested. Therefore, we conclude that bitter peptides released from casein during gastric digestion modulate digestive processes, namely, proton secretion activity, involving TAS2R16 and TAS2R38. Since proton secretion stimulated by bitter peptides was reduced to a greater extent in TAS2R16kd than in TAS2R38kd HGT-1 cells, it can be assumed that although both receptors are involved in the mechanism, TAS2R16 may be of higher functional importance. However, one has to note that differences in the effect size may also be caused by the different transfection efficiencies, as the gene expression of TAS2R16 was reduced by 20% more than that of TAS2R38.

A response of TAS2R16 to peptides in casein hydrolysates has already been detected by Maehashi *et al.*[19] Here, HEK293 cells expressing either TAS2R1, TAS2R4, TAS2R14, or TAS2R16 responded to casein hydrolysates. While activation of TAS2R1, TAS2R4, and TAS2R14 by amino acids and peptides could be confirmed by Kohl *et al.*, no unambiguous peptide sequences leading to activation of either TAS2R16 or TAS2R38 have yet been identified.[20] Our results indicate that both TAS2R16 and TAS2R38 play functional roles in the increased proton secretion in HGT-1 cells by the tested bitter peptides with clearly identified sequences at physiologically achievable concentrations.

In conclusion, our results demonstrate that bitter peptides are released from the non-bitter protein casein during gastric digestion. While intact casein had no or higher concentrations of inhibitory effect on proton secretion, representing a key mechanism of gastric acid secretion of HGT-1 cells, casein hydrolysate induced a stimulation. This effect was further enhanced upon treatment with isolated bitter peptides. While qPCR data suggest involvement of TAS2R16 and TAS2R38, co-incubation experiments with the antagonist probenecid showed that by blocking both receptors, no significant stimulation of mechanisms regulating gastric acid secretion was measurable, indicating a functional role of TAS2R16 and TAS2R38. These results were confirmed by knock-down experiments in which the gene expression of *TAS2R16* and *TAS2R38* was reduced by means of siRNA. Therefore, we verified a functional role of TAS2R16 and TAS2R38 in the bitter peptide-mediated stimulation of proton secretion in HGT-1 cells. This implicates a role of bitter peptides released during gastric cleavage from non-bitter-tasting proteins on gastric response mechanisms regulating digestion and food intake. Future clinical trials are warranted to determine respective effect sizes in human subjects in order to fully elucidate the potential of such peptides to modulate food intake and help to maintain a healthy body weight.

## ■ ASSOCIATED CONTENT

### Supporting Information

The Supporting Information is available free of charge at https://pubs.acs.org/doi/10.1021/acs.jafc.2c05228.

Changes in gene expression of the bitter receptors after incubation with peptides, optimized MS parameters for each peptide and transition, sequences of the primer pairs used for RT-qPCR, illustration of the proposed mechanism of proton secretion induced by bitter compounds in HGT-1 cells, comparison of retention times (UPLC) and SRM mass transitions (MS/MS) of the five peptides, effect on the proton secretion of HGT-1 cells incubated with VAPFPEVF, YFYPEL, and YQEPVLGPVRGPFPIIV, curve fit calculations of the proton secretion profile, results of sensory experiments, changes in gene expression of the TAS1Rs after incubation with peptides, identified degradation products of YQEPVLGPVRGPFPIIV, results of transient transfection, and results of histamine-induced stimulation of proton secretion of non-transfected and transfected HGT-1 cells (PDF)

## ■ AUTHOR INFORMATION


### Corresponding Author

**Veronika Somoza** − *Leibniz Institute for Food Systems Biology at the Technical University of Munich, 85354 Freising, Germany; Chair of Nutritional Systems Biology, TUM School of Life Sciences, Technical University of Munich, 85354 Freising, Germany; Department of Physiological Chemistry, Faculty of Chemistry, University of Vienna, 1090 Wien, Austria;* orcid.org/0000-0003-2456-9245; Phone: +49-8161-71-2700; Email: v.somoza.leibniz-lsb@tum.de

### Authors

**Phil Richter** − *Leibniz Institute for Food Systems Biology at the Technical University of Munich, 85354 Freising, Germany;* orcid.org/0000-0003-1026-4926

**Karin Sebald** − *Leibniz Institute for Food Systems Biology at the Technical University of Munich, 85354 Freising, Germany*

**Konrad Fischer** − *Chair of Livestock Biotechnology, TUM School of Life Sciences, Technical University of Munich, 85354 Freising, Germany*

**Maik Behrens** − *Leibniz Institute for Food Systems Biology at the Technical University of Munich, 85354 Freising, Germany;* orcid.org/0000-0003-2082-8860

**Angelika Schnieke** − *Chair of Livestock Biotechnology, TUM School of Life Sciences, Technical University of Munich, 85354 Freising, Germany*

Complete contact information is available at: https://pubs.acs.org/10.1021/acs.jafc.2c05228


### Notes

The authors declare no competing financial interest.

## ■ REFERENCES


(1) Moon, J.; Koh, G. Clinical Evidence and Mechanisms of High-Protein Diet-Induced Weight Loss. *J. Obes. Metab. Syndr.* **2020**, *29*, 166−173.

(2) Veldhorst, M. A. B.; Nieuwenhuizen, A. G.; Hochstenbach-Waelen, A.; Westerterp, K. R.; Engelen, M. P. K. J.; Brummer, R.-J.

M.; Deutz, N. E. P.; Westerterp-Plantenga, M. S. Comparison of the effects of a high- and normal-casein breakfast on satiety, "satiety" hormones, plasma amino acids and subsequent energy intake. *Br. J. Nutr.* **2009**, *101*, 295−303.
(3) Austin, J.; Marks, D. Hormonal Regulators of Appetite. *Int. J. Pediatr. Endocrinol.* **2009**, *2009*, 141753.
(4) van der Klaauw, A. A.; Keogh, J. M.; Henning, E.; Trowse, V. M.; Dhillo, W. S.; Ghatei, M. A.; Farooqi, I. S. High protein intake stimulates postprandial GLP1 and PYY release. *Obesity* **2013**, *21*, 1602−1607.
(5) Cummings, D. E.; Overduin, J. Gastrointestinal regulation of food intake. *J. Clin. Invest.* **2007**, *117*, 13−23.
(6) Kondrashina, A.; Brodkorb, A.; Giblin, L. Dairy-derived peptides for satiety. *J. Funct. Foods* **2020**, *66*, 103801.
(7) Tschöp, M.; Smiley, D. L.; Heiman, M. L. Ghrelin induces adiposity in rodents. *Nature* **2000**, *407*, 908−913.
(8) Blom, W. A. M.; Lluch, A.; Stafleu, A.; Vinoy, S.; Holst, J. J.; Schaafsma, G.; Hendriks, H. F. J. Effect of a high-protein breakfast on the postprandial ghrelin response. *Am. J. Clin. Nutr.* **2006**, *83*, 211−220.
(9) Uchida, M.; Kobayashi, O.; Saito, C. Correlation Between Gastric Emptying and Gastric Adaptive Relaxation Influenced by Amino Acids. *J. Neurogastroenterol. Motil.* **2017**, *23*, 400−408.
(10) Stoeger, V.; Lieder, B.; Riedel, J.; Schweiger, K.; Hoi, J.; Ruzsanyi, V.; Klieber, M.; Rust, P.; Hans, J.; Ley, J. P.; Krammer, G. E.; Somoza, V. Wheat Protein Hydrolysate Fortified With l-Arginine Enhances Satiation Induced by the Capsaicinoid Nonivamide in Moderately Overweight Male Subjects. *Mol. Nutr. Food Res.* **2019**, *63*, No. e1900133.
(11) Stoeger, V.; Holik, A.-K.; Hölz, K.; Dingjan, T.; Hans, J.; Ley, J. P.; Krammer, G. E.; Niv, M. Y.; Somoza, M. M.; Somoza, V. Bitter-Tasting Amino Acids l-Arginine and l-Isoleucine Differentially Regulate Proton Secretion via T2R1 Signaling in Human Parietal Cells in Culture. *J. Agric. Food Chem.* **2020**, *68*, 3434−3444.
(12) Stoeger, V.; Liszt, K. I.; Lieder, B.; Wendelin, M.; Zopun, M.; Hans, J.; Ley, J. P.; Krammer, G. E.; Somoza, V. Identification of Bitter-Taste Intensity and Molecular Weight as Amino Acid Determinants for the Stimulating Mechanisms of Gastric Acid Secretion in Human Parietal Cells in Culture. *J. Agric. Food Chem.* **2018**, *66*, 6762−6771.
(13) Liszt, K. I.; Ley, J. P.; Lieder, B.; Behrens, M.; Stöger, V.; Reiner, A.; Hochkogler, C. M.; Köck, E.; Marchiori, A.; Hans, J.; Widder, S.; Krammer, G.; Sanger, G. J.; Somoza, M. M.; Meyerhof, W.; Somoza, V. Caffeine induces gastric acid secretion via bitter taste signaling in gastric parietal cells. *Proc. Natl. Acad. Sci. U.S.A.* **2017**, *114*, E6260−E6269.
(14) Hochkogler, C. M.; Liszt, K.; Lieder, B.; Stöger, V.; Stübler, A.; Pignitter, M.; Hans, J.; Widder, S.; Ley, J. P.; Krammer, G. E.; Somoza, V. Appetite-Inducing Effects of Homoeriodictyol: Two Randomized, Cross-Over Interventions. *Mol. Nutr. Food Res.* **2017**, *61*, 1700459.
(15) Conigrave, A. D.; Quinn, S. J.; Brown, E. M. L-Amino acid sensing by the extracellular Ca2+-sensing receptor. *Proc. Natl. Acad. Sci. U.S.A.* **2000**, *97*, 4814−4819.
(16) Meyerhof, W.; Batram, C.; Kuhn, C.; Brockhoff, A.; Chudoba, E.; Bufe, B.; Appendino, G.; Behrens, M. The molecular receptive ranges of human TAS2R bitter taste receptors. *Chem. Senses* **2010**, *35*, 157−170.
(17) Bijl, E.; van Valenberg, H. J. F.; Huppertz, T.; van Hooijdonk, A. C. M. Protein, casein, and micellar salts in milk: Current content and historical perspectives. *J. Dairy Sci.* **2013**, *96*, 5455−5464.
(18) Raadsveld, C. W.Bitter Compounds from Cheese, 2nd ed.. *Proceedings 13th International Dairy Congress*, 1953.
(19) Maehashi, K.; Matano, M.; Wang, H.; Vo, L. A.; Yamamoto, Y.; Huang, L. Bitter peptides activate hTAS2Rs, the human bitter receptors. *Biochem. Biophys. Res. Commun.* **2008**, *365*, 851−855.
(20) Kohl, S.; Behrens, M.; Dunkel, A.; Hofmann, T.; Meyerhof, W. Amino acids and peptides activate at least five members of the human bitter taste receptor family. *J. Agric. Food Chem.* **2013**, *61*, 53−60.
(21) Kuhn, C.; Bufe, B.; Winnig, M.; Hofmann, T.; Frank, O.; Behrens, M.; Lewtschenko, T.; Slack, J. P.; Ward, C. D.; Meyerhof, W. Bitter taste receptors for saccharin and acesulfame K. *J. Neurosci.* **2004**, *24*, 10260−10265.
(22) Brockhoff, A.; Behrens, M.; Massarotti, A.; Appendino, G.; Meyerhof, W. Broad tuning of the human bitter taste receptor hTAS2R46 to various sesquiterpene lactones, clerodane and labdane diterpenoids, strychnine, and denatonium. *J. Agric. Food Chem.* **2007**, *55*, 6236−6243.
(23) Wettschureck, N.; Offermanns, S. Mammalian G proteins and their cell type specific functions. *Physiol. Rev.* **2005**, *85*, 1159−1204.
(24) Schubert, M. L. Gastric secretion. *Curr. Opin. Gastroenterol.* **2010**, *26*, 598−603.
(25) Laboisse, C. L.; Augeron, C.; Couturier-Turpin, M. H.; Gespach, C.; Cheret, A. M.; Potet, F. Characterization of a newly established human gastric cancer cell line HGT-1 bearing histamine H2-receptors. *Cancer Res.* **1982**, *42*, 1541−1548.
(26) Bumberger, E.; Belitz, H. D. Bitter taste of enzymic hydrolysates of casein. I. Isolation, structural and sensorial analysis of peptides from tryptic hydrolysates of beta-casein. *J. Food Compost. Anal.* **1993**, *197*, 14−19.
(27) Heda, R.; Toro, F.; Tombazzi, C. R.*Physiology, Pepsin*; StatPearls Publishing: Treasure Island (FL), 2021.
(28) Hornbuckle, W. E.; Simpson, K. W.; Tennant, B. C.Gastrointestinal Function. *Clinical Biochemistry of Domestic Animals*; Elsevier, 2008; pp 413−457.
(29) Keil, B.*Specificity of Proteolysis*; Springer Berlin/Heidelberg: Berlin, Heidelberg, 1992.
(30) Brodkorb, A.; Egger, L.; Alminger, M.; Alvito, P.; Assunção, R.; Ballance, S.; Bohn, T.; Bourlieu-Lacanal, C.; Boutrou, R.; Carrière, F.; Clemente, A.; Corredig, M.; Dupont, D.; Dufour, C.; Edwards, C.; Golding, M.; Karakaya, S.; Kirkhus, B.; Le Feunteun, S.; Lesmes, U.; Macierzanka, A.; Mackie, A. R.; Martins, C.; Marze, S.; McClements, D. J.; Ménard, O.; Minekus, M.; Portmann, R.; Santos, C. N.; Souchon, I.; Singh, R. P.; Vegarud, G. E.; Wickham, M. S. J.; Weitschies, W.; Recio, I. INFOGEST static in vitro simulation of gastrointestinal food digestion. *Nat. Protoc.* **2019**, *14*, 991−1014.
(31) Herraiz, T.; Casal, V. Evaluation of solid-phase extraction procedures in peptide analysis. *J. Chromatogr. A* **1995**, *708*, 209−221.
(32) Sebald, K.; Dunkel, A.; Schäfer, J.; Hinrichs, J.; Hofmann, T. Sensoproteomics: A New Approach for the Identification of Taste-Active Peptides in Fermented Foods. *J. Agric. Food Chem.* **2018**, *66*, 11092−11104.
(33) Sebald, K.; Dunkel, A.; Hofmann, T. Mapping Taste-Relevant Food Peptidomes by Means of Sequential Window Acquisition of All Theoretical Fragment Ion-Mass Spectrometry. *J. Agric. Food Chem.* **2020**, *68*, 10287−10298.
(34) Cox, J.; Mann, M. MaxQuant enables high peptide identification rates, individualized p.p.b.-range mass accuracies and proteome-wide protein quantification. *Nat. Biotechnol.* **2008**, *26*, 1367−1372.
(35) Frank, O.; Kreissl, J. K.; Daschner, A.; Hofmann, T. Accurate Determination of Reference Materials and Natural Isolates by Means of Quantitative 1H NMR Spectroscopy. *J. Agric. Food Chem.* **2014**, *62*, 2506−2515.
(36) Toelstede, S.; Hofmann, T. Sensomics mapping and identification of the key bitter metabolites in Gouda cheese. *J. Agric. Food Chem.* **2008**, *56*, 2795−2804.
(37) Walker, J.; Hell, J.; Liszt, K. I.; Dresel, M.; Pignitter, M.; Hofmann, T.; Somoza, V. Identification of beer bitter acids regulating mechanisms of gastric acid secretion. *J. Agric. Food Chem.* **2012**, *60*, 1405−1412.
(38) Tiroch, J.; Sterneder, S.; Di Pizio, A.; Lieder, B.; Hoelz, K.; Holik, A.-K.; Pignitter, M.; Behrens, M.; Somoza, M.; Ley, J. P.; Somoza, V. Bitter Sensing TAS2R50 Mediates the trans-Resveratrol-Induced Anti-inflammatory Effect on Interleukin 6 Release in HGF-1 Cells in Culture. *J. Agric. Food Chem.* **2021**, *69*, 13339−13349.

(39) Cox, J.; Neuhauser, N.; Michalski, A.; Scheltema, R. A.; Olsen, J. V.; Mann, M. Andromeda: a peptide search engine integrated into the MaxQuant environment. *J. Proteome Res.* **2011**, *10*, 1794−1805.
(40) Ney, K. H. Voraussage der Bitterkeit von Peptiden aus deren Aminosäurezu-sammensetzung. *Eur. Food Res. Technol.* **1971**, *147*, 64−68.
(41) Charoenkwan, P.; Yana, J.; Schaduangrat, N.; Nantasenamat, C.; Hasan, M. M.; Shoombuatong, W. iBitter-SCM: Identification and characterization of bitter peptides using a scoring card method with propensity scores of dipeptides. *Genomics* **2020**, *112*, 2813−2822.
(42) Charoenkwan, P.; Nantasenamat, C.; Hasan, M. M.; Manavalan, B.; Shoombuatong, W. BERT4Bitter: a bidirectional encoder representations from transformers (BERT)-based model for improving the prediction of bitter peptides. *Bioinformatics* **2021**, *37*, 2556−2562.
(43) Davies, D. T.; Law, A. J. R. The composition of whole casein from the milk of Ayrshire cows. *J. Dairy Res.* **1977**, *44*, 447−454.
(44) Jin, Y.; Yu, Y.; Qi, Y.; Wang, F.; Yan, J.; Zou, H. Peptide profiling and the bioactivity character of yogurt in the simulated gastrointestinal digestion. *J. Proteomics* **2016**, *141*, 24−46.
(45) Sandré, C.; Gleizes, A.; Forestier, F.; Gorges-Kergot, R.; Chilmonczyk, S.; Léonil, J.; Moreau, M. C.; Labarre, C. A peptide derived from bovine beta-casein modulates functional properties of bone marrow-derived macrophages from germfree and human flora-associated mice. *J. Nutr.* **2001**, *131*, 2936−2942.
(46) Coste, M.; Rochet, V.; Léonil, J.; Mollé, D.; Bouhallab, S.; Tomé, D. Identification of C-terminal peptides of bovine $\beta$-casein that enhance proliferation of rat lymphocytes. *Immunol. Lett.* **1992**, *33*, 41−46.
(47) Yamamoto, N.; Akino, A.; Takano, T. Antihypertensive Effect of the Peptides Derived from Casein by an Extracellular Proteinase from Lactobacillus helveticus CP790. *J. Dairy Sci.* **1994**, *77*, 917−922.
(48) Martínez-Maqueda, D.; Miralles, B.; Cruz-Huerta, E.; Recio, I. Casein hydrolysate and derived peptides stimulate mucin secretion and gene expression in human intestinal cells. *Int. Dairy J.* **2013**, *32*, 13−19.
(49) Tu, M.; Liu, H.; Cheng, S.; Xu, Z.; Wang, L.-S.; Du, M. Identification and analysis of transepithelial transport properties of casein peptides with anticoagulant and ACE inhibitory activities. *Food Res. Int.* **2020**, *138*, 109764.
(50) Patterson, J. K.; Lei, X. G.; Miller, D. D. The pig as an experimental model for elucidating the mechanisms governing dietary influence on mineral absorption. *Exp. Biol. Med.* **2008**, *233*, 651−664.
(51) Egger, L.; Schlegel, P.; Baumann, C.; Stoffers, H.; Guggisberg, D.; Brügger, C.; Dürr, D.; Stoll, P.; Vergères, G.; Portmann, R. Physiological comparability of the harmonized INFOGEST in vitro digestion method to in vivo pig digestion. *Food Res. Int.* **2017**, *102*, 567−574.
(52) Holik, A.-K.; Schweiger, K.; Stoeger, V.; Lieder, B.; Reiner, A.; Zopun, M.; Hoi, J. K.; Kretschy, N.; Somoza, M. M.; Kriwanek, S.; Pignitter, M.; Somoza, V. Gastric Serotonin Biosynthesis and Its Functional Role in L-Arginine-Induced Gastric Proton Secretion. *Int. J. Mol. Sci.* **2021**, *22*, 5881.
(53) Bufe, B.; Hofmann, T.; Krautwurst, D.; Raguse, J.-D.; Meyerhof, W. The human TAS2R16 receptor mediates bitter taste in response to $\beta$-glucopyranosides. *Nat. Genet.* **2002**, *32*, 397−401.
(54) Kim, U.-K.; Jorgenson, E.; Coon, H.; Leppert, M.; Risch, N.; Drayna, D. Positional cloning of the human quantitative trait locus underlying taste sensitivity to phenylthiocarbamide. *Science* **2003**, *299*, 1221−1225.
(55) Bufe, B.; Breslin, P. A. S.; Kuhn, C.; Reed, D. R.; Tharp, C. D.; Slack, J. P.; Kim, U.-K.; Drayna, D.; Meyerhof, W. The molecular basis of individual differences in phenylthiocarbamide and propylthiouracil bitterness perception. *Curr. Biol.* **2005**, *15*, 322−327.
(56) Zopun, M.; Liszt, K. I.; Stoeger, V.; Behrens, M.; Redel, U.; Ley, J. P.; Hans, J.; Somoza, V. Human Sweet Receptor T1R3 is Functional in Human Gastric Parietal Tumor Cells (HGT-1) and Modulates Cyclamate and Acesulfame K-Induced Mechanisms of Gastric Acid Secretion. *J. Agric. Food Chem.* **2018**, *66*, 4842−4852.
(57) Greene, T. A.; Alarcon, S.; Thomas, A.; Berdougo, E.; Doranz, B. J.; Breslin, P. A. S.; Rucker, J. B. Probenecid inhibits the human bitter taste receptor TAS2R16 and suppresses bitter perception of salicin. *PLoS One* **2011**, *6*, No. e20123.

Supporting Information

**Bitter peptides YFYPEL, VAPFPEVF and YQEPVLGPVRGPFPIIV, released during gastric digestion of casein, stimulate mechanisms of gastric acid secretion via bitter taste receptors TAS2R16 and TAS2R38**

Phil Richter[1], Karin Sebald[1], Konrad Fischer[2], Maik Behrens[1], Angelika Schnieke[2], Veronika Somoza[1,3,4*]

## Tables

Table-SI 1. Changes in gene expression of the bitter receptors after incubation for 15/30/60/120 min with peptides VAPFPEVF (17.5 µM), YFYPEL (0.03 µM) and YQEPVLGPVRGPFPIIV (0.4 µM). Normalized to the expression of PPIA and GAPDH and expression of the receptors in HGT-1 cells without treatment. Data shown as mean ± SEM, n = 3 – 5, t. r. = 3, Statistics: t test Holm-Šidák method; significant differences are expressed with * = $p \leq 0.05$.

| receptor | treatment | 15 min | | | 30 min | | | 60 min | | | 120 min | | |
|---|---|---|---|---|---|---|---|---|---|---|---|---|---|
| *TAS2R1* | VAPFPEVF | 0.79 | ± | 0.12 | 1.36 | ± | 0.20 | 0.44 | ± | 0.22 | 1.62 | ± | 0.61 |
| | YFYPEL | 0.36 | ± | 0.25 | 1.03 | ± | 0.38 | 0.55 | ± | 0.33 | 0.73 | ± | 0.29 |
| | YQEPVLGPVRGPFPIIV | 0.33 | ± | 0.43 | 0.43 | ± | 0.23 | 1.00 | ± | 0.63 | 0.84 | ± | 0.26 |
| *TAS2R3* | VAPFPEVF | **0.70** | **±** | **0.05*** | **1.56** | **±** | **0.22*** | 1.06 | ± | 0.04 | **1.72** | **±** | **0.12*** |
| | YFYPEL | **1.54** | **±** | **0.07*** | 1.08 | ± | 0.16 | 1.19 | ± | 0.12 | **1.34** | **±** | **0.08*** |
| | YQEPVLGPVRGPFPIIV | 1.03 | ± | 0.11 | **1.89** | **±** | **0.19*** | **1.61** | **±** | **0.22*** | **1.40** | **±** | **0.02*** |
| *TAS2R4* | VAPFPEVF | **0.50** | **±** | **0.06*** | 1.14 | ± | 0.19 | 0.95 | ± | 0.07 | **1.42** | **±** | **0.14*** |
| | YFYPEL | **1.24** | **±** | **0.07*** | 0.81 | ± | 0.12 | 0.92 | ± | 0.07 | 1.13 | ± | 0.11 |
| | YQEPVLGPVRGPFPIIV | 0.79 | ± | 0.08 | **1.71** | **±** | **0.19*** | **1.60** | **±** | **0.22*** | **1.21** | **±** | **0.03*** |
| *TAS2R5* | VAPFPEVF | 0.91 | ± | 0.04 | 1.05 | ± | 0.07 | 0.93 | ± | 0.06 | 1.23 | ± | 0.10 |
| | YFYPEL | **1.34** | **±** | **0.03*** | 1.03 | ± | 0.10 | 0.90 | ± | 0.04 | 1.02 | ± | 0.04 |
| | YQEPVLGPVRGPFPIIV | 1.25 | ± | 0.10 | **1.45** | **±** | **0.10*** | **1.39** | **±** | **0.13*** | **1.22** | **±** | **0.03*** |
| *TAS2R7* | VAPFPEVF | 1.20 | ± | 0.32 | 0.71 | ± | 0.34 | **1.05** | **±** | **1.05** | 0.62 | ± | 0.21 |
| | YFYPEL | 1.23 | ± | 0.83 | 2.50 | ± | 1.32 | **6.71** | **±** | **1.56*** | 1.18 | ± | 0.41 |
| | YQEPVLGPVRGPFPIIV | 0.49 | ± | 0.24 | 0.74 | ± | 0.35 | 0.70 | ± | 0.94 | 1.82 | ± | 1.25 |
| *TAS2R8* | VAPFPEVF | 1.24 | ± | 0.13 | **2.25** | **±** | **0.32*** | 1.34 | ± | 0.16 | **2.04** | **±** | **0.23*** |
| | YFYPEL | **1.62** | **±** | **0.22*** | **1.90** | **±** | **0.31*** | **1.87** | **±** | **0.39*** | **1.69** | **±** | **0.21*** |
| | YQEPVLGPVRGPFPIIV | 1.39 | ± | 0.23 | **2.45** | **±** | **0.28*** | **1.87** | **±** | **0.32*** | **1.93** | **±** | **0.23*** |
| *TAS2R9* | VAPFPEVF | 1.73 | ± | 0.08 | 1.08 | ± | 0.47 | 2.31 | ± | 0.75 | 0.99 | ± | 0.69 |
| | YFYPEL | 0.66 | ± | 0.42 | 2.64 | ± | 0.57 | 3.01 | ± | 0.75 | 1.41 | ± | 0.22 |
| | YQEPVLGPVRGPFPIIV | 0.43 | ± | 0.68 | 0.44 | ± | 0.80 | 1.91 | ± | 1.12 | 0.73 | ± | 0.32 |
| *TAS2R10* | VAPFPEVF | **0.34** | **±** | **0.05*** | 0.76 | ± | 0.14 | 0.91 | ± | 0.15 | 1.15 | ± | 0.10 |
| | YFYPEL | **0.64** | **±** | **0.08*** | **0.41** | **±** | **0.05*** | 0.72 | ± | 0.20 | 0.90 | ± | 0.11 |
| | YQEPVLGPVRGPFPIIV | **0.52** | **±** | **0.06*** | 0.78 | ± | 0.07 | 0.90 | ± | 0.12 | 1.04 | ± | 0.08 |
| *TAS2R13* | VAPFPEVF | **0.44** | **±** | **0.09*** | 1.28 | ± | 0.33 | 1.01 | ± | 0.05 | **1.92** | **±** | **0.36*** |
| | YFYPEL | 1.14 | ± | 0.07 | **0.53** | **±** | **0.11*** | 0.78 | ± | 0.06 | 0.88 | ± | 0.36 |
| | YQEPVLGPVRGPFPIIV | 0.70 | ± | 0.11 | **1.65** | **±** | **0.32*** | 1.16 | ± | 0.15 | 1.31 | ± | 0.08 |
| *TAS2R14* | VAPFPEVF | **0.67** | **±** | **0.02*** | 0.97 | ± | 0.05 | **0.86** | **±** | **0.03*** | 1.08 | ± | 0.03 |
| | YFYPEL | **1.11** | **±** | **0.01*** | 0.92 | ± | 0.05 | 0.99 | ± | 0.02 | **1.21** | **±** | **0.09*** |
| | YQEPVLGPVRGPFPIIV | **0.85** | **±** | **0.04*** | 1.08 | ± | 0.06 | 1.03 | ± | 0.04 | **1.08** | **±** | **0.02*** |
| *TAS2R16* | VAPFPEVF | **1.50** | **±** | **0.08*** | **3.70** | **±** | **0.97*** | **1.65** | **±** | **0.24*** | **2.88** | **±** | **0.28*** |
| | YFYPEL | **2.58** | **±** | **0.43*** | **3.19** | **±** | **0.50*** | **2.44** | **±** | **0.58*** | **2.51** | **±** | **0.83*** |
| | YQEPVLGPVRGPFPIIV | **2.61** | **±** | **0.58*** | **3.46** | **±** | **0.58*** | **2.50** | **±** | **0.41*** | **3.00** | **±** | **0.31*** |
| *TAS2R19* | VAPFPEVF | **0.66** | **±** | **0.07*** | 1.22 | ± | 0.17 | **0.69** | **±** | **0.02*** | **1.25** | **±** | **0.09*** |
| | YFYPEL | **1.60** | **±** | **0.02*** | 0.82 | ± | 0.09 | 0.79 | ± | 0.07 | 1.05 | ± | 0.14 |
| | YQEPVLGPVRGPFPIIV | 0.85 | ± | 0.14 | **1.58** | **±** | **0.09*** | 1.27 | ± | 0.17 | 1.05 | ± | 0.03 |
| *TAS2R20* | VAPFPEVF | **0.70** | **±** | **0.07*** | **1.33** | **±** | **0.13*** | **0.87** | **±** | **0.03*** | **1.78** | **±** | **0.20*** |
| | YFYPEL | **1.37** | **±** | **0.05*** | 0.93 | ± | 0.07 | 0.94 | ± | 0.09 | 1.16 | ± | 0.13 |
| | YQEPVLGPVRGPFPIIV | 0.95 | ± | 0.08 | **1.42** | **±** | **0.06*** | **1.38** | **±** | **0.08*** | **1.31** | **±** | **0.06*** |
| *TAS2R30* | VAPFPEVF | **0.56** | **±** | **0.09*** | **1.53** | **±** | **0.32*** | **0.75** | **±** | **0.04*** | **1.62** | **±** | **0.19*** |
| | YFYPEL | **1.79** | **±** | **0.06*** | **0.62** | **±** | **0.09*** | 0.89 | ± | 0.08 | 1.15 | ± | 0.31 |
| | YQEPVLGPVRGPFPIIV | 0.74 | ± | 0.13 | **1.88** | **±** | **0.20*** | 1.20 | ± | 0.17 | 0.89 | ± | 0.03 |
| *TAS2R31* | VAPFPEVF | **0.66** | **±** | **0.05*** | 1.14 | ± | 0.14 | **0.70** | **±** | **0.04*** | **1.22** | **±** | **0.07*** |
| | YFYPEL | **1.65** | **±** | **0.05*** | 0.91 | ± | 0.06 | 0.96 | ± | 0.05 | 1.09 | ± | 0.11 |
| | YQEPVLGPVRGPFPIIV | 0.86 | ± | 0.12 | **1.43** | **±** | **0.11*** | **1.33** | **±** | **0.12*** | 0.99 | ± | 0.04 |

| receptor | treatment | 15 min | | | 30 min | | | 60 min | | | 120 min | | |
|---|---|---|---|---|---|---|---|---|---|---|---|---|---|
| *TAS2R38* | VAPFPEVF | 1.31 | ± | 0.26 | **2.42** | ± | **0.55*** | 1.15 | ± | 0.23 | **2.45** | ± | **0.26*** |
| | YFYPEL | **2.96** | ± | **0.64*** | **3.40** | ± | **0.80*** | **2.39** | ± | **0.62*** | **2.91** | ± | **0.67*** |
| | YQEPVLGPVRGPFPIIV | **2.01** | ± | **0.41*** | **3.71** | ± | **0.93*** | **2.05** | ± | **0.49*** | **2.38** | ± | **0.34*** |
| *TAS2R39* | VAPFPEVF | **0.39** | ± | **0.13*** | 1.37 | ± | 0.34 | **0.55** | ± | **0.06*** | 1.16 | ± | 0.25 |
| | YFYPEL | 1.21 | ± | 0.16 | **0.42** | ± | **0.09*** | **0.62** | ± | **0.12*** | 0.45 | ± | 0.31 |
| | YQEPVLGPVRGPFPIIV | **0.53** | ± | **0.12*** | 1.16 | ± | 0.14 | 0.73 | ± | 0.13 | **0.53** | ± | **0.09*** |
| *TAS2R40* | VAPFPEVF | 0.81 | ± | 0.15 | 1.54 | ± | 0.37 | 0.88 | ± | 0.06 | 1.42 | ± | 0.28 |
| | YFYPEL | **1.90** | ± | **0.12*** | 0.82 | ± | 0.12 | **0.59** | ± | **0.06*** | 0.75 | ± | 0.14 |
| | YQEPVLGPVRGPFPIIV | 0.92 | ± | 0.14 | **1.78** | ± | **0.29*** | 0.96 | ± | 0.26 | 0.86 | ± | 0.07 |
| *TAS2R41* | VAPFPEVF | 0.95 | ± | 0.27 | 2.32 | ± | 1.06 | 0.98 | ± | 0.20 | 1.90 | ± | 0.68 |
| | YFYPEL | **2.82** | ± | **0.64*** | 1.56 | ± | 0.32 | **4.58** | ± | **2.91*** | 3.00 | ± | 2.14 |
| | YQEPVLGPVRGPFPIIV | 1.31 | ± | 0.67 | 1.71 | ± | 2.35 | 2.95 | ± | 1.80 | **4.61** | ± | **2.03*** |
| *TAS2R42* | VAPFPEVF | **0.52** | ± | **0.09*** | 0.88 | ± | 0.10 | **0.71** | ± | **0.03*** | 1.20 | ± | 0.14 |
| | YFYPEL | 1.17 | ± | 0.09 | **0.55** | ± | **0.12*** | **0.69** | ± | **0.11*** | 0.93 | ± | 0.09 |
| | YQEPVLGPVRGPFPIIV | 0.62 | ± | 0.19 | **1.38** | ± | **0.15*** | 1.18 | ± | 0.13 | 0.94 | ± | 0.06 |
| *TAS2R43* | VAPFPEVF | **0.57** | ± | **0.07*** | 1.14 | ± | 0.25 | **0.72** | ± | **0.03*** | **1.49** | ± | **0.15*** |
| | YFYPEL | **1.49** | ± | **0.04*** | **0.64** | ± | **0.06*** | 0.91 | ± | 0.04 | 1.02 | ± | 0.21 |
| | YQEPVLGPVRGPFPIIV | **0.69** | ± | **0.09*** | **1.44** | ± | **0.12*** | 1.15 | ± | 0.14 | 0.88 | ± | 0.04 |
| *TAS2R45* | VAPFPEVF | **0.52** | ± | **0.05*** | 1.08 | ± | 0.17 | **0.68** | ± | **0.03*** | 1.17 | ± | 0.11 |
| | YFYPEL | **1.15** | ± | **0.05*** | **0.54** | ± | **0.06*** | **0.70** | ± | **0.03*** | 0.94 | ± | 0.21 |
| | YQEPVLGPVRGPFPIIV | **0.63** | ± | **0.09*** | **1.25** | ± | **0.12*** | 1.06 | ± | 0.12 | **0.84** | ± | **0.04*** |
| *TAS2R46* | VAPFPEVF | **0.62** | ± | **0.07*** | **1.47** | ± | **0.29*** | 0.85 | ± | 0.05 | **1.95** | ± | **0.21*** |
| | YFYPEL | **1.70** | ± | **0.08*** | 0.73 | ± | 0.12 | 1.01 | ± | 0.11 | 1.30 | ± | 0.30 |
| | YQEPVLGPVRGPFPIIV | 0.69 | ± | 0.13 | **1.73** | ± | **0.18*** | 1.30 | ± | 0.17 | 1.06 | ± | 0.04 |
| *TAS2R50* | VAPFPEVF | **0.56** | ± | **0.06*** | 1.39 | ± | 0.35 | 0.83 | ± | 0.05 | **1.56** | ± | **0.18*** |
| | YFYPEL | **1.50** | ± | **0.06*** | 0.70 | ± | 0.11 | 0.92 | ± | 0.09 | 0.91 | ± | 0.25 |
| | YQEPVLGPVRGPFPIIV | **0.67** | ± | **0.08*** | **1.66** | ± | **0.19*** | 1.21 | ± | 0.13 | 1.07 | ± | 0.08 |
| *TAS2R60* | VAPFPEVF | not detected | | | | | | | | | | | |
| | YFYPEL | not detected | | | | | | | | | | | |
| | YQEPVLGPVRGPFPIIV | not detected | | | | | | | | | | | |

Table-SI 2. Optimized parameters declustering potential (DP), collision energy (CE), and collision cell exit potential (CXP) for each peptide and transition.

| peptide sequence | Q1 mass (Da) | DP (volts) | Q3 mass (Da) | CE (volts) | CXP (volts) |
|---|---|---|---|---|---|
| | | | 700.2 | 9 | 28 |
| | | | 571.2 | 13 | 24 |
| YFYPEL | 416.356 | 36 | 474.1 | 13 | 28 |
| | | | 358.1 | 11 | 22 |
| | | | 350.7 | 11 | 12 |
| | | | 1058.5 | 15 | 26 |
| | | | 978.5 | 23 | 28 |
| PVVVPPFLQPEVM | 726.897 | 180 | 977.5 | 21 | 26 |
| | | | 652.2 | 17 | 20 |
| | | | 475.2 | 21 | 30 |
| | | | 794.3 | 11 | 32 |
| | | | 636.4 | 11 | 18 |
| YYVPLGTQ | 470.592 | 21 | 614.2 | 15 | 20 |
| | | | 596.3 | 19 | 38 |
| | | | 515.2 | 13 | 16 |
| | | | 740.4 | 11 | 20 |
| | | | 735.3 | 11 | 16 |
| VAPFPEVF | 453.135 | 20 | 641.2 | 13 | 14 |
| | | | 570.2 | 15 | 30 |
| | | | 491.3 | 11 | 18 |
| | | | 1151.6 | 45 | 54 |
| | | | 1094.5 | 45 | 54 |
| YQEPVLGPVRGFPFIIV | 940.920 | 80 | 882.4 | 33 | 24 |
| | | | 730.6 | 39 | 38 |
| | | | 441.3 | 41 | 24 |

Table-SI 3. Sequences of the primer pairs used for RT-qPCR.[13,37,38]

| Gene | Direction | Sequence (5′ to 3′) | Amplicon length, bp |
|---|---|---|---|
| TAS2R1 | Forward | AAATGGCTCCGCTGGATCTC | 172 |
| | Reverse | GTGGCAAGCCAAAGTTCCAA | |
| TAS2R3 | Forward | GGGACTCACCGAGGGGGTGT | 160 |
| | Reverse | CCTCAAGAGTGCCAGGGTGGTG | |
| TAS2R4 | Forward | GCAGTGTCTGGTTTGTGACC | 168 |
| | Reverse | GCGTGATGTACAGGCAAGTG | |
| TAS2R5 | Forward | ACACTCATGGCAGCCTATCC | 107 |
| | Reverse | CGAGCACACACTGTCTTCCA | |
| TAS2R7 | Forward | GCAGGTGTGGATGTCAAACTC | 167 |
| | Reverse | TCTTGACCCAGTCCATGCAG | |
| TAS2R8 | Forward | ATGTGGATTACCACCTGCCT | 135 |
| | Reverse | GGAAATGGCAAAGCATCCCAG | |
| TAS2R9 | Forward | GCAGATTCGACTGCATGCTAC | 70 |
| | Reverse | TGCCTTTATGGCCCTCATGT | |
| TAS2R10 | Forward | GCTACGTGTAGTGGAAGGCA | 73 |
| | Reverse | TCCATTCCCCAAAACCCCAA | |
| TAS2R13 | Forward | GAAAGTGCCCTGCCGAGTAT | 177 |
| | Reverse | CCAGATCAGCCCAATTCTGGA | |
| TAS2R14 | Forward | CCAGGTGATGGGAATGGCTTA | 128 |
| | Reverse | AGGGCTCCCCATCTTTGAAC | |
| TAS2R16 | Forward | ATGGCATCACTGACCAAGCA | 255 |
| | Reverse | TTTCAACGTAGGGCTGCTCA | |
| TAS2R19 | Forward | TCTTAGGACACAGCAGAGCA | 146 |
| | Reverse | AGCGTGTCATCTGCCACAAAA | |
| TAS2R20 | Forward | ATTTGGGGGAACAAGACGCT | 183 |
| | Reverse | ACTACGGAAAAACTTGTGGGAA | |
| TAS2R30 | Forward | GGCTGGAAAAGCAACCTGTC | 191 |
| | Reverse | ACACAATGCCCCTCTTGTGA | |
| TAS2R31 | Forward | TTGAGGAGTGCAGTGTACCTTTC | 218 |
| | Reverse | ACGGCACATAACAAGAGGAAAA | |
| TAS2R38 | Forward | CCCAGCCTGGAGGCCCACATT | 216 |
| | Reverse | TCACAGCTCTCCTCAACTTGGCA | |
| TAS2R39 | Forward | TTCTGTGGCTGTCCGTGTTTA | 207 |
| | Reverse | GGGTGGCTGTCAGGATGAAC | |
| TAS2R40 | Forward | CGGTGAACACAGATGCCACAGATA | 150 |
| | Reverse | GTGTTTTGCCCCTGGCCCACT | |
| TAS2R41 | Forward | GCAGCGAATGGCTTCATTGT | 223 |
| | Reverse | TGGCTGAGTTCAGGAAGTGC | |
| TAS2R42 | Forward | TCCTCACCTGCTTGGCTATC | 161 |
| | Reverse | GGCAAGCCAGGTTGTCAAGT | |
| TAS2R43 | Forward | ATATCTGGGCAGTGATCAACC | 148 |
| | Reverse | CCCAACAACATCACCAGAATGAC | |
| TAS2R45 | Forward | AGTACCCTTTACTGTAACCC | 170 |
| | Reverse | AGTAAATGGCACGTAACAAG | |

| Gene | Direction | Sequence (5′ to 3′) | Amplicon length, bp |
|---|---|---|---|
| TAS2R46 | Forward | ACATGACTTGGAAGATCAAACTGAG | 200 |
| | Reverse | AGCTTTTATGTGGACCTTCATGC | |
| TAS2R50 | Forward | CGCAAGATCTCAGCACCAAGGTC | 151 |
| | Reverse | GCCTTGCTAACCATGACAACCGGG | |
| TAS2R60 | Forward | GGTGTTCAGTGCTGCAGGTA | 156 |
| | Reverse | CACCTTGAGGAACGACGACT | |
| GAPDH | Forward | AGGTCGGAGTCAACGGATTTG | 94 |
| | Reverse | GGGGTCATTGATGGCAACAATA | |
| PPIA | Forward | CCACCAGATCATTCCTTCTGTAGC | 144 |
| | Reverse | CTGCAATCCAGCTAGGCATGG | |

## Figures

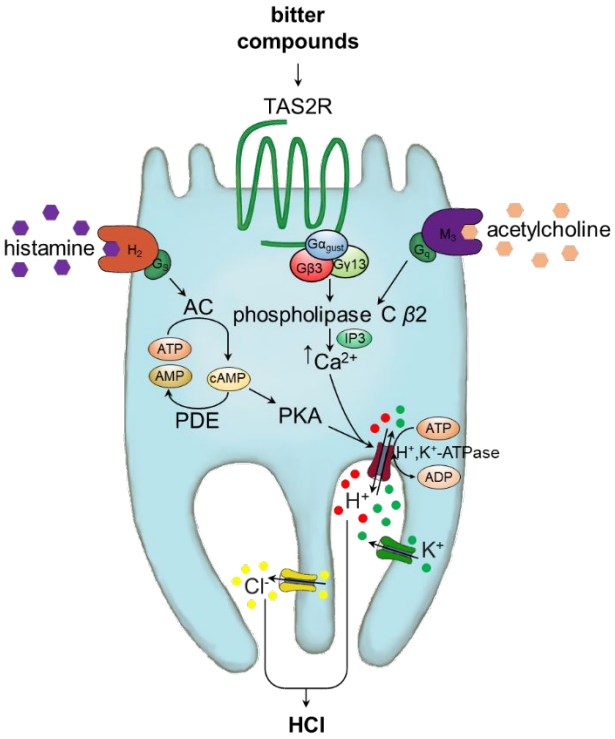


Figure-SI 1. Illustration of the proposed mechanism of proton secretion induced by bitter compounds in HGT-1 cells.[5,56]

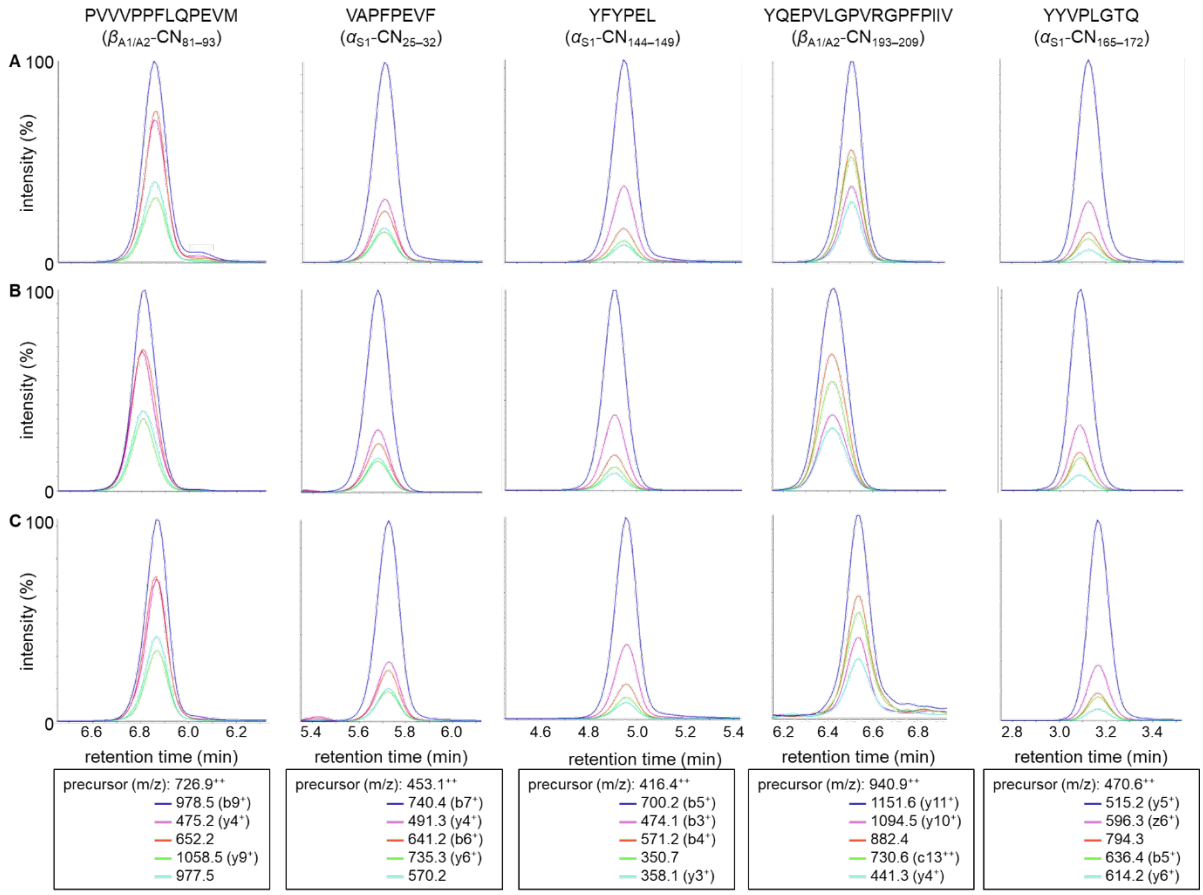


Figure-SI 2. Comparison of retention times (UPLC) and SRM mass transitions (MS/MS; 5 transitions per peptide; transitions identified with skyline 21.1.0.146) of PVVVPPFLQPEVM, VAPFPEVF, YFYPEL, YQEPVLGPVRGPFPIIV and YYVPLGTQ as (A) synthesized standard, (B) formed in *in vitro* digestion, and (C) formed in *in vivo* digestion.

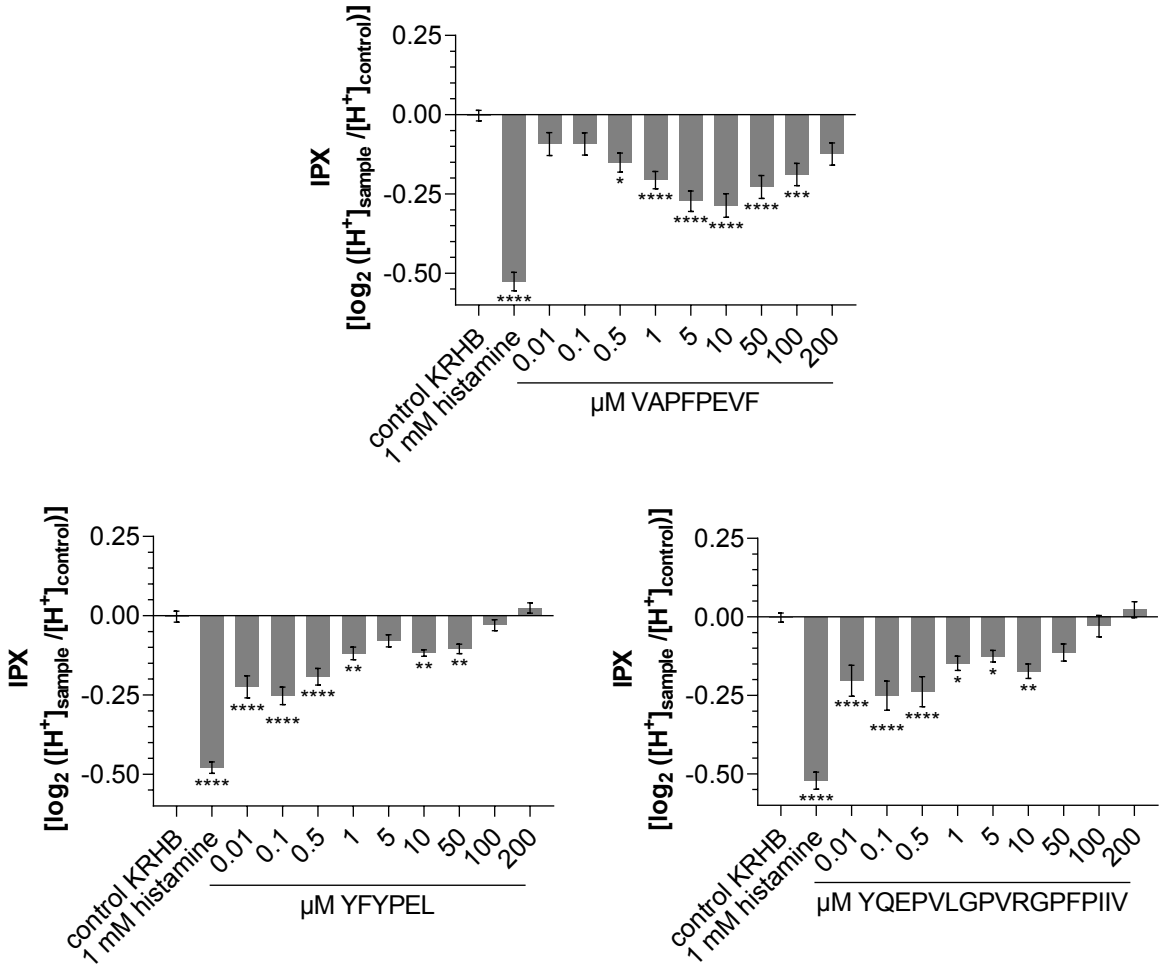


Figure-SI 3. Effect on proton secretion of HGT-1 cells incubated with VAPFPEVF (top) and the peptides YFYPEL and YQEPVLGPVRGPFPIIV with similar IPX profile (bottom). Data shown as mean ± SEM after incubation for 10 minutes, n = 4 – 8, t. r. = 4 – 6, control: KRHB, Statistics: one-way ANOVA Holm-Šidák post hoc test; significant differences are expressed with * = $p \leq 0.05$, ** = $p \leq 0.01$, *** = $p \leq 0.001$, **** = $p \leq 0.0001$.

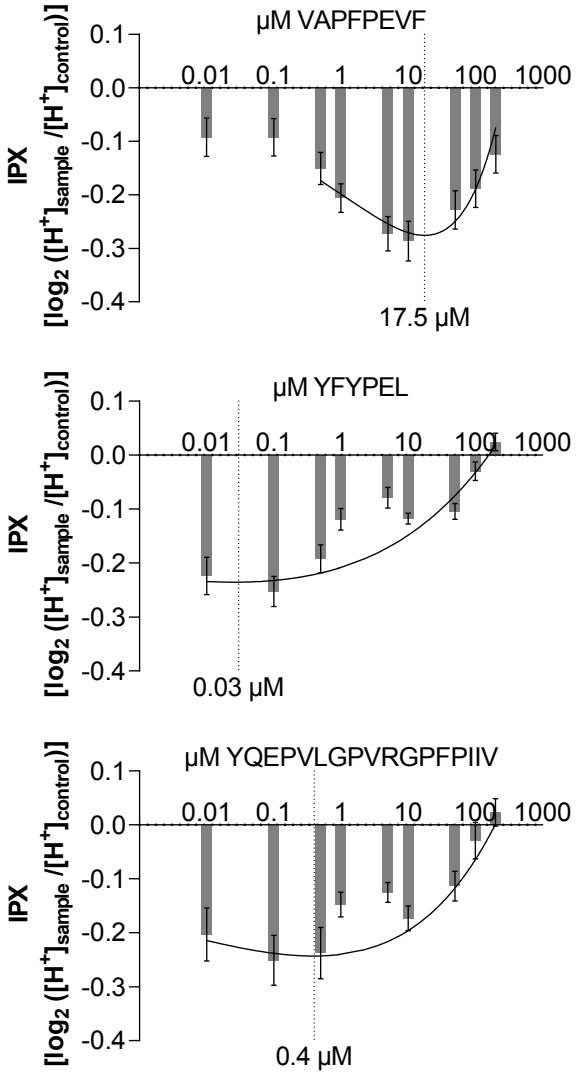


Figure-SI 4. Curve fit calculations of the proton secretion profile of the three peptides to determine which concentration has the greatest effect on proton secretion activity in HGT-1 cells in each case.

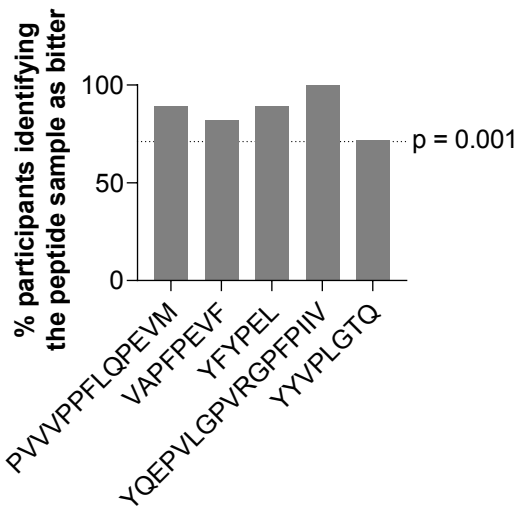


Figure-SI 5. Sensory experiments revealed significant bitterness ($p \leq 0.001$) toward water for all five selected peptides.

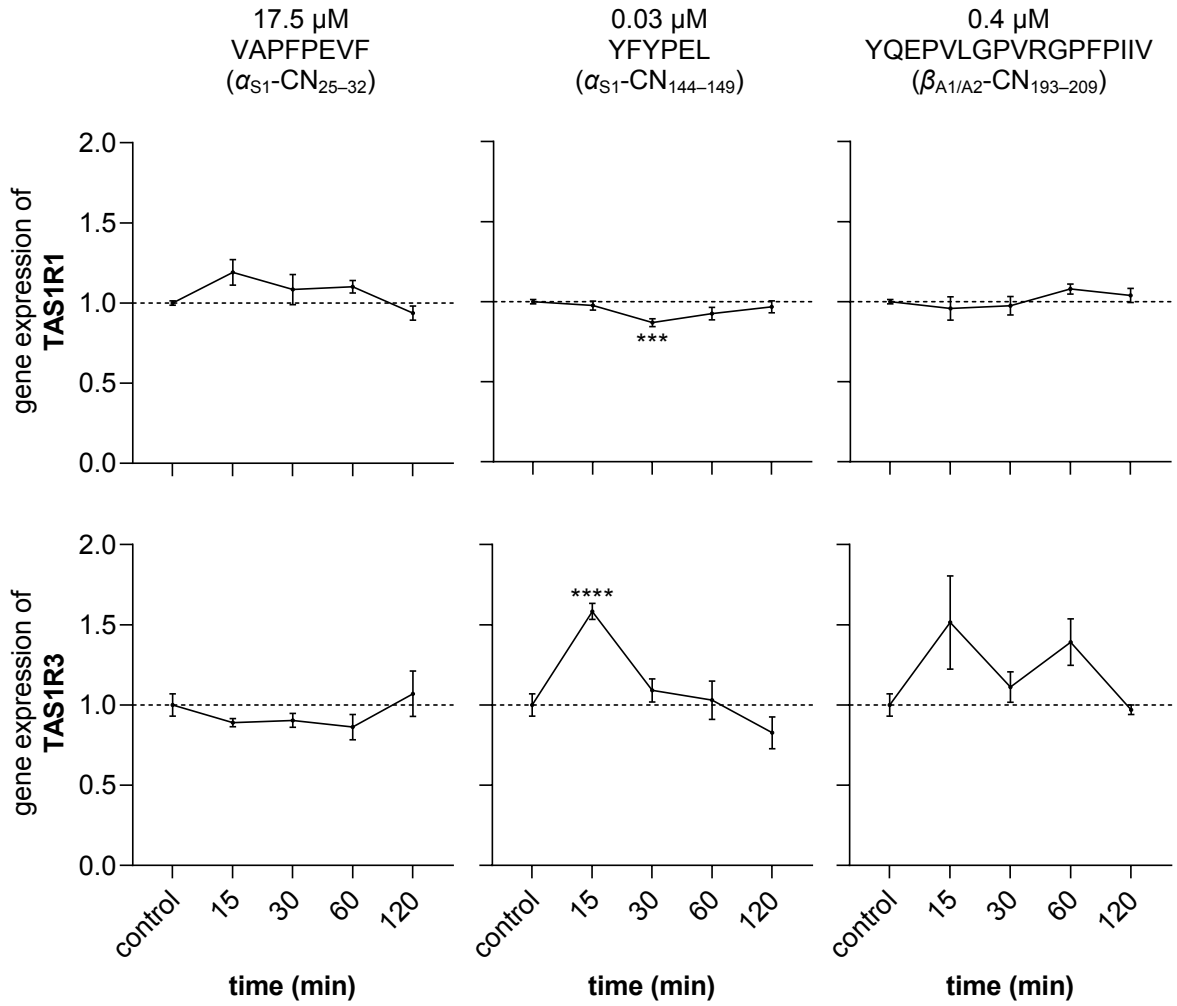


Figure-SI 6. Changes in gene expression (fold change) of taste receptors TAS1R1 (top) and TAS1R3 (bottom) as a function of incubation time with peptides VAPFPEVF (17.5 µM; left), YFYPEL (0.03 µM; center) and YQEPVLGPVRGPFPIIV (0.4 µM; right). Normalized to the expression of PPIA and GAPDH (reference genes). Data shown as mean ± SEM, n = 3, t. r. = 3, Statistics: t test Holm-Šidák method; significant differences are expressed with *** = $p \leq 0.001$, **** = $p \leq 0.0001$.

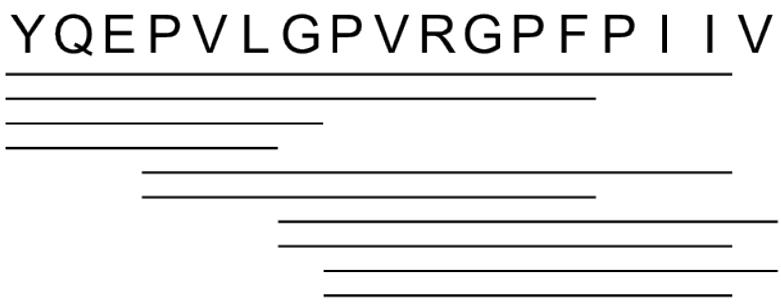


Figure-SI 7. Identified degradation products of YQEPVLGPVRGPFPIIV ($\beta_{A1/A2}$-$CN_{193–209}$) found in the further course of digestion explaining the degradation of the peptide.

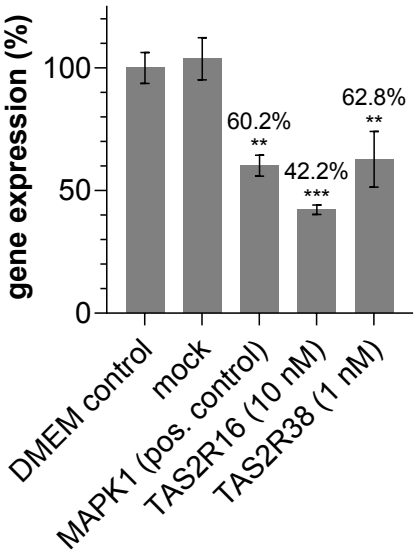


Figure-SI 8. Gene expression was reduced by transient transfection (knock-down) after 72 h. Mock transfections were performed with siRNA without target. Reduction in expression was best achieved with 10 nM siRNA targeting TAS2R16 (HSS121396) and 1 nM siRNA targeting TAS2R38 (HSS108754) to 42.2 and 62.8%, respectively.

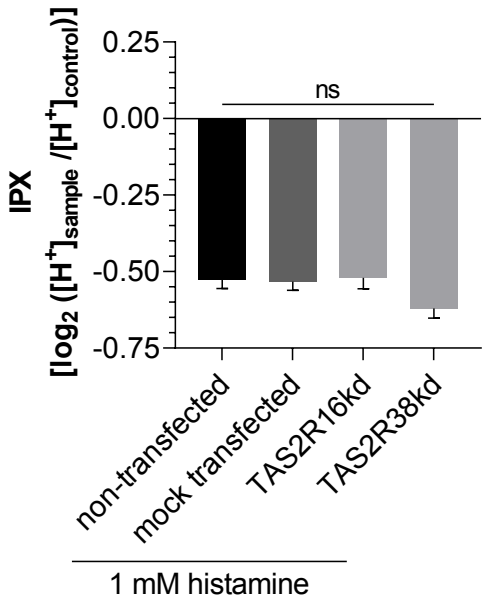


Figure-SI 9. TAS2R-independent histamine-induced stimulation of proton secretion does not differ from non-transfected cells in either mock-transfected or TAS2R16 or TAS2R38 knockdown HGT-1 cells.

## 6.2 Publication II and published supplementary data

Richter, P., Sebald, K., Fischer, K., Schnieke, A., Jlilati, M., Mittermeier-Klessinger, V., & Somoza, V. (2024).

**Gastric digestion of the sweet-tasting plant protein thaumatin releases bitter peptides that reduce *H. pylori* induced pro-inflammatory IL-17A release via the TAS2R16 bitter taste receptor.**

In: *Food Chemistry* (Vol. 448, p. 139157).

Elsevier BV. https://doi.org/10.1016/j.foodchem.2024.139157

Food Chemistry 448 (2024) 139157

Contents lists available at ScienceDirect

Food Chemistry

journal homepage: www.elsevier.com/locate/foodchem

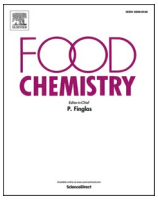

# Gastric digestion of the sweet-tasting plant protein thaumatin releases bitter peptides that reduce *H. pylori* induced pro-inflammatory IL-17A release *via* the TAS2R16 bitter taste receptor

Phil Richter [a,b], Karin Sebald [b], Konrad Fischer [c], Angelika Schnieke [c], Malek Jlilati [b], Verena Mittermeier-Klessinger [d], Veronika Somoza [b,e,f,*]

[a] TUM School of Life Sciences Weihenstephan, Technical University of Munich, Alte Akademie 8, 85354 Freising, Germany
[b] Leibniz Institute for Food Systems Biology at the Technical University of Munich, Lise-Meitner-Str. 34, 85354 Freising, Germany
[c] Livestock Biotechnology, TUM School of Life Sciences, Technical University of Munich, Liesel-Beckmann-Str. 1, 85,354 Freising, Germany
[d] Food Chemistry and Molecular Sensory Science, Technical University of Munich, Lise-Meitner-Str. 34, 85354 Freising, Germany
[e] Nutritional Systems Biology, TUM School of Life Sciences, Technical University of Munich, Lise-Meitner-Str. 34, 85,354 Freising, Germany
[f] Department of Physiological Chemistry, Faculty of Chemistry, University of Vienna, Josef-Holaubek-Platz 2 (UZA II), 1090 Wien, Austria

ARTICLE INFO

*Keywords:*
Thaumatin
Bitter peptides
Gastric digestion
Gastric acid secretion
Bitter taste receptors
Cytokines

ABSTRACT

About half of the world's population is infected with the bacterium *Helicobacter pylori*. For colonization, the bacterium neutralizes the low gastric pH and recruits immune cells to the stomach. The immune cells secrete cytokines, *i.e.*, the pro-inflammatory IL-17A, which directly or indirectly damage surface epithelial cells. Since (I) dietary proteins are known to be digested into bitter tasting peptides in the gastric lumen, and (II) bitter tasting compounds have been demonstrated to reduce the release of pro-inflammatory cytokines through functional involvement of bitter taste receptors (TAS2Rs), we hypothesized that the sweet-tasting plant protein thaumatin would be cleaved into anti-inflammatory bitter peptides during gastric digestion. Using immortalized human parietal cells (HGT-1 cells), we demonstrated a bitter taste receptor TAS2R16-dependent reduction of a *H. pylori*-evoked IL-17A release by up to 89.7 ± 21.9% ($p \leq 0.01$). Functional involvement of TAS2R16 was demonstrated by the study of specific antagonists and siRNA knock-down experiments.

## 1. Introduction

The sweet-tasting protein thaumatin is naturally occurring in *Thaumatococcus daniellii*, a plant found mainly in Africa. First described and isolated in 1972, its sweet intensity was demonstrated to be 1600 times that of sucrose on a weight basis (van der Wel & Loeve, 1972). Due to its intense sweetness, thaumatin (E 957) is added as sugar substitute to foods and beverages in concentrations between 0.5 and 400 mg/kg (Younes et al., 2021). Although the pharmacological characteristics of thaumatin have been extensively studied before the FDA has given GRAS notice (Gleba, 2017), peptides released after gastric digestion of thaumatin have so far not been characterized, neither for their taste quality nor for their (taste quality-associated) effects on the stomach's physiology.

Humans can perceive five recognized taste qualities: sweet, bitter, salty, sour and umami. The perception of these taste qualities after food intake is primarily mediated by taste receptors located on taste cells of the tongue. In extra-oral tissues, the expression of taste receptors, namely bitter taste receptors (TAS2Rs), have been demonstrated to play central roles in various physiological functions (Behrens & Meyerhof, 2013). While intestinal TAS2Rs modulate mechanisms regulating the control of food intake and the innate immune system, activation of gastric TAS2Rs stimulates proton secretion from parietal cells and are thereby involved in digestive mechanisms of gastric acid secretion (Liszt et al., 2017; Liszt et al., 2022).

However, an oral bitter taste perception of a given food constituent does not necessarily result in the activation of gastro-intestinal TAS2Rs. Digestive degradation might change the chemical structure and, in turn, the TAS2R activation profile and associated physiological functions of the parent compound. In one of our previous works, we have

* Corresponding author at: Leibniz Institute for Food Systems Biology at the Technical University of Munich, Lise-Meitner-Str. 34, 85354 Freising, Germany.
*E-mail addresses:* p.richter.leibniz-lsb@tum.de (P. Richter), k.sebald.leibniz-lsb@tum.de (K. Sebald), konrad.fischer@tum.de (K. Fischer), angelika.schnieke@wzw.tum.de (A. Schnieke), verena.mittermeier@tum.de (V. Mittermeier-Klessinger), v.somoza.leibniz-lsb@tum.de (V. Somoza).

https://doi.org/10.1016/j.foodchem.2024.139157
Received 23 December 2023; Received in revised form 8 March 2024; Accepted 25 March 2024
Available online 28 March 2024

demonstrated gastric digestion of the non-bitter tasting milk protein casein to release bitter peptides that stimulated mechanisms of gastric acid secretion by immortalized human parietal cells (HGT-1) *via* functional involvement of TAS2R16 and TAS2R38 (Richter et al., 2022). Besides digestive processes, TAS2Rs have also been shown to play a role in preventing immune competent cells from a stimulus-evoked release of pro-inflammatory cytokines (Liszt et al., 2022;Tiroch et al., 2021; Tiroch et al., 2023). In immortalized human gingival fibroblasts (HGF-1 cells), the release of the pro-inflammatory interleukin 6, evoked by treatment with lipopolysaccharides (LPS) from *Porphyromonas gingivalis*, was reduced by various TAS2R agonists and TAS2R50 siRNA knock-down (Tiroch et al., 2021; Tiroch et al., 2023).

From a mechanistic perspective, activation of TAS2R16 by its agonist salicin (Bufe, Hofmann, Krautwurst, Raguse, & Meyerhof, 2002) suppresses NF-κB p65 nuclear translocation and intracellular cAMP in HGF-1 cells, after treatment with LPS. In addition, down-regulation of gene expression of many pro-inflammatory cytokines occurred upon co-incubation of cells with LPS and salicin, which resulted in a decreased release of the pro-inflammatory cytokine IL-8 (Zhou et al., 2021). In the context of innate immunity, it has been shown that the activation of TAS2R38 by corresponding bitter substances leads to calcium mobilization, which might trigger the formation of NO as well-known antibacterial agent (Bethineedi et al., 2023).

Inflammatory processes in the stomach that are associated with the release of various cytokines are often caused by an infection with the bacterium *Helicobacter pylori* (*H. pylori*) (Bauditz et al., 1999; Beales & Calam, 1997; Lv et al., 2019; Yamauchi et al., 2008). Worldwide, about half of the population is infected with *H. pylori* (Suerbaum & Michetti, 2002). To protect itself from the human immune system, *H. pylori* has developed specific adaptations in order to be able to settle in the gastric mucosa. One of them is aimed at resisting the low pH in the stomach by producing the enzyme urease. This enzyme catalyzes the breakdown of urea into $CO_2$ and ammonia, neutralizing gastric acid (Salama, Hartung, & Müller, 2013).

Among the pro-inflammatory interleukins IL-17 is known to play a crucial role in *H. pylori* infections. In infected mice IL-17 protein expression was increased and associated with a strong neutrophil infiltration, which was significantly reduced in IL-17 knock-out mice. Moreover, the number of pathogens present in the stomach of the knock-out mice was significantly lower than in wild-type mice after 6 months of infection (Shiomi et al., 2008). In humans, sustained secretion of IL-17A, an important representative of the IL-17 family, by gastric cells has been hypothesized to promote the development of gastric tumors (Kang et al., 2023). Whether dietary peptides released during gastric digestion may counteract a *H. pylori*-evoked release of pro-inflammatory cytokines and whether TAS2Rs are involved herein, has not been studied so far.

We, therefore, hypothesized that gastric digestion of the sweet-tasting protein thaumatin generates bitter peptides that reduce an *H. pylori*-induced release of pro-inflammatory interleukins with functional involvement of TAS2Rs.

## 2. Material and methods

### 2.1. Chemicals

Thaumatin (mixture of the two forms thaumatin I and II, 99.4% purity) was purchased from TCI Chemicals (Portland, USA), 1,5-carboxy-seminaphtorhodafluor acetoxymethylester (SNARF-1-AM) and Dulbecco's modified Eagle's medium GlutaMAX (DMEM) were purchased from Thermo Fisher Scientific (USA). Fetal bovine serum (FBS Supreme), trypsin/ethylenediaminetetraacetic acid, and penicillin−streptomycin were obtained from PANBiotech GmbH (Aidenbach, Germany). Phosphate buffered saline was bought from Biozym Scientific GmbH (Hessisch Oldendorf, Germany). Dimethyl sulfoxide (DMSO) and 3-(4,5-dimethylthiazol-2-yl)-2,5-diphenyltetrazolium bromide (MTT) were purchased from Carl Roth (Karlsruhe, Germany). All other compounds were ordered from Merck KGaA (Darmstadt, Germany). Custom peptides (DAGGRQLNSGES, FNVPMDF, WTINVEPGTKGGKIW, and AAASKGDAAL) were synthesized by Genscript Biotech with a purity of >95% (New Jersey, USA). Double-distilled water ($ddH_2O$) from Elga Purelab Classic (Veolia Water Solutions & Technologies, France) was used for all experiments. The composition of Krebs-Ringer-HEPES buffer (KRHB), simulated salivary fluid (SSF), and simulated gastric fluid (SGF) is based on previously published work (Brodkorb et al., 2019; Richter et al., 2022).

### 2.2. In vitro digestion

For digestion of the intact plant protein thaumatin, 100 mg were dissolved in SSF as described before (Brodkorb et al., 2019; Richter et al., 2022) and incubated for 5 min at 37 °C and 5% $CO_2$ (standard conditions) in four biological replicates. After the first sampling, SGF was added and the pH was adjusted to 3. Pepsin was added to initiate simulated gastric digestion. The reaction was incubated under standard conditions and samples were taken at 0.25, 0.5, 0.75, 1, 2, 3, 4, 5, and 6 h. The samples were stored at −80 °C until peptide identification by LC-ToF-MS or quantitation by LC-MS/MS.

### 2.3. In vivo digestion

To carry out the *in vivo* digestion experiments, 1 g thaumatin was dissolved in 5 mL of water and administered to pigs (German Landrace, German Landrace × minipig, age: about 20 weeks) in 6 biological replicates. Two hours after thaumatin administration (Richter et al., 2022), the animals were euthanized and the stomach contents were collected and immediately frozen in liquid nitrogen. The following purification and desalting was carried out as previously published (Richter et al., 2022). The samples were stored at −80 °C until identification by LC-ToF-MS or quantitation by LC-MS/MS.

### 2.4. Peptide identification by means of Ultra-High-Performance Liquid Chromatography–Time-of-Flight Mass Spectrometry (UHPLC-ToF-MS)

Separations and measurements of peptides released from thaumatin digestion were performed using a Sciex ExionLC AC (Sciex, Darmstadt, Germany) coupled to a Sciex TripleTOF 6600 mass spectrometer (Sciex, Darmstadt, Germany) adapted from the previously published protocol (Richter et al., 2022). Data acquisition and instrumentation control were performed with AnalystTF software (v 1.7.1; Sciex, Darmstadt, Germany). The used gradient of 0.1% aqueous formic acid and acetonitrile containing 0.1% formic acid was only slightly adjusted according to the following scheme: 0 min, 5% B; 0.5 min, 5% B; 14 min, 60% B; 15 min, 98% B; 16 min, 98% B; 17 min, 5% B; and 20 min, 5% B. MaxQuant software (Cox & Mann, 2008) was used for the identification of the peptide sequences (version 1.6.3.4; unspecific digestion; variable modifications: oxidation M, acetyl protein N-term, carbamidomethyl C, phospho STY; peptide length between 4 and 25 amino acids; andromeda score > 10; max. Score: 202.27).

### 2.5. Quantitation of the thaumatin peptides via LC-MS/MS

Separations and measurements for peptide quantification were performed using a Sciex ExionLC AC (Sciex, Darmstadt, Germany) coupled to a 6500+ QTrap LC-MS/MS system (Sciex, Darmstadt, Germany) operating in the positive electrospray ionization mode. This was also based on the previously published methodology (Richter et al., 2022). While all other parameters were adopted, the gradient of 0.1% aqueous formic acid and acetonitrile containing 0.1% formic acid was modified as follows: 0 min, 10% B; 8 min, 40% B; 8.5 min, 98% B; 11 min, 98% B; 11.5 min, 10% B; and 15 min, 10% B. The optimal ionization parameters (DP, CE, and CXP; see supplementary data **Table S1**) for each peptide

transition were obtained by direct injection of the peptide solutions into the MS ion source.

### 2.6. Quantitative $^{1}H$ Nuclear Magnetic Resonance Spectroscopy

To verify the purity of the synthesized reference peptides, the peptides were dissolved in 600 μL $D_2O$ and filled into NMR tubes (178 × 5 mm inner diameter, USC tubes, Bruker, Rheinstetten, Germany). The 1H-qNMR spectra were recorded on a 400 MHz Avance III NMR spectrometer (Bruker, Rheinstetten, Germany), which was calibrated using caffeine and L-tyrosine before measurement as previously described (Frank, Kreissl, Daschner, & Hofmann, 2014).

### 2.7. Sensory study

After ensuring the purity of the identified peptides by LC-MS and $^{1}H$-qNMR (95.5–99.4%), sensory experiments were performed to confirm their predicted bitterness. Peptides were dissolved in non-carbonated, bottled water in a concentration of 1.5 mM (Richter et al., 2022). To determine the most dominant taste sensation (Labbe, Schlich, Pineau, Gilbert, & Martin, 2009), the 17–19 healthy, non-smoking trained panelists without known taste and smell disorders were asked to discriminate between sweet, bitter and another taste quality (Meilgaard & Carr, 2006).

### 2.8. Bradford assay

Thaumatin content of sweetener tablets was determined by the Bradford assay to associate the effect sizes demonstrated with a typical dietary thaumatin intake. For this purpose, one thaumatin sweetener tablet (71.04 mg) was dissolved in 5 mL of $H_2O$, and a calibration line of pure thaumatin (10, 5, 1, 0.5, 0.1, and 0.05 μg/mL) in water was prepared. Afterwards, the Bradford solution (BioRad, Feldkirchen, Germany) was added 1:1 to the sample solutions (four replicates) and the calibration solutions, and incubated for 20 min at room temperature. Absorbance was measured on a NanoDrop One$^{c}$ (Thermo Fisher Scientific Inc., USA) at 595 nm.

### 2.9. Cell culture

Immortalized human parietal cells (HGT-1), obtained from Dr. C. Laboisse (Laboratory of Pathological Anatomy, Nantes, Frances), were cultured under previously published standard conditions at 37 °C in a humidified atmosphere at 5% $CO_2$ in DMEM containing 10% FBS and 1% penicillin and streptomycin. Cells between passages 15 and 25 were used for all experiments (Liszt et al., 2017; Richter et al., 2022).

### 2.10. Cell viability

Exclusion of cytotoxic effects of all substances tested in cell assays was performed by MTT assay. For this, cells were incubated for six hours with thaumatin (100 μM), the peptides (100 μM), probenecid (1 mM) or native proteins of *H. pylori* (2.5–50 μg/mL) according to the previously published protocols (Richter et al., 2022). Viability was determined *via* reduction of MTT (0.83 mg/mL in DMEM) to the corresponding formazan dissolved in DMSO. Absorbance was measured at 570 nm (reference 650 nm) using an Infinite M200 plate reader (Tecan, Switzerland). Cell viability was calculated relative to cells treated with KRHB only (= 100%). DMSO (100%) and 5 mM quinine (Richter et al., 2024) were used as negative controls (see supplementary data **Fig. S1**).

### 2.11. Intracellular proton index (IPX) determined as indicator of parietal proton secretion

For the measurement of the intracellular proton index (IPX), based on the intracellular concentration of protons, 100,000 HGT-1 cells/well were seeded into a black 96 well plate on the previous day. On the day of measurement, cells were stained for 30 min with the pH sensitive fluorescent dye 1,5 carboxy-seminaphto-rhodafluor acetoxymethyl ester (SNARF-1-AM) at 37 °C and 5% $CO_2$. After removal of the dye and a washing step with KRHB, the cells were treated with thaumatin or the identified peptides in different concentrations (range: 1 pM – 100 μM) with and without 1 mM probenecid as TAS2R16 antagonist. After 10 min incubation under standard conditions, the dye was excited at 488 nm and emitted fluorescence was measured at 580 and 640 nm. All experiments and the calculation was done as previously described (Liszt et al., 2017; Richter et al., 2022).

### 2.12. Quantitation of mRNA expression

For analysis of gene expression, 500,000 cells/well were seeded into 24 well plates on the previous day. After incubation for different time periods with the respective substances, the cells were washed with PBS and lysed directly in the plate. Isolation of RNA followed by concentration and integrity determination, gDNA removal, synthesis of cDNA, and performance of real-time qPCR (RT-qPCR) were performed using the peqGOLD RNA Kit (VWR Peqlab, USA), the iScript gDNA Clear cDNA Synthesis Kit (BioRad, Feldkirchen, Germany), and the SsoAdvanced Universal SYBR Green Supermix (BioRad, Feldkirchen, Germany) as described previously (Richter et al., 2022). Primer sequences for the TAS2Rs were taken from Liszt et al., 2017. All other primers and plates with preloaded primers of common cytokines and chemokines (ID 10034128) were obtained from BioRad (Feldkirchen, Germany). PPIA and GAPDH were used as reference genes. The effects of the substances on gene expression were analyzed in comparison to untreated control cells.

### 2.13. Transient knock-down of TAS2R16 expression in HGT-1 cells

To determine transfection efficiency in this approach, 100,000 cells/well were seeded in 24-well plates the previous day. All reagents needed for transfection were purchased from Thermo Fisher Scientific, USA. To reduce the expression of *TAS2R16*, two different siRNA sequences (HSS121396 and HSS181763) were tested. After performing transfection with Lipofectamine RNAiMAX in Opti-Medium according to the manufacturer's protocol, cells were incubated for 72 h at standard conditions. Mock and positive control (MAPK1; VHS40312) transfections were performed as published previously (Richter et al., 2022). Transfection efficiency was determined by RT-qPCR. The siRNA sequence and concentration (HSS181763; 1 nM) with the most pronounced effect on reducing *TAS2R16* expression was used for the following ELISA experiments.

### 2.14. Determination of cytokine release from HGT-1 cells

To determine which cytokines are released by HGT-1 cells in response to *H. pylori* (10 μg/mL) exposure, 2,500,000 cells/well were seeded in 12 well plates the previous day. After incubation of cells with and without native proteins from *H. pylori*, cell supernatants were examined in four biological replicates according to the manufacturer's protocol using *Proteome Profiler Array Human XL Cytokine Array Kit* (R & D Systems, Minneapolis, USA). Afterwards, the membranes were imaged on a ChemiDoc MP Imaging System (BioRad, Feldkirchen, Germany). Quantification was subsequently performed using *ImageJ* (1.53 t) after background subtraction (Rolling Ball Radius 25 Pixels; light background; invert; size: 0.08 [23]). Here, normalization was performed to the positive controls located on the membrane.

### 2.15. Enzyme-linked Immunosorbent Assays (ELISA)

To quantitate the release of cytokine proteins by HGT-1 cells exposed to *H. pylori* (10 μg/mL), 750,000 cells/well were seeded in 96 well plates

the previous day. After transfection with siRNA targeting *TAS2R16* or nonspecific siRNA (mock), cells were incubated for 72 h under standard conditions as described. After six hours incubation with and without native proteins from *H. pylori* with and without the peptides under investigation in serum-free medium, the supernatants were collected and analyzed by ELISA. Human IL-17A High Sensitivity ELISA Kit (Thermo Fisher Scientific Inc., USA) was used for this purpose.

### 2.16. Statistics

Unless otherwise described, all data are presented as mean ± standard error of the mean (SEM). At least three biological replicates were prepared from each experiment. Statistical analyses of different treatments with the untreated control were performed after the Nalimov outlier test using *t*-test Holm-Šidák method or one-way ANOVA Holm-Šidák *post hoc* test. Different $p$ values are indicated with asterisks according to the following scheme: * = $p \leq 0.05$, ** = $p \leq 0.01$, *** = $p \leq 0.001$, **** = $p \leq 0.0001$.

## 3. Results and discussion

### 3.1. Identification of potentially bitter-tasting peptides released from thaumatin by gastric digestion in vitro

Thaumatin consists of two forms (UniProt Consortium, 2023), thaumatin I (UniProt P02883) and thaumatin II (UniProt P02884), which are 207 amino acids in length and differ structurally in four amino acids (46N>K; 63S>R; 67K>R; 76R>Q; see supplementary data **Table S2**). To identify the peptides released during gastric digestion of thaumatin, the intact protein was subjected to a previously validated *in vitro* digestion in four biological replicates (Richter et al., 2022). Analysis of these samples by LC-ToF-MS and the proteomics software MaxQuant (Cox & Mann, 2008; Tyanova, Temu, & Cox, 2016) led to the identification of 66 different peptides released over the complete digestion period of six hours.

Based on the amino acid sequence differences, eight peptides could be clearly assigned to thaumatin I and five to thaumatin II. The remaining 53 peptides could have resulted from the cleavage of thaumatin I as well as II. Peptide contamination of the intact thaumatin was excluded by LC-ToF-MS. To monitor the performance of the *in vitro* digestion, the effect of low pH (pH = 3) without pepsin addition and the stability of the protein under neutral conditions were tested. No release of peptides was observed. Hence, pepsin and pH 3 were required for the release of the 66 different peptides. As previously observed and described (Richter et al., 2022), there was no relevant formation or change in peptide concentrations after six hours of digestion, suggesting complete digestion.

To reduce the number of peptides to be investigated in the following experiments, only identified sequences with an andromeda score > 100 were used, reducing the number of peptides from 66 to 12 (Cox & Mann, 2008; Tyanova et al., 2016). To select potentially bitter-tasting peptides, various *in silico* prediction tools were applied, *e.g.* BERT4Bitter (Charoenkwan, Nantasenamat, Hasan, Manavalan, & Shoombuatong, 2021), iBitter-SCM (Charoenkwan et al., 2020), and prediction based on the amino acid composition according to Ney, 1971, which already proved successful in previous screenings (Richter et al., 2022). If at least two of the three tools declared the respective sequence as bitter, reference peptides were purchased to verify the bitterness by sensory trials and to perform subsequent experiments. To avoid testing similar peptides, overlapping sequences were excluded. Consequently, the following peptide sequences were assumed to be bitter-tasting: DAGGRQLNSGES (TH-I/II$_{25–36}$; iBitter-SCM score: 385.18 bitter; BERT4Bitter probability: 0.57 bitter; Ney: 435.8 non-bitter), FNVPMDF (TH-I/II$_{108–114}$; iBitter-SCM score: 393.17 bitter; BERT4Bitter probability: 0.00 non-bitter; Ney: 1710.0 bitter), WTINVEPGTKGGKIW (TH-II$_{37–51}$; iBitter-SCM score: 387.36 bitter; BERT4Bitter probability: 1.00 bitter; Ney: 1437.3 bitter). The likely non-bitter peptide AAASKGDAAL (TH-I/II$_{15–24}$; iBitter-SCM score: 247.44 non-bitter; BERT4Bitter probability: 0.00 non-bitter; Ney: 666.0 non-bitter) was selected to perform control experiments.

### 3.2. Identification of in vivo released thaumatin peptides showed high similarities to the in vitro model

To study the enzymatic cleavage of the intact protein thaumatin under *in vivo* conditions and to compare the results with the identified peptides of the *in vitro* approach, pigs were fed with 1 g thaumatin, and their stomach contents were analyzed *via* LC-ToF-MS after two hours of digestion. The time period of two hours was based on the results from the *in vitro* experiments, which demonstrated the major release of peptides within the first two hours of digestion. The porcine model was chosen because the digestive processes of pigs closely resemble those of humans (Patterson, Lei, & Miller, 2008). Determination of the pH of the pig's gastric contents resulted in a mean value of 3.15 ± 0.56. This result was in accordance with previously published data on studying the digestion products of casein (pH value 2.90 ± 0.74; $p \geq 0.77$), and justifies the use of pH value 3 for the *in vitro* digestion approach (Richter et al., 2022). LC-ToF-MS analysis of the peptides formed after two hours of gastric digestion revealed 68 different peptide sequences. Comparison of these peptides formed *in vivo* with those revealed from the *in vitro* approach showed a mean similarity of 83.7 ± 1.8%, including the three predicted bitter peptides and the likely non-bitter reference peptide. The high agreement of identified peptides between the *in vitro* and *in vivo* digestion confirmed, that the previously adapted *in vitro* digestion protocol provides a simple and suitable alternative to simulate protein digestion in the human stomach (Brodkorb et al., 2019; Richter et al., 2022).

To confirm the structure of the selected peptides, synthetic references were analyzed by LC-MS/MS and their retention times and MRM-pattern were compared to those of the selected peptides. This showed that both, the retention times (AAASKGDAAL: 1.41 ± 0.02 min; DAGGRQLNSGES: 0.97 ± 0.03 min; FNVPMDF: 6.74 ± 0.04 min; WTINVEPGTKGGKIW: 5.56 ± 0.02 min) and the ratios of specific transitions (5 per peptide) of the peptides formed *in vitro* and *in vivo*, were consistent with those of the synthesized reference peptides (see supplementary data **Fig. S2**). The recovery rates of the peptides in quality controls during the LC-MS measurements were 98.0 ± 1.5% for AAASKGDAAL, 94.6 ± 0.9% for DAGGRQLNSGES, 97.8 ± 1.3% for FNVPMDF, and 98.1 ± 0.3% for WTINVEPGTKGGKIW.

### 3.3. Sensory validation of the bitter taste of peptides released by gastric digestion of thaumatin

First, the bitter perception from the peptides DAGGRQLNSGES, FNVPMDF and WTINVEPGTKGGKIW, and the taste quality of the putatively non-bitter peptide AAASKGDAAL, predicted by using the prediction tools mentioned above, were evaluated by trained sensory panelists scoring (Fig. 1) according to a dominant sensation test (Labbe et al., 2009). This revealed that the three peptides classified as bitter by the preceding *in silico* approach, DAGGRQLNSGES (50.0 ± 1.4% of the panelists, $p \leq 0.01$), FNVPMDF (83.1 ± 4.2%, $p \leq 0.001$) and WTINVEPGTKGGKIW (100.0 ± 0.0%, $p \leq 0.001$), indeed exhibited a distinct bitter taste (see supplementary data **Table S3**). In addition, it was confirmed that the peptide AAASKGDAAL, which was predicted to be non-bitter, was neither perceived as bitter, nor as sweet (55.9 ± 0.8%, $p \leq 0.001$). For reference purposes, the intact thaumatin was also subjected to sensory analysis. Here, a sweet taste sensation was perceived (97.6 ± 0.6%, $p \leq 0.001$). This set of sensory experiments confirmed the *in silico* results obtained from the bitter prediction tools. Moreover, the sweet taste of thaumatin, already known from literature, could also be validated (van der Wel & Loeve, 1972). According to our hypothesis, it could be shown that the taste quality of the sweet-tasting plant protein

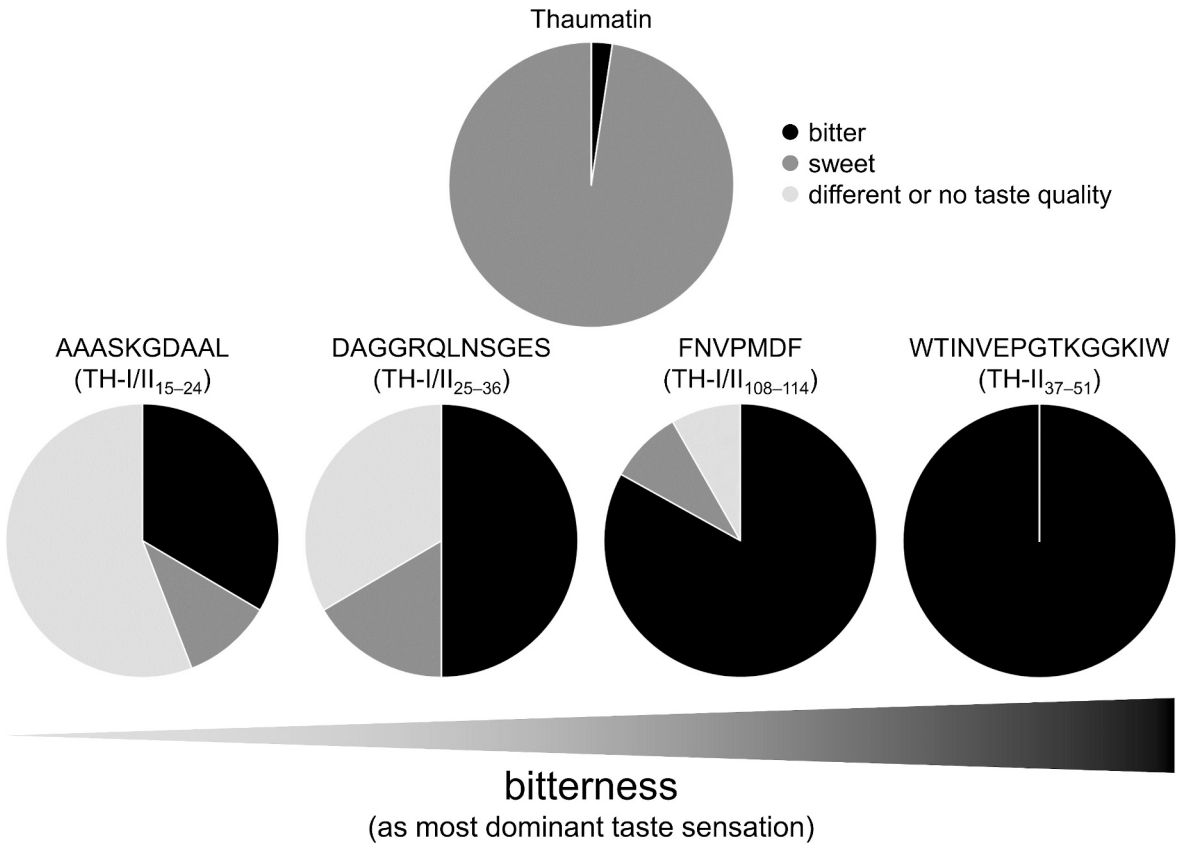


**Fig. 1.** Illustration of the results of the sensory experiments in which the bitterness of the three peptides DAGGRQLNSGES, FNVPMDF, and WTINVEPGTKGGKIW, the non-bitterness of AAASKGDAAL and the sweetness of thaumatin were validated; $n$ = 17–19, t. r. = 3.

thaumatin changes during gastric digestion and bitter-tasting peptides are released.

### 3.4. *Time-resolved quantitation of the thaumatin peptides AAASKGDAAL, FNVPMDF, DAGGRQLNSGES and WTINVEPGTKGGKIW released upon gastric digestion in vitro*

To investigate the peptide release over time, a LC-MS/MS method was developed and applied on the samples. Quantitation of the four peptides in the samples of the *in vitro* gastric digest revealed substantial cleavage of thaumatin (100 mg, 633.5 μM), resulting in a high release of the peptides within the first hour (Fig. 2). The highest concentrations of FNVPMDF (151.7 ± 1.6 μM) and AAASKGDAAL (61.3 ± 1.8 μM) were

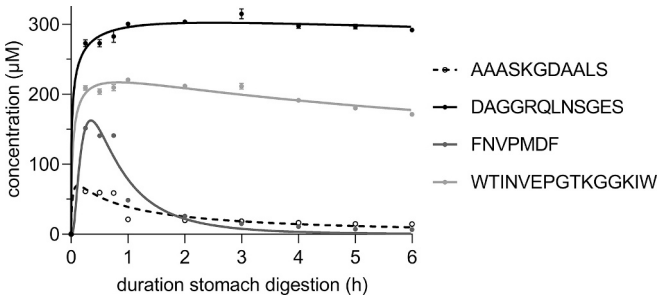


**Fig. 2.** Release of the three investigated bitter-tasting thaumatin peptides DAGGRQLNSGES (black line), WTINVEPGTKGGKIW (light gray line) and FNVPMDF (dark gray line) and the non-bitter tasting thaumatin peptide AAASKGDAAL (dashed line) during *in vitro* gastric digestion. Samples were taken after 0, 0.25, 0.5, 0.75, 1, 2, 3, 4, 5, and 6 h of digestion and quantitated by means of UHPLC−MS/MS-MRM measurements. Data shown as mean ± SEM, $n$ = 4, transitions per peptide = 5.

detected after 15 min of digestion, whereas lowest values were obtained at the last time point examined (6.6 ± 0.4 μM and 14.4 ± 0.8 μM, respectively), indicating a further breakdown of these peptides into smaller peptides and/or amino acids (Fig. 2, dark gray and dashed line). In contrast, mean concentrations of DAGGRQLNSGES and WTINVEPGTKGGKIW increased to 300.5 ± 2.3 μM, and 220.6 ± 1.3 μM, respectively, after the first hour of digestion, and were still at concentrations of 291.8 ± 2.3 μM and 171.4 ± 1.0 μM at the final time point of six hours of simulated gastric digestion (Fig. 2, black and light gray line). At time point 0, directly before initiation of the digestion process by enzyme addition, the release rates for all four peptides investigated were ≤ 0.5%. The highest release rate overall was observed for WTINVEPGTKGGKIW (originated from thaumatin II; see supplementary data **Table S2**), with 69.64 ± 0.42% after one hour of *in vitro* digestion and 54.12 ± 0.32% after six hours of *in vitro* digestion, based on the thaumatin concentrations used. The maximum release of DAGGRQLNSGES was reached at 49.70 ± 1.09% after three hours and was 46.05 ± 0.37% after six hours. After 15 min, the release of FNVPMDF was 23.94 ± 0.26% and decreased to 1.04 ± 0.06% at six hours. Following a similar pattern, the non-bitter peptide AAASKGDAAL was released at 9.67 ± 0.28% after 15 min and was further cleaved, resulting in a final concentration of 2.27 ± 0.11% after six hours.

Under *in vivo* conditions, release of the peptides by the two-hour gastric digestion resulted in the nanomolar range (Fig. 3). The highest release was found for the peptide FNVPMDF and was 1060 ± 276 nM. Concentrations of 179 ± 43 nM, 615 ± 135 nM, and 334 ± 108 nM were found for the peptides AAASKGDAAL, DAGGRQLNSGES, and WTINVEPGTKGGKIW, respectively.

Based on the quantitative data revealed for the formation of these four selected peptides, follow-up experiments, regarding their bitter taste receptor-mediated impact on *H. pylori*-induced pro-inflammatory cytokine release, were conducted.

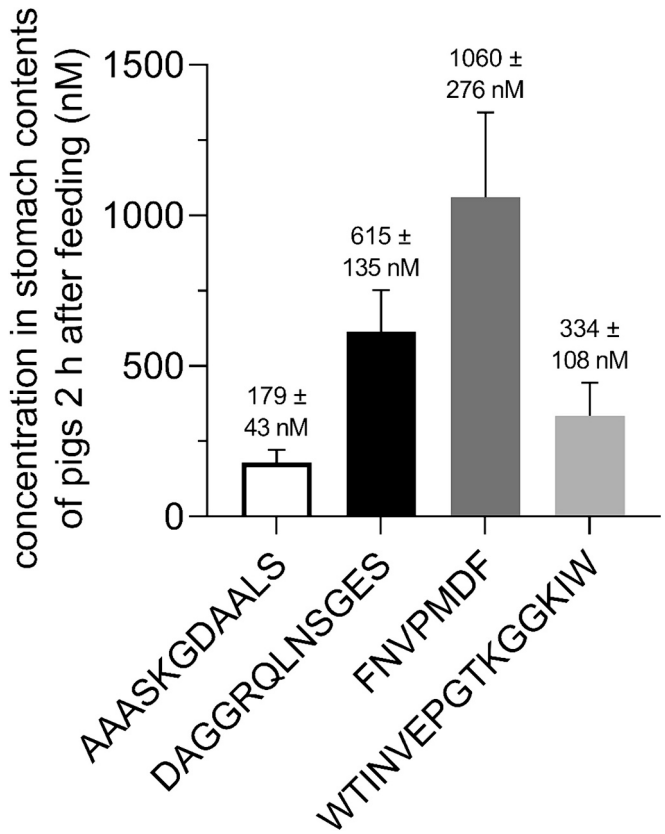


**Fig. 3.** Released concentrations of the four investigated peptides in the stomach contents of pigs after two hours of stomach digestion. Data shown as mean ± SEM, $n = 6$, transitions per peptide = 5.

### 3.5. Simulated *H. pylori* infection leads to regulation of gene expression of numerous chemokines and cytokines and leads to increased release of signaling proteins by HGT-1 cells

Expression analysis (RT-qPCR) of 55 common chemokines and cytokines using samples from HGT-1 cells cultured with native proteins from *H. pylori* (10 μg/mL; cytotoxic effect was excluded, see supplementary data **Fig. S3**) showed a variety of up- and down-regulations of mRNA levels (see supplementary data **Fig. S4** and **Table S4**).

Focusing on the release of cytokines, the cell supernatants of HGT-1 cells exposed to a mixture of native proteins of *H. pylori* for six hours demonstrated increasing concentrations of several cytokines compared to untreated control cells (Table 1). Specifically, a rise in interleukin concentration was observed for IL-1β (+44.0 ± 15.0%; $p \leq 0.05$); IL-6 (+29.4 ± 7.4%; $p \leq 0.01$); IL-11 (+32.9 ± 5.3%; $p \leq 0.001$); IL-15 (+23.7 ± 7.1%; $p \leq 0.05$); IL-16 (+47.4 ± 11.8%; $p \leq 0.01$); IL-17A (+41.4 ± 17.0%; $p \leq 0.05$); IL-19 (+38.0 ± 8.3%; $p \leq 0.01$); IL-31 (+19.2 ± 4.4%; $p \leq 0.05$); and IL-34 (+32.4 ± 8.2%; $p \leq 0.05$). Since gene expression of IL-19, IL-31, and IL-34 was not examined in the RT-qPCR experiments and no regulation at the mRNA level was detectable for the expression of IL-6 and IL-16, no link to the increased release of these proteins by the HGT-1 cells and their gene expression could be made. IL-18BP gene expression was not examined, but modulation of IL-18 expression was shown after 30 and 360 min treatment, which might be related to *H. pylori* induced IL-18BP release (+25.6 ± 6.3%; $p \leq 0.05$) (Harms, Creer, Lorenzo-Arteaga, Ostlund, & Sarvetnick, 2017). Although detection of an IL-1β-specific RNA transcript was not possible, increased secretion of IL-1β by HGT-1 cells occurred. Consistent with the observed down-regulations of gene expression of IL-11, IL-15, and IL-17A, an increased release were found for these representatives, possibly resulting in a negative feedback circuit (Vohradský, 2001). This suggests that the three cytokines IL-11, IL-15, and IL-17A might play a role in the *H. pylori* induced immune response.

**Table 1**
Human cytokines whose secretion was increased after incubation with native proteins of *H. pylori* for six hours. Data are shown as mean ± SEM after incubation for six hours, n = 4, t. r. = 2, statistics: *t*-test Holm-Šidák method.

| Protein | Increase over control (%) | *p* value | Bound protein normalized to positive control (%) |
|---|---|---|---|
| IL-1β | 44.0 ± 15.0 | ≤ 0.05 | 2.31 |
| IL-6 | 29.4 ± 7.4 | ≤ 0.01 | 3.49 |
| IL-11 | 32.9 ± 5.3 | ≤ 0.001 | 7.08 |
| IL-15 | 23.7 ± 7.1 | ≤ 0.05 | 3.42 |
| IL-16 | 47.4 ± 11.8 | ≤ 0.01 | 5.52 |
| **IL-17A** | **41.4 ± 17.0** | **≤ 0.05** | **11.82** |
| IL-18 BP | 25.6 ± 6.3 | ≤ 0.05 | 4.12 |
| IL-19 | 38.0 ± 8.3 | ≤ 0.01 | 2.76 |
| IL-31 | 19.2 ± 4.4 | ≤ 0.05 | 4.64 |
| IL-34 | 32.4 ± 8.2 | ≤ 0.05 | 2.79 |
| CCL17 | 52.7 ± 9.3 | ≤ 0.01 | 3.88 |
| CCL19 | 60.2 ± 14.3 | ≤ 0.05 | 4.12 |
| CCL20 | 26.0 ± 7.5 | ≤ 0.05 | 4.41 |
| CXCL5 | 43.6 ± 10.7 | ≤ 0.01 | 2.74 |
| CXCL10 | 45.5 ± 8.4 | ≤ 0.01 | 3.30 |
| CXCL11 | 31.0 ± 8.1 | ≤ 0.05 | 3.81 |
| C-Reactive Protein | 33.8 ± 5.5 | ≤ 0.01 | 4.39 |
| RAGE | 21.7 ± 4.5 | ≤ 0.01 | 7.14 |

While no detectable changes for *CCL19* and *CCL20* mRNA levels were observed, an increased protein release of these chemokines was detected after incubation with native proteins of *H. pylori*. The release for CCL19 increased by +60.2 ± 14.3% ($p \leq 0.05$), while for CCL20 a concentration increase of +26.0 ± 7.5% ($p \leq 0.05$) was detectable in the cell supernatants. Consistent with the down-regulation of *CCL17* gene expression found after 30 and 180 min, the release of this chemokine was increased by +52.7 ± 9.3% ($p \leq 0.01$) after six hours incubation with *H. pylori*.

From a gene regulation perspective, down-regulation of mRNA expression for CXC motif chemokines was found for the genes *CXCL5*, *CXCL10* and *CXCL11*, however their protein release into the medium was increased: CXCL5 (+43.6 ± 10.7%; $p \leq 0.01$), CXCL10 (+45.5 ± 8.4%; $p \leq 0.01$), and CXCL11 (+31.0 ± 8.1%; $p \leq 0.05$). Reduced mRNA levels and simultaneous increase in synthesis and release rates at the protein level are indications that CXCL5, CXCL10 and CXCL11 are also important signaling proteins involved in *H. pylori* infection.

Furthermore, after incubation of HGT-1 cells with native proteins from *H. pylori*, increased releases of C-Reactive Protein (+33.8 ± 5.5%; $p \leq 0.01$) and RAGE (+21.7 ± 4.5%; $p \leq 0.01$), were also detected.

Overall, treatment of HGT-1 cells with *H. pylori* protein induced a broad increase of chemokine protein release into the cell's supernatant. The next set of experiments was aimed at identifying whether the hypothesized modulating effects of bitter peptides, released from thaumatin during gastric digestion, is TAS2R-dependent and affects the *H. pylori*-induced release of the pro-inflammatory interleukin IL-17A, which was studied since its increase of bound protein relative to control was most pronounced (11.82%; Table 1).

### 3.6. Bitter peptides reduce a *H. pylori*-induced IL-17A release

For the *H. pylori*-evoked release of IL-17A, a cytokine that is known to be associated with *H. pylori* infections and to be involved in the initiation of gastritis and, in the long term, gastric cancer (Kang et al., 2023), the impact of the bitter peptides DAGGRQLNSGES, FNVPMDF and WTINVEPGTKGGKIW revealed a reduction by 66.6 ± 29.6% ($p \leq 0.05$), 89.7 ± 21.9% ($p \leq 0.01$), and 87.0 ± 38.0% ($p \leq 0.05$), respectively, whereas the non-bitter peptide AAASKGDAAL had no effect ($p = 0.75$; black bars in Fig. 5B). This demonstrates that, in human parietal HGT-1 cells, bitter peptides reduce the IL-17A release triggered by *H. pylori*.

To validate whether this reduction in the *H. pylori*-induced release of

IL-17A depends on the bitter taste quality of the peptides mediated by a bitter taste receptor (TAS2R), the cellular bitter response of HGT-1 cells was examined using an established assay based on parietal proton secretion (Liszt et al., 2017). In addition, as published previously (Richter et al., 2022), the effects of bitter peptides on *TAS2R* gene regulation was investigated in order to consider TAS2R involvement.

### 3.7. Cellular bitter response to intact thaumatin and bitter peptides generated upon gastric digestion thereof

Before the cellular bitter response was tested in the established HGT-1 cell model (Liszt et al., 2017), cell viability was tested by MTT assays. Here, no impaired cell viability (cell viability ≥96%) was detected (see supplementary data **Fig. S1**) after six hours of incubation with a concentration of either 100 μM of thaumatin or any of the four peptides tested (non-bitter: AAASKGDAAL; bitter: DAGGRQLNSGES, FNVPMDF and WTINVEPGTKGGKIW).

The cellular bitter response was tested by means of a proton-sensitive dye that allows to quantitate the intracellular concentration of protons (IPX) and is indicative of a TAS2R-associated proton secretion by HGT-1 cells (Liszt et al., 2017). While negative IPX values in the proton secretion assay represent an increased proton secretion as cellular bitter response, positive IPX values represent inhibition of these and an associated increased intracellular $H^+$ concentration, compared with untreated control cells (Liszt et al., 2017). Incubation of HGT-1 cells with the bitter peptides DAGGRQLNSGES and FNVPMDF resulted in stimulation of proton secretion at concentrations of 1 nM or lower (Fig. 4A). The strongest secretory activities were observed at peptide concentrations of 10 pM (IPX -0.218 ± 0.030; $p \leq 0.0001$) and 100 pM (IPX -0.224 ± 0.025; $p \leq 0.0001$), respectively (see supplementary data **Fig. S5B + C**). Notably, the solvent control to FNVPMDF, DMSO, did not affect IPX (final concentration of DMSO on cells: 0.03%). WTINVEPGTKGGKIW induced a stimulation of proton secretion at concentrations of 100 nM or lower, which was strongest at 100 pM with an IPX of −0.198 ± 0.029 ($p \leq 0.0001$; Fig. 4A). For each of the three bitter peptides, a hormetic concentration dependence, *i.e.*, a reduction of the effect size at lower and higher concentrations, was detectable (see supplementary data **Fig. S5B—D**). Similar effects were previously found for bitter peptides released upon gastric digestion of casein (Richter et al., 2022) and for cells stimulated with serotonin (Holik et al., 2021). Here, it is hypothesized that higher peptide concentrations lead to the involvement of specific proton-dependent peptide transporters, which also influence intercellular proton concentrations and therefore, at further increasing concentrations (>100 μM), lead to higher intracellular proton concentrations (symport with $H^+$) and decreased $H^+$-secretory activities (Rubio-Aliaga & Daniel, 2002). However, since daily intake of thaumatin does not lead to gastric peptide concentrations in this range, this mechanism was not considered in the context of this work.

Whereas the non-bitter peptide AAASKGDAAL did not affect IPX in a concentration range of 1 pM - 100 nM (see supplementary data **Fig. S5E**), treatment of the HGT-1 cells with 1 mM histamine as a positive control resulted in increased proton secretion ($p \leq 0.0001$), thereby allowing the functionality of the assay to be monitored.

Treatment of the cells with the TAS1R1/3 targeting protein thaumatin (Li et al., 2002) also decreased the IPX values (see supplementary data **Fig. S5A**), with the greatest effect observed at a concentration of 1 nM (IPX -0.279 ± 0.021; $p \leq 0.0001$; Fig. 4A). Although it is yet not known whether thaumatin activates TAS2Rs at a molecular level, a hormetic concentration dependence was also observed for its effect on intracellular proton concentrations (IPX).

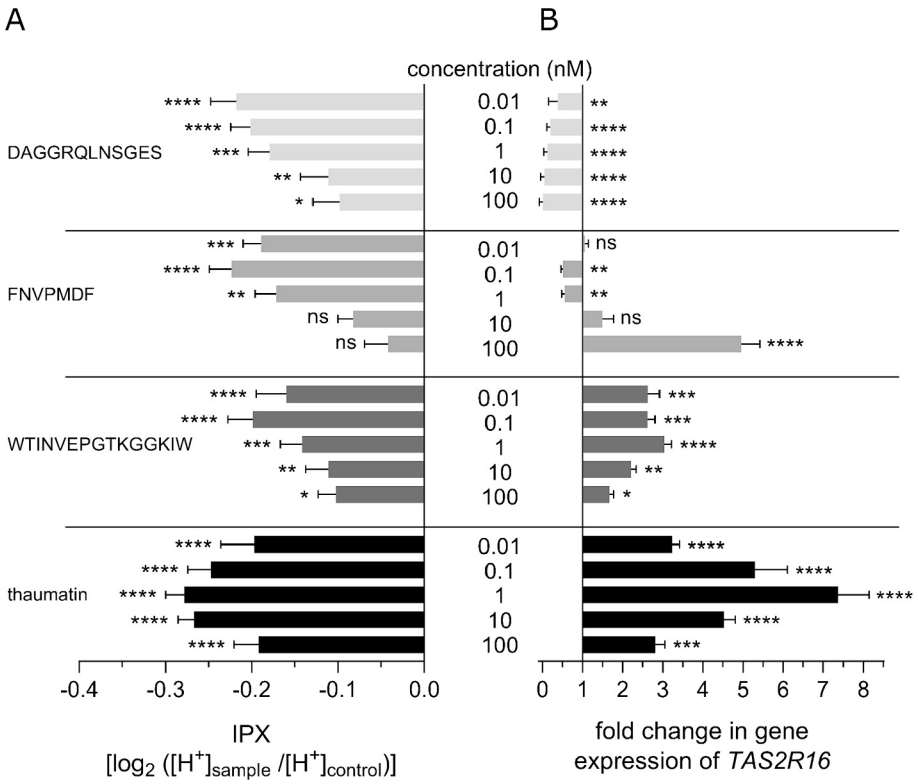


**Fig. 4.** (A) Effects of peptides DAGGRQLNSGES, FNVPMDF, WTINVEPGTKGGKIW, and intact thaumatin on proton secretion (untreated control cells represent an IPX of 0), with lower levels of IPX representing greater secretory activity. (B) Impact on *TAS2R16* mRNA levels (untreated control cells represent a fold-change of 1). Data shown as mean ± SEM, n = 4, t. r. = 4–6, control: KRHB, Statistics: one-way ANOVA Holm-Šidák *post hoc* test; significant differences are expressed with * = $p \leq 0.05$, ** = $p \leq 0.01$, *** = $p \leq 0.001$, **** = $p \leq 0.0001$.

### 3.8. Bitter peptides and thaumatin induce a concentration-dependent change in gene expression of TAS2R16

To investigate an involvement of TAS2Rs in the stimulation of proton secretion induced by bitter peptides and thaumatin, effects on gene expression were examined by RT-qPCR. Curve fit calculations allowed a determination of the concentrations with the strongest effect on secretory activity ($IPX_{min}$). An $IPX_{min}$ of 5 pM could be calculated for DAGGRQLNSGES and 30 pM for FNVPMDF and WTINVEPGTKGGKIW (see supplementary data **Fig. S6**). The lowest IPX value for thaumatin was obtained at a concentration of 2.3 nM. For better comparability, a concentration of 30 pM of the respective peptides and thaumatin was used to screen changes of mRNA transcript levels of all 25 TAS2Rs.

Incubation with thaumatin or the peptides resulted in a significant ($p \leq 0.05$) and distinct (fold-change $\geq 2$) up-regulation of the *TAS2R16*, *TAS2R38*, and *TAS2R41* genes, respectively (data not shown). This observation was consistent with previous experiments with bitter casein peptides, ultimately demonstrating the involvement of TAS2R16 and TAS2R38 in bitter peptide-mediated stimulation of mechanisms of gastric acid secretion (Richter et al., 2022). Comparison of the expression of these three TAS2Rs in the native cell line HGT-1 showed that *TAS2R16* was expressed most strongly ($p \leq 0.0001$; see supplementary data **Fig. S7**). Based on this and the fact that TAS2R16 activation by bitter peptides in casein hydrolysates in the HEK293 model was also shown by Maehashi et al., 2008, follow-up experiments focused on the involvement of TAS2R16.

To investigate whether the concentration-dependent stimulation of proton secretion by the bitter peptides and intact thaumatin is also reflected in *TAS2R16* expression, the effects of thaumatin and the selected bitter peptides generated upon gastric digestion of thaumatin on *TAS2R16* gene expression in HGT-1 cells were studied at concentrations between 0.01 and 100 nM (Fig. 4B). Positive correlations ($R^2 = 0.88$ and 0.57, respectively) were found for thaumatin and the peptide WTINVEPGTKGGKIW. While concentrations of 1 nM led to the strongest up-regulation of *TAS2R16* gene expression in both cases (fold-change 7.37 ± 0.77 for thaumatin, $p \leq 0.0001$; 3.03 ± 0.18 for WTINVEPGTKGGKIW, $p \leq 0.0001$), this effect decreased at higher and lower concentrations, but was statistically significant at all concentrations tested ($p \leq 0.05$). Again, the hormetic effect previously observed for IPX values indicating proton secretion was evident. While there was a reduction in the stimulatory effect of the bitter peptide DAGGRQLNSGES on the IPX with increasing concentrations from 10 pM, interestingly, an increase in concentration led to an enhanced down-regulation of *TAS2R16* expression ($R^2 = 0.97$). Therefore, there was a strong reduction of expression to 0.01 ± 0.01 (fold-change; $p \leq 0.0001$) after treatment with 100 nM DAGGRQLNSGES. Likewise, incubations with 0.1 and 1 nM FNVPMDF ($R^2 = 0.70$) resulted in down-regulation of *TAS2R16* mRNA levels to 0.51 ± 0.05 (fold-change; $p \leq 0.01$) and 0.55 ± 0.07 (fold-change; $p \leq 0.01$), respectively. However, this reduced gene expression was no longer observed as the concentration increased to 10 nM FNVPMDF and finally reversed at 100 nM, resulting in a strong up-regulation to 4.96 ± 0.46 (fold-change; $p \leq 0.0001$). Overall, the three bitter peptides studied as well as their parent protein thaumatin show a concentration-dependent influence on *TAS2R16* expression. These findings confirm that TAS2R16 is involved in the bitter peptide-mediated stimulation of the mechanisms of proton secretion in HGT-1 cells. As shown in past studies, both up- and down-regulation of the expression of specific genes may indicate the involvement of receptors, ion channels or other proteins (Gry et al., 2009; Vohradský, 2001). In this context, it should be noted that the involvement of receptors in cellular processes does not necessarily result in regulation of their mRNA levels. While desensitization has been shown for other membrane proteins in the past, there is no such evidence for TAS2Rs.

### 3.9. TAS2R16 antagonist probenecid inhibits bitter peptide-induced stimulation of proton secretion

Further evidence to support the assumption of a TAS2R16 involvement resulted from co-treatment of the cells with the organic anion transporter inhibitor probenecid (Nigam et al., 2015). In the past, the ability of this sulfobenzoic acid derivative to inhibit TAS2R16 activation has been described, making probenecid an antagonist of TAS2R16 (Greene et al., 2011; Richter et al., 2022).

Whereas incubation of HGT-1 cells with 1 mM probenecid solely showed no effect on proton secretion ($p = 0.22$; *vs.* untreated cells), co-incubation of 30 pM DAGGRQLNSGES, FNVPMDF, WTINVEPGTKGGKIW, or the intact protein thaumatin with 1 mM probenecid resulted in a reduction of the stimulatory effects of each peptide to baseline levels in all cases ($p > 0.05$; see supplementary data **Fig. S8**). Treatment of the cells with the peptides and protein alone again resulted in the already observed stimulation of the mechanisms of gastric acid secretion ($p \leq 0.0001$). To exclude the influence of probenecid on proton secretion in HGT-1 cells in a TAS2R-independent pathway, proton secretion was stimulated by activation of the $H_2$ receptor with 1 mM histamine. Here, no difference was found between the presence and absence of probenecid ($p = 0.92$). In addition to the antagonistic effect of probenecid on TAS2R16, inhibition of TAS2R38 and TAS2R43 has also been found in the past (Greene et al., 2011). Studies on casein peptides also showed a reduction in the stimulatory effects of bitter peptides when cells were co-treated with probenecid. Final knock-down experiments here showed actual involvement of both TAS2R16 and TAS2R38 (Richter et al., 2022).

### 3.10. Reduction of H. pylori evoked IL-17A release by bitter peptides is TAS2R16 dependent

Involvement of the bitter taste receptor TAS2R16, which already plays a central role in the bitter peptide-mediated stimulation of proton secretion from HGT-1 cells and the reduction of LPS-induced cytokine expression (Zhou et al., 2021), was demonstrated by knock-down experiments using siRNA (HSS181763; Fig. 5A). Here, the mRNA expression of *TAS2R16* was reduced by 51.6 ± 4.5% ($p \leq 0.0001$) *vs.* mock-transfected control cells. No difference in *H. pylori*-induced IL-17A secretion was observed between *TAS2R16*kd and mock-transfected cells ($p > 0.05$). In *TAS2R16*kd cells, the bitter peptides no longer caused the reducing effect ($p = 0.20$–$0.46$), making it clear that the involvement of TAS2R16 in bitter peptide-mediated reduced IL-17A release plays a crucial role (white bars in Fig. 5B). Nevertheless, it cannot be ruled out that other bitter taste receptors also contribute to this bitter peptide-mediated reduction of *H. pylori*-induced IL-17A release.

### 3.11. Achievable physiological peptide concentrations in the stomach are in the low nanomolar range

Based on the sweetening power of thaumatin (threshold <50 nM), which is equivalent to 1600 times that of sucrose (by weight), the habitual daily intake by humans is very low (van der Wel & Loeve, 1972). A common industrial use of thaumatin are as non-caloric sugar substitutes alongside acesulfame K, cyclamate, and saccharin, for example in sweetener tablets (Nikolelis & Pantoulias, 2001). The thaumatin content of a commercially available sweetener tablet determined by Bradford assay (pure thaumatin was used as an external standard) was 13.92 ± 0.80 μg per tablet. This corresponds to a thaumatin content of 0.02% based on the total weight of 71.04 mg per tablet and results in a maximum achievable concentration in the stomach between 0.5 and 3.8 nM for the respective peptides, considering the specific release rates and a stomach volume between 100 and 1000 mL. Since all thaumatin-derived bitter tasting peptides studied, namely DAGGRQLNSGES, FNVPMDF, WTINVEPGTKGGKIW, evoked cellular responses in the nanomolar range, thaumatin intake at habitual doses warrant further

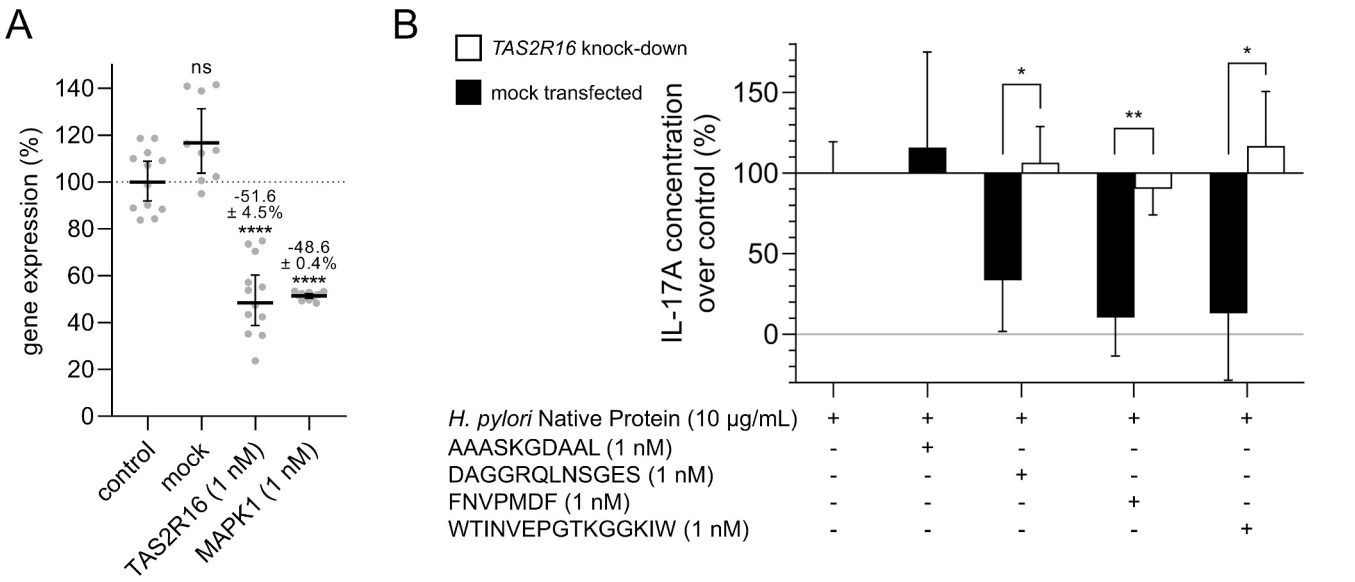


**Fig. 5.** (A) Reduction of gene expression using specific siRNA (*TAS2R16*; HSS181763) after 72 h. Mock control was performed using non-specific siRNA. As a positive control, the expression of MAPK1 (VHS40312) was reduced (−48.6 ± 0.4%; $p \leq 0.0001$). Gene expression of *TAS2R16* was reduced by −51.6 ± 4.5% ($p \leq 0.0001$). Data are shown as mean ± SEM after incubation with siRNA for 72 h, $n = 3$–4, t. r. = 3, control: DMEM; statistics: *t*-test Holm-Šidák method; significant differences are expressed with **** = $p \leq 0.0001$. (B) IL-17A release from HGT-1 cells incubated with *H. pylori* native protein (10 µg/mL; = 100%). Black bars represent mock-transfected cells, white bars *TAS2R16* knock-down cells. In all cases, co-incubation was performed with *H. pylori* Native Protein (10 µg/mL) and the respective peptide at a concentration of 1 nM. Data are shown as mean ± SEM, n = 4, t. r. = 1–2, statistics: *t*-test Holm-Šidák method; significant differences are expressed with * = $p \leq 0.05$, ** = $p \leq 0.01$.

studies to elucidate the potential anti-inflammatory effects associated with an *H. pylori* infection.

In conclusion, the sweet-tasting protein thaumatin was shown to be cleaved into bitter-tasting peptides during gastric digestion. Three of these bitter peptides, namely DAGGRQLNSGES, FNVPMDF, and WTINVEPGTKGGKIW, were demonstrated to stimulate proton secretion as a mechanism of gastric acid secretion of immortalized human parietal cells. Peptide concentrations in the nanomolar range, which can be achieved by ingestion of a single thaumatin-containing sweetener tablet, are sufficient to reduce the *H. pylori*-evoked release of the pro-inflammatory IL-17A protein *via* functional involvement of bitter taste receptor TAS2R16 in human parietal HGT-1 cells in culture.

## Funding

This research did not receive any specific grant from funding agencies in the public, commercial, or not-for-profit sectors.

## CRediT authorship contribution statement

**Phil Richter:** Writing – review & editing, Writing – original draft, Validation, Methodology, Investigation, Formal analysis, Conceptualization. **Karin Sebald:** Writing – review & editing, Methodology, Conceptualization. **Konrad Fischer:** Writing – review & editing, Methodology, Investigation. **Angelika Schnieke:** Writing – review & editing, Methodology. **Malek Jlilati:** Investigation. **Verena Mittermeier-Klessinger:** Writing – review & editing, Methodology. **Veronika Somoza:** Writing – review & editing, Validation, Supervision, Resources, Project administration, Methodology, Funding acquisition, Conceptualization.

## Declaration of competing interest

The authors declare the following financial interests/personal relationships which may be considered as potential competing interests: Phil Richter (co-author), Veronika Somoza (corresp. author) reports financial support, administrative support, article publishing charges, and equipment, drugs, or supplies were provided by Leibniz-Institute for Food Systems Biology at the Technical University of Munich. Veronika Somoza reports a relationship with Leibniz-Institute for Food Systems Biology at the Technical University of Munich that includes: employment. If there are other authors, they declare that they have no known competing financial interests or personal relationships that could have appeared to influence the work reported in this paper.

## Data availability

Data will be made available on request.

*Acknowledgements*

The authors thank Katrin Gradl for her support in developing the LC-MS/MS method, Kristin Kahlenberg for excellent technical assistance, Gaby Andersen for her help in answering scientific questions, Johanna Kreißl for her support in recording the NMR spectra, and Katharina Schiesser for her assistance with the sensory study.

*Ethical statement*

Sensory studies

This study was conducted in accordance with the principles of the Declaration of Helsinki. The trained panelists, who were asked to evaluate the taste quality of the thaumatin peptides as part of the sensory studies, were informed before the tests were carried out and provided written informed consent prior to enrollment. Thaumatin is an approved food protein (Gleba, 2017) that is already used in food. The purity of the resulting peptides, which are formed during the digestion of thaumatin, was checked by LC-MS and NMR. To further minimize the risk, the panelists were instructed not to swallow the sample solutions but to spit them out.

Gleba, Y. (2017). GRAS Notice for THAUMATIN Sweetener and Food Flavor Modifier, US FDA GRAS Notice No GRN 738. https://www.fda.gov/media/110043/download.

Animal experiments

Thaumatin was authorised as feed in the European Union under Implementing Regulation No 869/2012 in September 2012. Animal experiments were performed according to the European laws for handling and care of experimental animals.

## Appendix A. Supplementary data

Supporting information to this manuscript include optimized parameters of individual peptides for quantification by targeted proteomics (Table S1), amino acid sequences of the two thaumatin forms investigated (Table S2), results for the sensory study (Table S3), significant gene regulations of common chemo- and cytokines (Table S4), influence of thaumatin, the investigated peptides, probenecid and DMSO (solvent) on cell viability (Fig. S1), verification of retention times and SRM mass transitions of the four peptides studied (Fig. S2), influence of *H. pylori* native proteins on cell viability (Fig. S3), gene regulations of common chemo- and cytokines (Fig. S4), effects on proton secretion of HGT-1 cells incubated with intact thaumatin, the bitter peptides and the non-bitter reference peptide (Fig. S5), curve fit calculations of the proton secretion profiles (Fig. S6), representation of gene expression of *TAS2R16*, *TAS2R38*, and *TAS2R41* in HGT-1 cells (Fig. S7), co-incubation of HGT-1 cells with probenecid and the bitter peptides or thaumatin (Fig. S8). Supplementary data to this article can be found online at https://doi.org/10.1016/j.foodchem.2024.139157.

## References


Bauditz, J., Ortner, M., Bierbaum, M., Niedobitek, G., Lochs, H., & Schreiber, S. (1999). Production of IL-12 in gastritis relates to infection with Helicobacter pylori. *Clinical and Experimental Immunology, 117*, 316–323.

Beales, I. L., & Calam, J. (1997). Helicobacter pylori stimulates granulocyte-macrophage colony-stimulating factor (GM-CSF) production from cultured antral biopsies and a human gastric epithelial cell line. *European Journal of Gastroenterology & Hepatology, 9*, 451–455.

Behrens, M., & Meyerhof, W. (2013). Bitter taste receptor research comes of age: From characterization to modulation of TAS2Rs. *Seminars in Cell & Developmental Biology, 24*, 215–221.

Bethineedi, L. D., Baghsheikhi, H., Soltani, A., Mafi, Z., Samieefar, N., Sanjid Seraj, S., & Khazeei Tabari, M. A. (2023). Human T2R38 bitter taste receptor expression and COVID-19: From immunity to prognosis. *Avicenna Journal Of Medical Biotechnology, 15*, 118–123.

Brodkorb, A., Egger, L., Alminger, M., Alvito, P., Assunção, R., Ballance, S., … Recio, I. (2019). INFOGEST static in vitro simulation of gastrointestinal food digestion. *Nature Protocols, 14*, 991–1014.

Bufe, B., Hofmann, T., Krautwurst, D., Raguse, J.-D., & Meyerhof, W. (2002). The human TAS2R16 receptor mediates bitter taste in response to beta-glucopyranosides. *Nature Genetics, 32*, 397–401.

Charoenkwan, P., Nantasenamat, C., Hasan, M. M., Manavalan, B., & Shoombuatong, W. (2021). BERT4Bitter: A bidirectional encoder representations from transformers (BERT)-based model for improving the prediction of bitter peptides. *Bioinformatics, 37*, 2556–2562.

Charoenkwan, P., Yana, J., Schaduangrat, N., Nantasenamat, C., Hasan, M. M., & Shoombuatong, W. (2020). iBitter-SCM: Identification and characterization of bitter peptides using a scoring card method with propensity scores of dipeptides. *Genomics, 112*, 2813–2822.

Cox, J., & Mann, M. (2008). MaxQuant enables high peptide identification rates, individualized p.p.b.-range mass accuracies and proteome-wide protein quantification. *Nature Biotechnology, 26*, 1367–1372.

Frank, O., Kreissl, J. K., Daschner, A., & Hofmann, T. (2014). Accurate determination of reference materials and natural isolates by means of quantitative (1)h NMR spectroscopy. *Journal of Agricultural and Food Chemistry, 62*, 2506–2515.

Gleba, Y. (2017). GRAS notice for THAUMATIN sweetener and food flavor modifier, US FDA GRAS notice no GRN 738. https://www.fda.gov/media/110043/download.

Greene, T. A., Alarcon, S., Thomas, A., Berdougo, E., Doranz, B. J., Breslin, P. A. S., & Rucker, J. B. (2011). Probenecid inhibits the human bitter taste receptor TAS2R16 and suppresses bitter perception of salicin. *PLoS One, 6*, Article e20123.

Gry, M., Rimini, R., Strömberg, S., Asplund, A., Pontén, F., Uhlén, M., & Nilsson, P. (2009). Correlations between RNA and protein expression profiles in 23 human cell lines. *BMC Genomics, 10*, 365.

Harms, R. Z., Creer, A. J., Lorenzo-Arteaga, K. M., Ostlund, K. R., & Sarvetnick, N. E. (2017). Interleukin (IL)-18 binding protein deficiency disrupts natural killer cell maturation and diminishes circulating IL-18. *Frontiers in Immunology, 8*, 1020.

Holik, A.-K., Schweiger, K., Stoeger, V., Lieder, B., Reiner, A., Zopun, M., … Somoza, V. (2021). Gastric serotonin biosynthesis and its functional role in L-arginine-induced gastric proton secretion. *International Journal of Molecular Sciences, 22*.

Kang, J. H., Park, S., Rho, J., Hong, E.-J., Cho, Y.-E., Won, Y.-S., & Kwon, H.-J. (2023). IL-17A promotes Helicobacter pylori-induced gastric carcinogenesis via interactions with IL-17RC. *Gastric Cancer, 26*, 82–94.

Labbe, D., Schlich, P., Pineau, N., Gilbert, F., & Martin, N. (2009). Temporal dominance of sensations and sensory profiling: A comparative study. *Food Quality and Preference, 20*, 216–221.

Li, X., Staszewski, L., Xu, H., Durick, K., Zoller, M., & Adler, E. (2002). Human receptors for sweet and umami taste. *Proceedings of the National Academy of Sciences of the United States of America, 99*, 4692–4696.

Liszt, K. I., Ley, J. P., Lieder, B., Behrens, M., Stöger, V., Reiner, A., … Somoza, V. (2017). Caffeine induces gastric acid secretion via bitter taste signaling in gastric parietal cells. *PNAS, 114*, E6260–E6269.

Liszt, K. I., Wang, Q., Farhadipour, M., Segers, A., Thijs, T., Nys, L., … Depoortere, I. (2022). Human intestinal bitter taste receptors regulate innate immune responses and metabolic regulators in obesity. *Journal of Clinical Investigation, 132*.

Lv, Y.-P., Cheng, P., Zhang, J.-Y., Mao, F.-Y., Teng, Y.-S., Liu, Y.-G., … Zhuang, Y. (2019). Helicobacter pylori-induced matrix metallopeptidase-10 promotes gastric bacterial colonization and gastritis. *Science Advances, 5*, Article eaau6547.

Maehashi, K., Matano, M., Wang, H., Vo, L. A., Yamamoto, Y., & Huang, L. (2008). Bitter peptides activate hTAS2Rs, the human bitter receptors. *BBRC, 365*, 851–855.

Meilgaard, M. C., & Carr, B. T. (2006). *Sensory evaluation techniques*. CRC Press.

Ney, K. H. (1971). Voraussage der Bitterkeit von Peptiden aus deren Aminosäurezusammensetzung. *European Food Research and Technology, 147*, 64–68.

Nigam, S. K., Bush, K. T., Martovetsky, G., Ahn, S.-Y., Liu, H. C., Richard, E., … Wu, W. (2015). The organic anion transporter (OAT) family: A systems biology perspective. *Physiological Reviews, 95*, 83–123.

Nikolelis, D. P., & Pantoulias, S. (2001). Selective continuous monitoring and analysis of mixtures of acesulfame-K, cyclamate, and saccharin in artificial sweetener tablets, diet soft drinks, yogurts, and wines using filter-supported bilayer lipid membranes. *Analytical Chemistry, 73*, 5945–5952.

Patterson, J. K., Lei, X. G., & Miller, D. D. (2008). The pig as an experimental model for elucidating the mechanisms governing dietary influence on mineral absorption. *EBM, 233*, 651–664.

Richter, P., Andersen, G., Kahlenberg, K., Mueller, A. U., Pirkwieser, P., Boger, V., & Somoza, V. (2024). Sodium-permeable ion channels TRPM4 and TRPM5 are functional in human gastric parietal cells in culture and modulate the cellular response to bitter-tasting food constituents. *Journal of Agricultural and Food Chemistry, 72*, 4906–4917.

Richter, P., Sebald, K., Fischer, K., Behrens, M., Schnieke, A., & Somoza, V. (2022). Bitter peptides YFYPEL, VAPFPEVF, and YQEPVLGPVRGPFPIIV, released during gastric digestion of casein, stimulate mechanisms of gastric acid secretion via bitter taste receptors TAS2R16 and TAS2R38. *Journal of Agricultural and Food Chemistry, 70*, 11591–11602.

Rubio-Aliaga, I., & Daniel, H. (2002). Mammalian peptide transporters as targets for drug delivery. *Trends in Pharmacological Sciences, 23*, 434–440.

Salama, N. R., Hartung, M. L., & Müller, A. (2013). Life in the human stomach: Persistence strategies of the bacterial pathogen Helicobacter pylori. *Nature Reviews Microbiology, 11*, 385–399.

Shiomi, S., Toriie, A., Imamura, S., Konishi, H., Mitsufuji, S., Iwakura, Y., Yamaoka, Y., Ota, H., Yamamoto, T., Imanishi, J., & Kita, M. (2008). IL-17 is involved in Helicobacter pylori-induced gastric inflammatory responses in a mouse model. *Helicobacter, 13*, 518–524.

Suerbaum, S., & Michetti, P. (2002). Helicobacter pylori infection. *The New England Journal of Medicine, 347*, 1175–1186.

Tiroch, J., Dunkel, A., Sterneder, S., Zehentner, S., Behrens, M., Di Pizio, A., … Somoza, V. (2023). Human gingival fibroblasts as a novel cell model describing the association between bitter taste thresholds and Interleukin-6 release. *Journal of Agricultural and Food Chemistry, 71*, 5314–5325.

Tiroch, J., Sterneder, S., Di Pizio, A., Lieder, B., Hoelz, K., Holik, A.-K., … Somoza, V. (2021). Bitter sensing TAS2R50 mediates the trans -resveratrol-induced anti-inflammatory effect on interleukin 6 release in HGF-1 cells in culture. *Journal of Agricultural and Food Chemistry, 69*, 13339–13349.

Tyanova, S., Temu, T., & Cox, J. (2016). The MaxQuant computational platform for mass spectrometry-based shotgun proteomics. *Nature Protocols, 11*, 2301–2319.

UniProt Consortium. (2023). UniProt: The universal protein knowledgebase in 2023. *Nucleic Acids Research, 51*, D523–D531.

Vohradský, J. (2001). Neural network model of gene expression. *The FASEB Journal, 15*, 846–854.

van der Wel, H., & Loeve, K. (1972). Isolation and characterization of thaumatin I and II, the sweet-tasting proteins from *Thaumatococcus daniellii* Benth. *European Journal of Molecular Biology and Biochemistry, 31*, 221–225.

Yamauchi, K., Choi, I.-J., Lu, H., Ogiwara, H., Graham, D. Y., & Yamaoka, Y. (2008). Regulation of IL-18 in Helicobacter pylori Infection1. *Journal of Immunology, 180*, 1207–1216.

Younes, M., Aquilina, G., Castle, L., Engel, K.-H., Fowler, P., Frutos Fernandez, M. J., … Vianello, G. (2021). Re-evaluation of thaumatin (E 957) as food additive. *EFSA, 19*, Article e06884.

Zhou, Z., Xi, R., Liu, J., Peng, X., Zhao, L., Zhou, X., … Xu, X. (2021). TAS2R16 activation suppresses LPS-induced cytokine expression in human gingival fibroblasts. *Frontiers in Immunology, 12*, Article 726546.

# Supplementary data

## Gastric digestion of the sweet-tasting plant protein thaumatin releases bitter peptides that reduce *H. pylori* induced pro-inflammatory IL-17A release via the TAS2R16 bitter taste receptor

By

Phil RICHTER[1,2], Karin SEBALD[2], Konrad FISCHER[3], Angelika SCHNIEKE[3], Malek JLILATI[2], Verena MITTERMEIER-KLESSINGER[4], Veronika SOMOZA[2,5,6*]

*[1]TUM School of Life Sciences Weihenstephan, Technical University of Munich, Alte Akademie 8, 85354 Freising, Germany*

*[2]Leibniz Institute for Food Systems Biology at the Technical University of Munich, Lise-Meitner-Str. 34, 85354 Freising, Germany*

*[3]Chair of Livestock Biotechnology, TUM School of Life Sciences, Technical University of Munich, Liesel-Beckmann-Str. 1, 85354 Freising, Germany*

*[4]Chair of Food Chemistry and Molecular Sensory Science, Technical University of Munich, Lise-Meitner-Str. 34, 85354 Freising, Germany*

*[5]Chair of Nutritional Systems Biology, TUM School of Life Sciences, Technical University of Munich, Lise-Meitner-Str. 34, 85354 Freising, Germany*

*[6]Department of Physiological Chemistry, Faculty of Chemistry, University of Vienna, Josef-Holaubek-Platz 2 (UZA II), 1090 Wien, Austria*

**Correspondence to Veronika Somoza: telephone +49-8161-71-2700, E-mail: v.somoza.leibniz-lsb@tum.de*

**Table S1.** Optimized parameters of individual peptides for quantification by targeted proteomics.

| sequence | Q1 mass (Da) | DP (volts) | Q3 mass (Da) | CE (volts) | CXP (volts) |
|---|---|---|---|---|---|
| AAASKGDAAL | 437.985 | 114 | 486.5 | 36 | 18 |
| | | | 573.6 | 36 | 18 |
| | | | 574.7 | 36 | 18 |
| | | | 601.6 | 36 | 18 |
| | | | 644.7 | 36 | 18 |
| DAGGRQLNSGES | 595.869 | 61 | 543.1 | 23 | 26 |
| | | | 586.8 | 23 | 28 |
| | | | 812.2 | 29 | 22 |
| | | | 187.0 | 33 | 22 |
| | | | 159.0 | 39 | 18 |
| FNVPMDF | 870.328 | 141 | 870.4 | 11 | 24 |
| | | | 509.7 | 37 | 26 |
| | | | 509.1 | 37 | 24 |
| | | | 119.9 | 125 | 12 |
| | | | 387.1 | 21 | 20 |
| WTINVEPGTKGGKIW | 562.815 | 71 | 699.9 | 23 | 12 |
| | | | 557.0 | 21 | 10 |
| | | | 159.3 | 33 | 10 |
| | | | 188.0 | 41 | 10 |
| | | | 170.1 | 41 | 20 |

**Table S2.** Amino acid sequences of the two thaumatin forms investigated. Quantified and tested peptides are marked in bold, underlined amino acids differ in the forms of thaumatin I to II.

| sequence of thaumatin I |
| --- |
| ATFEIVNRCSYTVW **AAASKGDAAL DAGGRQLNSGES** WTINVEPGTNGGKIW ARTDCYFDDSGSGICKTGDCGGLLRCKRFGRPPTTLAEFSLNQYGKDYIDISNIK G **FNVPMDF** SPTTRGCRGVRCAADIVGQCPAKLKAPGGGCNDACTVFQTSEYC CTT GKCGPTEYSRFFKRLCPDAFSYVLDKPTTVTCPGSSNYRVTFCPTA |
| sequence of thaumatin II |
| ATFEIVNRCSYTVW **AAASKGDAAL DAGGRQLNSGES WTINVEPGTKGGKIW** ARTDCYFDDSGRGICRTGDCGGLLQCKRFGRPPTTLAEFSLNQYGKDYIDISNIK G **FNVPMDF** SPTTRGCRGVRCAADIVGQCPAKLKAPGGGCNDACTVFQTSEYC CTTGKCGPTEYSRFFKRLCPDAFSYVLDKPTTVTCPGSSNYRVTFCPTA |

**Table S3.** Results for the sensory study, in which the indication of the most dominant taste quality of the individual peptides and the protein had to be given. Data are shown as mean ± SEM, n = 17-19, t. r. = 3, significant differences are expressed with ** = $p \leq 0.001$, *** = $p \leq 0.001$.

| | AAASK GDAAL (TH-I/II$_{15–24}$) | DAGGRQ LNSGES (TH-I/II$_{25–36}$) | FNVPMDF (TH-I/ II$_{108–114}$) | WTINVEPG TKGGKIW (TH-II$_{37–51}$) | Thaumatin |
|---|---|---|---|---|---|
| bitter | ns<br>33.5 ± 1.4% | **<br>50.0 ± 1.4% | ***<br>83.1 ± 4.2% | ***<br>100 ± 0.0% | ns<br>2.4 ± 0.6% |
| sweet | ns<br>10.6 ± 1.5% | ns<br>16.5 ± 0.3% | ns<br>8.7 ± 2.9% | ns<br>0.0 ± 0.0% | ***<br>97.6 ± 0.6% |
| different or no taste quality | ***<br>55.9 ± 0.8% | ns<br>33.5 ± 1.4% | ns<br>8.3 ± 1.4% | ns<br>0.0 ± 0.0% | ns<br>0.0 ± 0.0% |

**Table S4.** Significant ($p \leq 0.05$) gene regulations (mRNA) of common chemo- and cytokines after time-dependent incubation with native proteins of *H. pylori* (10 µg/mL). Significant regulations are shown as fold-change, n = 3-4, statistics: *t*-test Holm-Šidák method.

| gene | 0 min | 30 min | 60 min | 180 min | 360 min |
|---|---|---|---|---|---|
| *C5* | 1.00 | 0.42 | 0.52 | 0.57 | ns |
| *CCL1* | 1.00 | - | - | - | ns |
| *CCL2* | 1.00 | 4.62 | 2.91 | ns | ns |
| *CCL3* | 1.00 | 0.07 | 0.07 | 0.06 | 0.11 |
| *CCL5* | 1.00 | ns | ns | ns | ns |
| *CCL7* | 1.00 | 0.01 | ns | 0.07 | ns |
| *CCL8* | 1.00 | ns | ns | ns | ns |
| *CCL11* | 1.00 | ns | ns | ns | ns |
| *CCL13* | - | - | - | - | - |
| *CCL17* | 1.00 | 0.08 | ns | 0.06 | ns |
| *CCL18* | 1.00 | 0.07 | 0.08 | 0.09 | 0.14 |
| *CCL19* | 1.00 | ns | ns | ns | ns |
| *CCL20* | 1.00 | ns | ns | ns | ns |
| *CCL21* | 1.00 | 0.02 | 0.01 | 0.01 | 0.03 |
| *CCL22* | 1.00 | 0.61 | ns | 0.60 | ns |
| *CCL24* | 1.00 | 0.02 | ns | 0.05 | 0.01 |
| *CSF1* | 1.00 | 0.79 | ns | 0.70 | 0.79 |
| *CSF2* | 1.00 | 0.05 | 0.04 | 0.04 | 0.02 |
| *CSF3* | 1.00 | 0.08 | ns | 0.07 | 0.08 |
| *CX3CL1* | 1.00 | 0.54 | ns | ns | 0.66 |
| *CXCL1* | 1.00 | ns | ns | ns | ns |
| *CXCL2* | 1.00 | ns | ns | ns | ns |
| *CXCL5* | 1.00 | 0.01 | ns | 0.08 | 0.01 |
| *CXCL9* | 1.00 | ns | ns | ns | ns |
| *CXCL10* | 1.00 | ns | ns | 0.06 | ns |
| *CXCL11* | 1.00 | ns | ns | 0.06 | ns |
| *CXCL12* | 1.00 | - | - | - | ns |
| *CXCL13* | 1.00 | ns | ns | ns | ns |
| *CXCL16* | 1.00 | ns | 1.20 | ns | ns |

| gene | 0 min | 30 min | 60 min | 180 min | 360 min |
|---|---|---|---|---|---|
| *IL1A* | 1.00 | ns | ns | ns | ns |
| *IL1B* | - | - | - | - | - |
| *IL1RN* | 1.00 | - | ns | - | ns |
| *IL2* | 1.00 | ns | ns | ns | ns |
| *IL3* | 1.00 | ns | ns | ns | ns |
| *IL4* | - | - | - | - | - |
| *IL5* | 1.00 | ns | 0.24 | ns | 1.86 |
| *IL6* | 1.00 | ns | ns | ns | ns |
| *IL7* | 1.00 | ns | ns | 0.04 | 0.11 |
| *IL8* | 1.00 | 0.08 | ns | 0.05 | 0.08 |
| *IL9* | - | - | - | - | - |
| *IL10* | 1.00 | ns | 0.03 | 0.01 | 0.06 |
| *IL11* | 1.00 | 0.22 | 0.20 | 0.22 | 0.35 |
| *IL12A* | 1.00 | 1.76 | 2.13 | ns | ns |
| *IL12B* | 1.00 | ns | ns | ns | ns |
| *IL13* | 1.00 | ns | ns | 0.02 | ns |
| *IL15* | 1.00 | 0.34 | 0.44 | 0.51 | ns |
| *IL16* | 1.00 | ns | ns | ns | ns |
| *IL17A* | 1.00 | ns | ns | ns | 0.29 |
| *IL17F* | 1.00 | ns | ns | ns | 1.94 |
| *IL18* | 1.00 | 0.73 | ns | ns | 1.24 |
| *IL21* | - | - | - | - | - |
| *IL22* | 1.00 | 0.02 | ns | ns | ns |
| *IL23A* | 1.00 | 0.48 | 0.43 | 0.76 | ns |
| *IL24* | 1.00 | 0.14 | ns | 0.32 | ns |
| *IL27* | 1.00 | ns | ns | ns | ns |

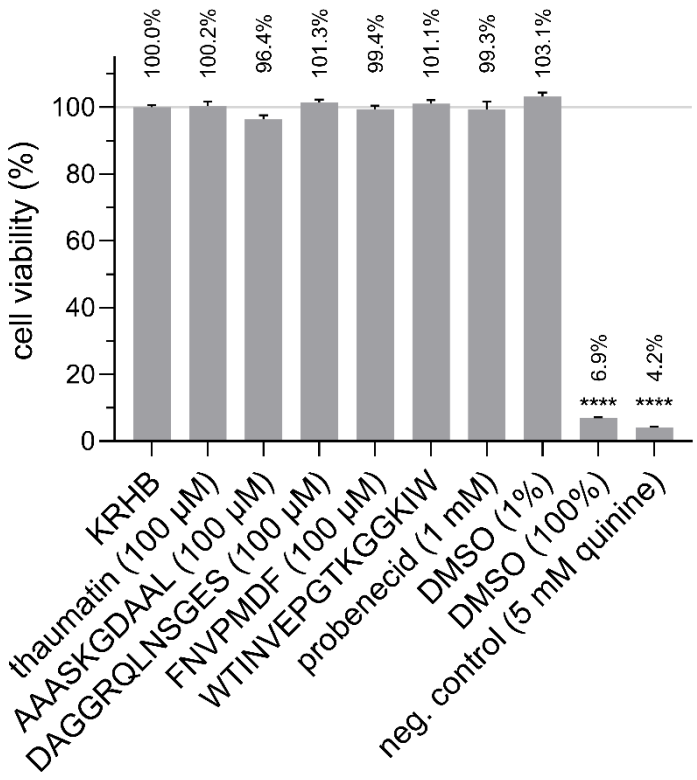


**Fig. S1.** Influence of 100 µM thaumatin, 100 µM of the investigated peptides, 1 mM probenecid and DMSO (solvent) on cell viability. Data are shown as mean ± SEM after incubation for six hours, n = 3-4, t. r. = 3, control: KRHB, statistics: one-way ANOVA Holm-Šidák post hoc test, significant differences are expressed with **** = $p \leq 0.0001$.

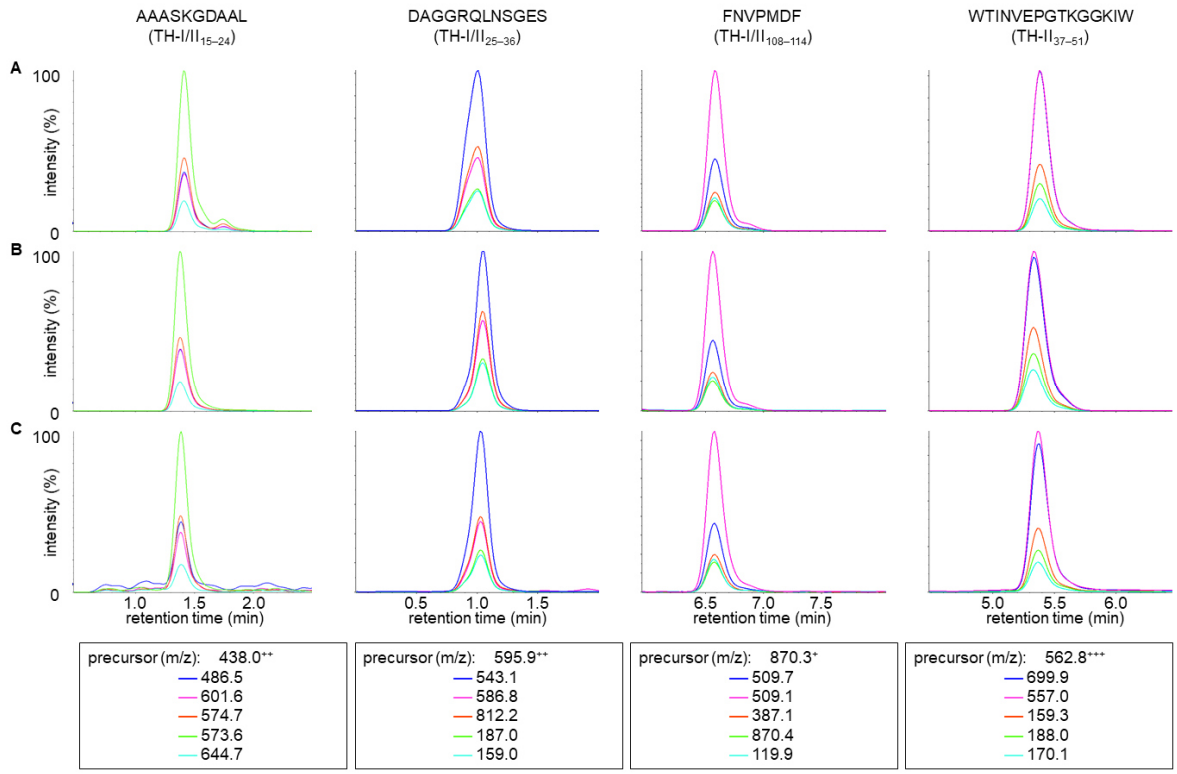


**Fig. S2.** Verification of retention times (UPLC) and MRM mass transitions (MS/MS, 5 transitions per peptide) of the four peptides studied as (A) synthesized standard, (B) formed in *in vitro* digestion, and (C) formed in *in vivo* digestion.

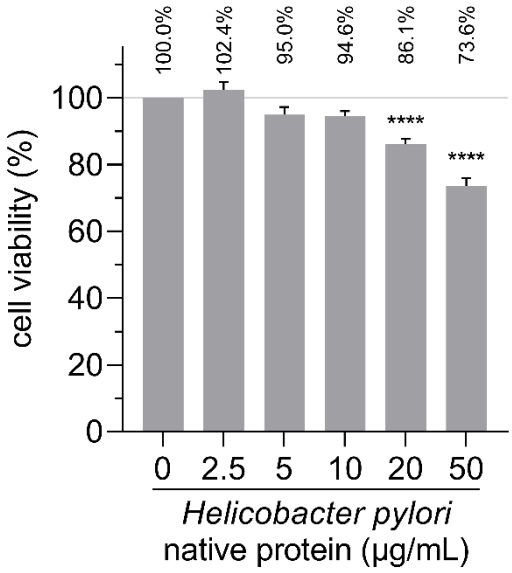


**Fig. S3.** Influence of *H. pylori* native proteins on cell viability. Data are shown as mean ± SEM after incubation for six hours, n = 3, t. r. = 3, control: DMEM, statistics: one-way ANOVA Holm-Šidák post hoc test, significant differences are expressed with **** = $p \leq 0.0001$.

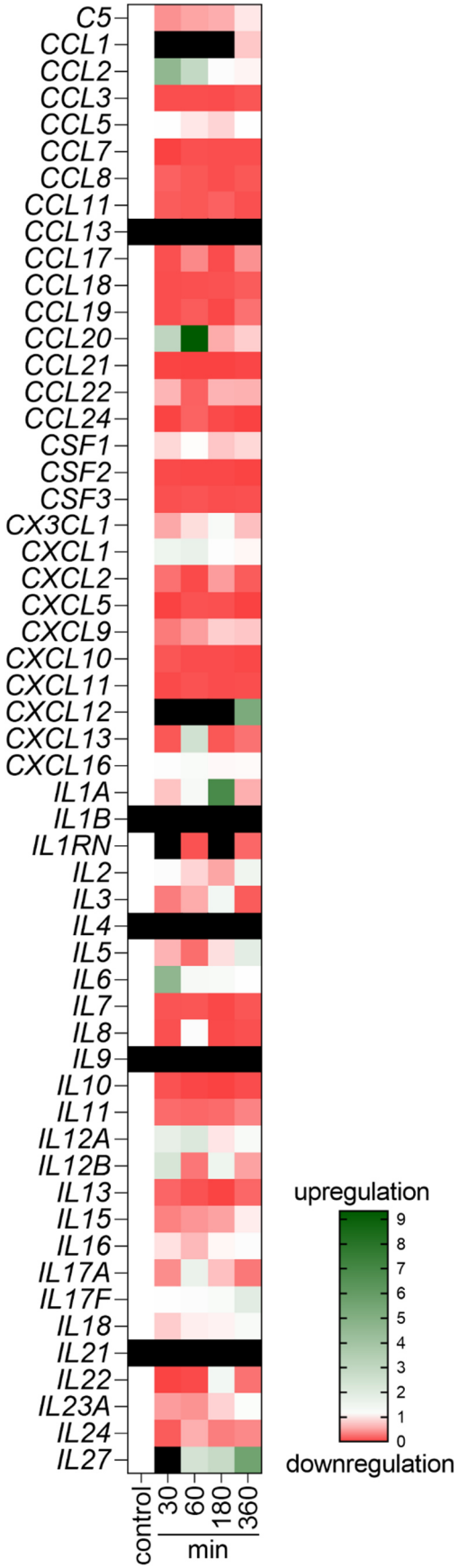


**Fig. S4.** Gene regulations of common chemo- and cytokines after time-dependent incubation with native proteins of *H. pylori* (10 µg/mL), n = 3-4.

**A**

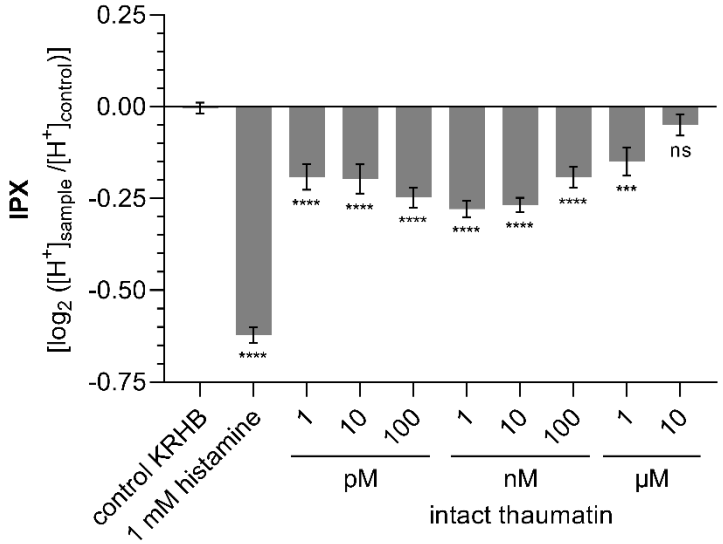
IPX
[log2 ([H+]sample /[H+]control)]
0.25
0.00
-0.25
-0.50
-0.75
ns
control KRHB
1 mM histamine
1
10
100
1
10
100
1
10
pM
nM
µM
intact thaumatin

**B**

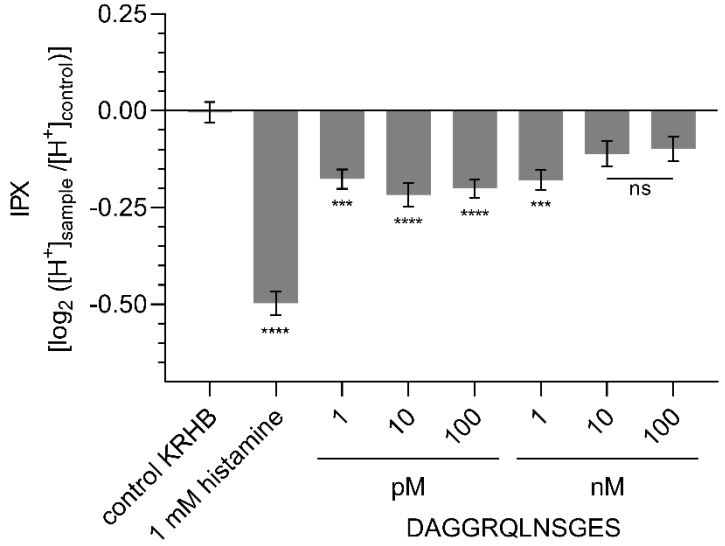
IPX
[log2 ([H+]sample /[H+]control)]
0.25
0.00
-0.25
-0.50
ns
control KRHB
1 mM histamine
1
10
100
1
10
100
pM
nM
DAGGRQLNSGES

**C**

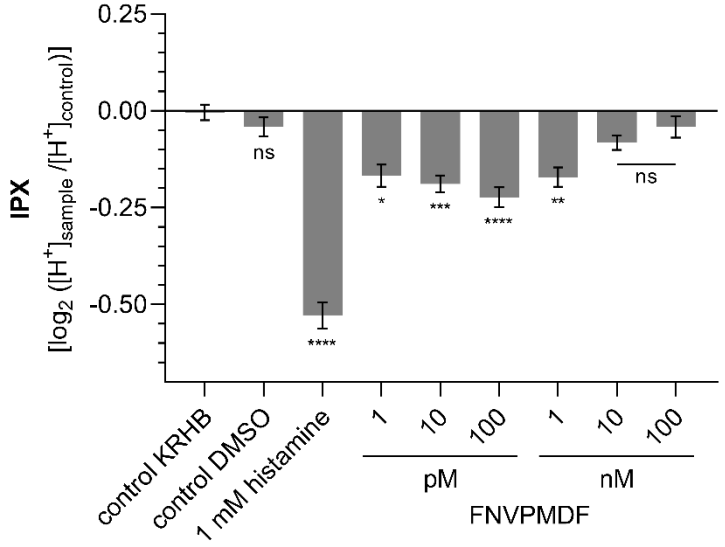
IPX
[log2 ([H+]sample /[H+]control)]
0.25
0.00
-0.25
-0.50
ns
ns
control KRHB
control DMSO
1 mM histamine
1
10
100
1
10
100
pM
nM
FNVPMDF

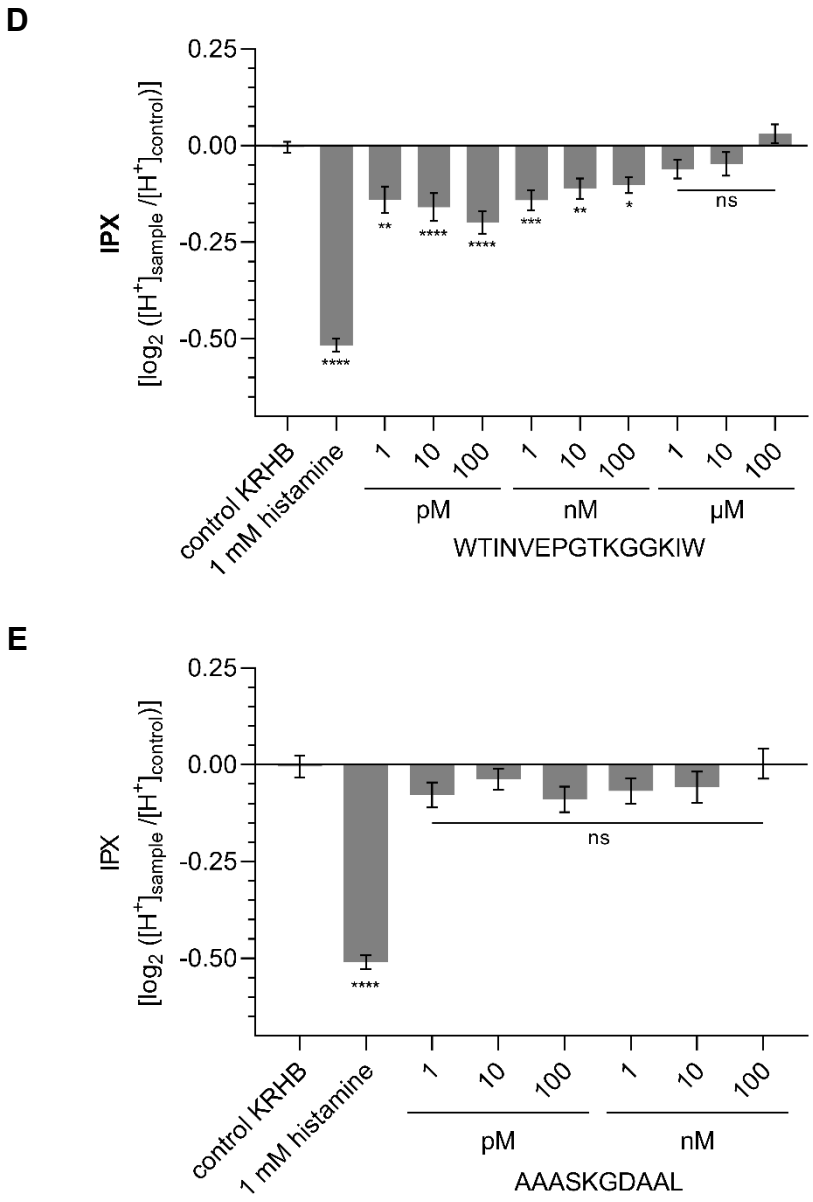


**Fig. S5.** Effects on proton secretion of HGT-1 cells incubated with intact thaumatin (A), the bitter peptides DAGGRQLNSGES (B), FNVPMDF (C), and WTINVEPGTKGGKIW (D) and the non-bitter reference peptide AAASKGDAAL (E). Data shown as mean ± SEM after incubation for 10 minutes, n = 4-6, t. r. = 4-6, control: KRHB, Statistics: one-way ANOVA Holm-Šidák post hoc test, significant differences are expressed with * = $p \leq 0.05$, ** = $p \leq 0.01$, *** = $p \leq 0.001$, **** = $p \leq 0.0001$, 1 mM histamine was used as a positive control.

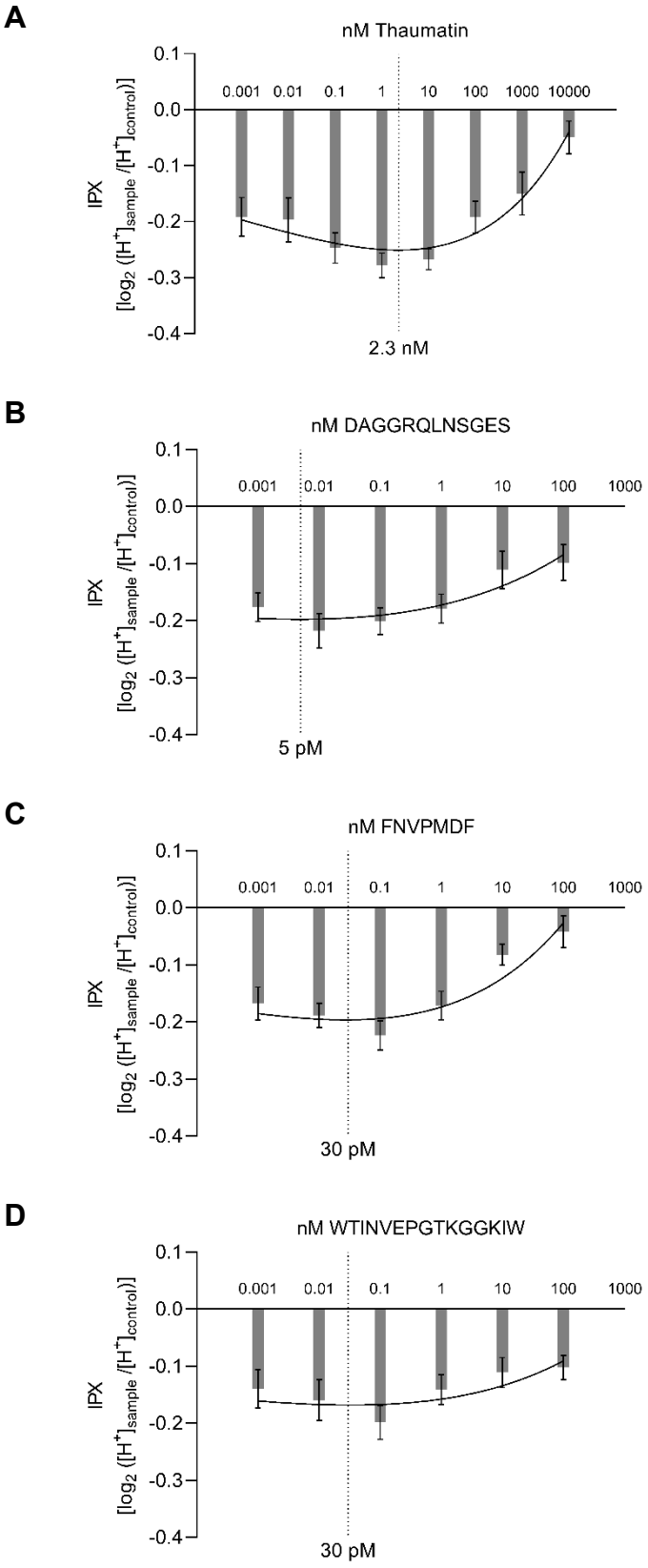


**Fig. S6.** Curve fit calculations of the proton secretion profiles of thaumatin (A) and the three bitter peptides DAGGRQLNSGES (B), FNVPMDF (C), and WTINVEPGTKGGKIW (D), to determine the concentrations with the strongest effect on secretory activity ($IPX_{min}$) in HGT-1 cells. Data shown as mean ± SEM after incubation for 10 minutes, n = 4-6, t. r. = 4-6.

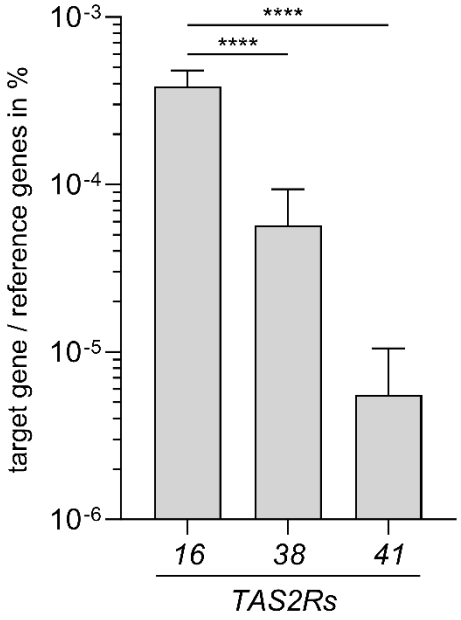


**Fig. S7.** Representation of gene expression of *TAS2R16*, *TAS2R38*, and *TAS2R41* in HGT-1 cells normalized to the reference genes GAPDH and PPIA. Data are shown as mean ± SEM, n = 4, t. r. = 3, Statistics: one-way ANOVA Holm-Šidák post hoc test; significant differences are expressed with **** = $p \leq 0.0001$.

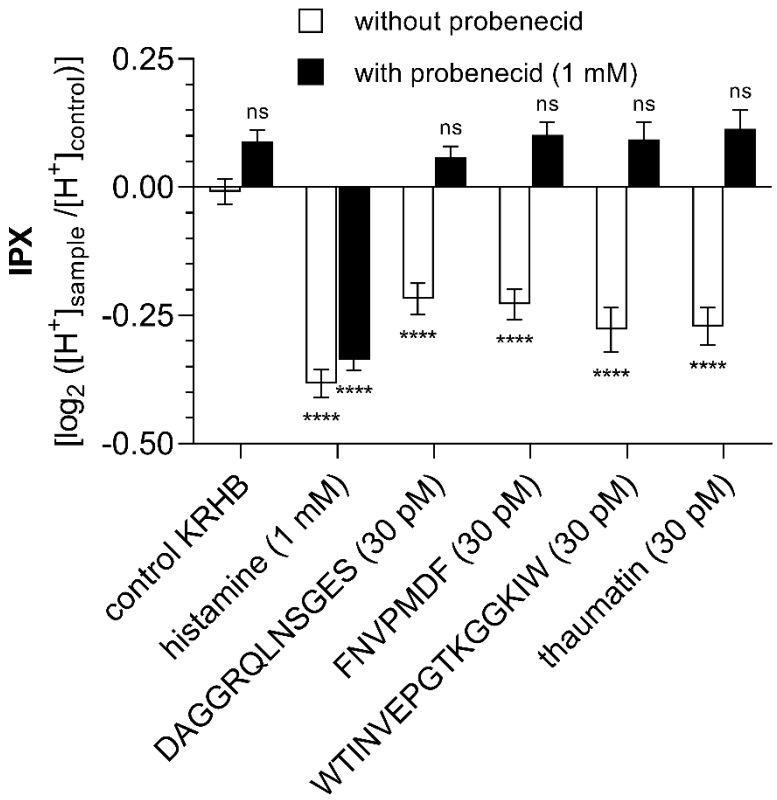


**Fig. S8.** Co-incubation of HGT-1 cells with probenecid (1 mM) and the bitter peptides or thaumatin abolishes the stimulation of proton secretion. Probenecid alone has no effect on proton secretion. To exclude the influence of probenecid on proton secretion in HGT-1 cells in a TAS2R-independent pathway, proton secretion was stimulated by activation of the $H_2$ receptor with 1 mM histamine. Here, no difference was found between the presence and absence of probenecid. Data shown as mean ± SEM, n = 4, t. r. = 4-6, control: KRHB, Statistics: one-way ANOVA Holm-Šidák post hoc test, significant differences are expressed with * = $p \leq 0.05$, ** = $p \leq 0.01$, *** = $p \leq 0.001$, **** = $p \leq 0.0001$.

## 6.3 Publication III and published supplementary data

Richter, P., Andersen, G., Kahlenberg, K., Mueller, A. U., Pirkwieser, P., Boger, V., & Somoza, V. (2024).

**Sodium-Permeable Ion Channels TRPM4 and TRPM5 are Functional in Human Gastric Parietal Cells in Culture and Modulate the Cellular Response to Bitter-Tasting Food Constituents.**

In: *Journal of Agricultural and Food Chemistry* (Vol. 72, Issue 9, pp. 4906–4917).

American Chemical Society (ACS). https://doi.org/10.1021/acs.jafc.3c09085

JOURNAL OF AGRICULTURAL AND FOOD CHEMISTRY



pubs.acs.org/JAFC
Article

# Sodium-Permeable Ion Channels TRPM4 and TRPM5 are Functional in Human Gastric Parietal Cells in Culture and Modulate the Cellular Response to Bitter-Tasting Food Constituents

*Published as part of Journal of Agricultural and Food Chemistry virtual special issue "13th Wartburg Symposium on Flavor Chemistry and Biology".*

Phil Richter,[⊥] Gaby Andersen,[⊥] Kristin Kahlenberg, Alina Ulrike Mueller, Philip Pirkwieser, Valerie Boger, and Veronika Somoza*

Cite This: J. Agric. Food Chem. 2024, 72, 4906−4917



**ABSTRACT:** Gastric parietal cells secrete chloride ions and protons to form hydrochloric acid. Besides endogenous stimulants, e.g., acetylcholine, bitter-tasting food constituents, e.g., caffeine, induce proton secretion via interaction with bitter taste receptors (TAS2Rs), leading to increased cytosolic $Ca^{2+}$ and cAMP concentrations. We hypothesized TAS2R activation by bitter tastants to result in proton secretion via cellular $Na^+$ influx mediated by transient receptor potential channels (TRP) M4 and M5 in immortalized human parietal HGT-1 cells. Using the food-derived TAS2R agonists caffeine and L-arginine, we demonstrate both bitter compounds to induce a TRPM4/M5-mediated $Na^+$ influx, with $EC_{50}$ values of 0.65 and 10.38 mM, respectively, that stimulates cellular proton secretion. Functional involvement of TAS2Rs in the caffeine-evoked effect was demonstrated by means of the TAS2R antagonist homoeriodictyol, and stably CRISPR-Cas9-edited TAS2R43ko cells. Building on previous results, these data further support the suitability of HGT-1 cells as a surrogate cell model for taste cells. In addition, TRPM4/M5 mediated a $Na^+$ influx after stimulating HGT-1 cells with the acetylcholine analogue carbachol, indicating an interaction of the digestion-associated cholinergic pathway with a taste-signaling pathway in parietal cells.

**KEYWORDS:** *transient receptor potential channels (TRP) M4/M5, taste receptors, TAS2Rs, bitter taste signaling, sodium pathway*

## INTRODUCTION

Parietal cells are highly specialized cells located within the gastric glands in the stomach. They are responsible for gastric acid production from the secretion of chloride ions and protons. Upon stimulation of the cells, $H^+/K^+$-ATPase-containing tubulovesicles are translocated to the apical membrane via exocytotic fusion, thereby enabling the secretion of protons into the stomach lumen. While gastric acid is essential for the digestion of dietary proteins and suppressing pathogens, any imbalance contributes to pathophysiological conditions like atrophic gastritis, peptic ulcers, gastroesophageal reflux disease, and vitamin B12 deficiency.[1]

*In vivo* gastric acid secretion is triggered by endocrine, paracrine, and neuronal signals. Two different intracellular signaling pathways have particularly been described to play a crucial role: the cAMP-mediated PKA activation pathway, which is induced by histaminergic stimulation of the $H_2$ receptor, and the $Ca^{2+}$ pathway, typically induced by binding of gastrin to the $CCK_B$ receptor and cholinergic stimulation of the muscarinic $M_3$ receptor.[2] The latter positively couples to phospholipase C through $G_{q/11}$, inducing inositol 1,4,5-trisphosphate ($IP_3$) and diacylglycerol generation, followed by increased intracellular $Ca^{2+}$.[3] Yet, interactions between the two pathways may occur.[4] With respect to food ingredients, the bitter-tasting compound caffeine was shown to induce gastric acid secretion via the activation of bitter taste receptors (TAS2Rs).[5] Moreover, a positive correlation was shown between the perceived bitterness of caffeine and the extent of its ability to stimulate gastric acid secretion,[5] implicating the activation of similar intracellular signaling pathways in taste and parietal cells by bitter compounds targeting TAS2Rs.

In taste cells located on the tongue, activation of TAS2Rs by bitter compounds initiates dissociation of the G protein $\alpha$-gustducin from its $\beta3\gamma13$ subunits. The latter activates PLC$\beta2$ (1-phosphatidylinositol-4,5-bisphosphate phosphodiesterase beta-2), leading to $IP_3$ (inositol-1,4,5-trisphosphate) generation and a release of $Ca^{2+}$ from $IP_3$ sensitive $Ca^{2+}$ stores, resulting in $Na^+$ influx through the transient receptor potential cation channel subfamily M (M for melastatin) members 4 and 5 (TRPM4/5),[6−8] subsequent ATP release, and finally activation of the gustatory cortex.[9,10]

The TRPM subfamily comprises eight members with diverse functional properties.[11] TRPM4 and M5 are activated by

Received: December 3, 2023
Revised: January 28, 2024
Accepted: January 29, 2024
Published: February 20, 2024

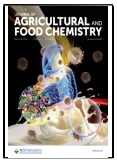





https://doi.org/10.1021/acs.jafc.3c09085
J. Agric. Food Chem. 2024, 72, 4906−4917

increased cytosolic $Ca^{2+}$ concentrations and are insofar exceptional since they are the only two TRP channels that are monovalent, cation-selective, and impermeable to divalent cations, e.g., $Ca^{2+}$.[6,7,12,13] In contrast, most TRPs are nonselective cation channels that are permeable to monovalent and divalent cations like $Na^+$ and $Ca^{2+}$, and despite the fact that TRPM5 is about 20-fold more sensitive to $Ca^{2+}$ than TRPM4,[14] both channels contribute about equally to taste perception.[8] TRPM4 and TRPM5 were found to be expressed in the stomach, albeit the respective cell type was not identified.[15] A more detailed analysis revealed the expression of TRPM5 in the principal part of the gastric glands, most abundantly in the cardiac region.[16] The functional roles of TRPM4 and M5 in this tissue, however, have yet to be elucidated.

A well-established model for the analyses of mechanisms of gastric acid secretion and gastric cancer is the HGT-1 cell line, a human gastric cancer cell line that was established from a primary tumor of a 60-year-old male patient.[17] HGT-1 cells do not secrete mucus but maintain expression of functional histamine $H_2$ receptors and the principal transporters found in primary nontumor acid-secreting parietal cells.[18] Additionally, these cells express functional taste receptors as well as PLC$\beta$2, GNAT2 (G Protein Subunit Alpha Transducin 2), GNAT3 (Gustducin alpha-3 chain), and $IP_3$Rs ($IP_3$ receptors), some of the main components of the taste signaling pathway.[5,19] Moreover, results from HGT-1 cells regarding proton secretion upon stimulation with bitter compounds were verified *in vivo*.[5] Whether the HGT-1 cells also express the TRP channels M4 and M5, and if so, whether TRPM4 and TRPM5 play a role in the signaling process of food-derived bitter compounds, comparable to taste cells, is not known. This, however, would allow the conclusion that HGT-1 cells may serve as a suitable surrogate for investigating taste-active compounds and their ability to induce cellular and physiological responses, e.g., taste perception.

Yet, the available data suggest that HGT-1 cells express a fully functional bitter taste signaling pathway. It is, therefore, of great interest not only to investigate the impact of bitter compounds on cellular $Ca^{2+}$ mobilization in response to TAS2R activation, but also to clarify the possible secondary effects resulting from activated signaling pathways, such as an activity of cellular ion channels. Thus, we hypothesized that the ion channels TRPM4 and TRPM5 are expressed in the parietal cell line HGT-1 and are functionally linked to TAS2R signaling pathways, thereby contributing to proton secretion induced by bitter compounds.

## MATERIALS AND METHODS

**Chemicals.** $Na^+$ binding benzofuran isophthalate acetoxymethyl ester (SBFI-AM), 1,5 carboxy-seminaphtorhodafluor acetoxymethyl ester (SNARF-1-AM), 3-(4,5-dimethylthiazol-2-yl)-2,5-diphenyltetrazolium bromide (MTT), triphenylphosphine oxide (TPPO, 99.4% purity), nicotine (99.8% purity), 9-phenanthrol (99.9% purity), L-arginine (99.0% purity), carbachol (99.7% purity), quinine (99.6% purity), 2-mercaptoethanol, 16% formaldehyde solution methanol-free, Hoechst-3334, Fluoromount-G™, and Pluronic F-127 were obtained from Thermo Fisher Scientific. Fluorogenic $Ca^{2+}$ sensitive dye Cal-520 AM was received from Biomol (Hamburg, Germany). Fetal bovine serum (FBS), penicillin–streptomycin, and trypsin/ethylenediaminetetraacetic acid were purchased from PAN-Biotech GmbH (Aidenbach, Germany). Homoeriodictyol (HED, purity >95%) was kindly provided by Symrise AG (Holzminden).[20] Dimethyl sulfoxide (DMSO) was purchased from Carl Roth (Karlsruhe, Germany). PeqGOLD RNA Kit was obtained from VWR Peqlab (USA). All items for performing real-time qPCR (RT-qPCR) were purchased from BioRad (Feldkirchen, Germany). All reagents and siRNA for transient knockdown were obtained from Thermo Fisher Scientific (USA). Krebs-Ringer HEPES buffer (KRHB) is composed of 130 mM NaCl, 4.7 mM KCl, 1.3 mM $CaCl_2$, 1.2 mM $MgSO_4$, 1.2 mM $KH_2PO_4$, 11.7 mM D-glucose, and 10 mM HEPES; pH was adjusted to 7.4 with KOH. $Na^+$ free KRHB is composed of 134.7 mM KCl, 1.3 mM $CaCl_2$, 1.2 mM $MgSO_4$, 1.2 mM $KH_2PO_4$, 11.7 mM D-glucose, and 10 mM HEPES; pH was adjusted to 7.4 with KOH. Caffeine (99.9% purity), histamine (99.6% purity), and concanavalin A biotin-conjugated were purchased from Sigma-Aldrich (Munich, Germany) and horse serum from Biowest (Nuaillé, France).

**Cell Culture.** Human gastric tumor cells (HGT-1, RRID: CVCL_A609), provided by Dr. C. Laboisse, Nantes (France), were cultivated in DMEM containing 10% FBS and 1% penicillin and streptomycin at 37 °C, 5% $CO_2$, and in a humidified atmosphere (standard conditions). Cells between passages 15 and 25 were used for all experiments.

**Cell Viability.** To determine cell viability, 100,000 cells per well of a transparent 96-well plate were seeded the previous day. On the day of the experiment, the cells were washed with KRHB and then incubated for 60 min with the substances of interest. For the $Na^+$ sensitive fluorescent dye SBFI (5 $\mu$M), the agonists caffeine (10 mM), L-arginine (50 mM), and histamine (1 mM), the antagonists HED (0.3 mM), TPPO (1 mM), nicotine (0.5 mM), and 9-phenanthrol (50 $\mu$M), and the solvent controls ethanol (1%) and DMSO (0.05%) were not found to affect cell viability (>88%). DMSO (100%) and quinine (5 mM) were used as negative controls (Figure S1). Cells were then washed again with KRHB and incubated with MTT (0.83 mg/mL in DMEM) for 15 min under standard conditions. Formazan formed was dissolved in DMSO, and the absorbance was measured (570 nm; reference 650 nm) on an Infinite M200 plate reader (Tecan, Switzerland). Untreated control cells (KRHB) were used to normalize and calculate the cell viability.

**Localization of TRPM4 and TRPM5 by Immunocytochemistry.** For fluorescence labeling of HGT-1 cells, 50,000 cells were seeded at standard conditions for 24 h in a poly-D-lysine (10 $\mu$g/mL)-coated glass bottom 10-well plate (Greiner Bio-One GmbH, Leipzig, Germany). Then, the cells were incubated with PBS for 30 min before cell membrane staining with (1:2000) biotin-conjugated concanavalin A on ice for 1 h, followed by fixation with 4% formaldehyde for 10 min. After washing steps with PBS (3×, 5 min), 0.5% Triton-X-100 (1×, 5 min), and PBS (3×, 5 min), cells were incubated in a blocking solution with 5% horse serum and 0.3% Triton X-100 for 45 min to reduce the level of unspecific binding. Primary antibodies anti-TRPM4 antibody (RRID: AB_2040250) or anti-TRPM5 antibody (RRID: AB_2040252) (Alomone Labs, Jerusalem, Israel) (1:100) and corresponding blocking peptide (1:50) were incubated in blocking solution for approximately 1 h before applying to the cells. As a secondary antibody (Alexa Fluor 488 antirabbit IgG (RRID: AB_2536097) (Thermo Fisher Scientific Inc., USA) (1:1000) and for cell membrane staining streptavidin, Alexa Fluor 633 conjugate (RRID: AB_2313500) (Thermo Fisher


https://doi.org/10.1021/acs.jafc.3c09085
J. Agric. Food Chem. 2024, 72, 4906−4917

Scientific Inc., USA) (1:1000) was selected and incubated for 1 h. The nucleus was labeled with Hoechst-33342 (1:2000) for 5 min, and the stained cells were embedded in Fluoromount-G™. Immunofluorescence images were acquired and analyzed by confocal laser scanning microscopy using a Zeiss LSM 780 instrument (Carl Zeiss AG, Munich, Germany). For super-resolution imaging, an Airyscan detector was used.

**Determination of Intercellular Sodium Concentration Using Sodium-Sensitive Fluorescent Dye SBFI.** To determine the intracellular sodium concentration, 50,000 cells per well of a black 96-well plate were seeded the previous day. On the experimental day, cells were washed with KRHB and then incubated with 5 $\mu$M $Na^+$ sensitive fluorescent dye SBFI-AM (in KRHB containing 0.1% DMSO and 0.01% Pluronic F-127) for 2 h under standard conditions. Then, the cells were washed again with KRHB and incubated for another 30 min under standard conditions to allow complete de-esterification of the dye. After adding the test solutions, the plate was incubated in a FlexStation 3 (Molecular Devices, USA) for 60 min at 37 °C and fluorescence (excitation: 340/380 nm, emission: 500 nm) was recorded every 5 min. After calculation, according to the manufacturer's protocol, fluorescence intensity was determined after 30 min and normalized to untreated control cells.

**Characterization of Intracellular Calcium Mobilization Using Calcium-Sensitive Fluorescent Dye Cal-520.** To measure intracellular calcium mobilization, 50,000 cells per well of a black 96-well plate with a transparent bottom were seeded the previous day. On the experimental day, cells were washed with KRHB and then incubated with 1 $\mu$M Cal-520 AM (in KRHB containing 0.02% DMSO and 0.004% Pluronic F-127) for 2 h under standard conditions. Cells were then washed again with KRHB and incubated at 37 °C in a FlexStation 3. Fluorescence (excitation: 495 nm, emission: 515 nm) was recorded at 1 s intervals. After 60 s, the test substances were added in an automated setting and the fluorescence was recorded continuously. The fluorescence intensity was normalized to the first 60 s of the measurement before addition of each substance.

**Determination of the Intracellular Proton Concentration.** To examine the effects of the investigated compounds on the proton secretion activity of HGT-1 cells, 100,000 cells per well of a black 96-well plate were seeded the previous day and incubated under standard conditions. After washing with KRHB, cells were incubated for 30 min with 3 $\mu$M of the pH-sensitive fluorescent dye SNARF-1-AM as previously described.[5,21] After another washing step, the cells were stimulated with the test substances, and their intracellular proton secretion was determined using a FlexStation 3. The intracellular proton index (IPX) calculated from the measured data reflects the change in proton concentration compared to that of untreated control cells. Negative IPX values represent a stimulation of proton secretion, while positive IPX values indicate an inhibition of proton secretion.

**Determination of Gene Expression via RT-qPCR.** For gene expression studies, 500,000 cells per well of a 24-well plate were seeded the previous day. On the day of the experiment, the cells were washed with PBS and incubated with the appropriate test solutions. This was followed by lysis of the cells and RNA isolation according to the manufacturer's protocol using the peqGOLD RNA Kit (VWR Peqlab, USA). When the general expression of TRP channels was examined, the cells were directly lysed, and the RNA was extracted. The concentration of RNA was determined on NanoDrop One$^c$ (Thermo Fisher Scientific Inc., USA). According to the manufacturer's instructions, removing gDNA contaminants and synthesizing cDNA was performed using iScript gDNA Clear cDNA Synthesis Kit (BioRad, Feldkirchen, Germany). RT-qPCR was performed using SsoAdvanced Universal SYBR Green Supermix (Bio-Rad Laboratories, Inc., USA) and the previously published primers.[22] All determined gene expressions were normalized to those of the reference genes GAPDH[23] and PPIA[24].

**Measurement of Intracellular Sodium Concentrations via LA−ICP−MS.** To validate intracellular sodium concentrations in HGT-1 cells via single-cell laser ablation−inductively coupled plasma−mass spectrometry (LA−ICP−MS), 20,000 cells per well of a Cellview cell culture slide (Greiner Bio-One, Austria) were seeded the previous day. On the day of the experiment, the cells were washed with KRHB and then incubated with caffeine (10 mM) or L-arginine (50 mM) for 30 min under standard conditions. This was followed by another washing step with KRHB and drying of the slides for 2 h under standard conditions.

All laser ablation measurements were carried out with an Iridia 193 nm laser ablation system (Teledyne CETAC Technologies, USA), coupled to a NexION 5000 multiquadrupole ICP−MS instrument (PerkinElmer, USA). The laser ablation system was equipped with a cobalt long pulse ablation cell and connected to the ICP−MS via the Aerosol Rapid Introduction System (ARIS). Helium was used as a carrier gas (0.3 L/min) for aerosol transport from the ablation cell to the ICP. The LA−ICP−MS conditions were optimized on a daily basis using the NIST SRM 612 glass certified reference material (National Institute of Standards and Technology, USA). The nebulizer gas flow (~0.92−0.98 L/min) was fine-tuned, generating maximum $^{140}Ce^+$ signals, low oxide formation based on $^{232}Th^{+16}O^+$ (<100) and low elemental fractionation based on the $^{238}U^+/^{232}Th^+$ ratio (~1). The quadrupole ion deflector (QID) parameters were optimized by adjusting the QID lens scanning system for maximum efficiency, measuring $^7Li^+$, $^{24}Mg^+$, $^{115}In^+$, $^{140}Ce^+$, $^{208}Pb^+$, and $^{238}U^+$ as representatives of the entire mass spectrum. A radio frequency power of 1600 W, an auxiliary argon gas flow rate of 1.2 L/min, and a plasma gas flow rate of 16 L/min were used. The LA−ICP−MS imaging experiments were measured in the MS/MS standard mode (dwell time $^{23}Na^+$: 50 ms) and ablating an area of ~200 × 175 $\mu$m line by line (unidirectional, laser off between rows). Quantitative ablation was achieved by selecting a fluence of 1.0 J/cm$^2$ with a fixed dosage of 9, at a repetition rate of 162 Hz and using a 3 $\mu$m circle spot size. The integration and readout rate were optimized to match the laser ablation repetition rate. The ICP−MS signal, received from Syngistix v.3.3 (PerkinElmer, USA) was synchronized with the timestamps in the laser log files from Chromium v.3.1 (Teledyne CETAC Technologies, USA) and further processed with the laser ablation data software HDIP-v1.7.1 (Teledyne CETAC Technologies, USA). Single cells were extracted as regions of interest and visualized via HDIP-v1.7.1. The complete instrument settings are listed in Table S1.

**Transient Knockdown of TRPM4 and TRPM5 in HGT-1 Cells.** To quantitate the functional role of the two ion channels TRPM4 and TRPM5, a knockdown (kd) was performed using siRNA. The procedure was analogous to the already published protocol.[25] Stealth siRNA TRPM4 (HSS123260) and TRPM5


https://doi.org/10.1021/acs.jafc.3c09085
J. Agric. Food Chem. 2024, 72, 4906−4917

(HSS179077) were purchased from Thermo Fisher Scientific (USA).

**Stable TAS2R43 Knockout Using CRISPR-Cas9.** For experiments with TAS2R43 homozygote KO HGT-1 cells, the same clone was used as previously published.[5]

**Statistical Analysis.** Unless otherwise described, all data are presented as box plots with 10th and 90th percentiles. Data points outside of this range are indicated as dots. At least four independent biological replicates were used for each experiment. Data were subjected to a Nalimov outlier test and then analyzed via a one-way ANOVA Holm-Šidák *post hoc* test. Different $p$ values are indicated with asterisks according to the following scheme: *$p \leq 0.05$, **$p \leq 0.01$, ***$p \leq 0.001$, and ****$p \leq 0.0001$.

## RESULTS

**TRPM4 and TRPM5 are Expressed in HGT-1 Cells.** First, the RNA expression of all 27 members of the human TRP superfamily was investigated via RT-qPCR. Except for TRPC5, the RNA expression of all TRP channels could be detected in HGT-1 cells (Figure 1). Regarding the respective transcript levels, TRPM4 revealed a slightly, yet statistically significant, higher RNA expression level compared with TRPM5 ($p \leq 0.0001$; Figure 1).

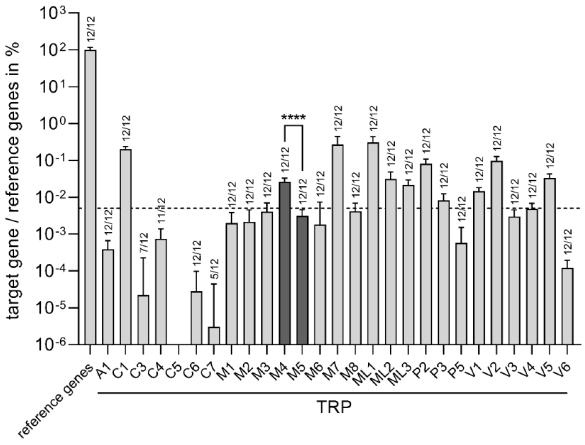


**Figure 1.** Representation of gene expression of TRP channels in HGT-1 cells normalized to the reference genes GAPDH and PPIA. Four different passages in three technical replicates were examined. Numbers above the bars indicate in how many samples the specific PCR product was found. The dashed line represents the mean gene expression of all 27 TRP channels. Data are shown as mean ± SEM, $n$ = 4, t. r. = 3.

Following our hypothesis, we next analyzed whether TRPM4 and TRPM5 are expressed in HGT-1 cells on the protein level via immunocytochemistry. Staining of HGT-1 cells for TRPM4 and TRPM5 led to a fluorescence signal in the plasma membrane and the cytoplasm (Figure 2a,b). Application of the respective blocking peptides diminished these signals (Figure S2), thereby confirming the expression of TRPM4 and TRPM5 on the protein level in HGT-1 cells.

**Bitter Compounds but Not Histamine Increased Intracellular Fluorescence Signals of the $Na^+$ Sensitive Dye SBFI.** According to our hypothesis, a bitter signaling pathway like in taste cells should lead to $Ca^{2+}$ mobilization from the endoplasmic reticulum and, consequently, to TRPM4/M5-mediated $Na^+$ influx after applying bitter

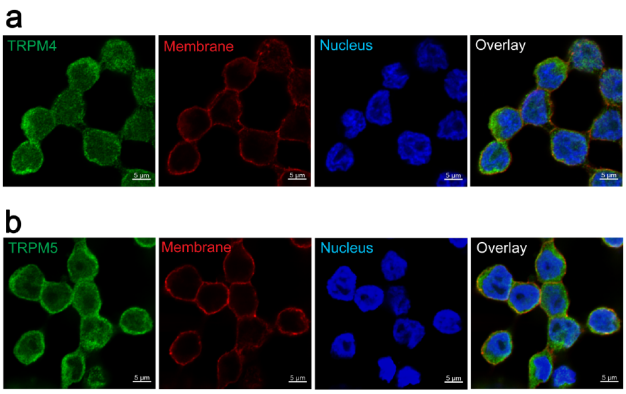


**Figure 2.** TRPM4 and TRPM5 are expressed in HGT-1 cells. Super-resolution images were acquired with the Airyscan detector of Zeiss LSM 780. Ion channel expression is detected by anti-TRPM4 antibody (a) and anti-TRPM5 antibody (b) in combination with an Alexa Fluor 488 antirabbit IgG (green). The nucleus is visualized by Hoechst-33342 (blue), and the plasma membrane by biotin-conjugated concanavalin A in combination with Alexa Fluor 633 conjugate (red). Scale: 5 $\mu$m.

compounds via activation of TAS2Rs expressed in HGT-1 cells. Therefore, we assessed whether incubation of HGT-1 cells with different concentrations of the TAS2R agonists caffeine and L-arginine for 30 min results in an increase in the intracellular $Na^+$-dependent fluorescence of the dye SBFI. The two compounds were selected based on their different TAS2R target profile and their ability to induce proton secretion in HGT-1 cells. While caffeine is the prototypical coffee bitter substance activating 5 of the 25 human TAS2Rs (TAS2R7, 10, 14, 43, and 46)[26] and demonstrated to induce gastric acid secretion in healthy subjects,[5] L-arginine is the third most bitter amino acid[27] and also a potent inducer of proton secretion in HGT-1 cells.[28] L-arginine induced a robust increase of the cytosolic $Ca^{2+}$ concentration (Figure S3), while caffeine application resulted in a notable dip in the fluorescence intensity (Figure S3), probably due to its well-known quenching properties.[29] However, concentration−response analyses revealed a caffeine-concentration-dependent increase in SBFI-fluorescence intensity. For the caffeine-concentration-dependent rise in the intracellular $Na^+$ concentration, an $EC_{50}$ value of 0.65 mM was calculated (Figure 3a orange line). The bitter compound L-arginine also induced a concentration-dependent increase in the intracellular SBFI-fluorescence (Figure 3a blue line) with an $EC_{50}$ value of 10.38 mM. However, the efficacy was higher for L-arginine compared to that of caffeine ($p \leq 0.0001$). By incubating cells from four different cell passages with varying concentrations of caffeine (1, 3, 5, and 10 mM), we could show that these changes in the SBFI-fluorescence intensity are stable and repeatable (Figure S4). Since histamine stimulates gastric acid secretion in HGT-1 cells TAS2R-independent[30] via the $H_2$ receptor, HGT-1 cells were incubated with two different histamine concentrations, and the SBFI-fluorescence was analyzed. As hypothesized, stimulating the cells with histamine did not increase the SBFI-fluorescence signal ($p > 0.60$; Figure 3b), indicating that the increased SBFI-fluorescence is TAS2R dependent.

**Pharmacological Inhibition of TAS2Rs and Genetic Knockout of TAS2R43 Diminishes the $Na^+$ Influx.** We next aimed to analyze whether the influx of $Na^+$ is initiated via binding of bitter compounds to TAS2Rs provoking taste-cell-


https://doi.org/10.1021/acs.jafc.3c09085
J. Agric. Food Chem. 2024, 72, 4906−4917

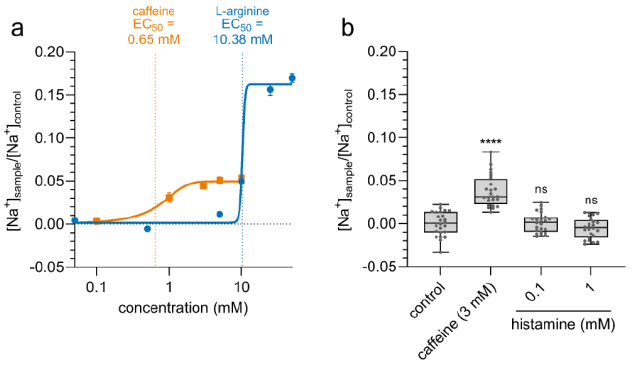


**Figure 3.** (a) Caffeine and L-arginine lead to a concentration-dependent $Na^+$ influx into HGT-1 cells. For caffeine, the $EC_{50}$ is reached at 0.65 mM, whereas the $EC_{50}$ of L-arginine is 10.38 mM. (b) Treatment of cells with caffeine (3 mM) increases intracellular $Na^+$ concentrations compared to untreated control cells. However, the $Na^+$ concentration of histamine-treated cells (0.1 or 1 mM) does not differ from untreated cells. Statistics: $n$ = 4, t. r. = 6, one-way ANOVA Holm-Šidák *post hoc* test; significant differences are expressed with ****$p \leq 0.0001$.

like signaling. For this, the bitter-masking TAS2R antagonist homoeriodictyol (HED), which has been described to reduce the bitter taste of caffeine in human sensory panels by up to 49%,[20,31] as well as the caffeine-evoked proton secretion in HGT-1 cells[5] by inhibiting TAS2R20/31/43/50,[5] was applied. When HGT-1 cells were coincubated with caffeine and HED, the caffeine-induced $Na^+$ influx (+3.89 ± 0.20%; $p \leq 0.0001$) was reduced by 61.8 ± 2.5% ($p \leq 0.0001$; Figure 4a). Incubation of the cells with 0.3 mM HED alone led to a small, yet statistically significant, influx of $Na^+$ (+0.96 ± 0.12%; $p \leq 0.0001$). The respective solvent control (0.05% DMSO) had no impact ($p > 0.99$). In addition to caffeine, bitter-tasting amino acid L-arginine also increased $Na^+$ influx into HGT-1 cells (+10.24 ± 1.00%; $p \leq 0.0001$; Figure 4b). This stimulatory effect was reversed by coincubation with HED (−131.7 ± 4.8%; $p \leq 0.0001$) so that coincubated cells revealed a lower intracellular $Na^+$ concentration than untreated cells.

Since HED targets TAS2R43, and caffeine has been shown to activate, among others, TAS2R43, we next analyzed whether the $Na^+$ influx upon caffeine stimulation of HGT-1 cells is reduced in CRISPR/Cas TAS2R43 knockout (TAS2R43ko) cells, which were established previously.[5] Upon stimulation with different concentrations of caffeine, the TAS2R43ko cells revealed a lower $Na^+$ influx compared to that of the wild-type cells ($p$ = 0.038; effect size −17.30 ± 6.17% for 5 mM caffeine) (Figure 4c).

**The Increased Intracellular SBFI-Fluorescence is $Na^+$ Specific and Results from $Na^+$ Influx.** Next, we wanted to confirm that SBFI-fluorescence is a suitable indicator for intracellular $Na^+$ concentrations in HGT-1 cells. Therefore, we determined intracellular Na+ concentrations via single-cell LA−ICP−MS after incubating HGT-1 cells with concentrations for which the most pronounced effects of caffeine and L-arginine are demonstrated in Figure 3a for the respective solvent control. These analyses revealed that incubation of HGT-1 cells with 10 mM caffeine (+42.5 ± 11.6%; $p \leq 0.01$)

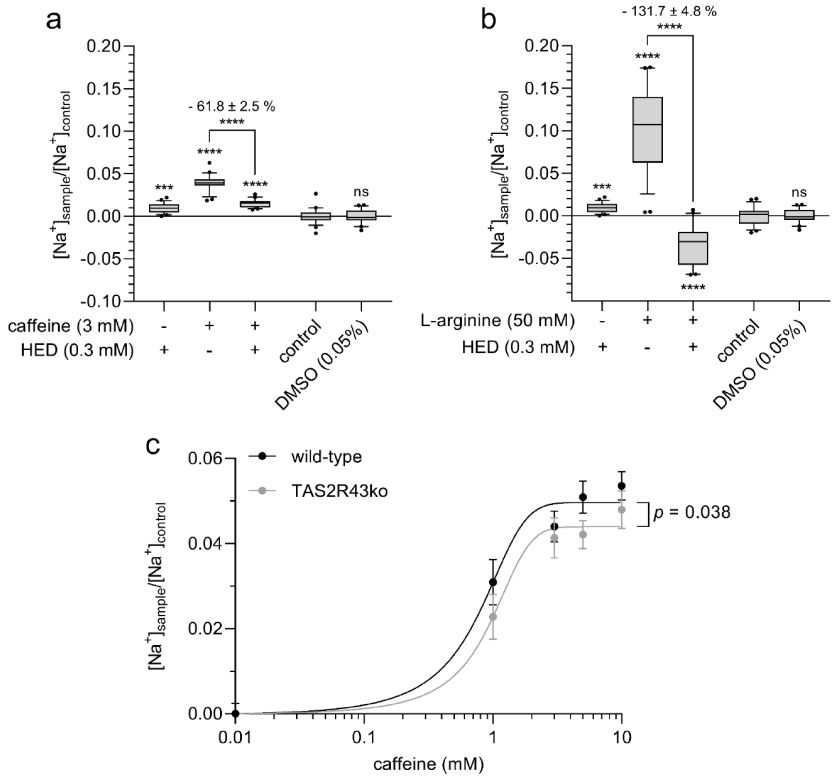


**Figure 4.** Pharmacological inhibition of TAS2Rs by homoeriodictyol (0.3 mM) leads to a reduction in (a) caffeine- (3 mM) and (b) L-arginine-induced (50 mM) $Na^+$ influx in cells. (c) Stable TAS2R43 knockout by CRISPR-Cas9 reduces caffeine-induced $Na^+$ influx into cells at different caffeine concentrations (0.01−10 mM). Statistics: $n$ = 4, t. r. = 6, one-way ANOVA Holm-Šidák *post hoc* test; significant differences are expressed with ***$p \leq 0.001$, ****$p \leq 0.0001$.


https://doi.org/10.1021/acs.jafc.3c09085
J. Agric. Food Chem. 2024, 72, 4906−4917

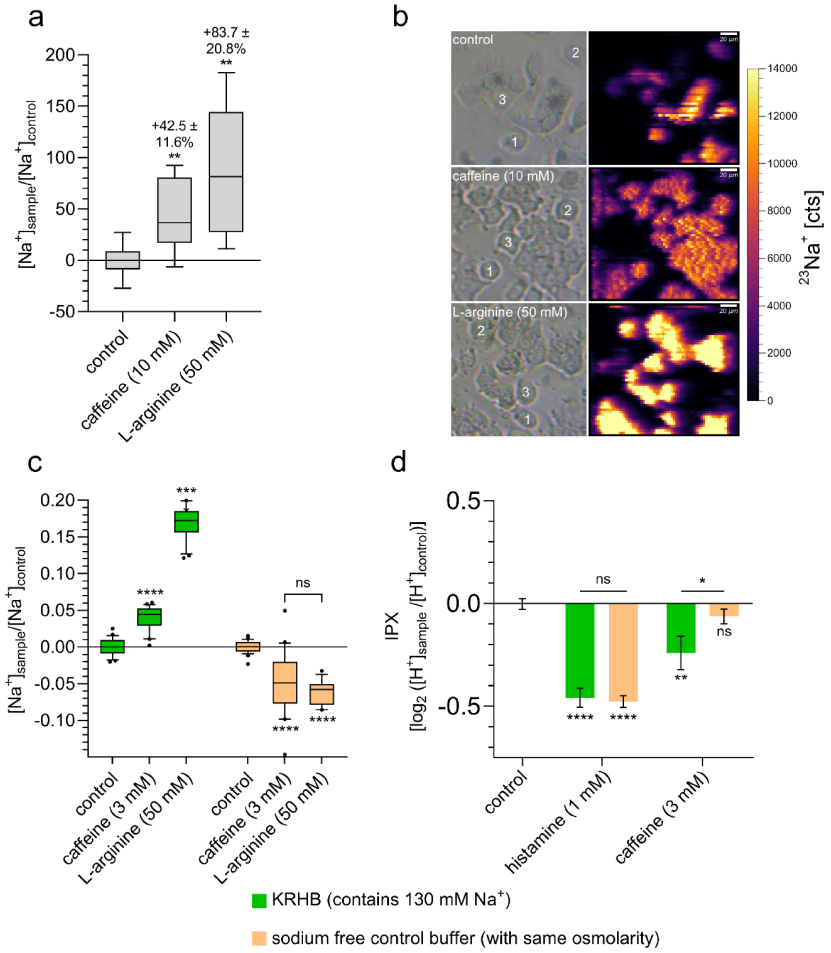


**Figure 5.** (a) Measurement of intracellular $Na^+$ concentration by LA−ICP−MS validated the results obtained by using $Na^+$ sensitive fluorescent dye. Incubation of HGT-1 cells with caffeine (10 mM) and L-arginine (50 mM) increases $Na^+$concentration in the cell. (b) Bright-field images of HGT-1 cells (left). Signal intensity maps of $^{23}Na^+$ in HGT-1 cells obtained by LA−ICP−MS imaging (right). LA-Parameters: fluence: 1.0 J/cm$^2$; repetition rate: 162 Hz; spot size: 3 $\mu$m circle; fixed dosage mode: 9; dwell time $^{23}Na^+$: 50 ms. (c) Treatment of cells with caffeine (3 mM) or L-arginine (50 mM) in $Na^+$-containing buffer (KRHB) resulted in an increase in the $Na^+$-dependent fluorescence signal within the cells. Incubation with the same substances but in $Na^+$-free buffer did not increase the $Na^+$ concentration within the cells. (d) Similar results were obtained when measuring caffeine-induced stimulation of proton secretion. Here, treatment of cells with caffeine in the presence of $Na^+$ in the external medium resulted in increased proton secretion, whereas this was no longer detectable when measured in $Na^+$-free buffer. However, treatment of the cells with histamine (1 mM) resulted in stimulation of proton secretion in both cases. In (d), data are shown as mean ± SEM. Statistics: $n$ = 4−5, t. r. = 6, one-way ANOVA Holm-Šidák *post hoc* test; significant differences are expressed with *$p \leq 0.05$, **$p \leq 0.01$, ****$p \leq 0.0001$.

or 50 mM L-arginine (+83.7 ± 20.8%; $p \leq 0.01$) leads to an increase in intracellular $Na^+$ concentrations (Figure 5ab), validating the measurements using the $Na^+$ sensitive fluorescent dye SBFI.

To verify that the increased intracellular $Na^+$ concentrations are based on $Na^+$ influx from the extracellular space, HGT-1 cells were stimulated with either 3 mM caffeine or 50 mM L-arginine in KRHB containing 130 mM $Na^+$ and in nominal $Na^+$-free KRHB, respectively, followed by monitoring the resulting SBFI-fluorescence. The presence of $Na^+$ in the KRHB solution led to the already observed increase of the intracellular $Na^+$ concentration after incubation with 3 mM caffeine (+4.00 ± 0.32%; $p \leq 0.0001$) and 50 mM L-arginine (+16.97 ± 0.47%; $p \leq 0.0001$; Figure 5c, left), whereas incubation of HGT-1 cells with caffeine and L-arginine in a nominal $Na^+$-free KRHB even led to lower intracellular $Na^+$ concentrations compared to untreated control cells (−4.73 ± 0.85% and −6.22 ± 0.46%, respectively; $p \leq 0.0001$; Figure 5c, right), confirming that incubation of HGT-1 cells with the bitter compounds caffeine and L-arginine induces an influx of $Na^+$ from the extracellular space. Also, the proton secretion induced by caffeine was reduced in nominal $Na^+$-free buffer ($p \leq 0.05$), indicating the involvement of $Na^+$ influx in this mechanism (Figure 5d). This was not the case when proton secretion was TAS2R-independently induced by histamine.

**The $Na^+$ Influx Induced by Bitter Compounds is TRPM4 and TRPM5 Dependent.** To test whether the $Na^+$ influx elicited by the binding of bitter compounds to TAS2Rs is mediated via TRPM4 and/or TRPM5, different antagonists of TRPM4 and TRPM5 were applied (Figure 6). Pharmacological inhibition of TRPM5 with nicotine[32] led to a lower $Na^+$ influx in HGT-1 cells when costimulated with 3 mM caffeine (−47.1 ± 11.6%; $p \leq 0.01$; Figure 6a). Notably, this effect could not be detected, when the TRPM5-specific inhibitor TPPO[33] was applied (Figure 6b). Since the TRPM4-specific inhibitor 9-phenanthrol[34] could not be entirely removed from the cells and reveals spectral overlapping with the $Na^+$ dye


https://doi.org/10.1021/acs.jafc.3c09085
J. Agric. Food Chem. 2024, 72, 4906−4917

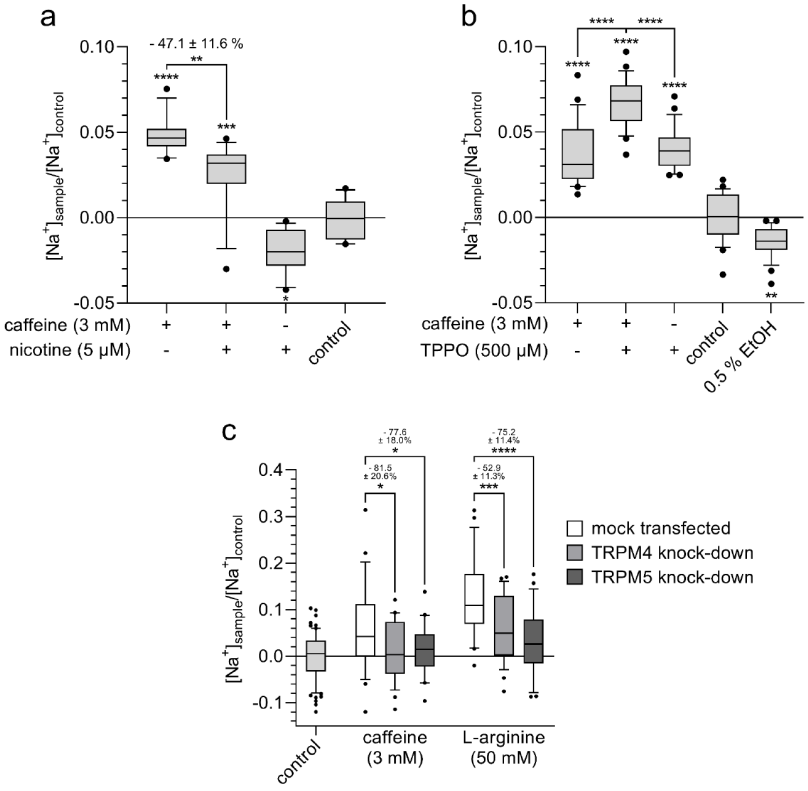


**Figure 6.** Whereas coincubation of cells with caffeine (3 mM) and the (a) TRPM5 inhibitor nicotine (5 $\mu$M) leads to a reduction in $Na^+$ influx, (b) simultaneous treatment with the TRPM5 inhibitor TPPO (500 $\mu$M) increases $Na^+$ influx. (c) Transient reduction of TRPM4 or TRPM5 expression by siRNA leads to decreased $Na^+$ influx upon stimulation with caffeine (3 mM) or L-arginine (50 mM), respectively, compared with mock-transfected cells. Statistics: $n$ = 4, t. r. = 6, one-way ANOVA Holm-Šidák *post hoc* test; significant differences are expressed with *$p \leq 0.05$, **$p \leq 0.01$, ***$p \leq 0.001$, ****$p \leq 0.0001$.

SBFI, pharmacological inhibition of TRPM4 was, for technical reasons, unsuccessful (data not shown).

Since the pharmacological inhibition experiments provided inconclusive results, TRPM4 and TRPM5 siRNA knockdown (kd) experiments were performed. The mean knockdown efficiency was determined as −42.1 ± 7.0% ($p \leq 0.01$) for TRPM4 and 68.7 ± 4.9% ($p \leq 0.0001$) for TRPM5 (Figure S5). Knockdown of TRPM4 or TRPM5 independently reduced the $Na^+$ influx induced by caffeine (−81.5 ± 20.6% for TRPM4kd cells; $p \leq 0.05$ and −77.6 ± 18.0% for TRPM5kd cells; $p \leq 0.05$) and L-arginine (−52.9 ± 11.3% for TRPM4kd cells; $p \leq 0.001$ and −75.2 ± 11.4% for TRPM5kd cells; $p \leq 0.0001$), thereby confirming the involvement of TRPM4 and TRPM5 in the $Na^+$ influx in HGT-1 cells upon stimulation with bitter compounds (Figure 6c). No difference was observed regarding the effect size for TRPM4 vs TRPM5 ($p$ = 0.90 for caffeine, $p$ = 0.15 for L-arginine), indicating that both channels contribute about equally to the $Na^+$ influx.

Also, bitter compounds impact not only TRPM4 and TRPM5 on the functional level but also on the transcript level. Incubation of the cells with 3 mM caffeine led to reduced transcript levels of TRPM4 after only 10 min, while TRPM5 transcript levels were reduced after 30 min (Figure S6).

**Activation of Muscarinic Acetylcholine Receptor Leads to $Na^+$ Influx by TRPM4 and TRPM5.** Since activation of the muscarinic acetylcholine receptor ($M_3$) leads to a mobilization of $Ca^{2+}$ from the endoplasmic reticulum to the cytosol, and both TRPM4 and M5 are activated by increased cytosolic $Ca^{2+}$ concentrations, we next investigated whether activation of the cholinergic pathway also triggers TRPM4- and TRPM5-mediated $Na^+$ influx into HGT-1 cells. Therefore, the cells were treated with carbachol, a well-known structural analog of acetylcholine.[35] As hypothesized, exposure of the cells to 1 mM carbachol led to $Ca^{2+}$ mobilization (Figure S3) and increased the intracellular $Na^+$ concentration by +5.14 ± 2.05% ($p \leq 0.05$). Again, the involvement of TRPM4 and M5 was investigated by knockdown experiments. A reduction in intracellular $Na^+$ concentration of −90.9 ± 32.3% ($p \leq 0.05$) for TRPM4kd and −116.9 ± 51.4% ($p \leq 0.05$) for TRPM5kd cells, respectively, was detected (Figure 7).

**TRPM4- and TRPM5-Dependent $Na^+$ Influx is Involved in Proton Secretion.** Next, we hypothesized that the TRPM4/5-evoked $Na^+$ influx induced by food constituents modulates the proton secretion of HGT-1 cells. For this purpose, the proton-secreting activity was analyzed after stimulation of wild-type cells as well as TRPM4kd and TRPM5kd cells with histamine, caffeine, and L-arginine, respectively (Figure 8). We could show that both TRPM4 or TRPM5 knockdown reduced the proton secretion upon stimulation with 3 mM caffeine (−28.2 ± 6.5%; $p \leq 0.01$ and −36.3 ± 12.6%; $p \leq 0.05$) and 50 mM L-arginine (−15.1 ± 1.2%; $p \leq 0.0001$ and −11.6 ± 1.3%; $p \leq 0.0001$), respectively. This result was confirmed for caffeine by applying TRPM5- (Figure S7a,b) and TRPM4-specific (Figure S7c) antagonists. In contrast, incubation of TRPM4kd or TRPM5kd cells with 1 mM histamine did not show any deviation from mock-transfected cells regarding proton secretion.


https://doi.org/10.1021/acs.jafc.3c09085
J. Agric. Food Chem. 2024, 72, 4906−4917

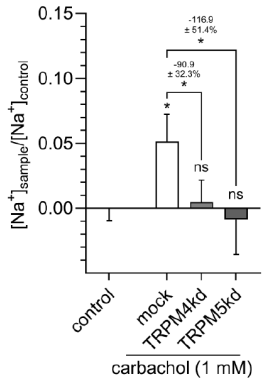


**Figure 7.** Treating mock-transfected HGT-1 cells with the muscarinic acetylcholine receptor agonist carbachol (1 mM) increases intracellular $Na^+$ concentrations. This increase cannot be detected in TRPM4 or TRPM5 knockdown cells. Data are shown as mean ± SEM, $n = 4$, t. r. = 6, statistics: one-way ANOVA Holm-Šidák *post hoc* test; significant differences are expressed with $*p \leq 0.05$.

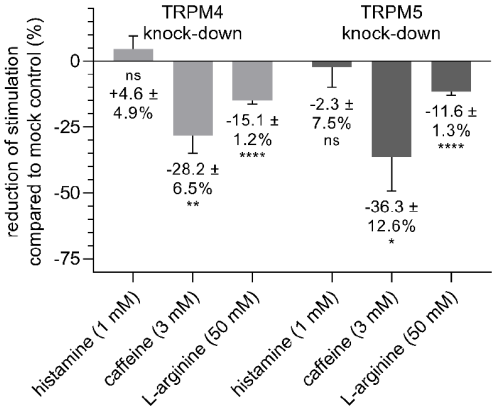


**Figure 8.** Transient knockdown of TRPM4 or TRPM5 leads to a reduction in the stimulation of proton secretion induced by caffeine (3 mM) or L-arginine (50 mM). Treatment with histamine (1 mM) did not result in differentiation between TRPM4 or TRPM5 knockdown and mock-transfected cells. Data are shown as mean ± SEM, $n = 4$, t. r. = 6, statistics: one-way ANOVA Holm-Šidák *post hoc* test; significant differences are expressed with $*p \leq 0.05$, $**p \leq 0.01$, $****p \leq 0.0001$.

## DISCUSSION

Gastric acid secretion is a vital, yet tightly regulated process. The physiological stimuli of proton secretion as key mechanisms of gastric acid formation include acetylcholine, gastrin, and especially, histamine. Apart from endogenous signals, food-derived bitter compounds have also been shown to induce proton secretion via binding to TAS2Rs located on parietal cells.[5] However, the particular underlying signaling cascade, finally leading to proton secretion, has yet to be fully elucidated. In contrast, the mode of action of bitter compounds in taste cells located on the tongue has been very well described and includes activation of the TRP channels M4 and M5 leading to an influx of $Na^+$.[8,10] Here, we hypothesized a similar cellular signaling pathway of bitter compounds in the parietal cell line HGT-1, a well-established surrogate model of human parietal cells.[5,18]

First of all, we analyzed the expression of all members of the TRP superfamily on the RNA level and the expression of TRPM4 and M5 also on the protein level. We could

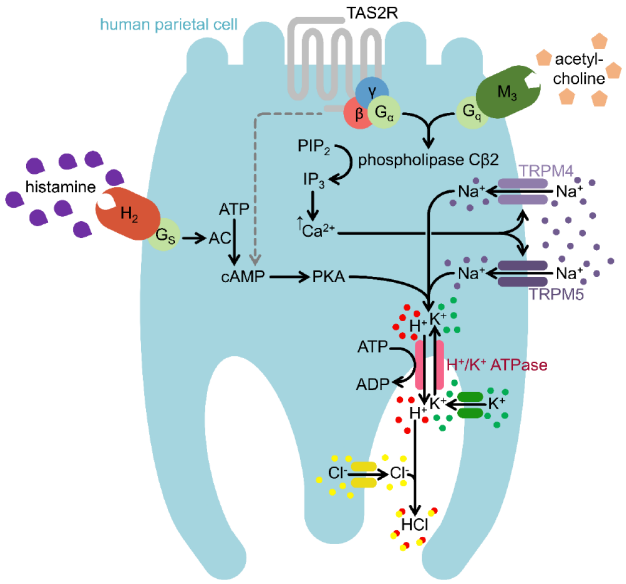


**Figure 9.** TRPM4 and TRPM5 mediate $Na^+$ influx upon stimulation with bitter compounds and carbachol (acetylcholine) in parietal cells from the cell line HGT-1 as major signaling pathway. AC: adenylylcyclase; ADP: adenosinediphosphate; ATP: adenosintriphosphate; cAMP: cyclic adenosinmonophosphate; $IP_3$: inositol-1,4,5-trisphosphate; $PIP_2$: phosphatidylinositol-4,5-bisphosphate; PKA: protein kinase A; $H_2$: histamine-$H_2$-receptor; $M_3$: muscarinic acetylcholine receptor; TAS2R: family 2 of taste receptors; TRPM4: transient receptor potential M4; TRPM5: transient receptor potential M5; $H^+/K^+$ ATPase: hydrogen potassium ATPase; G$\alpha$: G protein subunit alpha; $G_s$: G protein subunit s; $\beta$, $\gamma$: G protein beta-gamma complex.

demonstrate the expression of a variety of TRP-specific transcripts and, most importantly, the expression of TRPM4 and M5 on the protein level. Both channels are located in the cytoplasm and the plasma membrane, which may indicate regulation of cell surface expression via internalization in HGT-1 cells, which was shown before for the TRPM4 channel in a variety of cells.[36−38] In the colorectal cancer cell line HCT116, increasing concentrations of intracellular $Ca^{2+}$ led to the delivery of TRPM4-containing vesicles to the plasma membrane.[39] This presumed regulation of TRPM4 and TRPM5 in HGT-1 cells could also explain the downregulation of their specific transcripts due to a stimulation of the cells with 3 mM caffeine for 10 and 30 min, respectively.

According to our hypothesis, TRPM4 and TRPM5 are functionally linked to TAS2Rs in HGT-1 cells. Therefore, we tested whether stimulation of the cells with bitter compounds leads to an influx of $Na^+$. For this, the $Na^+$ sensitive fluorescence dye SBFI was applied. Incubation of the cells with the food-derived bitter compounds caffeine, targeting the bitter receptors TAS2R7, 10, 14, 43, and 46,[26] as well as L-arginine, targeting at least TAS2R1,[28] led to concentration-dependent increases in SBFI-fluorescence. Caffeine showed a higher potency with an $EC_{50}$ value of 0.65 mM but a lower efficacy (maximal efficacy: 5.0%) than L-arginine ($EC_{50}$: 10.38 mM; maximal efficacy: 16.3%). The higher potency of caffeine for inducing a $Na^+$ influx compared to L-arginine can be linked to the lower bitter recognition threshold of caffeine, which has been determined as ranging from 0.7 to 3.7 mM[40,41] compared to 75 mM for L-arginine.[42] To our knowledge, no data are


https://doi.org/10.1021/acs.jafc.3c09085
J. Agric. Food Chem. 2024, 72, 4906−4917

available on whether the bitter perceptions of L-arginine and caffeine in equimolar concentrations differ.

By additionally applying the fluorescence-independent and direct method single-cell LA−ICP−MS, we could clearly demonstrate that the SBFI-fluorescence not only is a suitable indicator for intracellular $Na^+$ concentrations in HGT-1 cells but furthermore can be used in a semiquantitative manner. In addition, the observed increased intracellular $Na^+$ concentrations result from an influx of $Na^+$ since the SBFI-fluorescence did not increase when HGT-1 cells were stimulated with caffeine and L-arginine in a nominal $Na^+$ free buffer. These results confirm former analyzes using SBFI to measure $Na^+$ fluxes in parietal cells from New Zealand White rabbits, although the ion channel responsible was not identified.[43] Also, the detected $Na^+$ influx is linked to TAS2Rs since stimulating HGT-1 cells with histamine, whose signaling pathway in parietal cells is mediated via the $H_2$ receptor, did not impact intracellular $Na^+$ concentrations. In fact, coincubating HGT-1 cells with caffeine or L-arginine and the bitter-masking compound HED led to lower ($-61.8 \pm 2.5\%$ for caffeine and $-131.7 \pm 4.8\%$ for L-arginine) intracellular $Na^+$ concentrations. These findings strongly suggest that $Na^+$ influx in HGT-1 cells upon stimulation with bitter compounds is mediated via the interaction with TAS2Rs. Interestingly, stimulation of the cells with HED alone did induce a $Na^+$ influx ($+0.96 \pm 0.12\%$; $p \leq 0.0001$), which might be due to the fact that HED was identified not only as an antagonist for the TAS2Rs 31, 43, 20, and 50 but also as an agonist for TAS2R14 and TAS2R39.[44] According to this knowledge, the activation of TAS2R14 and/or TAS2R39 by HED would lead to an influx of $Na^+$, as measured.

As TAS2R43 can be activated by caffeine,[26] the effect of caffeine on $Na^+$ influx was further investigated using TAS2R43ko HGT-1 cells.[5] The results obtained further evidenced the contribution of TAS2Rs in initiating the $Na^+$ influx since the TAS2R43 knockout cells demonstrated a decreased $Na^+$ influx as compared to the HGT-1 wild-type cells (Figure 4c). The remaining $Na^+$ influx in TAS2R43 knockout cells is very likely caused by the activation of other TAS2Rs (7, 10, 14, and 46), which are also targeted by caffeine.[26] Since we hypothesized a non TAS2R43-specific effect here, we also tested L-arginine, which is not a ligand for this receptor. The results presented in Figure 4c support this hypothesis. Which of the TAS2Rs has the greatest impact in stimulation $Na^+$ influx has to be investigated in future studies. However, these results implicate that, as in taste cells, the $Na^+$ influx is activated downstream of TAS2Rs.

Pharmacological inhibitors were applied to verify the involvement of TRP channels M4 and M5 in the $Na^+$ influx triggered by bitter compounds. Co-incubation of the cells with caffeine and the TRPM5 inhibitor nicotine led to a nearly 50% lower $Na^+$ influx than cells treated with caffeine. Incubation of the cells with nicotine alone resulted in lower intracellular $Na^+$ concentrations compared with control cells. This may indicate a more general function of TRPM5 in the control of intracellular $Na^+$ concentrations. In addition, nicotine may interact with other receptors in HGT-1 cells, leading to the observed effects. However, contrarily, application of the TRPM5-specific inhibitor TPPO[33] alone led to a $Na^+$ influx in HGT-1 cells comparable to caffeine. In contrast, coapplication with TPPO and caffeine doubled the impact of the single compounds. Here, we hypothesize TPPO to interact nonselectively with other ion channels in HGT-1 cells, which has already been shown for Chinese ovarian hamster (CHO) cells expressing P2X2/P2X3 receptors.[45]

Nevertheless, genetic knockdown of TRPM4 and TRPM5 decreased the $Na^+$ influx in HGT-1 cells upon stimulation with caffeine and L-arginine by 52.9−81.5%. These results show that the $Na^+$ influx in HGT-1 cells upon stimulation with food-derived bitter compounds is mediated via TRPM4 and TRPM5. A significant difference between the impact of TRPM4 and TRPM5 was not detected. Thus, both channels account for the $Na^+$ influx about equally. This also reflects the situation in taste cells, where TRPM4 and TRPM5 act downstream of TAS2Rs and contribute to a similar degree to the $Na^+$ influx upon stimulation with bitter compounds.[8] However, we cannot fully rule out the possibility that other $Na^+$ permeable ion channels, like the epithelial sodium channel (ENaC), may also contribute, albeit to a smaller extent, to the $Na^+$ influx.[46] On the other hand, activation of ENaC by bitter compounds has not been described so far. Nonetheless, TRPM4 and TRPM5 are also involved in the $Na^+$ influx induced by the structural acetylcholine analogue carbachol since the knockdown of either ion channel decreased the carbachol-induced proton secretion of HGT-1 cells up to 100%. This finding aligns with former results by Negulescu et al., who detected a $Na^+$ influx in parietal cells from New Zealand White rabbits upon stimulation with 100 $\mu$M carbachol.[43] One open question to be elucidated in future studies is whether carbachol targets, in addition to the $M_3$ receptor, e.g., taste receptors.

In nonsensory tissue other than parietal cells, bitter substances stimulated CCK secretion from enteroendocrine STC-1 cells with the participation of TRPM5.[47] Shah et al. observed that bitter compounds elicited a TRPM5-specific inward current, which might be responsible for the release of CCK.[48] In *trpm5*$^{-/-}$ mice, not only the glucose-induced insulin secretion was reduced, but also the L-arginine-induced insulin secretion.[49] This finding was confirmed for L-arginine-induced insulin secretion from rat $\beta$-cells using the TRPM5-specific inhibitor TPPO.[50] TRPM4, on the other hand, was shown to be involved in glucose-induced insulin secretion but not L-arginine-induced insulin secretion.[51] However, L-arginine-induced insulin secretion is mediated, at least partly, via GPRC6A,[52] and participation of bitter taste receptors in this process has, to our knowledge, not been demonstrated so far. Based on our findings, TRPM4 and M5 are cellular targets for taste-active food ingredients, although knowledge regarding food constituents that are capable of directly activating or inhibiting TRPM4 or TRPM5 is scarce. For example, TRPM5 was shown to be modulated by the sweetener stevioside,[53] which could imply an impact of this taste-active compound on gastric acid secretion. Furthermore, the results presented may raise the question of whether the observed physiological functions of taste-active food constituents, especially those for which beneficial health effects have been shown, e.g., coumaric acid[54] and polyphenols,[55−57] are mediated via a taste-like signaling pathway in nonsensory tissue.

To conclude, we provide evidence for the functional role of TRPM4 and TRPM5 in immortalized human parietal cells, wherein both channels are necessary for proton secretion upon stimulation with food-derived bitter compounds by mediating $Na^+$ influx. Specifically, our results indicate that HGT-1 cells possess a signal transduction pathway for bitter compounds, which is equal to taste cells, thereby rendering HGT-1 cells a suitable surrogate cell model for investigating the gustatory


https://doi.org/10.1021/acs.jafc.3c09085
J. Agric. Food Chem. 2024, 72, 4906−4917

impact of taste-active compounds. As summarized in Figure 9, the taste signaling pathway partially interacts with the well-known signaling pathway of the secretagogue acetylcholine. Although the precise mode of action and a potential interaction with the cAMP pathway remain to be clarified, this finding may help develop novel approaches that may contribute to treating pathophysiological conditions due to increased gastric acid secretion.

## ■ ASSOCIATED CONTENT

### Data Availability Statement

The data sets generated during and/or analyzed during the current study are not publicly available due to the institutional statutes but are available from the corresponding author on reasonable request.

### Supporting Information

The Supporting Information is available free of charge at https://pubs.acs.org/doi/10.1021/acs.jafc.3c09085.

LA−ICP−MS parameters (Table S1), cell viability (Figure S1), immunostaining (Figure S2), intracellular $Ca^{2+}$ measurements (Figure S3), intracellular $Na^{+}$ measurements (Figure S4), knockdown efficiency (Figure S5), gene regulation (Figure S6), and pharmacological inhibition (Figure S7) (PDF)

## ■ AUTHOR INFORMATION


### Corresponding Author

**Veronika Somoza** − *Leibniz Institute for Food Systems Biology at the Technical University of Munich, Freising 85354, Germany; Chair of Nutritional Systems Biology, TUM School of Life Sciences, Technical University of Munich, Freising 85354, Germany; Department of Physiological Chemistry, Faculty of Chemistry, University of Vienna, Vienna 1090, Austria;* orcid.org/0000-0003-2456-9245; Phone: +49-8161-71-2700; Email: v.somoza.leibniz-lsb@tum.de

### Authors

**Phil Richter** − *TUM School of Life Sciences Weihenstephan, Technical University of Munich, Freising 85354, Germany; Leibniz Institute for Food Systems Biology at the Technical University of Munich, Freising 85354, Germany;* orcid.org/0000-0003-1026-4926

**Gaby Andersen** − *Leibniz Institute for Food Systems Biology at the Technical University of Munich, Freising 85354, Germany*

**Kristin Kahlenberg** − *Leibniz Institute for Food Systems Biology at the Technical University of Munich, Freising 85354, Germany*

**Alina Ulrike Mueller** − *Leibniz Institute for Food Systems Biology at the Technical University of Munich, Freising 85354, Germany*

**Philip Pirkwieser** − *Leibniz Institute for Food Systems Biology at the Technical University of Munich, Freising 85354, Germany*

**Valerie Boger** − *Leibniz Institute for Food Systems Biology at the Technical University of Munich, Freising 85354, Germany*

Complete contact information is available at: https://pubs.acs.org/10.1021/acs.jafc.3c09085


### Author Contributions

⊥P.R. and G.A. contributed equally to this work. G.A., P.R., and V.S. conceived and planned the experiments. V.S. supervised the project. Material preparation, data collection, and analysis were performed by P.R., K.K., A.U.M., P.P., and V.B. The first draft of the manuscript was written by G.A., and all authors commented on previous versions of the manuscript. All authors read and approved the final manuscript.


### Funding

The authors declare that no funds, grants, or other support were received during the preparation of this manuscript.


### Notes

The authors declare no competing financial interest.


## ■ ACKNOWLEDGMENTS

The authors kindly acknowledge Dr. Jakob Ley (Symrise AG, Holzminden, Germany) for providing homoeriodictyol.


## ■ REFERENCES


(1) Schubert, M. L.; Peura, D. A. Control of gastric acid secretion in health and disease. *Gastroenterology* **2008**, *134* (7), 1842−1860.

(2) Yao, X.; Forte, J. G. Cell biology of acid secretion by the parietal cell. *Annu. Rev. Physiol.* **2003**, *65*, 103−131.

(3) Wess, J. Molecular biology of muscarinic acetylcholine receptors. *Crit. Rev. Neurobiol.* **1996**, *10* (1), 69−99.

(4) Li, Z. Q.; Mårdh, S. Interactions between $Ca^{2+}$- and cAMP-dependent stimulatory pathways in parietal cells. *Biochim. Biophys. Acta* **1996**, *1311* (2), 133−142.

(5) Liszt, K. I.; Ley, J. P.; Lieder, B.; Behrens, M.; Stöger, V.; Reiner, A.; Hochkogler, C. M.; Köck, E.; Marchiori, A.; Hans, J.; et al.et al. Caffeine induces gastric acid secretion via bitter taste signaling in gastric parietal cells. *Proc. Natl. Acad. Sci. U. S. A.* **2017**, *114* (30), No. E6260−E6269.

(6) Prawitt, D.; Monteilh-Zoller, M. K.; Brixel, L.; Spangenberg, C.; Zabel, B.; Fleig, A.; Penner, R. TRPM5 is a transient $Ca^{2+}$-activated cation channel responding to rapid changes in $[Ca^{2+}]i$. *Proc. Natl. Acad. Sci. U. S. A.* **2003**, *100* (25), 15166−15171.

(7) Liu, D.; Liman, E. R. Intracellular $Ca^{2+}$ and the phospholipid PIP2 regulate the taste transduction ion channel TRPM5. *Proc. Natl. Acad. Sci. U. S. A.* **2003**, *100* (25), 15160−15165.

(8) Dutta Banik, D.; Martin, L. E.; Freichel, M.; Torregrossa, A. M.; Medler, K. F. TRPM4 and TRPM5 are both required for normal signaling in taste receptor cells. *Proc. Natl. Acad. Sci. U. S. A.* **2018**, *115* (4), No. E772−e781.

(9) Margolskee, R. F. Molecular mechanisms of bitter and sweet taste transduction. *J. Biol. Chem.* **2002**, *277* (1), 1−4.

(10) Roper, S. D. Signal transduction and information processing in mammalian taste buds. *Pflugers Arch. - Eur. J. Physiol.* **2007**, *454* (5), 759−776.

(11) Clapham, D. E. TRP channels as cellular sensors. *Nature* **2003**, *426* (6966), 517−524.

(12) Hofmann, T.; Chubanov, V.; Gudermann, T.; Montell, C. TRPM5 is a voltage-modulated and Ca(2+)-activated monovalent selective cation channel. *Curr. Biol.* **2003**, *13* (13), 1153−1158.

(13) Launay, P.; Fleig, A.; Perraud, A. L.; Scharenberg, A. M.; Penner, R.; Kinet, J. P. TRPM4 is a $Ca^{2+}$-activated nonselective cation channel mediating cell membrane depolarization. *Cell* **2002**, *109* (3), 397−407.

(14) Ullrich, N. D.; Voets, T.; Prenen, J.; Vennekens, R.; Talavera, K.; Droogmans, G.; Nilius, B. Comparison of functional properties of the $Ca^{2+}$-activated cation channels TRPM4 and TRPM5 from mice. *Cell Calcium* **2005**, *37* (3), 267−278.

(15) Fonfria, E.; Murdock, P. R.; Cusdin, F. S.; Benham, C. D.; Kelsell, R. E.; McNulty, S. Tissue distribution profiles of the human TRPM cation channel family. *J. Recept. Signal Transduction Res.* **2006**, *26* (3), 159−178.

(16) Kaske, S.; Krasteva, G.; König, P.; Kummer, W.; Hofmann, T.; Gudermann, T.; Chubanov, V. TRPM5, a taste-signaling transient receptor potential ion-channel, is a ubiquitous signaling component in chemosensory cells. *BMC Neurosci.* **2007**, *8* (1), 49.
(17) Laboisse, C. L.; Augeron, C.; Couturier-Turpin, M. H.; Gespach, C.; Cheret, A. M.; Potet, F. Characterization of a newly established human gastric cancer cell line HGT-1 bearing histamine H2-receptors. *Cancer Res.* **1982**, *42* (4), 1541−1548.
(18) Carmosino, M.; Procino, G.; Casavola, V.; Svelto, M.; Valenti, G. The cultured human gastric cells HGT-1 express the principal transporters involved in acid secretion. *Pflugers Arch. - Eur. J. Physiol.* **2000**, *440* (6), 871−880.
(19) Zopun, M.; Liszt, K. I.; Stoeger, V.; Behrens, M.; Redel, U.; Ley, J. P.; Hans, J.; Somoza, V. Human Sweet Receptor T1R3 is Functional in Human Gastric Parietal Tumor Cells (HGT-1) and Modulates Cyclamate and Acesulfame K-Induced Mechanisms of Gastric Acid Secretion. *J. Agric. Food Chem.* **2018**, *66* (19), 4842−4852.
(20) Ley, J. P.; Krammer, G.; Reinders, G.; Gatfield, I. L.; Bertram, H. J. Evaluation of bitter masking flavanones from Herba Santa (*Eriodictyon californicum* (H. and A.) Torr., Hydrophyllaceae). *J. Agric. Food Chem.* **2005**, *53* (15), 6061−6066.
(21) Liszt, K. I.; Walker, J.; Somoza, V. Identification of organic acids in wine that stimulate mechanisms of gastric acid secretion. *J. Agric. Food Chem.* **2012**, *60* (28), 7022−7030.
(22) Andersen, G.; Kahlenberg, K.; Krautwurst, D.; Somoza, V. [6]-Gingerol Facilitates CXCL8 Secretion and ROS Production in Primary Human Neutrophils by Targeting the TRPV1 Channel. *Mol. Nutr. Food Res.* **2023**, *67* (4), No. e2200434.
(23) Tiroch, J.; Sterneder, S.; Di Pizio, A.; Lieder, B.; Hoelz, K.; Holik, A. K.; Pignitter, M.; Behrens, M.; Somoza, M.; Ley, J. P.; et al.etal. Bitter Sensing TAS2R50 Mediates the trans-Resveratrol-Induced Anti-inflammatory Effect on Interleukin 6 Release in HGF-1 Cells in Culture. *J. Agric. Food Chem.* **2021**, *69* (45), 13339−13349.
(24) Walker, J.; Hell, J.; Liszt, K. I.; Dresel, M.; Pignitter, M.; Hofmann, T.; Somoza, V. Identification of beer bitter acids regulating mechanisms of gastric acid secretion. *J. Agric. Food Chem.* **2012**, *60* (6), 1405−1412.
(25) Richter, P.; Sebald, K.; Fischer, K.; Behrens, M.; Schnieke, A.; Somoza, V. Bitter Peptides YFYPEL, VAPFPEVF, and YQEPVLGPVRGPFPIIV, Released during Gastric Digestion of Casein, Stimulate Mechanisms of Gastric Acid Secretion via Bitter Taste Receptors TAS2R16 and TAS2R38. *J. Agric. Food Chem.* **2022**, *70* (37), 11591−11602.
(26) Meyerhof, W.; Batram, C.; Kuhn, C.; Brockhoff, A.; Chudoba, E.; Bufe, B.; Appendino, G.; Behrens, M. The molecular receptive ranges of human TAS2R bitter taste receptors. *Chem. Senses* **2010**, *35* (2), 157−170.
(27) Stoeger, V.; Liszt, K. I.; Lieder, B.; Wendelin, M.; Zopun, M.; Hans, J.; Ley, J. P.; Krammer, G. E.; Somoza, V. Identification of Bitter-Taste Intensity and Molecular Weight as Amino Acid Determinants for the Stimulating Mechanisms of Gastric Acid Secretion in Human Parietal Cells in Culture. *J. Agric. Food Chem.* **2018**, *66* (26), 6762−6771.
(28) Stoeger, V.; Holik, A. K.; Hölz, K.; Dingjan, T.; Hans, J.; Ley, J. P.; Krammer, G. E.; Niv, M. Y.; Somoza, M. M.; Somoza, V. Bitter-Tasting Amino Acids l-Arginine and l-Isoleucine Differentially Regulate Proton Secretion via T2R1 Signaling in Human Parietal Cells in Culture. *J. Agric. Food Chem.* **2020**, *68* (11), 3434−3444.
(29) Muschol, M.; Dasgupta, B. R.; Salzberg, B. M. Caffeine interaction with fluorescent calcium indicator dyes. *Biophys. J.* **1999**, *77* (1), 577−586.
(30) Engevik, A. C.; Kaji, I.; Goldenring, J. R. The Physiology of the Gastric Parietal Cell. *Physiol. Rev.* **2020**, *100* (2), 573−602.
(31) Ley, J. P.; Dessoy, M.; Paetz, S.; Blings, M.; Hoffmann-Lücke, P.; Reichelt, K. V.; Krammer, G. E.; Pienkny, S.; Brandt, W.; Wessjohann, L. Identification of enterodiol as a masker for caffeine bitterness by using a pharmacophore model based on structural analogues of homoeriodictyol. *J. Agric. Food Chem.* **2012**, *60* (25), 6303−6311.
(32) Gees, M.; Alpizar, Y. A.; Luyten, T.; Parys, J. B.; Nilius, B.; Bultynck, G.; Voets, T.; Talavera, K. Differential effects of bitter compounds on the taste transduction channels TRPM5 and IP3 receptor type 3. *Chem. Senses* **2014**, *39* (4), 295−311.
(33) Palmer, R. K.; Atwal, K.; Bakaj, I.; Carlucci-Derbyshire, S.; Buber, M. T.; Cerne, R.; Cortés, R. Y.; Devantier, H. R.; Jorgensen, V.; Pawlyk, A.; et al.et al. Triphenylphosphine oxide is a potent and selective inhibitor of the transient receptor potential melastatin-5 ion channel. *Assay Drug Dev. Technol.* **2010**, *8* (6), 703−713.
(34) Grand, T.; Demion, M.; Norez, C.; Mettey, Y.; Launay, P.; Becq, F.; Bois, P.; Guinamard, R. 9-phenanthrol inhibits human TRPM4 but not TRPM5 cationic channels. *Br. J. Pharmacol.* **2008**, *153* (8), 1697−1705.
(35) Dell'acqua, M. L.; Carroll, R. C.; Peralta, E. G. Transfected m2 muscarinic acetylcholine receptors couple to G alpha i2 and G alpha i3 in Chinese hamster ovary cells. Activation and desensitization of the phospholipase C signaling pathway. *J. Biol. Chem.* **1993**, *268* (8), 5676−5685.
(36) Ghosh, D.; Segal, A.; Voets, T. Distinct modes of perimembrane TRP channel turnover revealed by TIR-FRAP. *Sci. Rep.* **2014**, *4* (1), 7111.
(37) Crnich, R.; Amberg, G. C.; Leo, M. D.; Gonzales, A. L.; Tamkun, M. M.; Jaggar, J. H.; Earley, S. Vasoconstriction resulting from dynamic membrane trafficking of TRPM4 in vascular smooth muscle cells. *Am. J. Physiol. Cell Physiol.* **2010**, *299* (3), C682−C694.
(38) Kruse, M.; Schulze-Bahr, E.; Corfield, V.; Beckmann, A.; Stallmeyer, B.; Kurtbay, G.; Ohmert, I.; Schulze-Bahr, E.; Brink, P.; Pongs, O. Impaired endocytosis of the ion channel TRPM4 is associated with human progressive familial heart block type I. *J. Clin. Invest.* **2009**, *119* (9), 2737−2744.
(39) Stokłosa, P.; Kappel, S.; Peinelt, C. A Novel Role of the TRPM4 Ion Channel in Exocytosis. *Cells* **2022**, *11* (11), 1793.
(40) Izawa, K.; Amino, Y.; Kohmura, M.; Ueda, Y.; Kuroda, M. 4.16 - Human−Environment Interactions − Taste. In *Comprehensive Natural Products II*; Liu, H.-W.; Mander, L., Eds.; Elsevier: Oxford, 2010; pp. 631671.
(41) Guinard, J.-X.; Hong, D. Y.; Zoumas-Morse, C.; Budwig, C.; Russell, G. F. Chemoreception and perception of the bitterness of isohumulones. *Physiol. Behav.* **1994**, *56* (6), 1257−1263.
(42) Sonntag, T.; Kunert, C.; Dunkel, A.; Hofmann, T. Sensory-Guided Identification of N -(1-Methyl-4-oxoimidazolidin-2-ylidene)-α-amino Acids as Contributors to the Thick-Sour and Mouth-Drying Orosensation of Stewed Beef Juice. *J. Agric. Food Chem.* **2010**, *58* (10), 6341−6350.
(43) Negulescu, P. A.; Harootunian, A.; Tsien, R. Y.; Machen, T. E. Fluorescence measurements of cytosolic free Na concentration, influx and efflux in gastric cells. *Cell Regul.* **1990**, *1* (3), 259−268.
(44) Roland, W. S. U.; van Buren, L.; Gruppen, H.; Driesse, M.; Gouka, R. J.; Smit, G.; Vincken, J. P. Bitter taste receptor activation by flavonoids and isoflavonoids: Modeled structural requirements for activation of hTAS2R14 and hTAS2R39. *J. Agric. Food Chem.* **2013**, *61* (44), 10454−10466.
(45) Huang, Y. A.; Roper, S. D. Intracellular Ca(2+) and TRPM5-mediated membrane depolarization produce ATP secretion from taste receptor cells. *J. Physiol.* **2010**, *588* (Pt13), 2343−2350.
(46) Bigiani, A. Does ENaC Work as Sodium Taste Receptor in Humans? *Nutrients* **2020**, *12* (4), 1195.
(47) Chen, M. C.; Wu, S. V.; Reeve, J. R., Jr.; Rozengurt, E. Bitter stimuli induce $Ca^{2+}$ signaling and CCK release in enteroendocrine STC-1 cells: Role of L-type voltage-sensitive $Ca^{2+}$ channels. *Am. J. Physiol. Cell Physiol.* **2006**, *291* (4), C726−C739.
(48) Shah, B. P.; Liu, P.; Yu, T.; Hansen, D. R.; Gilbertson, T. A. TRPM5 is critical for linoleic acid-induced CCK secretion from the enteroendocrine cell line, STC-1. *Am. J. Physiol. Cell Physiol.* **2012**, *302* (1), C210−C219.
(49) Brixel, L. R.; Monteilh-Zoller, M. K.; Ingenbrandt, C. S.; Fleig, A.; Penner, R.; Enklaar, T.; Zabel, B. U.; Prawitt, D. TRPM5 regulates

glucose-stimulated insulin secretion. *Pflugers Arch. - Eur. J. Physiol.* **2010**, *460* (1), 69−76.
(50) Krishnan, K.; Ma, Z.; Björklund, A.; Islam, M. S. Role of transient receptor potential melastatin-like subtype 5 channel in insulin secretion from rat β-cells. *Pancreas* **2014**, *43* (4), 597−604.
(51) Cheng, H.; Beck, A.; Launay, P.; Gross, S. A.; Stokes, A. J.; Kinet, J. P.; Fleig, A.; Penner, R. TRPM4 controls insulin secretion in pancreatic β-cells. *Cell Calcium* **2007**, *41* (1), 51−61.
(52) Pi, M.; Wu, Y.; Lenchik, N. I.; Gerling, I.; Quarles, L. D. GPRC6A mediates the effects of L-arginine on insulin secretion in mouse pancreatic islets. *Endocrinology* **2012**, *153* (10), 4608−4615.
(53) Philippaert, K.; Pironet, A.; Mesuere, M.; Sones, W.; Vermeiren, L.; Kerselaers, S.; Pinto, S.; Segal, A.; Antoine, N.; Gysemans, C.; et al.et al. Steviol glycosides enhance pancreatic beta-cell function and taste sensation by potentiation of TRPM5 channel activity. *Nat. Commun.* **2017**, *8* (1), 14733.
(54) Pei, K.; Ou, J.; Huang, J.; Ou, S. p-Coumaric acid and its conjugates: Dietary sources, pharmacokinetic properties and biological activities. *J. Sci. Food Agric.* **2016**, *96* (9), 2952−2962.
(55) Soares, S.; Silva, M. S.; García-Estevez, I.; Groβmann, P.; Brás, N.; Brandão, E.; Mateus, N.; de Freitas, V.; Behrens, M.; Meyerhof, W. Human Bitter Taste Receptors Are Activated by Different Classes of Polyphenols. *J. Agric. Food Chem.* **2018**, *66* (33), 8814−8823.
(56) Yamashita, Y.; Sakakibara, H.; Toda, T.; Ashida, H. Insights into the potential benefits of black soybean (Glycine max L.) polyphenols in lifestyle diseases. *Food Funct.* **2020**, *11* (9), 7321−7339.
(57) Xing, L.; Zhang, H.; Qi, R.; Tsao, R.; Mine, Y. Recent Advances in the Understanding of the Health Benefits and Molecular Mechanisms Associated with Green Tea Polyphenols. *J. Agric. Food Chem.* **2019**, *67* (4), 1029−1043.


https://doi.org/10.1021/acs.jafc.3c09085
*J. Agric. Food Chem.* 2024, 72, 4906−4917

# Supporting information to

**Sodium Permeable Ion Channels TRPM4 and TRPM5 are Functional in Human Gastric Parietal Cells in Culture and Modulate the Cellular Response to Bitter Tasting Food Constituents**

By

P. Richter[1,2#], G. Andersen[2#], K. Kahlenberg[2], A. U. Mueller[2], P. Pirkwieser[2], V. Boger[2], V. Somoza[2,3,4*]

*[1]TUM School of Life Sciences Weihenstephan, Technical University of Munich, Alte Akademie 8, 85354 Freising, Germany*

*[2]Leibniz Institute for Food Systems Biology at the Technical University of Munich, Lise-Meitner-Str. 34, 85354 Freising, Germany*

*[3]Chair of Nutritional Systems Biology, TUM School of Life Sciences, Technical University of Munich, Lise-Meitner-Str. 34, 85354 Freising, Germany*

*[4]Department of Physiological Chemistry, Faculty of Chemistry, University of Vienna, Josef-Holaubek-Platz 2 (UZA II), 1090 Wien, Austria*

[#]The authors contributed equally to this work

**Correspondence to Veronika Somoza: telephone +49-8161-71-2700, E-mail: v.somoza.leibniz-lsb@tum.de*

**Table S1:** Instrumental parameters for the LA-ICP-MS measurements.

| **NexION 5000 Multi-Quadrupole ICP-MS** | | **Iridia 193 nm Laser Ablation System** | |
|---|---|---|---|
| **Software** | Syngistix v.3.3 | **Software** | Chromium v.3.1 |
| **Nebulizer Gas Flow [L/min]** | 0.82-0.94 | **Data Processing Software** | HDIP-v1.7.1 |
| **Auxiliary Gas Flow [L/min]** | 1.20 | **Ablation Cell Type** | Cobalt Long Pulse with Z-prime (100 mm x 100 mm) |
| **Plasma Gas Flow [L/min]** | 16 | **Fluence [J/cm$^2$]** | 1.0 |
| **ICP RF Power [W]** | 1600 | **Repetition Rate [Hz]** | 162 |
| **Profile** | standard | **Spot size [µm]** | 3 |
| **Analyte** | Na | **Mask shape** | circle |
| **Scan Mode** | MS/MS | **Image xy dimensions [µm]** | 200x175 |
| **Q1/Q3 Begin Mass** | 22.9898 | **Lateral scan speed [µm/s]** | 52 |
| **IGM** | focusing | **Dosage** | 9 |
| **Dwell Time Per AMU** | 50 | **Scan mode** | line by line uni-directional, laser off between rows |
| **Rpq [V]** | 0.25 | **Image xy dimensions [µm]** | 200x175 |

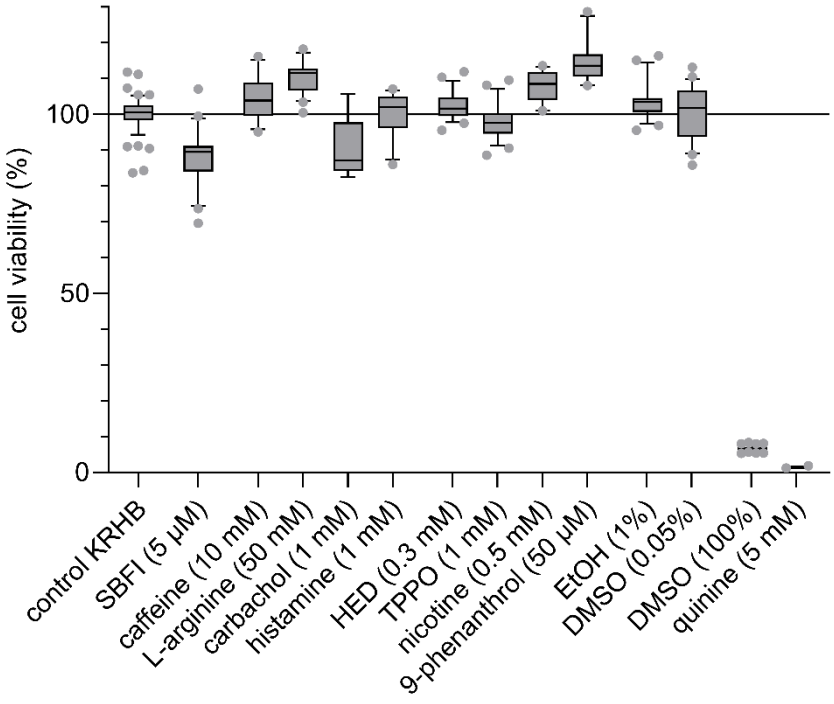


**Figure S1:** Results of the experiments on cell viability. No relevant effects of viability after incubation of the investigated substances were found. DMSO (100%) and quinine (5 mM) were used as negative controls. Data were normalized to HGT-1 cells treated with KRHB only, n = 4-5, t. r. = 3-6.

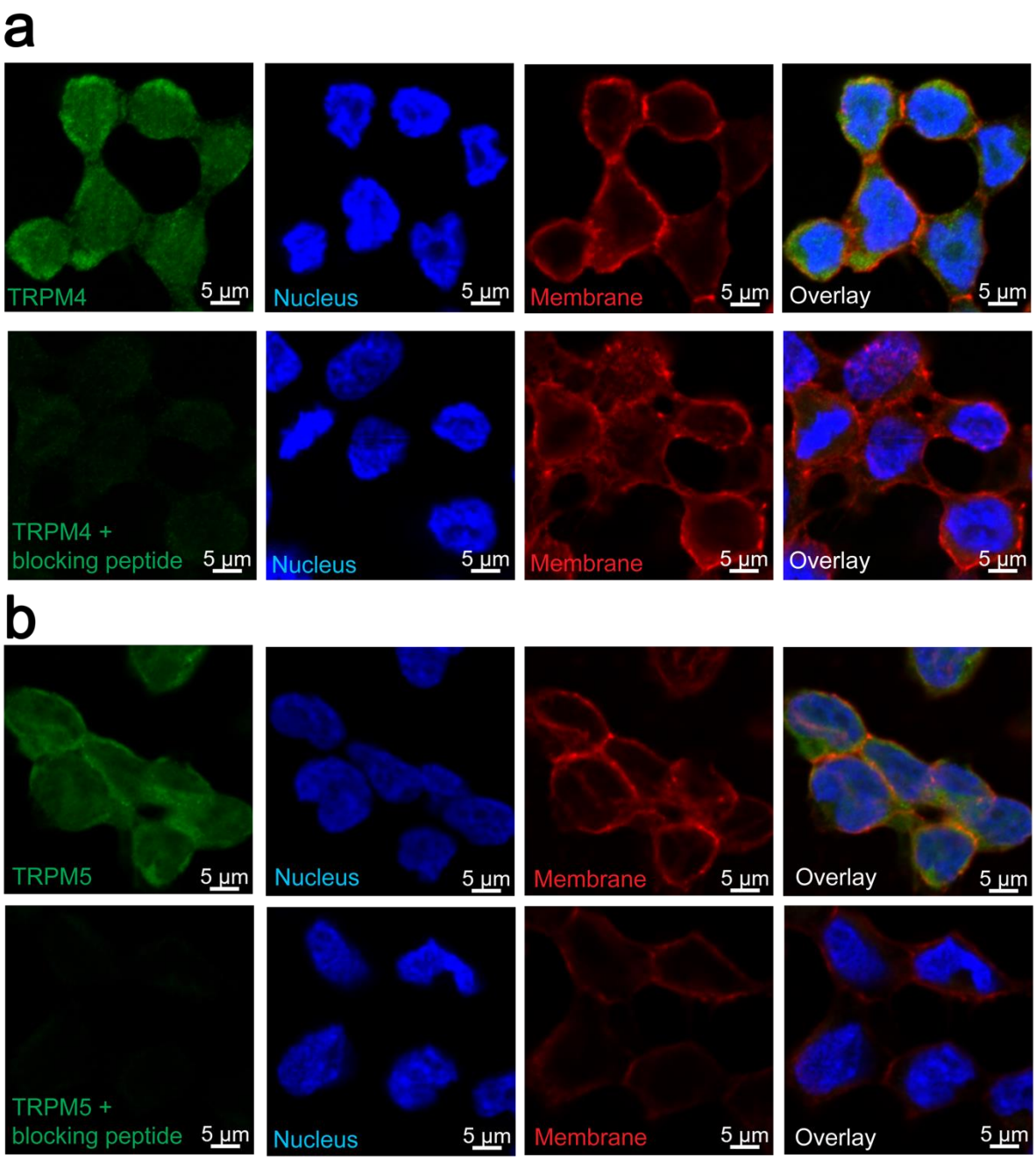


**Figure S2:** Specific immunostaining of TRPM4 and TRPM5 in HGT-1 cells. Receptor expression is detected by anti-TRPM4 antibody (a) and anti-TRPM5 antibody (b) in combination with an Alexa Fluor 488 anti-rabbit IgG (green). The nucleus is visualized by Hoechst-33342 (blue), and the plasma membrane by biotin-conjugated concanavalin A binding in combination with Alexa Fluor 633 conjugate (red). As antibody specificity control, primary antibodies were preincubated with the corresponding blocking peptide. Scale: 5 µM.

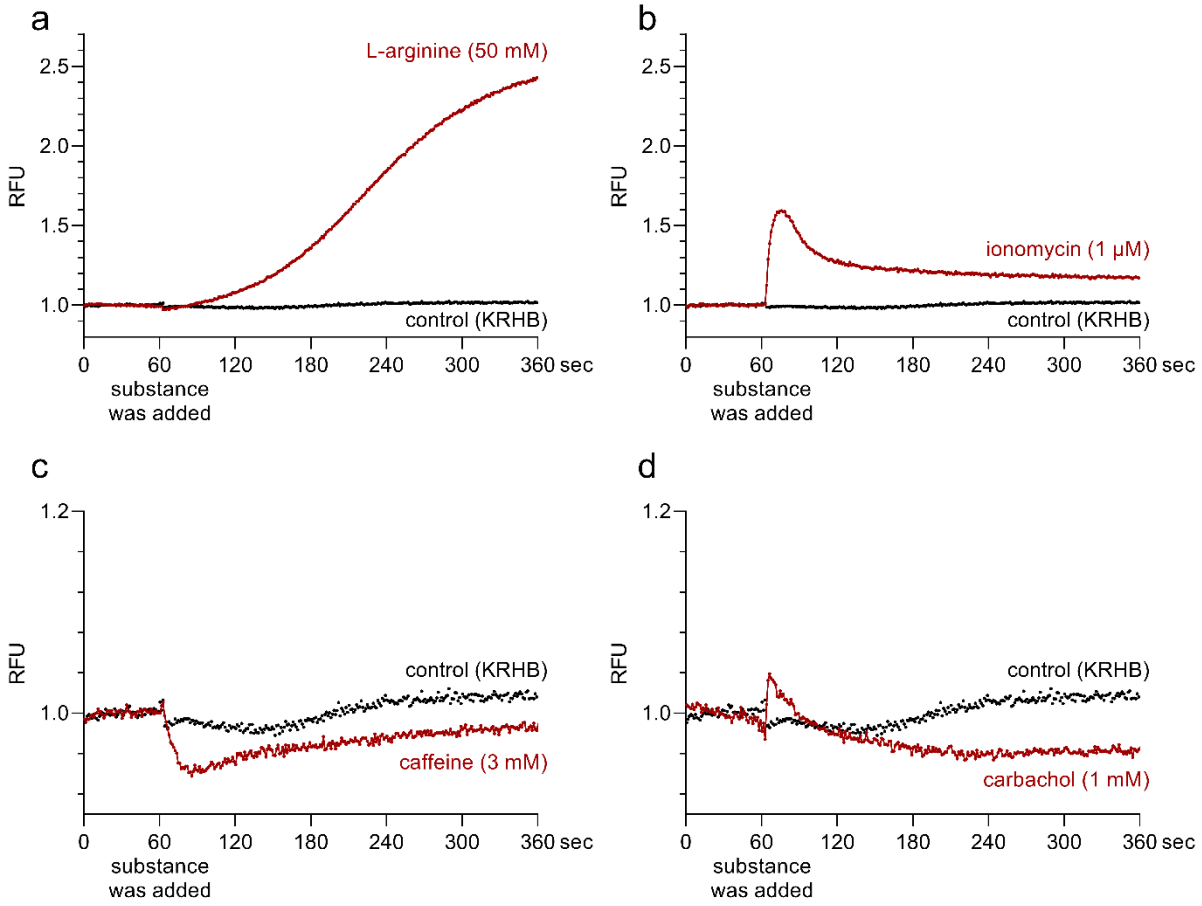


**Figure S3**: L-arginine (50 mM, a) and carbachol (1 mM, d) lead to an increase in intracellular $Ca^{2+}$ concentration in HGT-1 cells, whereas this is not measurable for caffeine due to its already described quenching effect (3 mM, c). Ionomycin (1 µM, b) was used as a positive control. Substances were added after 60 seconds. In comparison, the untreated control (black) is shown. Data are shown as mean, n = 4, t. r. = 2.

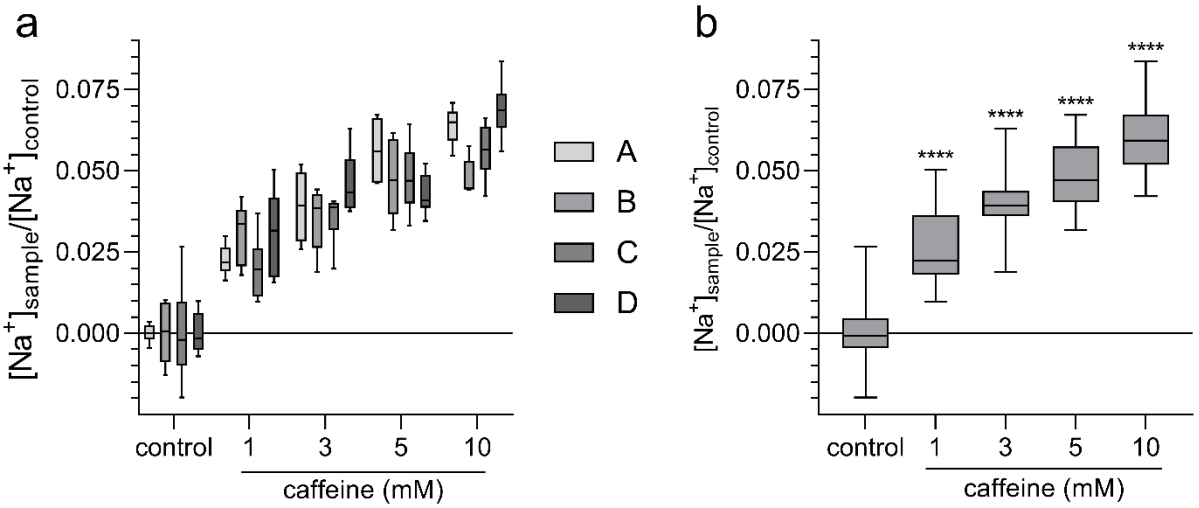


**Figure S4:** Caffeine induced increases in intracellular $Na^+$ are stable and reproducible. (a) Each grayscale represents the results of one biological replicate (t. r. = 6). In all cases, a reproducible increase in sodium concentrations in HGT-1 cells was shown starting at concentrations of 1 mM caffeine. (b) The combined results of the four biological replicates. Statistics: n = 4, t. r. = 6, one-way ANOVA Holm-Šidák *post hoc* test; significant differences are expressed with **** = $p \leq 0.0001$.

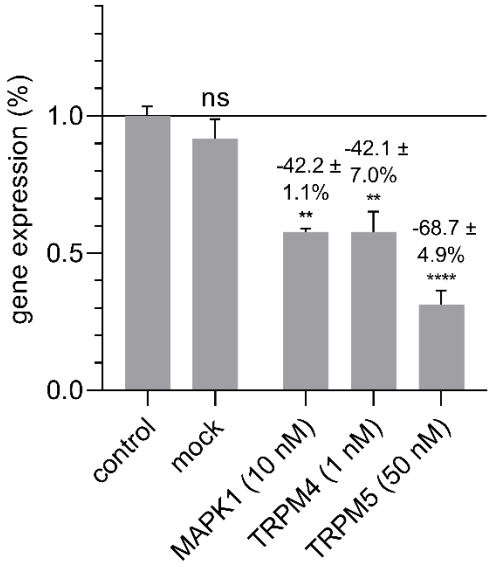


**Figure S5:** Gene expression of TRPM4 and TRPM5 were reduced by incubating HGT-1 cells with lipofectamine and siRNA for 72 hours. The expression of MAPK1 was downregulated as a positive control. Nonspecific siRNA was used as a negative control (mock). Knock-down efficiencies are shown as mean ± SEM, n = 4, t. r. = 3, statistics: one-way ANOVA Holm-Šidák *post hoc* test; significant differences are expressed with ** = $p \leq 0.01$, **** = $p \leq 0.0001$.

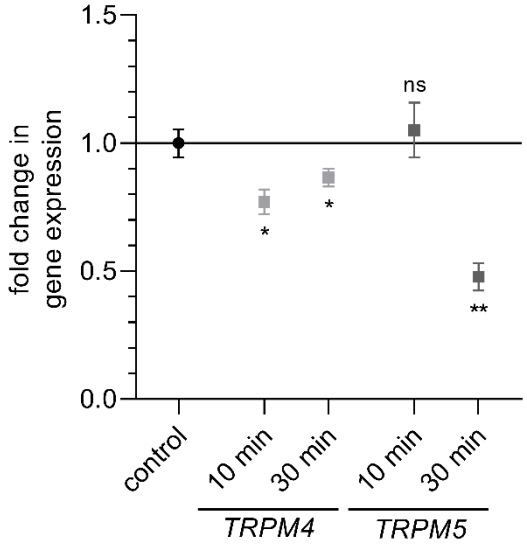


**Figure S6:** Incubation of the cells with caffeine (3 mM) resulted in a significant down-regulation of TRPM4 at the RNA level after only 10 minutes. This regulation was also still present after 30 minutes. For the expression of TRPM5, there was no significant change after 10 minutes, but after 30 minutes the expression was strongly downregulated. Data are shown as mean ± SEM, n = 4, t. r. = 3, statistics: one-way ANOVA Holm-Šidák *post hoc* test; significant differences are expressed with * = $p \leq 0.05$, ** = $p \leq 0.01$.

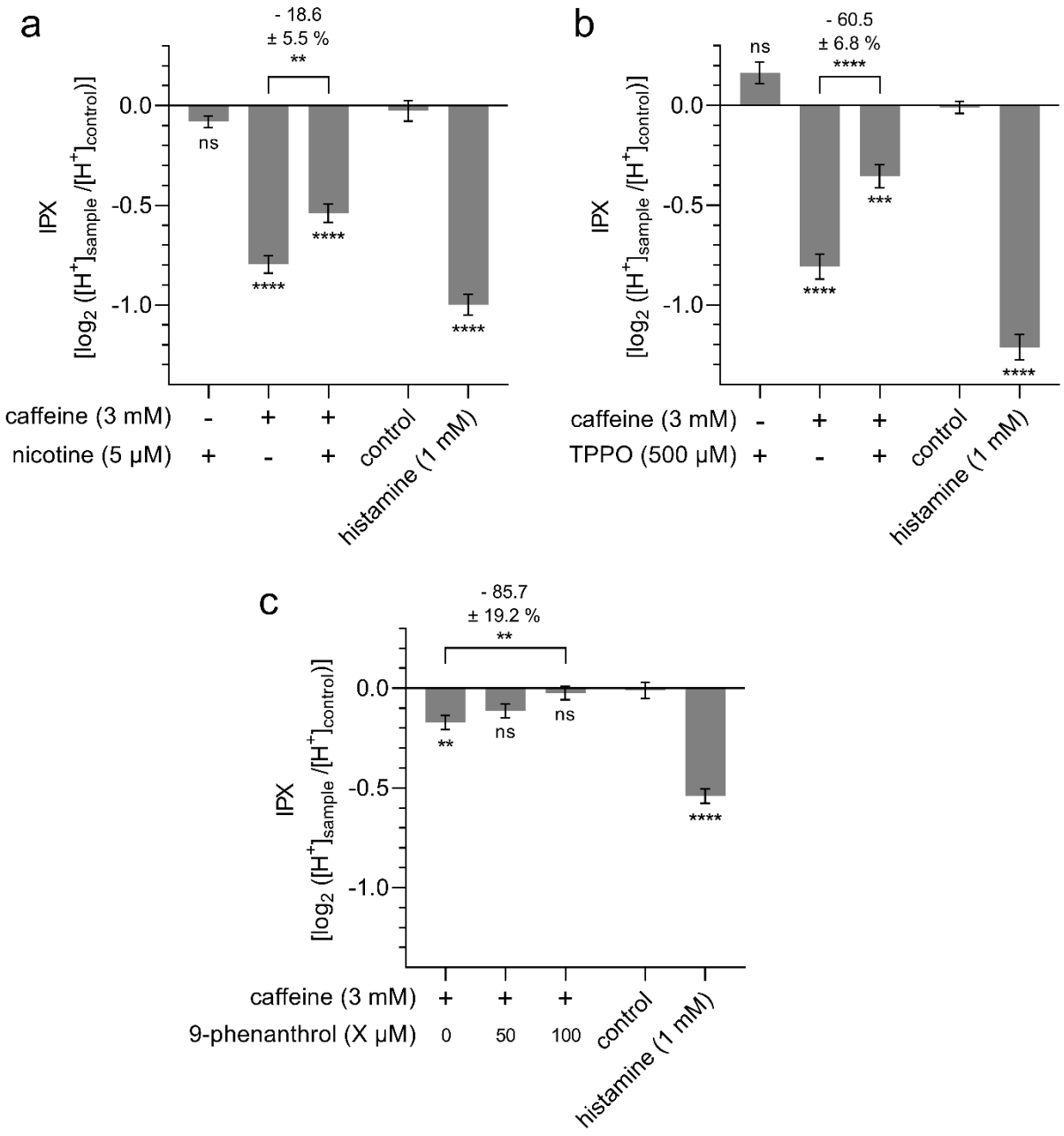


**Figure S7:** Pharmacological inhibition with the TRPM5-specific inhibitors (a) nicotine and (b) TPPO and the TRPM4-specific inhibitor (c) 9-phenanthrol resulted in a reduction in caffeine-induced (3 mM) stimulation of proton secretion of HGT-1 cells. Data are shown as mean ± SEM, n = 4, t. r. = 6, statistics: one-way ANOVA Holm-Šidák *post hoc* test; significant differences are expressed with ** = $p \leq 0.01$, *** = $p \leq 0.001$, **** = $p \leq 0.0001$.